DISSERTATION

NOVEL APPROACHES TO CHARACTERIZING FELINE-ASSOCIATED DERMATOPHYTIC FUNGI

Submitted by

Alexandra Elizabeth Moskaluk

Department of Microbiology, Immunology, and Pathology

In partial fulfillment of the requirements

For the Degree of Doctor of Philosophy

Colorado State University

Fort Collins, Colorado

Fall 2022

Doctoral Committee:

Advisor: Sue VandeWoude

Josh Daniels
Jennifer Schissler
Melissa Reynolds

ABSTRACT

NOVEL APPROACHES TO CHARACTERIZING FELINE-ASSOCIATED DERMATOPHYTIC FUNGI

Dermatophytes are highly infectious fungi that cause superficial infections in keratinized tissues in humans and animals. This group of fungi is defined by their ability to digest keratin and encompasses a wide range of species. Classification of many of these species has recently changed due to genetic analysis, potentially affecting clinical diagnosis and disease management. In Chapter One, we review dermatophyte classification including name changes for medically important species, current and potential diagnostic techniques for detecting dermatophytes, and an in-depth review of *Microsporum canis*, a prevalent zoonotic dermatophyte.

M. canis commonly causes dermatophytosis in humans and cats, and is adapting to its primary host (domestic cats) as one of its mating types (MAT1-2) appears to be going extinct. Assessment of genetic variation among *M. canis* isolates in the United States has not been conducted. Further, *M. canis* mating type and assessment of disease severity associated with genotypic characteristics have not been rigorously evaluated. In Chapter Two, *M. canis* was isolated from 191 domestic cats across the US and characterized genotypes by evaluation of ITS sequence, MAT locus, and microsatellite loci analysis. The genes SSU1 and SUB3, which are associated with keratin adhesion and digestion, were sequenced from a subset of isolates to evaluate potential genetic associations with virulence. Analysis of microsatellite makers revealed three *M. canis* genetic clusters. Both clinic location and disease severity were significant predictors of microsatellite variants. 100% of the *M. canis* isolates were MAT1-1 mating gene

type, indicating that MAT1-2 is very rare or extinct in the US and that asexual reproduction is the dominant form of replication. No genetic variation at SSU1 and SUB3 was observed. These findings pave the way for novel testing modalities for *M. canis* and provide insights about transmission and ecology of this ubiquitous and relatively uncharacterized agent.

Chapter Three evaluated four dermatophytosis cases occurring in kittens collected from the study in Chapter Two that yielded fungi with colony morphology more similar to *Arthroderma* species than *Microsporum*. Morphologic and microscopic examinations were conducted, and gene segments for the ITS, β-tubulin, and translation elongation factor 1-alpha (TEF1) regions were sequenced from DNA extracted from these cultures. Sequences were aligned to other dermatophytes using maximum likelihood and neighbor-joining trees and were compared to previously described fungal species to assess nucleotide homology. We identified two previously undescribed fungal species, herein as *Arthroderma lilyanum* sp. nov. and *Arthroderma mcgillisianum* sp. nov. *M. canis* co-cultured in two of the four cases. Other physiologic tests supported this diagnosis. These species have significance as potential pathogens and should be considered as rule-outs for dermatophytosis in cats. The potential for infection of other species, including humans, should be considered.

In Chapter Four, we investigated a critical adhesion protein (Sub3) utilized by *M. canis* during initial stages of infection, analyzing its production and expression under varying growth conditions. Additionally, as this protein must be expressed and produced for dermatophyte infections to occur, we developed and optimized a diagnostic antibody assay targeting this protein. While clinical samples of *M. canis* were found to have low Sub3 production, Sub3 levels were increased in culture when grown in baffled flasks and supplemented with either L-cysteine or cat hair. As Sub3 was also produced in cultures not supplemented with keratin or cysteine, this

study demonstrated that Sub3 expression is not reliant on the present of keratin or its derivatives. These findings could help direct future metabolic studies of dermatophytes, particularly during the adherence phase of infections.

Chapter Five explored two molecular approaches for developing diagnostic assays for dermatophytosis based on keratin metabolites: sulfite and S-sulfocysteine (SSC). Currently, fungal culture is still considered the "gold standard" for diagnosing dermatophytosis, however, modern molecular assays have overcome the main disadvantages of culture, allowing for tandem use with cultures. The first approach involved a starch and iodine indicator that reacts with sulfite and SSC, resulting in a visual color change. While this method had a low limit of detection, the indicator had many off-target reactions, leading to low specificity for dermatophyte metabolites. The second approach utilized tandem liquid chromatography with mass spectrometry, targeting SSC. Using the same cultures performed in Chapter Four, we were able to detect and quantify SSC from *M. canis* cultures grown with hair at days 15 and 18 post inoculation. These findings demonstrated that SSC is consumed/degraded by the fungi, particularly during early growth stages.

Collectively, this work provides future directions for genetic and metabolic studies of dermatophytes and how to leverage unique characteristics of dermatophytes for developing novel diagnostic assays. We conclude that *M. canis* genetics influence clinical disease presentation and further whole genome studies could help elucidate key genetic regions involved in dermatophyte pathogenesis. Furthermore, as *M. canis* continues to adapt to its primary host of cats, having a rapid, accurate diagnostic assay will become even more critical, particularly in high-density populations.

ACKNOWLEDGEMENTS

First and foremost, I would not be where I am today without the love, support, and encouragement from my husband, Benjamin Shupe. He has been my rock through both veterinary and graduate school. Through his dedication, support, and amazing cooking skills, he has helped me continue the marathon that is a PhD. Thanks for being my partner in life!

As young as I can remember, my parents have been supportive of me pursuing my dreams in life. They have believed in my goals throughout the years, always offering words of encouragement, and being there since day one through the journey of life for all of the ups and downs as well as attending all of the important milestones along this journey from graduations to my white coat ceremony for vet school. I also want to thank my family including my pets (Isaac, Lily, Ghost, and Sylvie) for encouraging me to follow my dreams through multiple degrees.

During undergraduate and veterinary schools, I was incredibly lucky to have multiple supportive professors who shaped my views on research. Dr. Karen McDonald and Dr. Bruno Chomel introduced me to how animal health can greatly impact human health. Dr. Patricia Pesavento has been and continues to be a wonderful mentor in guiding me through the difficult waters of pursuing a research career as a veterinarian. I want to thank my graduate committee for their support during my PhD: Sue VandeWoude, Josh Daniels, Melissa Reynolds and Jennifer Schissler. All of the people involved in my projects along the way during graduate school have also been a tremendous help. Additionally, I want to thank all the animals involved in the studies as without them, none of this would have been possible.

Thank you for helping me become the person I am today, for supporting me in pursuit of my dreams, and for showing me the important things in life. Let the next chapter in life begin.

DEDICATION

I would like to dedicate my dissertation and all my graduate work to Lily Moskaluk. She was my soulmate and my shining star, guiding me through life. May we meet again in this life or the next.

TABLE OF CONTENTS

CHAPTER ONE: CURRENT TOPICS IN DERMATOPHYTE CLASSIFICATION AND CLINICAL DIAGNOSIS

Dermatophytes are the most ubiquitous fungal pathogens worldwide, responsible for a majority of skin and nail infections [Havlickova *et al.* 2008, Seebacher *et al.* 2008, Hay 2017][1]. Globally, the estimated lifetime risk of developing dermatophytosis is 10-20%, with infections of feet being the most common [Drake *et al.* 1996, Nussipov *et al.* 2017]. Given the high infection rates, treating dermatophytes globally costs $500 million annually [Gräser *et al.* 2008]. Accurate diagnosis is key for patient management and implementation of appropriate therapies. Many forms of dermatophytosis can be difficult to clinically distinguish from other skin ailments as clinical presentation overlaps between the diseases [Garg *et al.* 2009]. Additionally, a significant portion of dermatophyte cases occur in developing countries, where populations are unable to access health care [Richard *et al.* 1994, Nweze *et al.* 2017]. Misdiagnosis can result in dangerous consequences, particularly in immunocompromised patients, as disease can progress to deeper invasion, leading to disseminated dermatophytosis and invasive dermatitis [Marconi *et al.* 2010, Peres *et al.* 2010, Rouzaud *et al.* 2015, Benedict *et al.* 2018]. Misdiagnosis can also occur due to misidentification of the dermatophyte responsible for infection. As with other fields in mycology, medical mycology has recently experienced reclassification of various species as the use of genetics has become more prevalent in defining species [Gräser *et al.* 1999, de Hoog *et al.* 2017]. Name changing has affected many genera of dermatophytes, which can impact clinical databases and certain diagnostic techniques. In this review, we discuss (1) dermatophyte classification with regard to human and animal infections, (2) diagnostic techniques currently

[1] Work presented in this chapter has been published under the following citation Moskaluk, Alex E., and Sue VandeWoude. "Current Topics in Dermatophyte Classification and Clinical Diagnosis." Pathogens, vol. 11, no. 9, Aug. 2022, p. 957. Crossref, https://doi.org/10.3390/pathogens11090957.

used for detecting dermatophytes in clinical settings, (3) potential future directions for dermatophytosis diagnostics, and (4) a comprehensive clinical review on prevalent zoophile *Microsporum canis*. We focused on *M. canis* as it frequently infects both humans and animals, making it one of the most encountered dermatophytes in clinical settings [Gräser *et al.* 2000, Moriello *et al.* 2017].

1.1 Introduction to dermatophytes

Dermatophytes are a classification of fungi that invade and degrade keratinized tissues including hair, skin, nails, and feathers [Weitzman *et al.* 1995]. These fungi belong to the Ascomycota phylum, Eurotiomycetes class, Onygenales order, and Arthrodermataceae family [de Hoog *et al.* 2017, Segal *et al.* 2021]. There are currently seven accepted genera of dermatophytes: *Trichophyton*, *Epidermophyton*, *Nannizzia*, *Paraphyton*, *Lophophyton*, *Microsporum* and *Arthroderma* [de Hoog *et al.* 2017]. As with other fungi families, names of species have continuously changed as the field of mycology has switched from naming based on morphology and clinical disease of isolates to including a molecular approach [Gräser *et al.* 1999, de Hoog *et al.* 2017]. Additionally, the sexual form (teleomorph) and asexual form (anamorph) used to be classified as two separate species with different names [Moriello *et al.* 2017]. Recently, names of teleomorphs and anamorphs have been consolidated, resulting in the "One Fungus = One Name" system for species identification [Hawksworth *et al.* 2011, Taylor 2011]. Further categorization of dermatophytes places species into three different groups based on their habitat: anthropophilic (living on humans), zoophilic (living on animals), and geophilic (living in the environment) [Gräser *et al.* 1999, de Hoog *et al.* 2017, Baert *et al.* 2020]. As mycological naming systems have continued to evolve, molecular characterization has been implemented in conjunction with other approaches to better define dermatophyte species.

1.1.1 Molecular characterization of dermatophytes

Molecular approaches have been applied to dermatophytes to assist in classification and epidemiological studies. Dermatophyte genomes range from 2.25Mb to 24.1Mb, and the full genomes of several species, including *Microsporum canis* have been annotated [Martinez *et al.* 2012]. Dermatophyte genomes are haploid and contain relatively little repetitive DNA [White *et al.* 2014]. Conidia (spores) have a single nucleus and hyphae generally are multinucleated cells with genetically unique nuclei [Achterman *et al.* 2011]. The genomes of dermatophyte species are relatively conserved, with over 6,000 orthologs shared among anthropophiles, zoophiles, and geophiles [Martinez *et al.* 2012]. *M. canis* has 943 unique genes, the most heterogeneity characterized to date amongst dermatophytes [Martinez *et al.* 2012]. Using two gene regions (internal transcriber spacer region ITS and partial β-tubulin), Baert *et al.* recently proposed a new classification scheme for dermatophyte species using a phylogenetic approach [Baert *et al.* 2020]. This resulted in numerous species being reclassified, expanding the *Nannizzia*, *Paraphyton*, *Lophophyton* and *Trichophyton* genera while condensing the *Arthroderma* and *Microsporum* genera [Baert *et al.* 2020]. This included renaming the clinically important species *Nannizzia persicolor* (former name *Arthroderma persicolor*), *Nannizzia nana* (former name *Microsporum nanum*), *Trichophyton mentagrophytes* (former name *Arthroderma vanbreuseghemii*) and *Nannizzia gypsea* (former name *Microsporum gypseum*) [Baert *et al.* 2020]. This reclassification also shifted the percentage of species in a genus that are anthropophiles, zoophiles and geophiles [Baert *et al.* 2020], making it more critical to identify down to the species level, instead of genus in clinical infections.

In addition to genus' and species' classification, epidemiological studies have been conducted to characterize dermatophyte genetic variations, evaluating DNA sequences of mitochondria [Wu *et al.* 2009], non-transcribed spacer regions (rDNA) [Jackson *et al.* 1999], random amplified polymorphic DNA [Mochizuki *et al.* 1997, Kim *et al.* 2001], microsatellites [Sharma *et al.* 2007, da Costa *et al.* 2013, Pasquetti *et al.* 2013], and RNA sequencing [Martins *et al.* 2020]. Microsatellite DNA polymorphisms have been identified in dermatophytes [Sharma *et al.* 2007, Pasquetti *et al.* 2013], providing a technique to rapidly characterize strain variation at low cost, and offering a useful method for genotypic comparisons among large sample sets. Several studies have implemented this approach for *M. canis* sample sets from various regions in the world, demonstrating intraspecies genetic differences [Sharma *et al.* 2007, da Costa *et al.* 2013, Pasquetti *et al.* 2013, Watanabe *et al.* 2017, Aneke *et al.* 2021, Moskaluk *et al.* 2022, Yamada *et al.* 2022]. Genetic understanding of dermatophytes has greatly increased in recent years, allowing for a better comprehension of basic dermatophyte processes including how infections begin.

1.1.2 Initiation of dermatophyte infections

Dermatophytes are free-living in the environment, but under certain conditions can cause infections in humans and animals. These fungi are septate, hyaline, filamentous molds that can produce spores (conidia) and are mainly composed of mycelium [Samanta 2015]. Mycelium structures are formed from the amalgamation fungal tubular structures known as hyphae [Samanta 2015]. Mycelium performs the physiologic functions of nutrient absorption, spore creation, and environmental sensing of light, temperature, and nutrients [Brand *et al.* 2009, Köhler *et al.* 2014, Samanta 2015, Roberson 2020]. Different types of conidia are formed

depending on the dermatophyte species and environmental conditions [Samanta 2015]. For example, asexual spores can form as macroconidia (large, multi-septate conidia), microconidia (small, unicellular conidia), and arthroconidia (infectious fragments of hyphae) [Samanta 2015]. The initiation of a dermatophyte infection begins when infectious portions of dermatophytes called arthroconidia adhere to keratinized tissues [Zurita *et al.* 1987, Vermout *et al.* 2008, Baldo *et al.* 2012] (Figure 1.1). Arthroconidia first adhere to the epidermis within two to six hours after contact and begin to germinate in the stratum corneum [Zurita *et al.* 1987, Vermout *et al.* 2008, Baldo *et al.* 2012] (Figure 1.1). As arthroconidia begin to germinate, these spores develop germ tubes that can penetrate the first layer of the epidermis, the stratum corneum [Baldo *et al.* 2012] (Figure 1.1). The pH at the site of infection becomes more basic as the dermatophyte degrades keratin, aiding in the activity of downstream fungal proteases [Kasperova *et al.* 2013]. Fungal hyphae continue to grow and invade keratinized tissues, and begin producing arthroconidia within seven days of infection, allowing the fungus to spread to other anatomical locations of the original host, to other hosts, or to contaminate the environment [Aljabre *et al.* 1992] (Figure 1.1).

Arthroconidia cannot invade healthy tissue because the host's immune system prevents the fungi from infecting healthy epidermis [Weitzman *et al.* 1995, Duek *et al.* 2004, Havlickova *et al.* 2008, Ziółkowska *et al.* 2015, Gnat *et al.* 2019]. Therefore, predisposing factors are typically present for an infection to occur. Common predisposing factors for infection are young age, immunosuppression, nutritional deficiency, skin trauma, and high environmental temperature and/or humidity [Weitzman *et al.* 1995, Havlickova *et al.* 2008, Ziółkowska *et al.* 2015, Moriello *et al.* 2017, Gnat *et al.* 2019]. One study demonstrated that cats experimentally exposed to dermatophyte spores remained uninfected unless a predisposing factor was induced; factors in this study were occlusive bandage and restricted grooming [DeBoer *et al.* 1994]. The

unique metabolic pathways of dermatophytes that facilitate keratin invasion and digestion are potential sites for novel therapeutic development and intervention.

1.1.3 Dermatophyte viability

While infections can result from direct transmission from an infected animal, dermatophytosis can also result following contact with viable environmental conidia. Environmental contamination with arthroconidia is very common in places where infected individuals reside such as animal shelters or animal raising establishments [Courtellemont *et al.* 2017, Seyedmousavi *et al.* 2018, Yamada *et al.* 2019]. High exposure locations such as swimming pools, nails salons, wrestling mats can also lead to dermatophytosis from environmental contamination [Hedayati *et al.* 2007, Segal *et al.* 2015, Nowicka *et al.* 2016]. While the length of infectivity of arthroconidia in the environment for inducing dermatophytosis in a host is uncertain, under laboratory conditions, arthroconidia have remained viable for up to 4.5 years, depending on the dermatophyte species [McPherson 1957, Rosenthal *et al.* 1962, Guirges 1981, Sparkes *et al.* 1994]. Long-term viability is critical for laboratory analysis of isolates, particularly of rare dermatophyte species [Baker *et al.* 2006, García-Martínez *et al.* 2018]. Long-term preservation methods for dermatophytes include lyophilization and cryopreservation using liquid nitrogen vapor, storage at low temperatures (-20°C to -70°C), and commercial cryopreservation kits [Meyer 1955, Hwang *et al.* 1976, Schipper *et al.* 1976, Stalpers *et al.* 1987, Pasarell *et al.* 1992, Baker *et al.* 2006], with commercial kits used most successfully (Microbank; Pro-Labs Diagnostics, Richmond Hill, Ontario, Canada). These protocols harvest mycelium and conidia that are subsequently stored at -80°C on porous beads suspended in a cryopreservative fluid, allowing recovery over a two-year period for a variety of dermatophyte

species [Baker *et al.* 2006]. Understanding viability of arthroconidia in clinical and laboratory settings can help improve decontamination protocols, reduce potential outbreaks, and assist in maintaining bioarchives for future studies.

1.2 Dermatophyte classification

Dermatophytes are broadly classified into three groups depending on their environmental habitat, and include anthropophiles (living on humans), zoophiles (living on animals), and geophiles (living in the soil) [Gräser *et al.* 1999, de Hoog *et al.* 2017, Baert *et al.* 2020]. The distinction between these groups can be blurred as species can become adapted to certain hosts, switching its preferred habitat [Rippon 1988, Makimura *et al.* 1998, Gräser *et al.* 1999, Summerbell *et al.* 2000, Moriello *et al.* 2017]. Group classification is important as clinical presentation can be influenced by the type of dermatophyte causing the infection [White *et al.* 2014, de Hoog *et al.* 2017]. Over 40 species from all three classifications have the potential to cause infections in humans [Gräser *et al.* 1999, White *et al.* 2014]. The following subsections examine habitat classification groups and the type of infections caused by the most clinically relevant species.

1.2.1 Anthropophilic dermatophytes

Dermatophytes that preferentially infect humans are classified as anthropophilic dermatophytes which theoretically evolved from geophilic dermatophytes [Rippon 1988, Makimura *et al.* 1998, Gräser *et al.* 1999]. Animals can sometime be infected with anthropophilic dermatophytes following anthropo-zoonotic transmission [Ranganathan *et al.* 1997, Brilhante *et al.* 2006]. Approximately 10 dermatophyte species belong to this group with

the main genera including *Trichophyton* and *Epidermophyton* [de Hoog *et al.* 2017]. The majority of infections are caused by *Trichophyton rubrum*, *Trichophyton interdigitale*, and *Epidermophyton floccosum*, with *T. rubrum* being the most widely spread dermatophyte that infects humans [Kidd *et al.* 2016, Burstein *et al.* 2020]. These species are well-adapted to the human physiology and immune system, resulting in a dampened immune response and mild clinical signs [White *et al.* 2014]. Occasionally, non-inflammatory, chronic infections with more significant clinical features can last months to years [de Hoog *et al.* 2017]. Only one mating type has been documented per species, suggesting that they rely exclusively on asexual reproduction [White *et al.* 2008, de Hoog *et al.* 2017, Kosanke *et al.* 2018]. It has been theorized that since these species have adapted to humans, they face less selective pressure, resulting in loss of one mating type [Kaszubiak *et al.* 2004].

As anthropophiles have become adapted to humans, species have developed preferences for specific locations on the body. For example, infection of the feet is called tinea pedis ("athlete's foot") [Hay 2000, White *et al.* 2014]. Other forms of localized dermatophytosis include tinea capitis (infection of the scalp), tinea unguium (infection of nails), tinea barbae (infection of the beard), tinea faciei (infection of the face), tinea corporis (infection of the body), tinea manuum (infection of the hands), and tinea cruris (infection of the groin region) [Weitzman *et al.* 1995] (Figure 1.2). *T. rubrum* is the most prevalent dermatophyte infecting humans worldwide and is responsible for the majority of tinea pedis cases [Seebacher *et al.* 2008, Achterman *et al.* 2011, White *et al.* 2014]. *T. interdigitale* also causes tinea pedis and is a clonal offshoot of *T. mentagrophytes* [Kidd *et al.* 2016, de Hoog *et al.* 2017]. *T. tonsurans* is one of the primary agents responsible for tinea capitis infections around the world [Gupta *et al.* 2000, White *et al.* 2014] (Figure 1.2, Table 1.1). A rare form of tinea capitis called tinea capitis favosa is

caused by *Trichophyton schoenleinii* and usually occurs in children and adolescences [Li *et al.* 2013, Kidd *et al.* 2016, Daadaa *et al.* 2022]. Distribution of these infections varies according to geographic and socioeconomic factors, with tinea pedis occurring more frequently in developed countries and tinea capitis in developing countries [Martinez *et al.* 2012]. Age also plays a role in which type of dermatophytosis is present, as older patients tend to have tinea unguium, whereas children more frequently acquire tinea capitis [Lipner *et al.* 2019]. Tinea unguium can also be referred to as onychomycosis which encompasses all fungal infections of the nail [Bodman *et al.* 2022]. Most of these infections are due to *T. rubrum* and zoophile *Trichophyton mentagrophytes* [Weitzman *et al.* 1995]. Tinea barbae infections are mostly caused by zoophilic dermatophytes, *T. mentagrophytes* and *T. verrucosum*, and anthropophilic *T. rubrum* [Rippon 1988, Rutecki *et al.* 2000, Bonifaz *et al.* 2003]. The dermatophytes responsible for tinea corporis infections can depend on the route of transmission [Leung *et al.* 2020]. Human-to-human transmission infections are generally due to *T. rubrum* and *T. tonsurans*, whereas contact with animals can lead to infection from *M. canis* [Leung *et al.* 2020]. Tinea faciei is considered a special form of tinea corporis and is usually caused by *T. rubrum*, *T. mentagrophytes*, *T. tonsurans*, or *M. canis* [Alteras *et al.* 1988, Belhadjali *et al.* 2009, Atzori *et al.* 2012] (Table 1.1). *T. rubrum* and *E. floccosum* are responsible for the majority of tinea cruris ("jock itch") infections [Weitzman *et al.* 1995]. Tinea manuum infections are caused mostly by *T. rubrum* or *M. canis* and is usually associated with tinea pedis infections [Weitzman *et al.* 1995, Veraldi *et al.* 2019, Chamorro *et al.* 2021] (Figure 1.2, Table 1.1). While the majority of dermatophytosis cases in humans are due to anthropophiles, zoophiles can also cause infections in humans and zoonotic dermatophyte infections can also occur (further discussed below).

Recently, a new anthropophile species (*Trichophyton indotineae*) has become widespread, causing recurrent infections where some isolates are resistant to terbinafine treatment [Verma *et al.* 2021, Uhrlaß *et al.* 2022]. This fungus can cause various forms of dermatophytosis including tinea pedis, tinea unguium, tinea cruris, tinea corporis and tinea faciei [Verma 2018, Uhrlaß *et al.* 2022]. Current treatment involves other anti-fungal medications such as itraconazole, however strains from Germany have been shown to have reduced sensitivity to this drug [Brasch *et al.* 2021, Uhrlaß *et al.* 2022]. As this species continues to spread to more countries, it is important for healthcare workers to be aware of this dermatophyte and its potential resistance to therapies.

1.2.2 Zoophilic dermatophytes

Zoophilic dermatophyte species have evolved to live on non-human animals [Moriello *et al.* 2017]. The main species that cause infections in animals are *Microsporum canis*, *Nannizzia persicolor*, *Nannizzia nana*, *Trichophyton equinum*, *Trichophyton mentagrophytes*, and *Trichophyton verrucosum* [Moriello *et al.* 2017]. In humans, the infections are mostly caused by *M. canis*, *T. mentagrophytes*, and *T. verrucosum* [Pier *et al.* 1994]. When these infections occur in humans, there is usually significantly more inflammation and there is a shorter course of infection course than those noted for anthropophilic dermatophytosis infections [de Hoog *et al.* 2017]. It is thought that the more robust inflammatory response may be attributed to lack of host-pathogen adaptation. As a corollary to this relationship, these fungi can also undergo sexual reproduction [Hube *et al.* 2015, Kosanke *et al.* 2018] as two mating types exist in nature and can reproduce when two isolates of opposite types encounter each other [White *et al.* 2008, de Hoog *et al.* 2017, Kosanke *et al.* 2018]. However, for many of these species, it has been shown that the

proportion of the two mating types has become unequal, leading to increasingly more reliance on asexual reproduction [Kosanke *et al.* 2018]. Zoophiles that infect soil-dwelling animals are more likely to have both mating type isolates and undergo sexual reproduction than zoophiles from non-soil-associated animals [Summerbell *et al.* 2000]. As these fungal species become more adapted to a particular host species, infections tend to become more reliant on asexual reproduction as noted in human infections. Dermatophytosis occurs more often in mammals than in reptiles and birds [Rees 1967, Rees 1968, Cabañes 2000].

Dermatophytosis, or ringworm, in animals is generally not further classified based on infection location as is standard for human infections. Clinical signs typically include circular alopecic lesions with erythematous margins and pruritus is not commonly observed [Chermette *et al.* 2008]. Animals can be asymptomatic carriers of dermatophytes, resulting in occult transmission to other animals or humans in close contact [Chermette *et al.* 2008].

Cats are the primary host for *M. canis* and will be explored further in later sections. Other zoophiles infect livestock such as pigs and ruminants, putting farmers and livestock handlers at higher risk for zoonotic infection [Courtellemont *et al.* 2017, Segal *et al.* 2021]. The most frequently isolated dermatophyte species on ruminants is *Trichophyton verrucosum* [Moretti *et al.* 1998] (Table 1.1). An increase in dermatophytosis prevalence in cattle is associated with intensively bred beef cattle farms as these animals are living in higher density populations [Moretti *et al.* 1998, Chermette *et al.* 2008]. Pigs are another livestock species that frequently experience dermatophytosis, usually caused by *Nannizzia nana* [Weitzman *et al.* 1995] (Table 1.1). Dogs and goats can be infected by *N. nana* [Begum *et al.* 2020]. *Trichophyton equinum* is the primary dermatophyte that infects horses and rarely causes dermatophytosis in humans [Veraldi *et al.* 2018]. *Trichophyton mentagrophytes* is most commonly isolated from rodents and

can be found worldwide [Pier *et al.* 1994, Kidd *et al.* 2016] (Table 1.1). *Nannizzia persicolor* (former name *Trichophyton persicolor*) was first isolated from voles and bats and occasionally causes infections in humans [English 1966, Krzyściak *et al.* 2015] (Table 1.1). Zoophiles can be propagate in the soil, blurring the distinction between zoophiles and geophiles [Summerbell *et al.* 2000].

1.2.3 Geophilic dermatophytes

Geophilic dermatophytes mainly reside in soil and keratinous debris shed from animals and rarely cause infections in humans and animals [de Hoog *et al.* 2017, Moriello *et al.* 2017]. These fungi are ecologically important as they are responsible for degrading keratin and returning the nutrients to the soil [Dolenc-Voljč *et al.* 2017]. Infections caused by geophiles are generally not transmitted between hosts and are acquired from the environment [Weitzman *et al.* 1995, Dolenc-Voljč *et al.* 2017]. When a geophile continues to maintain a population on particular hosts and causes more frequent infections, it would be reclassified as a zoophile [Summerbell *et al.* 2000]. The most common species to cause infection in humans and animals is *Nannizzia gypsea* (former name *Microsporum gypseum*) [Moriello *et al.* 2017, Segal *et al.* 2021]. Having frequent outdoor contact with soil, particularly without protection is a risk factor for geophilic dermatophytosis [Chermette *et al.* 2008]. Certain professions such as farmers also have a higher risk for acquiring this infection [Dolenc-Voljč *et al.* 2017].

While infections are rare, clinical presentation of dermatophytosis caused by geophiles differs from anthropophilic and zoophilic dermatophytosis. The inflammatory response is usually more severe in these cases, and the duration of infection is generally shorter, reinforcing that host-fungus adaptation ultimately results in a diminished immune response and protracted period

of replication [White *et al.* 2014]. As geophiles have not adapted to a host species, they have not been under host-specific selective pressures as much as anthropophiles [Wu *et al.* 2009]. Clinical signs can be similar to other dermatological diseases/disorders, resulting in difficulty in diagnosis unless culture or sequence analysis is performed [Dolenc-Voljč *et al.* 2017]. *N. gypsea* can cause tinea corporis and infrequently tinea capitis in people [García-Agudo *et al.* 2018] (Table 1.1). Geophilic species have maintained two mating types and are more likely to undergo sexual reproduction than host-adapted species [White *et al.* 2008, de Hoog *et al.* 2017, Kosanke *et al.* 2018]. It is theorized that the humid environment of soil provides a favorable condition for fruiting bodies to form, which occur during sexual reproduction. Such structures have not been isolated directly from an infected animal [Summerbell *et al.* 2000]. While habitat and other features such as reproduction differ among dermatophyte species of different classification, the same clinical diagnostic approaches can be utilized for all dermatophytes.

1.3 Diagnostic approaches to dermatophytosis

Accurate diagnosis is critical for dermatophytosis to allow for early treatment and to reduce transmission to other humans or animals. When diagnosing dermatophytosis in animals, fomite carriage must be considered especially for cases without clinical signs as these cases can be positive for dermatophytosis [Moriello *et al.* 2017]. Given the clinical presentation similarities between dermatophytosis and other skin diseases, accurate diagnosis is also important before starting treatment [Outerbridge 2006]. Prior treatment can interfere with many diagnostic assays, leading to inaccurate results [Moriello *et al.* 2017]. Collecting appropriate clinical samples greatly increases diagnostic accuracy. Samples should be performed near the edge of well-defined skin lesions, as the center of the lesions may contain lowly viable to non-viable material

[Weitzman *et al.* 1995]. Skin infections with poorly defined lesions should be sampled via skin scrape, covering a representative area of infection [Weitzman *et al.* 1995]. Hair samples can be collected either by plucking or using the "Mackenzie" brush technique [Mackenzie 1963]; this technique is commonly used for animals as thorough sampling of a large area can be performed [Moriello *et al.* 2017]. For this technique, the patient is brushed for 2-3 minutes or until the bristles contain a sufficient amount of hair [Moriello *et al.* 2017]. Whole nail clippings or nail scrapings can be collected depending on the location and severity of the infection [Weitzman *et al.* 1995]. The type of clinical sample collected from the patient will influence which diagnostic approaches can be utilized as sensitivity and specificity of assays can depend on clinical sample type.

1.3.1 Direct examination

Dermoscopy involves using a hand-held magnification tool for examining cutaneous lesions including lesions involving hair and nails [Lim *et al.* 2022]. Direct examination of the patient using dermoscopy is common in clinical practice, especially in human medicine [Lim *et al.* 2022]. As it is non-invasive, dermoscopy can be utilized for both diagnosis and for monitoring infections during treatment [Lallas *et al.* 2012, Bhat *et al.* 2019, Lim *et al.* 2022]. Modern advancements for dermoscopy including using polarized light sources and attaching the scope to a mobile device to enhance observation of dermatological features [Piliouras *et al.* 2014]. Dermoscopy is mainly used in veterinary patients for examining hair follicles and skin [Scarampella *et al.* 2015, Zanna *et al.* 2015]. A disadvantage for veterinary dermoscopy is compliance, as the patient needs to remain still long enough for images to be digitally captured

[Dong *et al.* 2016] (Table 1.2). Consequently, the accuracy of this technique relies heavily on the skills and expertise of the examiner [Dong *et al.* 2016] (Table 1.2).

1.3.2 Wood's lamp

Application of a Wood's lamp to examine for fluorescence is a commonly utilized diagnostic tool for dermatophytosis, particularly in screening animals in shelter situations [Scarampella *et al.* 2015]. This tool uses UV light (wavelength ranges between 320 and 400 nm) to detect fluorescence on skin and hair characteristic of active dermatophyte infection [Asawanonda *et al.* 1999, Klatte *et al.* 2015]. Dermatophytes that have been reported to fluoresce under the Wood's lamp UV light are *M. canis*, *M. audouinii*, *M. ferrugineum*, *M. disortum* phenotype, *N. gypsea*, and *Trichophyton schoenleinii* [Asawanonda *et al.* 1999]. The percent of *M. canis* isolates that exhibit fluorescence has been reported to range from 30 to 100% of cases [Kaplan *et al.* 1958, Kaplan *et al.* 1959, Keep 1959, Collins *et al.* 1960, Kaplan *et al.* 1960, Cafarchia *et al.* 2004]. As not all species of dermatophytes can fluoresce, a negative Wood's lamp examination cannot rule out dermatophytosis as a diagnosis [Klatte *et al.* 2015] (Table 1.2). Fluorescence can be identified even after initiation of topical therapies including lime sulfur dips and topical shampoos [DeBoer *et al.* 1995, Sparkes *et al.* 2000, Guillot *et al.* 2002, Newbury *et al.* 2007, Mancianti *et al.* 2009]. Other infections and dermatological disorders such as bacterial infections, yeast infections, and pigmentary disorders can also fluoresce under Wood's lamp, which can lead to false positives for dermatophytosis [Klatte *et al.* 2015] (Table 1.2).

1.3.3 Microscopy and histopathology

Clinical samples can be prepared and stained with various stains to enhance different fungal elements. Potassium hydroxide (KOH) can be applied to hair or skin scrapes to detect the presence of fungal elements [Aslanzadeh *et al.* 1991, Jang *et al.* 2006]. While this technique is very sensitive in determining if fungi are present, it cannot discriminate between living and dead cells, and cannot determine specific species [Gupta *et al.* 2008] (Table 1.2). Other disadvantages of this diagnostic technique are that it requires mycological equipment and trained personnel [Bhat *et al.* 2019] (Table 1.2). Lactophenol cotton blue is another stain that targets chitin in fungal cell walls, enhancing the visualization of fungal structures [Leck 1999]. This stain kills the fungi, reducing potential contamination of handling the sample [Leck 1999]. Mineral oil is another mounting medium for clinical samples with the advantage of not interfering with fluorescent metabolites [Moriello 2001, Moriello 2014, Moriello *et al.* 2017]. Compared to other diagnostic methods, microscopy is relatively quick as the sample can be evaluated immediately (under one hour) after collection [Moriello 2001] and has a reported false negative rate between 5 to 15% in clinical settings [Weitzman *et al.* 1995] (Table 1.2).

Examination of hair samples can determine if the dermatophyte species is ectothrix or endothrix as most anthropophiles are endothrix while geophiles and zoophiles are usually ectothrix [Moriello 2001, Gupta *et al.* 2008]. Ectothrix means the hyphae and conidia do not invade the hair shaft and instead degrade the cuticle, while endothrix refers to fungi that invade the hair shaft [Hay 2017]. Hyphal structures can also be used to distinguish dermatophyte species. *T. mentagrophytes* has spiral hyphae, nodular bodies or racquet hyphae [Samanta 2015]. *M. audouinii* is identified by pectinate bodies, which are small hyphal projections that look like a comb [Samanta 2015]. Both *T. schoenleinii* and *T. violaceum* can produce favic chandeliers, which are irregular hyphal projections that look like a chandelier [Samanta 2015].

Histopathology is a commonly utilized technique for visualizing fungal cells in tissues. While this method is rarely used for dermatophytosis, it can be beneficial for deep dermatophyte infections as the dermatophytes have invaded the dermis or deeper tissues [Marconi *et al.* 2010]. Histologic features observed in active dermatophytosis includes parakeratosis, basket weave of the keratin layer, neutrophils in the base layers of the epidermis, neutrophilic crusts, spongiotic changes, eosinophils in the dermis, acanthosis or hyperkeratosis, epidermal pustules, and visualization of hyphae [Gross *et al.* 2008, Park *et al.* 2014, Wang *et al.* 2017] (Figure 1.3). Inflammation can also be visualized around hair follicles and can potentially observe mural and luminal folliculitis with occasional furunculosis [Gross *et al.* 2008]. For dermatophytic kerions, both marked, focal inflammation and follicular destruction can be observed [Gross *et al.* 2008]. Stains that can be applied to the tissues to visualize the fungi include Periodic acid Schiff (PAS), Gomori's modification of methenamine silver (GMS), and calcofluor white stain [Aslanzadeh *et al.* 1991, Park *et al.* 2014, Wang *et al.* 2017] (Figure 1.3). Given that these stains are generally not available in clinical settings and the technical skills required for histopathology, this method is infrequently used [Aslanzadeh *et al.* 1991].

1.3.4 Fungal culture

Isolating and identifying dermatophytes from a clinical sample grown in culture has been considered the "gold standard" for diagnosing dermatophytosis [Frymus *et al.* 2013, Moriello 2014, Begum *et al.* 2020]. Dermatophyte test medium (DTM) contains phenol red, a dye that changes color when the pH increases, indicating the presence of a dermatophyte [Weitzman *et al.* 1995]. A major disadvantage of this medium is that the gross colony and microscopic morphology of the dermatophyte are altered, making it harder to determine the fungal species

[Jang *et al.* 2006]. DTM is generally paired with Sabouraud dextrose agar (SDA) medium as the latter medium is less discriminatory and interferes less with colony morphology than DTM [Poluri *et al.* 2015] (Figure 1.4). These media usually contain cycloheximide to slow the growth of non-dermatophytic fungi [Weitzman *et al.* 1995]. When trying to differentiate between *Trichophyton* species, media such as SDA with 5% salt added, vitamin free agar, Bromocresol purple milk solid glucose agar, Lactritmel agar, Littman oxgall agar, and 1% peptone agar can be utilized because soil-associated *Trichophyton* species tend to be nutrient-independent [Kidd *et al.* 2016]. Rice grain slopes can be employed to distinguish *Microsporum* species because this medium induces sporulation for *M. canis* but not *M. audounii* [Kidd *et al.* 2016]. When grown in media, dermatophytes can produce three types of asexual conidia: macroconidia, microconidia, and arthroconidia [Summerbell *et al.* 2000]. Macroconidia have been considered to have various potential purposes from being energy sources to aiding in longevity in environments without a host [Summerbell *et al.* 2000]. These larger conidia tend to have features that deter arthropods from grazing on them, allowing for higher survival in the environment [Summerbell *et al.* 2000].

Culture is essential for tinea unguium as direct examination and microscopy can be impractical for these samples [Weitzman *et al.* 1995]. False negatives can occur due to overgrowth of non-dermatophytic fungi, insufficient clinical material, or improper inoculation of clinical material on culture (particularly for toothbrush samples) [Sparkes *et al.* 1993, Dong *et al.* 2016, Moriello *et al.* 2017] (Table 1.2). False positives can occur when samples are collected from patients in contaminated environments [Dong *et al.* 2016] (Table 1.2).

Cultures for dermatophytosis are grown at room temperature (25°C±5°C) with no enhanced growth observed at human body temperature (37°C) [Guillot *et al.* 2001]. In clinical practice and reference laboratories, cultures are generally grown in complete darkness [Elwart *et*

al. 2021]. However, one report did not detect a difference in dermatophyte growth when incubated with 24 hours or light or darkness, 12 hours of light with 12 hours of darkness or room lighting [Moriello *et al.* 2010]. Cultures should be observed frequently for up to four weeks as some species are very slow growing [Morris *et al.* 1996] (Table 1.2). Determining the species growing in culture requires diagnostic expertise as pleomorphism commonly occurs [Gräser *et al.* 2000, Brillowska-Dabrowska *et al.* 2013] (Table 1.2).

1.3.5 DNA-based assays

Polymerase chain reaction (PCR) has increased in use as a diagnostic assay for detecting dermatophytes. PCR is a more sensitive technique than culture as it can detect fungal DNA even if the culture is negative [Arabatzis *et al.* 2007, Jacobson *et al.* 2017] (Table 1.2). However, similar to microscopy, it cannot distinguish between living and dead fungal cells [Moriello *et al.* 2017]. False negatives can occur due to improper sampling technique, while false positives can occur due to nonviable fungus present on the host [Moriello *et al.* 2017] (Table 1.2). A major factor that can influence the accuracy of PCR is the DNA extraction method employed; the use of these techniques for fungal detection (versus bacteria or viruses) requires special extraction protocols that can digest the fungal cell [Wickes *et al.* 2018]. These extra steps can involve freeze/thaw cycles, heat, or mechanical or chemical disruptions (such as beads or additional lysis buffers) [Brillowska-Dąbrowska 2006, Bergman *et al.* 2013].

Qualitative (conventional) PCRs for dermatophyte detection and identification generally target the internal transcriber spacer (ITS) region as this region can identify many isolates down to the species level [Turin *et al.* 2000]. Primers have been developed to target conserved regions of the ITS that specifically belong to dermatophytes, making it easier to identify dermatophyte

positive samples [Bergmans *et al.* 2010]. Quantitative PCRs (real-time PCR, RT-PCR) have also been developed for dermatophyte identification from clinical samples. Using the ITS primers specifically targeting dermatophytes, RT-PCRs have been able to distinguish between dermatophyte species detected in clinical samples (hair, skin, nail) [Bergmans *et al.* 2010].

1.3.6 Antibody-based assays

Enzyme-linked immunosorbent assay (ELISA) is a common antibody-antigen-based assay that can be used for detecting various diseases [Magnarelli *et al.* 1989, Ferreira *et al.* 2001, Lagousi *et al.* 2021, Moskaluk *et al.* 2021]. Direct, indirect, sandwich, and competitive/inhibition ELISA techniques offer different advantages and disadvantages [Aydin 2015]. ELISA makes use of a variety of detection systems, including colorimetric/chromogenic, chemiluminescence, and fluorescent. Colorimetric is most commonly used as a standard plate reader can be utilized [Soderstrom *et al.* 2011]. Sensitivity due to a low signal can be increased by optimizing reagents with higher affinity for the target, by switching the type of ELISA performed, increasing incubation times, or changing incubation temperatures [Sittampalam *et al.* 1996, Aydin 2015].

ELISAs have been developed to detect dermatophytes using serum samples from clinical cases and evaluation of antibody binding to purified *M. canis* antigen [Peano *et al.* 2005, Santana *et al.* 2018]. The *M. canis* specific IgG antibody from cats and dogs have been detected using ELISA and had similar sensitivity to fungal cultures [Peano *et al.* 2005, Santana *et al.* 2018] (Table 1.2). As antibodies can persist after an infection has cleared, false positives can occur with this assay [Peano *et al.* 2005, Santana *et al.* 2018] (Table 1.2). Additionally, this assay requires serum, making sample collection more invasive than other diagnostic approaches (Table 1.2).

1.3.7 Mass spectrometry

Matrix assisted laser desorption ionization time of flight mass spectrometry (MALDI-ToF MS) is gaining popularity as a diagnostic method for detecting and identifying fungal species. Filamentous fungi can have varying phenotypes which can be detected by changes in the protein spectra [Patel 2019]. While this technique is relatively fast compared to culture, it is limited by the organism library available, making it difficult to identify novel species or rare species that are not included in the library [Patel 2019] (Table 1.2). Additional limitations include needing an adequate sample amount, unreliable results if a sample has multiple fungal species present, spreading occurring between loaded samples, cost of initial equipment, training personnel on specialized instruments, and improper cleaning between runs [Patel 2019].

Libraries have been curated for dermatophyte species with over 20 species included for analysis [Theel *et al.* 2011, de Respinis *et al.* 2013, Nenoff *et al.* 2013]. While this method is faster than other assays, it requires access to specialized equipment and requires that the libraries be constantly updated with name changes for the different dermatophyte species [Patel 2019] (Table 1.2). As many of the current diagnostic approaches for dermatophyte diagnosis have major drawbacks, there is a great need for novel assays that are affordable, provide rapid results, and are user-friendly.

1.4 Potential targets of diagnostic assays for dermatophytosis

Current diagnostic assays for detecting and diagnosing dermatophytosis have various disadvantages, particularly in clinical settings. One of the main challenges is distinguishing between dead and alive fungi, particularly after therapy has been implemented. A potential

approach for overcoming this obstacle is to target dermatophyte-specific metabolic products as the presence of these metabolites would indicate living, metabolically active fungi. Dermatophytes produce a variety of unique metabolic products ranging from simple chemicals to complex proteins, allowing for a wide range of potential targets to be utilized for diagnostic assays [Asawanonda *et al.* 1999, Martinez *et al.* 2012, Grumbt *et al.* 2013]. Compared to other orders of fungi, dermatophyte genomes encode for a greater number of secondary metabolites including proteases [Martinez *et al.* 2012, White *et al.* 2014]. Metabolic pathways unique to dermatophytes include those associated with keratin degradation and production of fluorescent metabolites [Asawanonda *et al.* 1999, Martinez *et al.* 2012, Grumbt *et al.* 2013]. These pathways and metabolites will be explored below as potential targets for dermatophyte detection assays.

1.4.1 Unique dermatophytic keratin metabolism, Sulfite efflux pump (SSU1)

Dermatophytes are unique in their ability to metabolize keratin because these proteins are, by necessity, very resistant to microbial degradation [Grumbt *et al.* 2013]. Dermatophytes secrete sulfite as well as keratinases in order to accomplish keratinolysis [Grumbt *et al.* 2013]. The *sulfite efflux pump* (SSU1) secretes sulfite to break the disulfide bonds in keratinized tissues, releasing cysteine and S-sulfocysteine (SSC), and furthering the digestion of keratin to supply fungal nutrients [Léchenne *et al.* 2007, Grumbt *et al.* 2013, Mercer *et al.* 2018]. Cysteine, a nonessential amino acid that constitutes approximately 20% of the amino acid residues in hair, is taken up by dermatophyte fungus and internally converted to sulfite through multiple reactions [Kasperova *et al.* 2013]. Once inside the fungal cell, cysteine is oxidized to cysteine sulfinic acid by cysteine dioxygenase (Cdo1) [Grumbt *et al.* 2013]. The conversion of cysteine sulfinic acid to

sulfite is theorized to occur by transamination and spontaneous decomposition, allowing for the degradation cycle to continue [Griffith 1983, Mercer *et al.* 2018].

The SSU1 gene of a dermatophyte (*T. mentagrophytes*) has been shown to be essential for keratin degradation and clinical infection, demonstrating the potential role of this gene as a virulence factor [Grumbt *et al.* 2013]. SSU1 thus makes an attractive target for assessment of active infection and virulence and as a factor underlying dermatophyte strain variation. Detecting metabolic products reliant on SSU1 (such as sulfite or SSC) would indicate the presence of metabolically active dermatophytes as other bacteria and yeast on the skin do not actively breakdown keratin as a nutrient source [Irwin *et al.* 2017]. A key factor for detecting these metabolites is determining how long they can remain present on the host after the fungi has been killed to ensure false positives do not occur. Further investigation into these metabolites would be warranted for designing diagnostic assays for dermatophytosis.

1.4.2 UV fluorescent metabolites

Certain dermatophyte species have been documented to fluoresce under UV light including *M. canis*, *M. audouinii, M. ferrugineum, N. gypsea,* and *Trichophyton schoenleinii* [Asawanonda *et al.* 1999]. Pteridine has been reported to be the fluorescent compound produced by *M. canis* and *N. gypsea* [Wolf 1957, Wolf *et al.* 1958]. Both pteridine and xanthurenic acid derivatives contribute to the fluorescence of *T. schoenleinii* [Chattaway *et al.* 1966]. These compounds produce a blue-green and yellow color when exposed to UV light, respectively [Klatte *et al.* 2015]. Other dermatological conditions produce different colors including coral-red (bacterial infections, skin cancer), bluish-white (vitiligo and other pigmentary disorders), and brown (melasma) [Klatte *et al.* 2015]. Detecting these fluorescent metabolites using mass

spectrometry or fluorometric approaches or developing an antibody assay against the metabolites could enhance the sensitivity and specificity of diagnosing dermatophytosis compared to Wood's lamp. Furthermore, exploring the metabolic pathways that produce these metabolites can help elucidate if all strains of the same dermatophyte species have the potential to create these compounds.

1.4.3 Dermatophyte-specific Proteases

Proteases are a classification of enzymes that can degrade proteins into amino acids or peptides [Monod 2008]. Dermatophytes express high amounts of proteases compared to other groups of fungi, particularly when exposed to keratin [Martinez *et al.* 2012, Tran *et al.* 2016]. Endo- and exoproteases are produced in order to degrade keratin and downstream degradation products [White *et al.* 2014]. The proteases involved in keratin hydrolysis include groups of endoproteases and exoproteases [Mercer *et al.* 2018]. While endoproteases break internal bonds of polypeptides, exoproteases can only target the polypeptide bonds at the N- or C-terminus [Monod 2008]. The major categories of endoproteases are fungalysins, subtilisins, and neutral proteases [Rawlings *et al.* 2016, Mercer *et al.* 2018]. Production of these proteases have been associated with increased disease severity [Viani *et al.* 2001]. The most important class of proteases for dermatophytes is the secreted subtilisin proteases as this family of enzymes is responsible for degrading keratin [Mercer *et al.* 2018]. These proteins have undergone extensive expansion within dermatophytes with most species having 12 subtilisin proteases [Martinez *et al.* 2012].

Subtilisin 3, (Sub3) is produced by *M. canis* and is essential for adherence to keratinized tissues during early phases of infection [Mignon *et al.* 1998, Baldo *et al.* 2008, Monod 2008,

Baldo *et al.* 2010, Băguţ *et al.* 2012]. Given that SUB3 expression is active during infection, detecting this protein is an indicator of metabolically active *M. canis* [Grumbt *et al.* 2013]. Sub3 produced by *M. canis* fungal cells has been detected by immunohistochemistry in domestic cat hair follicles in clinical biopsy specimens [Mignon *et al.* 1998], suggesting that antibodies can be created to specifically target this protein. Further exploration into these potential targets could help improve dermatophyte detection with possible speciation at diagnosis.

1.5 Introduction to *Microsporum canis*

All of the species within the *Microsporum* genus cause significant amount of disease in both humans and animals, making this genus clinically important [Gräser *et al.* 1999, Summerbell *et al.* 2000]. *Microsporum* includes three species: *Microsporum canis*, *Microsporum audouinii*, and *Microsporum ferrugineum*, each with genomes of approximately 23 Mbp [Kidd *et al.* 2016]. *M. canis* is a zoophilic dermatophyte that is soil-associated [Gräser *et al.* 1999, Summerbell *et al.* 2000]. It was first described from cats and represents the earliest dermatophyte that branched from other dermatophyte species [Hasegawa *et al.* 1975, Gräser *et al.* 2000, Martinez *et al.* 2012, de Hoog *et al.* 2017]. *M. audouinii* and *M. ferrugineum* are anthropophiles that evolved from *M. canis* [Gräser *et al.* 1999, Summerbell *et al.* 2000]. Within the *Microsporum* genus, *M. canis* causes the majority of human infections, which are usually spread from an infected domestic cat [Moriello *et al.* 2017]. *M. canis* used to only refer to the anamorphic form, while the teleomorph was called *Arthroderma otae* or *Nannizzia otae*; now *M. canis* refers to both forms [Hasegawa *et al.* 1975, de Hoog *et al.* 2017]. The following subsections will discuss clinically relevant topics of *M. canis* including diagnosis, prevalence, infection, and unique characteristics of *M. canis*.

1.5.1 Morphology and laboratory characteristics of M. canis

When grown in culture, colonies of *M. canis* are white to cream colored with the reverse pigment ranging from golden yellow to brownish yellow [Kidd *et al.* 2016]. The topography is usually flat and spreading with radial grooves and the texture is cottony to wooly [Gräser *et al.* 2000, Kidd *et al.* 2016]. *M. canis* is a septate, hyaline, filamentous mold that can produce different types of conidia including spindle-shaped macroconidia and microconidia [Samanta 2015, Kidd *et al.* 2016]. Macroconidia have thickened cell walls, making them less digestible by arthropods that graze on conidia [Summerbell *et al.* 2000]. *M. canis* can be grown on specialized media such as lactrimel agar or rice grains to induce sporulation [Kidd *et al.* 2016]. Unlike some *Trichophyton* species, *M. canis* does not require specialized nutrients for growth in culture [Summerbell *et al.* 2000].

Similar to other soil-associated dermatophytes, *M. canis* is positive for hair perforation test by day 14 and about 80% of isolates are urease positive [Gräser *et al.* 2000, Brilhante *et al.* 2005, Kidd *et al.* 2016]. When grown on hair, *M. canis* is ectothrix, meaning the hyphae and conidia do not invade the hair shaft and instead degrade the cuticle [Carter 1990]. The hair perforation test involves incubating the dermatophyte with hair and periodically observing the hair under a microscope to see if the hair shaft has been perforated [Ajello *et al.* 1957]. *M. canis* isolates generally fluoresce yellow green under UV light. [Asawanonda *et al.* 1999, Moriello *et al.* 2017].

1.5.2 M. canis habitat and transmission

Cats are the primary reservoir for *M. canis* with certain populations having up to 100% infection rates [Brilhante *et al.* 2003, Khosravi *et al.* 2003, Cafarchia *et al.* 2004, Wiegand *et al.* 2019]. Dogs are the second most common animal reservoir, with 40-90% of dermatophytosis cases in dogs being caused by *M. canis* [Jungerman *et al.* 1972, Cabañes 2000]. While cats and dogs frequently encounter this dermatophyte, *M. canis* is not considered a normal microbe of the host's skin [Moriello *et al.* 2017]. *M. canis* has rarely been isolated from horses, cattle, goats, sheep, rabbits and pigs [Stenwig 1985, Pier *et al.* 1994, González Cabo *et al.* 1995, Cabañes *et al.* 1997, Cabañes 2000]. Transmission generally occurs by direct contact with an infected animal or contact with fomites [Frymus *et al.* 2013, Subelj *et al.* 2014, Brosh-Nissimov *et al.* 2018]. Outbreaks frequently occur in high density populations including animal shelters and catteries [Newbury *et al.* 2007, Moriello 2014, Seyedmousavi *et al.* 2018]. Human-to-human *M. canis* infections have been described; however, transmission wanes after a few transmission events [Shah *et al.* 1988, Snider *et al.* 1993, Brosh-Nissimov *et al.* 2018]. Given the high transmissibility of *M. canis*, it has been able to spread worldwide [Seebacher *et al.* 2008, Kidd *et al.* 2016].

1.5.3 M. canis distribution

M. canis is distributed worldwide though prevalence varies among countries [Seebacher *et al.* 2008, Kidd *et al.* 2016]. *M. canis* has been found to be the leading cause of tinea capitis infection in Great Britain, Ireland, Western Europe, Spain, Greece, Kuwait, Hong Kong, Malaysia, Australia, New Zealand, USA, Canada, Venezuela, Brazil, Uruguay, Argentina, Chile, Algeria, Sudan, and South Africa [Marples 1959, Ridley *et al.* 1961, Carlier 1963, Londero 1964, Mackenzie 1964, Vanbreuseghem *et al.* 1970, Ross *et al.* 1971, Zaror 1974, Dion *et al.*

1975, Gaisin *et al.* 1977, Mahgoub 1977, Philpot 1978, al-Fouzan *et al.* 1993, Fernandes *et al.* 2001]. *M. canis* is also the primary agent for tinea corporis in Australia, New Zealand, Brazil, Uruguay, and South Africa [Marples 1959, Ridley *et al.* 1961, Londero 1964, Philpot 1978]. Over the past several decades, infections due to *M. canis* have decreased due to various factors such as stray animal management [Maraki *et al.* 2000, Yamada *et al.* 2019].

1.5.4 M. canis mating types

As noted above, dermatophytes can undergo sexual or asexual reproduction depending on access to a compatible mating partner [Kosanke *et al.* 2018, Metin *et al.* 2020]. The two mating types of dermatophytes are high-mobility group (HMG) and alpha-box genes, respectively. Mating type genes, also be referred to as MAT1-1 (for alpha-box) and MAT1-2 (for HMG) [Li *et al.* 2010, Kosanke *et al.* 2018, Metin *et al.* 2020]. There have been reports of two *M. canis* mating types; however, the positive type has only been isolated from Japan [Hasegawa *et al.* 1975, Weitzman *et al.* 1978, Marchisio *et al.* 1995]. It has been hypothesized that *M. canis* is becoming more reliant on asexual reproduction given the lack of MAT1-2 identification [Moskaluk *et al.* 2022].

1.5.5 M. canis associated clinical disease

After keratinized tissue is exposed to *M. canis* arthroconidia, lesions generally begin appearing one to three weeks later [DeBoer *et al.* 1994]. *M. canis* infections in humans have been shown to be more inflammatory than anthropophilic *M. audouinii* infections, suggesting that *M. canis* has not adapted to human hosts [Gräser *et al.* 2000]. Clinical signs can range from mild scaling and alopecia to severe inflammation with pustules and invasion of the dermis via

the hair follicles, developing into Majocchi's granuloma [Voisard *et al.* 1999, Ratajczak-Stefańska *et al.* 2010, da Costa *et al.* 2013]. *M. canis* generally causes dermatophytosis in humans as tinea corporis and tinea capitis [Weitzman *et al.* 1995]. Tinea unguium, or infection of the nails, due to *M. canis* is rare in humans [Kidd *et al.* 2016].

Cats with dermatophytosis generally present with mild circular alopecia and scaling [Frymus *et al.* 2013]. Pruritus and miliary dermatitis can be variable upon presentation [Moriello *et al.* 2017]. Dermatophytosis in cats is caused by *M. canis* in 90% to 100% of cases depending on geographic region [Sparkes *et al.* 1993, Marchisio *et al.* 1995, Cabañes 2000]. *M. canis* has been shown to elicit a weaker immune response in cats compared to other dermatophyte species, suggesting cats are the primary host [Moriello *et al.* 2003, Chermette *et al.* 2008]. *M. canis* infections in cats are less susceptible to treatment than other dermatophytes [Brillowska-Dabrowska *et al.* 2013]. Treatment is implemented to reduce spreading of the fungi and reduce the length of infection [Stuntebeck *et al.* 2017]. Clinical disease generally resolves between seven to 17 weeks post exposure to arthroconidia [Sparkes *et al.* 1995, Sparkes *et al.* 2000].

6.1 Conclusions

Numerous dermatophyte species that infect humans and animals have recently been renamed, potentially impacting diagnosis and treatment plans. A variety of diagnostic methods have been developed for dermatophytosis with fungal culture still being considered the "gold standard". Novel approaches for improving diagnostics include investigating assays based on fungal metabolites (sulfite metabolism, UV fluorescent metabolites, and proteases).

M. canis is a clinically important dermatophyte as it is a common pathogen in human and veterinary medicine, and represents the most common zoonotic dermatophyte. This agent causes

dermatophytosis in cats and tinea capitis and tinea corporis in humans and appears to be adapting to the feline host with the loss of one of its mating types (MAT1-2). Current diagnostic assays can identify *M. canis* and can distinguish it from other *Microsporum* species. Further investigations of the genetics and metabolism of *M. canis* (and other dermatophytes) are warranted to develop novel, rapid, and inexpensive diagnostic tests, and new therapies for dermatophytosis of animals and humans.

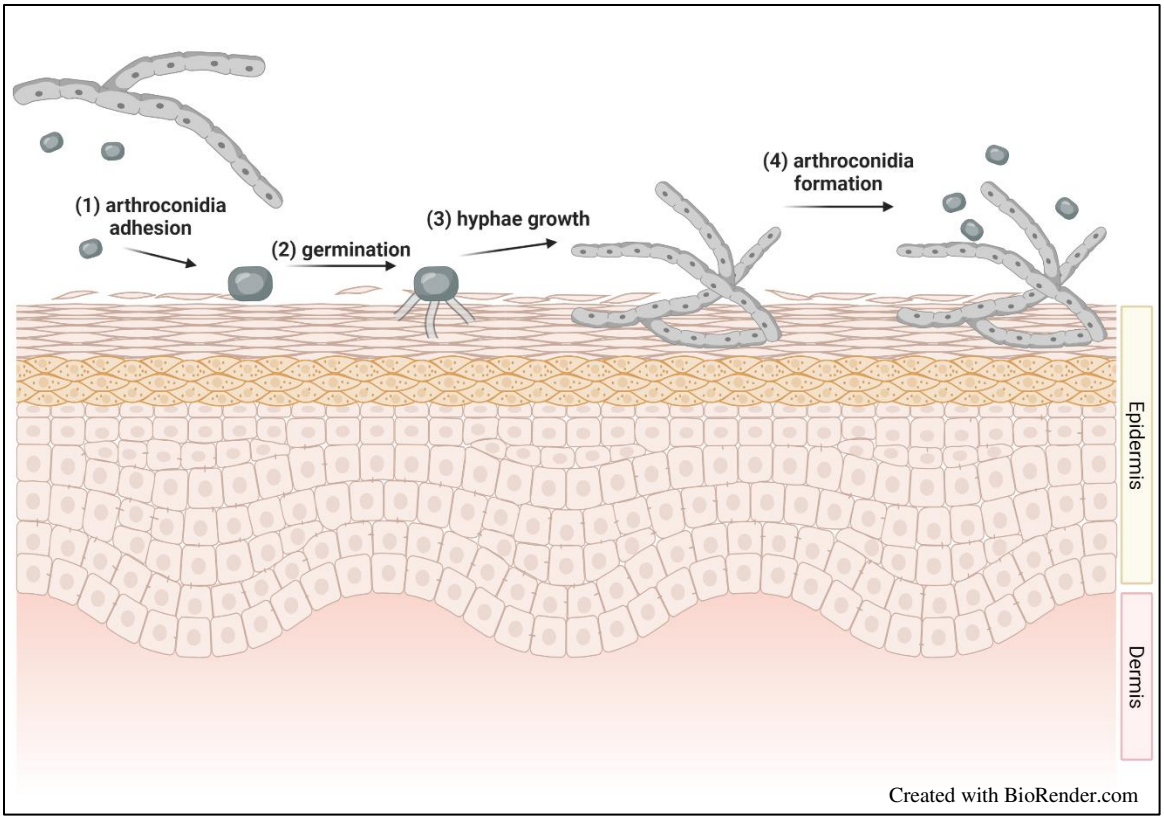

Figure 1.1. Initiation of dermatophyte infection in skin. (1) Arthroconidia from environment or other infected host comes in contact with new host's skin. Adhesion to skin occurs between 2-6 hours after contact. (2) Arthroconidia begins to germinate in the top layer of the epidermis, forming germ tubes. (3) Hyphae continue to grow within the epidermis. (4) Within 7 days of infection, arthroconidia are formed, allowing for the cycle to repeat.

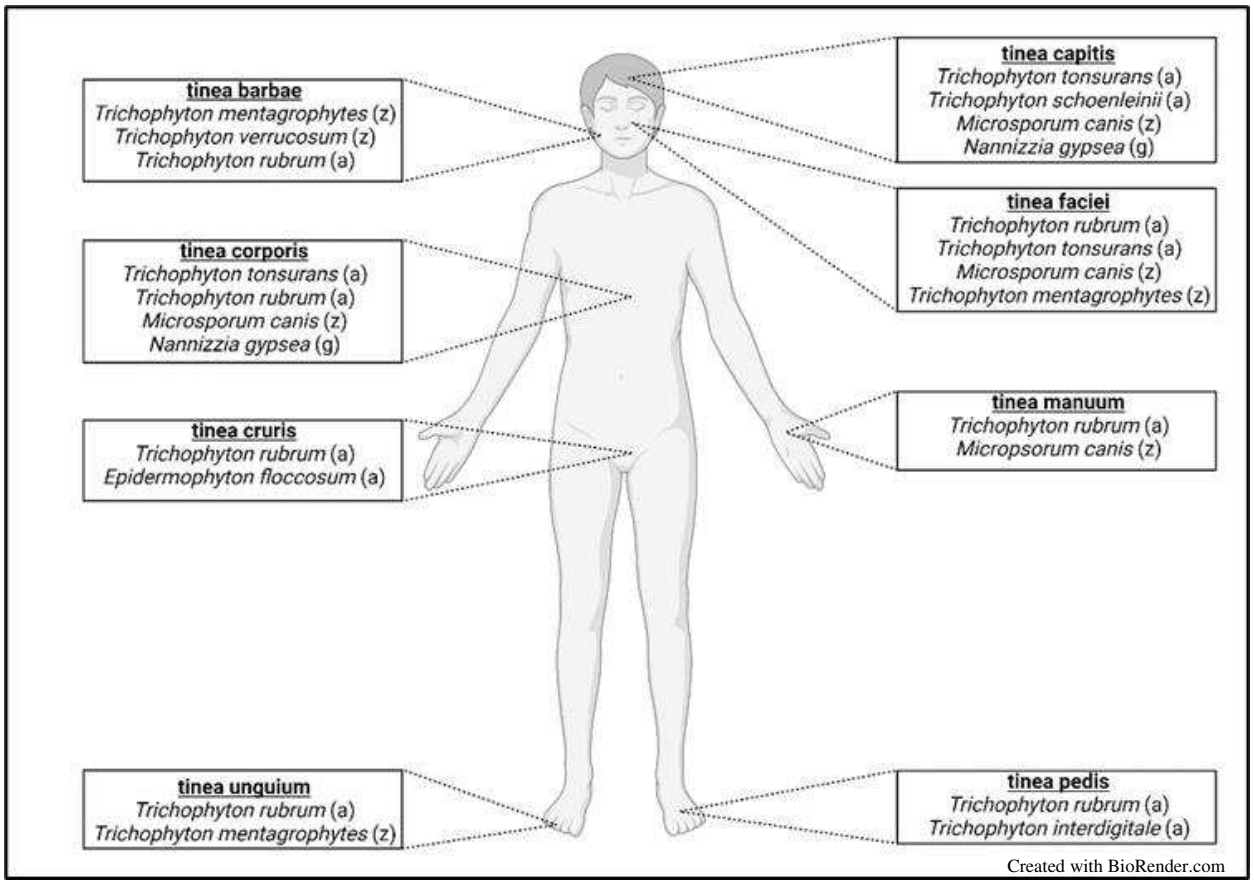

Figure 1.2. Classification of dermatophytosis in humans. Anatomic location of infection determines the type of dermatophytosis. For each classification, the most prevalent fungal species that cause infection are listed. (a) = anthropophile; (z) = zoophile; (g) = geophile.

Table 1.1. Classification of most common dermatophytes causing infections in humans and animals. Infection nomenclature is based on infection in primary host.

Classification	Species	Primary Host/Habitat	Main Type of Infection	Geographical Distribution	Reference
Anthropophilic	*Trichophyton rubrum*	Humans	tinea pedis, tinea unguium, tinea cruris, tinea faciei, tinea corporis, tinea manuum, tinea barbae	Worldwide	[Alteras *et al.* 1988, Weitzman *et al.* 1995, Seebacher *et al.* 2008, Belhadjali *et al.* 2009, Achterman *et al.* 2011, White *et al.* 2014, Kidd *et al.* 2016, Leung *et al.* 2020]
	Trichophyton tonsurans	Humans	tinea capitis, tinea corporis, tinea faciei	Worldwide	[Gupta *et al.* 2000, White *et al.* 2014, Kidd *et al.* 2016, Leung *et al.* 2020]
	Epidermophyton floccosum	Humans	tinea cruris	Worldwide	[Kidd *et al.* 2016]
	Trichophyton digitale	Humans	tinea pedis	Worldwide	[Kidd *et al.* 2016, Taghipour *et al.* 2019]
	Trichophyton schoenleinii	Humans	tinea capitis favosa	Asia, Europe, Africa	[Li *et al.* 2013, Kidd *et al.* 2016]
Zoophilic	*Microsporum canis*	Cats	Ringworm	Worldwide	[Pier *et al.* 1994, Kidd *et al.* 2016, Moriello *et al.* 2017]
	Nannizzia persicolor (former name *Arthroderma persicolor*)	Voles, bats	Ringworm	Africa, Australia, Europe, N. America	[English 1966, Krzyściak *et al.* 2015,

					Kidd *et al.* 2016]
	Nannizzia nana (former name *Microsporum nanum*)	Pigs	Ringworm	Worldwide	[Weitzman *et al.* 1995, Kidd *et al.* 2016, Begum *et al.* 2020]
	Trichophyton equinum	Horses	Ringworm	Worldwide	[Kidd *et al.* 2016, Veraldi *et al.* 2018]
	Trichophyton mentagrophytes (former name *Arthroderma vanbreuseghemii*)	Mice, guinea pigs	Ringworm	Worldwide	[Pier *et al.* 1994, Kidd *et al.* 2016]
	Trichophyton verrucosum	Cattle	Ringworm	Worldwide	[Moretti *et al.* 1998, Chermette *et al.* 2008, Kidd *et al.* 2016]
Geophilic	*Nannizzia gypsea* (former name *Microsporum gypseum*)	Soil	Ringworm (animals), tinea capitis/tinea corporis (humans)	Worldwide	[Kidd *et al.* 2016, Moriello *et al.* 2017, García-Agudo *et al.* 2018, Segal *et al.* 2021]

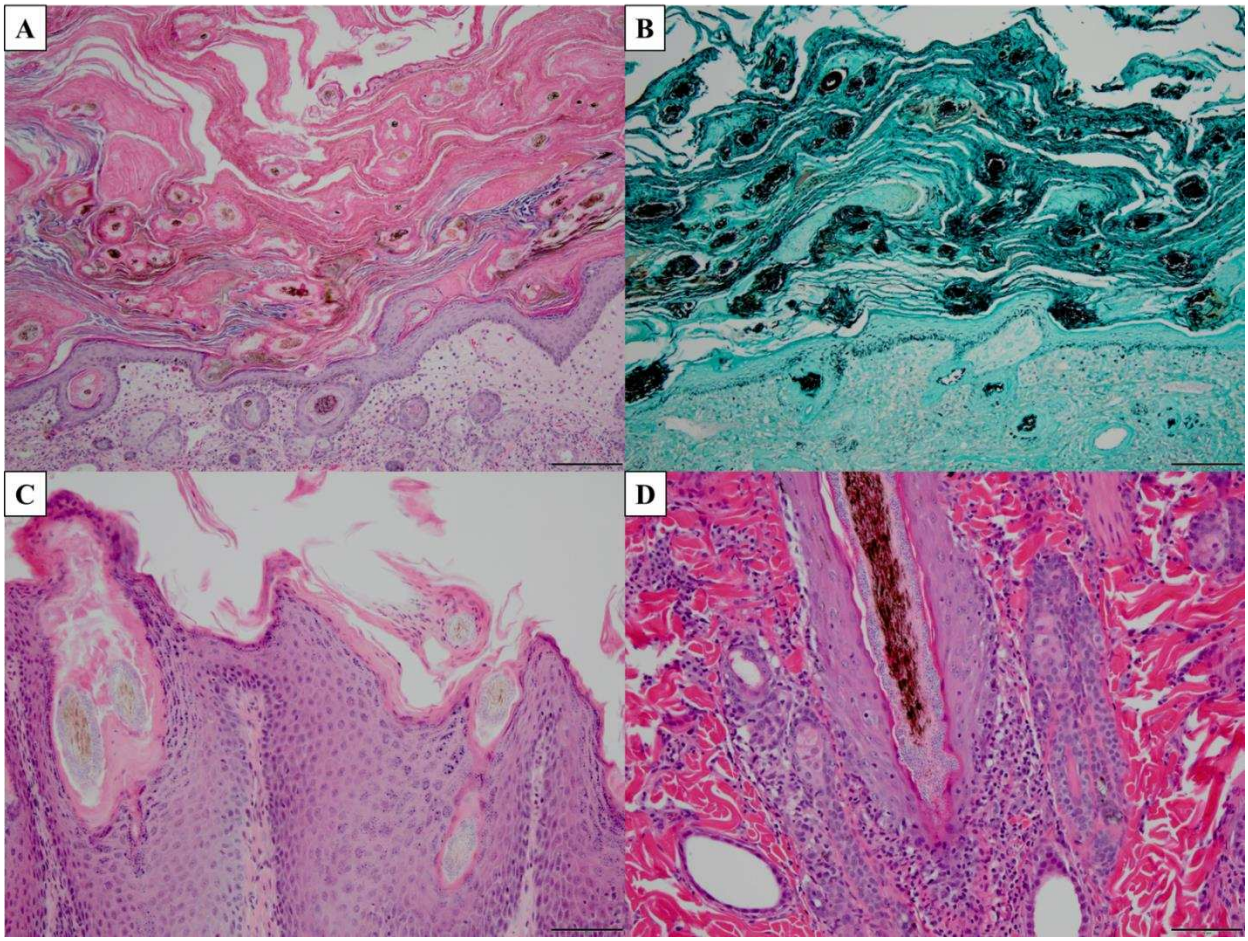

Figure 1.3. Histopathology of common histologic features of dermatophytosis. A, C, D – tissue stained with Periodic acid Schiff (PAS). B – tissue stained with Gomori's modification of methenamine silver (GMS). A – marked hyperkeratosis (both orthokeratotic and parakeratotic), 10X magnification, scale bar = 100 µm. B – visualization of fungal hyphae, 10X magnification, scale bar = 100 µm. C – Parakeratotic hyperkeratosis, acanthosis, numerous fungi associated with hair shaft, 20X magnification, scale bar = 50 µm. D – Neutrophils infiltrating basal layer of hair follicle with hyphae in hair follicle lumen, 20X magnification, scale bar = 50 µm.

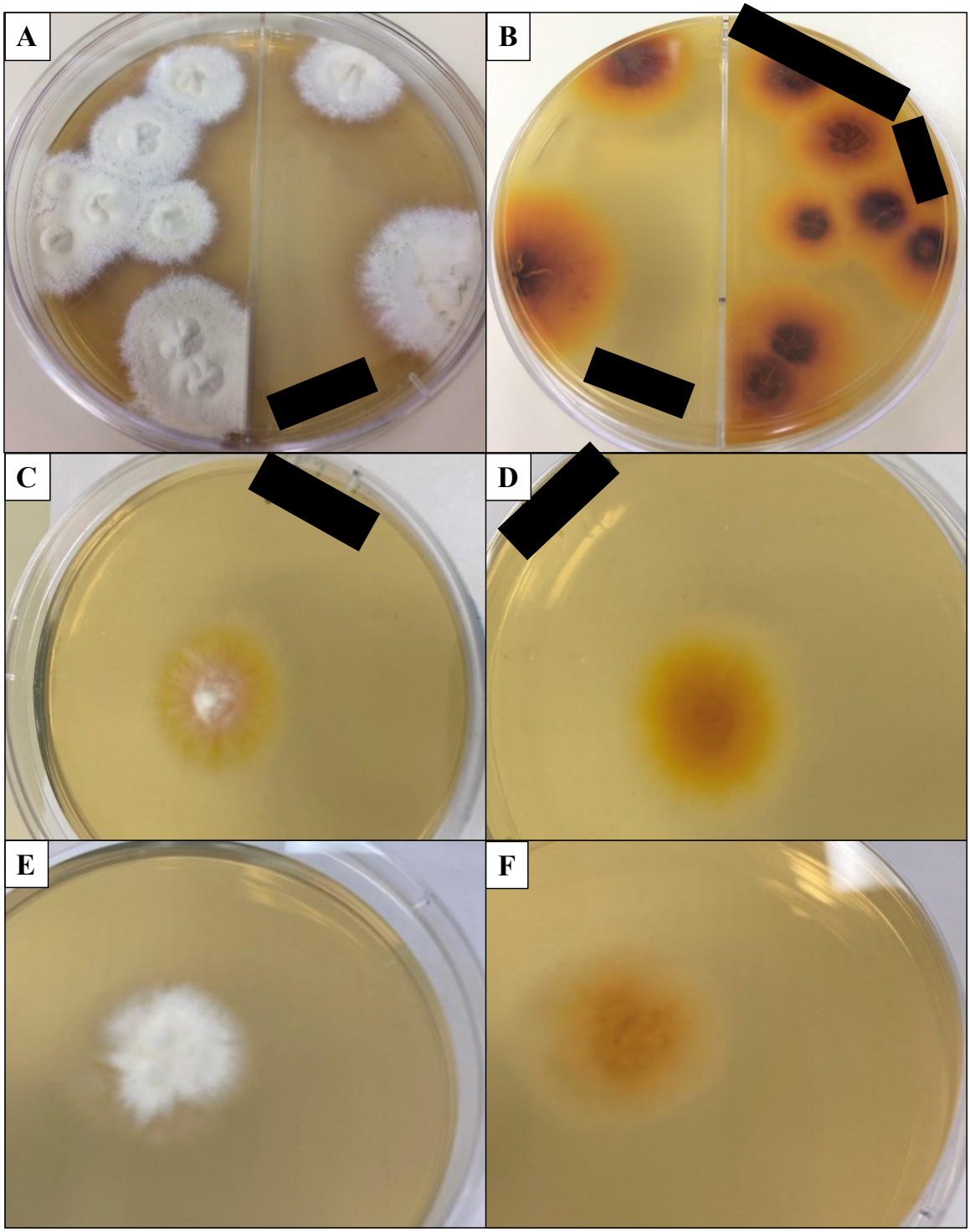

Figure 1.4. Common dermatophytes grown on Sabouraud dextrose agar (SDA) medium. A – colony surface and B – colony reverse of *T. mentagrophytes* grown for 19 days isolated from domestic cat. C – colony surface and D – colony reverse of *M. canis* grown for 7 days isolated from domestic cat. E – colony surface and F – colony reverse of CBS 118893 *N. gypsea* grown for 7 days. Black bars – deidentifying patient information. Cultures were incubated at 20-25°C in the dark. CBS – Westerdijk Fungal Biodiversity Institute.

Table 1.2. Comparison of diagnostic methods for detecting dermatophytes.

Diagnostic method	Advantages	Disadvantages	Time to Results	Reference
Direct examination	• Non-invasive • Low cost	• Unable to determine species	Minutes	[Scarampella *et al.* 2015, Zanna *et al.* 2015]
Wood's lamp	• Non-invasive • Low cost	• Not all species fluoresce	Minutes	[Asawanonda *et al.* 1999, Klatte *et al.* 2015]
Microscopy*	• Can detect unique features of species • Low cost	• Unable to distinguish dead and alive fungi	Minutes	[Moriello 2001, Samanta 2015]
Culture	• Low cost • Easy to perform • Can distinguish between species	• Requires expertise to determine species • Can be contaminated by saprophytes	Days – Weeks	[Frymus *et al.* 2013, Moriello 2014, Begum *et al.* 2020]
PCR*	• Highly sensitive • Can distinguish between species	• Unable to distinguish dead and alive fungi	Hours – Days	[Arabatzis *et al.* 2007, Jacobson *et al.* 2017, Moriello *et al.* 2017]
ELISA	• Highly specific	• False positives due to past infections	Hours – Days	[Peano *et al.* 2005, Aydin 2015, Santana *et al.* 2018]
MALDI-ToF*	• Highly sensitive • Can distinguish between species	• Only detect species in library	Minutes – Hours	[Theel *et al.* 2011, de Respinis *et al.* 2013, Nenoff *et al.* 2013, Patel 2019]

Genetic analysis*	• Highly sensitive • Can distinguish between species	• Unable to distinguish dead and alive fungi	Hours – Days	[Turin *et al.* 2000, Sharma *et al.* 2007, Pasquetti *et al.* 2013]

* These techniques can use culture material for analysis resulting in higher sensitivity, but longer time to diagnosis. Using clinical samples, these assays can be used as point-of-care/clinical diagnostic tests. However, not all clinical sample types can be used for each type of assay.

Literature Cited

Achterman RR, Smith AR, Oliver BG, et al. (2011). Sequenced dermatophyte strains: growth rate, conidiation, drug susceptibilities, and virulence in an invertebrate model. *Fungal Genet Biol* **48**(3):335-341.

Ajello L and Georg LK. (1957). In vitro hair cultures for differentiating between atypical isolates ofTrichophyton mentagrophytes andTrichophyton rubrum. *Mycopathologia et mycologia applicata* **8**(1):3-17.

al-Fouzan AS, Nanda A, and Kubec K. (1993). Dermatophytosis of children in Kuwait: a prospective survey. *Int J Dermatol* **32**(11):798-801.

Aljabre SH, Richardson MD, Scott EM, et al. (1992). Germination of Trichophyton mentagrophytes on human stratum corneum in vitro. *J Med Vet Mycol* **30**(2):145-52.

Alteras I, Sandbank M, David M, et al. (1988). 15-year survey of tinea faciei in the adult. *Dermatologica* **177**(2):65-9.

Aneke CI, Čmoková A, Hubka V, et al. (2021). Subtyping Options for Microsporum canis Using Microsatellites and MLST: A Case Study from Southern Italy. *Pathogens* **11**(1).

Arabatzis M, Bruijnesteijn van Coppenraet LES, Kuijper EJ, et al. (2007). Diagnosis of common dermatophyte infections by a novel multiplex real-time polymerase chain reaction detection/identification scheme. *British Journal of Dermatology* **157**(4):681-689.

Asawanonda P and Taylor CR. (1999). Wood's light in dermatology. *International Journal of Dermatology* **38**(11):801-807.

Aslanzadeh J and Roberts GD. (1991). Direct microscopic examination of clinical specimens for the laboratory diagnosis of fungal infections. *Clinical Microbiology Newsletter* **13**(24):185-188.

Atzori L, Aste N, Aste N, et al. (2012). Tinea Faciei Due to Microsporum canis in Children: A Survey of 46 Cases in the District of Cagliari (Italy). *Pediatric Dermatology* **29**(4):409-413.

Aydin S. (2015). A short history, principles, and types of ELISA, and our laboratory experience with peptide/protein analyses using ELISA. *Peptides* **72**(4-15.

Baert F, Stubbe D, D'hooge E, et al. (2020). Updating the Taxonomy of Dermatophytes of the BCCM/IHEM Collection According to the New Standard: A Phylogenetic Approach. *Mycopathologia* **185**(1):161-168.

Băguţ ET, Baldo A, Mathy A, et al. (2012). Subtilisin Sub3 is involved in adherence of Microsporum canis to human and animal epidermis. *Veterinary microbiology* **160**(3-4):413-9.

Baker M and Jeffries P. (2006). Use of commercially available cryogenic vials for long-term preservation of dermatophyte fungi. *Journal of clinical microbiology* **44**(2):617-618.

Baldo A, Mathy A, Tabart J, et al. (2010). Secreted subtilisin Sub3 from Microsporum canis is required for adherence to but not for invasion of the epidermis. *Br J Dermatol* **162**(5):990-7.

Baldo A, Monod M, Mathy A, et al. (2012). Mechanisms of skin adherence and invasion by dermatophytes. *Mycoses* **55**(3):218-223.

Baldo A, Tabart J, Vermout S, et al. (2008). Secreted subtilisins of Microsporum canis are involved in adherence of arthroconidia to feline corneocytes. *Journal of Medical Microbiology* **57**(9):1152-1156.

Begum J and Kumar R. (2020). Prevalence of dermatophytosis in animals and antifungal susceptibility testing of isolated Trichophyton and Microsporum species. *Tropical Animal Health and Production* **53**(1):3.
Begum J, Mir NA, Lingaraju MC, et al. (2020). Recent advances in the diagnosis of dermatophytosis. *Journal of Basic Microbiology* **60**(4):293-303.
Belhadjali H, Aounallah A, Youssef M, et al. (2009). [Tinea faciei, underrecognized because clinically misleading. 14 cases]. *Presse Med* **38**(9):1230-4.
Benedict K, Jackson BR, Chiller T, et al. (2018). Estimation of Direct Healthcare Costs of Fungal Diseases in the United States. *Clinical Infectious Diseases* **68**(11):1791-1797.
Bergman A, Heimer D, Kondori N, et al. (2013). Fast and specific dermatophyte detection by automated DNA extraction and real-time PCR. *Clinical Microbiology and Infection* **19**(4):E205-E211.
Bergmans AMC, van der Ent M, Klaassen A, et al. (2010). Evaluation of a single-tube real-time PCR for detection and identification of 11 dermatophyte species in clinical material. *Clinical Microbiology and Infection* **16**(6):704-710.
Bhat YJ, Keen A, Hassan I, et al. (2019). Can Dermoscopy Serve as a Diagnostic Tool in Dermatophytosis? A Pilot Study. *Indian dermatology online journal* **10**(5):530-535.
Bodman MA and Krishnamurthy K, *Onychomycosis*, in *StatPearls*. 2022, StatPearls Publishing Copyright © 2022, StatPearls Publishing LLC.: Treasure Island (FL).
Bonifaz A, Ramírez-Tamayo T, and Saúl A. (2003). Tinea barbae (tinea sycosis): experience with nine cases. *J Dermatol* **30**(12):898-903.
Brand A and Gow NAR. (2009). Mechanisms of hypha orientation of fungi. *Current opinion in microbiology* **12**(4):350-357.
Brasch J, Gräser Y, Beck-Jendroscheck V, et al. (2021). "Indian" strains of Trichophyton mentagrophytes with reduced itraconazole susceptibility in Germany. *J Dtsch Dermatol Ges* **19**(12):1723-1727.
Brilhante RS, Cavalcante CS, Soares-Junior FA, et al. (2003). High rate of Microsporum canis feline and canine dermatophytoses in Northeast Brazil: epidemiological and diagnostic features. *Mycopathologia* **156**(4):303-8.
Brilhante RSN, Cordeiro RA, Gomes JMF, et al. (2006). Canine dermatophytosis caused by an anthropophilic species: molecular and phenotypical characterization of Trichophyton tonsurans. *Journal of Medical Microbiology* **55**(11):1583-1586.
Brilhante RSN, Rocha MFG, Cordeiro RA, et al. (2005). Phenotypical and molecular characterization of Microsporum canis strains in north-east Brazil. *J Appl Microbiol* **99**(4):776-782.
Brillowska-Dąbrowska A, *DNA preparation from nail samples*, W.I.P. Organization, Editor. 2006: Denmark.
Brillowska-Dabrowska A, Michałek E, Saunte DML, et al. (2013). PCR test for Microsporum canis identification. *Medical Mycology* **51**(6):576-579.
Brosh-Nissimov T, Ben-Ami R, Astman N, et al. (2018). An Outbreak of Microsporum canis infection at a military base associated with stray cat exposure and person-to-person transmission. *Mycoses* **61**(7):472-476.
Burstein VL, Beccacece I, Guasconi L, et al. (2020). Skin Immunity to Dermatophytes: From Experimental Infection Models to Human Disease. *Frontiers in Immunology* **11**(
Cabañes F. (2000). Dermatophytes in domestic animals. *Rev Iberoam Micol* **17**(104-108.

Cabañes FJ, Abarca ML, and Bragulat MR. (1997). Dermatophytes isolated from domestic animals in Barcelona, Spain. *Mycopathologia* **137**(2):107-13.
Cafarchia C, Romito D, Sasanelli M, et al. (2004). The epidemiology of canine and feline dermatophytoses in southern Italy. *Mycoses* **47**(11-12):508-13.
Carlier GI. (1963). A SEVENTEEN-YEAR SURVEY OF THE RINGWORM FLORA OF BIRMINGHAM. *The Journal of hygiene* **61**(3):291-305.
Carter GR, *29 - Dermatophytes and Dermatophytoses11This chapter is a revision of a chapter prepared by Dr. H. A. McAllister for the Fourth Edition. Much of his material has been retained and his contribution is gratefully acknowledged*, in *Diagnostic Procedure in Veterinary Bacteriology and Mycology (Fifth Edition)*, G.R. Carter and J.R. Cole, Editors. 1990, Academic Press: San Diego. p. 381-404.
Chamorro MJ and House SA, *Tinea Manuum*. 2021: StatPearls Publishing, Treasure Island (FL).
Chattaway FW and Barlow AJE. (1966). Further studies of the fluorescent compounds produced in vivo by Trichophyton schoenleinii. *Sabouraudia* **4**(4):265-272.
Chermette R, Ferreiro L, and Guillot J. (2008). Dermatophytoses in Animals. *Mycopathologia* **166**(5):385-405.
Collins GD and Smith OG. (1960). Ringworm in a Siamese Cattery. *Can Vet J* **1**(9):412-5.
Courtellemont L, Chevrier S, Degeilh B, et al. (2017). Epidemiology of Trichophyton verrucosum infection in Rennes University Hospital, France: A 12-year retrospective study. *Medical Mycology* **55**(7):720-724.
da Costa FVA, Farias MR, Bier D, et al. (2013). Genetic variability in Microsporum canis isolated from cats, dogs and humans in Brazil. *Mycoses* **56**(5):582-588.
Daadaa N and Ben Tanfous A, *Favus*, in *StatPearls*. 2022, StatPearls Publishing
Copyright © 2022, StatPearls Publishing LLC.: Treasure Island (FL).
de Hoog GS, Dukik K, Monod M, et al. (2017). Toward a Novel Multilocus Phylogenetic Taxonomy for the Dermatophytes. *Mycopathologia* **182**(1):5-31.
de Respinis S, Tonolla M, Pranghofer S, et al. (2013). Identification of dermatophytes by matrix-assisted laser desorption/ionization time-of-flight mass spectrometry. *Medical Mycology* **51**(5):514-521.
DeBoer DJ and Moriello KA. (1994). Development of an experimental model of Microsporum canis infection in cats. *Veterinary microbiology* **42**(4):289-295.
DeBoer DJ and Moriello KA. (1995). Inability of two topical treatments to influence the course of experimentally induced dermatophytosis in cats. *J Am Vet Med Assoc* **207**(1):52-7.
Dion WM and Kapica L. (1975). Isolation of dermatophytes, Candida species and systemic fungi from dermatologic specimens in Montréal, 1963 to 1973. *Can Med Assoc J* **112**(6):712-6.
Dolenc-Voljč M and Gasparič J. (2017). Human Infections with Microsporum gypseum Complex (Nannizzia gypsea) in Slovenia. *Mycopathologia* **182**(11):1069-1075.
Dong C, Angus J, Scarampella F, et al. (2016). Evaluation of dermoscopy in the diagnosis of naturally occurring dermatophytosis in cats. *Veterinary Dermatology* **27**(4):275-e65.
Drake LA, Dinehart SM, Farmer ER, et al. (1996). Guidelines of care for superficial mycotic infectionsof the skin: Tinea corporis, tinea cruris, tinea faciei, tinea manuum, and tinea pedis. *Journal of the American Academy of Dermatology* **34**(2, Part 1):282-286.
Duek L, Kaufman G, Ulman Y, et al. (2004). The pathogenesis of dermatophyte infections in human skin sections. *Journal of Infection* **48**(2):175-180.
Elwart OE, Pieper JB, Oh S-H, et al. (2021). Effect of light exposure on growth rate of veterinary clinical dermatophyte isolates. *Veterinary Dermatology* **32**(3):234-e61.

English MP. (1966). Trichophyton persicolor infection in the field vole and pipistrelle bat. *Sabouraudia* **4**(4):219-222.
Fernandes NC, Akiti T, and Barreiros MG. (2001). Dermatophytoses in children: study of 137 cases. *Rev Inst Med Trop Sao Paulo* **43**(2):83-5.
Ferreira AW, Belem ZR, Lemos EA, et al. (2001). Enzyme-linked immunosorbent assay for serological diagnosis of Chagas' disease employing a Trypanosoma cruzi recombinant antigen that consists of four different peptides. *Journal of clinical microbiology* **39**(12):4390-5.
Frymus T, Gruffydd-Jones T, Pennisi MG, et al. (2013). Dermatophytosis in Cats: ABCD guidelines on prevention and management. *Journal of feline medicine and surgery* **15**(7):598-604.
Gaisin A, Holzwanger JM, and Leyden JJ. (1977). Endothrix tinea capitis in Philadelphia. *Int J Dermatol* **16**(3):188-90.
García-Agudo L and Espinosa-Ruiz JJ. (2018). [Tinea capitis by Microsporum gypseum, an infrequent species]. *Arch Argent Pediatr* **116**(2):e296-e299.
García-Martínez J, López Lacomba D, and Castaño Pascual A. (2018). Evaluation of a Method for Long-Term Cryopreservation of Fungal Strains. *Biopreserv Biobank* **16**(2):128-137.
Garg J, Tilak R, Garg A, et al. (2009). Rapid detection of dermatophytes from skin and hair. *BMC research notes* **2**(60.
Gnat S, Nowakiewicz A, Łagowski D, et al. (2019). Host- and pathogen-dependent susceptibility and predisposition to dermatophytosis. *Journal of Medical Microbiology* **68**(6):823-836.
González Cabo JF, Bárcena Asensio MC, Gómez Rodriguez F, et al. (1995). An outbreak of dermatophytosis in pigs caused by Microsporum canis. *Mycopathologia* **129**(2):79-80.
Gräser Y, El Fari M, Vilgalys R, et al. (1999). Phylogeny and taxonomy of the family Arthrodermataceae (dermatophytes) using sequence analysis of the ribosomal ITS region. *Medical Mycology* **37**(2):105-114.
Gräser Y, Kuijpers AF, El Fari M, et al. (2000). Molecular and conventional taxonomy of the Microsporum canis complex. *Med Mycol* **38**(2):143-53.
Gräser Y, Scott J, and Summerbell R. (2008). The New Species Concept in Dermatophytes—a Polyphasic Approach. *Mycopathologia* **166**(5):239.
Griffith OW. (1983). Cysteinesulfinate metabolism. altered partitioning between transamination and decarboxylation following administration of beta-methyleneaspartate. *J Biol Chem* **258**(3):1591-8.
Gross TL, Affolter VK, Ihrke PJ, et al., *Skin Diseases of the Dog and Cat: Clinical and Histopathologic Diagnosis*. 2. Aufl. ed. 2008, Chichester: Wiley-Blackwell.
Grumbt M, Monod M, Yamada T, et al. (2013). Keratin Degradation by Dermatophytes Relies on Cysteine Dioxygenase and a Sulfite Efflux Pump. *Journal of Investigative Dermatology* **133**(6):1550-1555.
Guillot J, Latié L, Deville M, et al. (2001). Evaluation of the dermatophyte test medium RapidVet-D. *Vet Dermatol* **12**(3):123-7.
Guillot J, Malandain E, Jankowski F, et al. (2002). Evaluation of the efficacy of oral lufenuron combined with topical enilconazole for the management of dermatophytosis in catteries. *Vet Rec* **150**(23):714-8.
Guirges SY. (1981). Viability of Trichophyton schoenleinii in epilated hairs. *Sabouraudia* **19**(2):155-6.

Gupta AK and Cooper EA, *Dermatophytosis (Tinea) and Other Superficial Fungal Infections*, in *Diagnosis and Treatment of Human Mycoses*, D.R. Hospenthal and M.G. Rinaldi, Editors. 2008, Humana Press: Totowa, NJ. p. 355-381.

Gupta AK and Summerbell RC. (2000). Tinea capitis. *Medical Mycology* **38**(4):255-287.

Hasegawa A and Usui K. (1975). Nannizzia otae sp. nov, the perfect state of Microsporum canis Bodin. *Japanese Journal of Medical Mycology* **16**(3):148-153.

Havlickova B, Czaika VA, and Friedrich M. (2008). Epidemiological trends in skin mycoses worldwide. *Mycoses* **51**(s4):2-15.

Hawksworth DL, Crous PW, Redhead SA, et al. (2011). The amsterdam declaration on fungal nomenclature. *IMA fungus* **2**(1):105-112.

Hay RJ, *Dermatophytoses and Other Superficial Mycoses*, in *Atlas of Infectious Diseases: Fungal Infections*, G.L. Mandell and R.D. Diamond, Editors. 2000, Current Medicine Group: London. p. 191-203.

Hay RJ. (2017). Tinea Capitis: Current Status. *Mycopathologia* **182**(1-2):87-93.

Hedayati MT, Afshar P, Shokohi T, et al. (2007). A study on tinea gladiatorum in young wrestlers and dermatophyte contamination of wrestling mats from Sari, Iran. *Br J Sports Med* **41**(5):332-4.

Hube B, Hay R, Brasch J, et al. (2015). Dermatomycoses and inflammation: The adaptive balance between growth, damage, and survival. *Journal de Mycologie Médicale* **25**(1):e44-e58.

Hwang S-W, Kwolek W, and Haynes W. (1976). Investigation of ultralow temperature for fungal cultures III. Viability and growth rate of mycelial cultures following cryogenic storage. *Mycologia* **68**(2):377-387.

Irwin SV, Fisher P, Graham E, et al. (2017). Sulfites inhibit the growth of four species of beneficial gut bacteria at concentrations regarded as safe for food. *PloS one* **12**(10):e0186629-e0186629.

Jackson CJ, Barton RC, and Evans EG. (1999). Species identification and strain differentiation of dermatophyte fungi by analysis of ribosomal-DNA intergenic spacer regions. *Journal of clinical microbiology* **37**(4):931-6.

Jacobson LS, McIntyre L, and Mykusz J. (2017). Comparison of real-time PCR with fungal culture for the diagnosis of Microsporum canis dermatophytosis in shelter cats: a field study. *Journal of feline medicine and surgery* **20**(2):103-107.

Jang S and Walker R. (2006). Laboratory diagnosis of fungal and algal infections. *GREENE CE. Infectious Disease of the Dog and Cat* **3**(533-542.

Jungerman PF and Schwartzman RM, *Veterinary medical mycology*. 1972.

Kaplan W and Ajello L. (1959). Oral treatment of spontaneous ringworm in cats with griseofulvin. *J Am Vet Med Assoc* **135**(253-61.

Kaplan W and Ajello L. (1960). Therapy of spontaneous ringworm in cats with orally administered griseofulvin. *Arch Dermatol* **81**(714-23.

Kaplan W, Georg LK, and Ajello L. (1958). Recent developments in animal ringworm and their public health implications. *Ann N Y Acad Sci* **70**(3):636-49.

Kasperova A, Kunert J, and Raska M. (2013). The possible role of dermatophyte cysteine dioxygenase in keratin degradation. *Medical Mycology* **51**(5):449-454.

Kaszubiak A, Klein S, de Hoog GS, et al. (2004). Population structure and evolutionary origins of Microsporum canis, M. ferrugineum and M. audouinii. *Infection, Genetics and Evolution* **4**(3):179-186.

Keep JM. (1959). THE EPIDEMIOLOGY AND CONTROL OP MICROSPORUM CANIS BODIN IN A CAT COMMUNITY. *Australian Veterinary Journal* **35**(8):374-378.
Khosravi AR and Mahmoudi M. (2003). Dermatophytes isolated from domestic animals in Iran. *Mycoses* **46**(5-6):222-5.
Kidd S, Halliday CL, Alexiou H, et al., *Descriptions of Medical Fungi*. 2016: CutCut Digital.
Kim JA, Takahashi Y, Tanaka R, et al. (2001). Identification and subtyping of Trichophyton mentagrophytes by random amplified polymorphic DNA. *Mycoses* **44**(5):157-65.
Klatte JL, van der Beek N, and Kemperman PMJH. (2015). 100 years of Wood's lamp revised. *Journal of the European Academy of Dermatology and Venereology* **29**(5):842-847.
Köhler JR, Casadevall A, and Perfect J. (2014). The spectrum of fungi that infects humans. *Cold Spring Harbor perspectives in medicine* **5**(1):a019273-a019273.
Kosanke S, Hamann L, Kupsch C, et al. (2018). Unequal distribution of the mating type (MAT) locus idiomorphs in dermatophyte species. *Fungal Genet Biol* **118**(45-53.
Krzyściak P, Al-Hatmi AMS, Ahmed SA, et al. (2015). Rare zoonotic infection with Microsporum persicolor with literature review. *Mycoses* **58**(9):511-515.
Lagousi T, Routsias J, and Spoulou V. (2021). Development of an Enzyme-Linked Immunosorbent Assay (ELISA) for Accurate and Prompt Coronavirus Disease 2019 (COVID-19) Diagnosis Using the Rational Selection of Serological Biomarkers. *Diagnostics (Basel)* **11**(11).
Lallas A, Kyrgidis A, Tzellos TG, et al. (2012). Accuracy of dermoscopic criteria for the diagnosis of psoriasis, dermatitis, lichen planus and pityriasis rosea. *British Journal of Dermatology* **166**(6):1198-1205.
Léchenne B, Reichard U, Zaugg C, et al. (2007). Sulphite efflux pumps in Aspergillus fumigatus and dermatophytes. *Microbiology* **153**(3):905-913.
Leck A. (1999). Preparation of lactophenol cotton blue slide mounts. *Community eye health* **12**(30):24-24.
Leung AK, Lam JM, Leong KF, et al. (2020). Tinea corporis: an updated review. *Drugs in context* **9**(2020-5-6.
Li H, Wu S, Mao L, et al. (2013). Human pathogenic fungus Trichophyton schoenleinii activates the NLRP3 inflammasome. *Protein Cell* **4**(7):529-38.
Li W, Metin B, White Theodore C, et al. (2010). Organization and Evolutionary Trajectory of the Mating Type (MAT) Locus in Dermatophyte and Dimorphic Fungal Pathogens. *Eukaryotic Cell* **9**(1):46-58.
Lim SS, Shin K, and Mun J-H. (2022). Dermoscopy for cutaneous fungal infections: A brief review. *Health science reports* **5**(1):e464-e464.
Lipner SR and Scher RK. (2019). Onychomycosis: Clinical overview and diagnosis. *Journal of the American Academy of Dermatology* **80**(4):835-851.
Londero AT. (1964). DERMATOMYCOSS IN THE HINTERLAND OF RIO GRANDE DO SUL (BRAZIL). *Dermatol Trop Ecol Geogr* **35**(64-8.
Mackenzie DW. (1963). "Hairbrush Diagnosis" in Detection and Eradication of Non-fluorescent Scalp Ringworm. *Br Med J* **2**(5353):363-5.
Mackenzie DW. (1964). The mycological diagnostic service: a five-year survey (1959-1963). *The Ulster medical journal* **33**(2):94-100.
Magnarelli LA, Anderson JF, and Barbour AG. (1989). Enzyme-linked immunosorbent assays for Lyme disease: reactivity of subunits of Borrelia burgdorferi. *J Infect Dis* **159**(1):43-9.
Mahgoub ES. (1977). Mycoses of the Sudan. *Trans R Soc Trop Med Hyg* **71**(3):184-8.

Makimura K, Mochizuki T, Hasegawa A, et al. (1998). Phylogenetic classification of Trichophyton mentagrophytes complex strains based on DNA sequences of nuclear ribosomal internal transcribed spacer 1 regions. *Journal of clinical microbiology* **36**(9):2629-2633.
Mancianti F, Dabizzi S, and Nardoni S. (2009). A lufenuron pre-treatment may enhance the effects of enilconazole or griseofulvin in feline dermatophytosis? *Journal of feline medicine and surgery* **11**(2):91-5.
Maraki S and Tselentis Y. (2000). Survey on the epidemiology of Microsporum canis infections in Crete, Greece over a 5-year period. *International Journal of Dermatology* **39**(1):21-24.
Marchisio VF, Gallo MG, Tullio V, et al. (1995). Dermatophytes from cases of skin disease in cats and dogs in Turin, Italy. *Mycoses* **38**(5-6):239-244.
Marconi VC, Kradin R, Marty FM, et al. (2010). Disseminated dermatophytosis in a patient with hereditary hemochromatosis and hepatic cirrhosis: case report and review of the literature. *Medical Mycology* **48**(3):518-527.
Marples MJ. (1959). Some problems in the ecology of the dermatophytes. *N Z Med J* **58**(323):64-9.
Martinez DA, Oliver BG, Gräser Y, et al. (2012). Comparative genome analysis of Trichophyton rubrum and related dermatophytes reveals candidate genes involved in infection. *mBio* **3**(5):e00259.
Martins MP, Rossi A, Sanches PR, et al. (2020). Comprehensive analysis of the dermatophyte Trichophyton rubrum transcriptional profile reveals dynamic metabolic modulation. *Biochem J* **477**(5):873-885.
McPherson E. (1957). The influence of physical factors on dermatomycosis in domestic animals. *Veterinary Record* **69**(43).
Mercer DK and Stewart CS. (2018). Keratin hydrolysis by dermatophytes. *Medical Mycology* **57**(1):13-22.
Metin B and Heitman J. (2020). She Loves Me, She Loves Me Not: On the Dualistic Asexual/Sexual Nature of Dermatophyte Fungi. *Mycopathologia* **185**(1):87-101.
Meyer E. (1955). The preservation of dermatophytes at sub-freezing temperatures. *Mycologia* **47**(5):664-668.
Mignon B, Swinnen M, Bouchara JP, et al. (1998). Purification and characterization of a 315 kDa keratinolytic subtilisin-like serine protease from and evidence of its secretion in naturally infected cats. *Medical Mycology* **36**(6):395-404.
Mochizuki T, Sugie N, and Uehara M. (1997). Random amplification of polymorphic DNA is useful for the differentiation of several anthropophilic dermatophytes. *Mycoses* **40**(11-12):405-9.
Monod M. (2008). Secreted proteases from dermatophytes. *Mycopathologia* **166**(5-6):285-94.
Moretti A, Boncio L, Pasquali P, et al. (1998). Epidemiological aspects of dermatophyte infections in horses and cattle. *Zentralbl Veterinarmed B* **45**(4):205-8.
Moriello K. (2014). Feline dermatophytosis: aspects pertinent to disease management in single and multiple cat situations. *Journal of feline medicine and surgery* **16**(5):419-431.
Moriello KA. (2001). Diagnostic techniques for dermatophytosis. *Clinical Techniques in Small Animal Practice* **16**(4):219-224.
Moriello KA, Coyner K, Paterson S, et al. (2017). Diagnosis and treatment of dermatophytosis in dogs and cats. *Veterinary Dermatology* **28**(3):266-e68.

Moriello KA, DeBoer DJ, Greek J, et al. (2003). The prevalence of immediate and delayed type hypersensitivity reactions to Microsporum canis antigens in cats. *Journal of feline medicine and surgery* **5**(3):161-166.
Moriello KA, Verbrugge MJ, and Kesting RA. (2010). Effects of temperature variations and light exposure on the time to growth of dermatophytes using six different fungal culture media inoculated with laboratory strains and samples obtained from infected cats. *Journal of feline medicine and surgery* **12**(12):988-90.
Morris AJ, Byrne TC, Madden JF, et al. (1996). Duration of incubation of fungal cultures. *Journal of clinical microbiology* **34**(6):1583-1585.
Moskaluk A, Darlington L, Kuhn S, et al. (2022). Genetic Characterization of Microsporum canis Clinical Isolates in the United States. *Journal of Fungi* **8**(7).
Moskaluk A, Nehring M, and VandeWoude S. (2021). Serum Samples from Co-Infected and Domestic Cat Field Isolates Nonspecifically Bind FIV and Other Antigens in Enzyme-Linked Immunosorbent Assays. *Pathogens* **10**(6):665.
Nenoff P, Erhard M, Simon JC, et al. (2013). MALDI-TOF mass spectrometry – a rapid method for the identification of dermatophyte species. *Medical Mycology* **51**(1):17-24.
Newbury S, Moriello K, Verbrugge M, et al. (2007). Use of lime sulphur and itraconazole to treat shelter cats naturally infected with Microsporum canis in an annex facility: an open field trial. *Vet Dermatol* **18**(5):324-31.
Nowicka D, Nawrot U, Włodarczyk K, et al. (2016). Detection of dermatophytes in human nail and skin dust produced during podiatric treatments in people without typical clinical signs of mycoses. *Mycoses* **59**(6):379-82.
Nussipov Y, Markabayeva A, Gianfaldoni S, et al. (2017). Clinical and Epidemiological Features of Dermatophyte Infections in Almaty, Kazakhstan. *Open access Macedonian journal of medical sciences* **5**(4):409-413.
Nweze EI and Eke IE. (2017). Dermatophytes and dermatophytosis in the eastern and southern parts of Africa. *Medical Mycology* **56**(1):13-28.
Outerbridge CA. (2006). Mycologic disorders of the skin. *Clin Tech Small Anim Pract* **21**(3):128-34.
Park YW, Kim DY, Yoon SY, et al. (2014). 'Clues' for the histological diagnosis of tinea: how reliable are they? *Annals of dermatology* **26**(2):286-288.
Pasarell L and McGinnis MR. (1992). Viability of fungal cultures maintained at -70 degrees C. *Journal of clinical microbiology* **30**(4):1000-1004.
Pasquetti M, Peano A, Soglia D, et al. (2013). Development and validation of a microsatellite marker-based method for tracing infections by Microsporum canis. *Journal of Dermatological Science* **70**(2):123-129.
Patel R. (2019). A Moldy Application of MALDI: MALDI-ToF Mass Spectrometry for Fungal Identification. *Journal of fungi (Basel, Switzerland)* **5**(1):4.
Peano A, Rambozzi L, and Gallo MG. (2005). Development of an enzyme-linked immunosorbant assay (ELISA) for the serodiagnosis of canine dermatophytosis caused by Microsporum canis. *Veterinary Dermatology* **16**(2):102-107.
Peres NT, Maranhao FC, Rossi A, et al. (2010). Dermatophytes: host-pathogen interaction and antifungal resistance. *An Bras Dermatol* **85**(5):657-67.
Philpot CM. (1978). Geographical distribution of the dermatophytes: a review. *The Journal of hygiene* **80**(2):301-313.

Pier AC, Smith JMB, Alexiou H, et al. (1994). Animal ringworm — its aetiology, public health significance and control. *Journal of Medical and Veterinary Mycology* **32**(Supplement_1):133-150.
Piliouras P, Buettner P, and Soyer HP. (2014). Dermoscopy use in the next generation: A survey of Australian dermatology trainees. *Australasian Journal of Dermatology* **55**(1):49-52.
Poluri LV, Indugula JP, and Kondapaneni SL. (2015). Clinicomycological Study of Dermatophytosis in South India. *Journal of laboratory physicians* **7**(2):84-89.
Ranganathan S, Arun Mozhi Balajee S, and Mahendra Raja S. (1997). A survey of dermatophytosis in animals in Madras, India. *Mycopathologia* **140**(3):137-140.
Ratajczak-Stefańska V, Kiedrowicz M, Maleszka R, et al. (2010). Majocchi's granuloma caused by Microsporum canis in an immunocompetent patient. *Clinical and Experimental Dermatology* **35**(4):445-447.
Rawlings ND, Barrett AJ, and Finn R. (2016). Twenty years of the MEROPS database of proteolytic enzymes, their substrates and inhibitors. *Nucleic Acids Res* **44**(D1):D343-50.
Rees RG. (1967). Keratinophilic fungi from Queensland. I. Isolations from animal hair and scales. *Sabouraudia* **5**(3):165-72.
Rees RG. (1968). Keratinophilic Fungi from Queensland—II. Isolations from Feathers of Wild Birds. *Sabouraudia* **6**(1):14-18.
Richard JL, Debey MC, Chermette R, et al. (1994). Advances in veterinary mycology. *Journal of Medical and Veterinary Mycology* **32**(Supplement_1):169-187.
Ridley MF, Wilson E, and Harrington M. (1961). The occurrence of dermatophytes in Queensland. *Aust J Dermatol* **6**(24-8.
Rippon JW, *Medical Mycology: The Pathogenic Fungi and the Pathogenic Actinomycetes*. 1988: Saunders.
Roberson RW. (2020). Subcellular structure and behaviour in fungal hyphae. *Journal of Microscopy* **280**(2):75-85.
Rosenthal SA and Vanbreuseghem R. (1962). Viability of dermatophytes in epilated hairs. *Arch Dermatol* **85**(103-5.
Ross JB, Butler RW, Cross RJ, et al. (1971). A retrospective study of dermatophyte infection in Newfoundland for the period 1962-1968. *Can Med Assoc J* **104**(6):492-6.
Rouzaud C, Hay R, Chosidow O, et al. (2015). Severe Dermatophytosis and Acquired or Innate Immunodeficiency: A Review. *Journal of fungi (Basel, Switzerland)* **2**(1):4.
Rutecki GW, Wurtz R, and Thomson RB. (2000). From Animal to Man: Tinea Barbae. *Curr Infect Dis Rep* **2**(5):433-437.
Samanta I, *Veterinary Mycology*. 2015: Springer India.
Santana AE, Taborda CP, Severo JS, et al. (2018). Development of enzyme immunoassays (ELISA and Western blot) for the serological diagnosis of dermatophytosis in symptomatic and asymptomatic cats. *Medical Mycology* **56**(1):95-102.
Scarampella F, Zanna G, Peano A, et al. (2015). Dermoscopic features in 12 cats with dermatophytosis and in 12 cats with self-induced alopecia due to other causes: an observational descriptive study. *Veterinary Dermatology* **26**(4):282-e63.
Schipper MA and Bekker-Holtman J. (1976). Viability of lyophilized fungal cultures. *Antonie Van Leeuwenhoek* **42**(3):325-8.
Seebacher C, Bouchara J-P, and Mignon B. (2008). Updates on the Epidemiology of Dermatophyte Infections. *Mycopathologia* **166**(5):335-352.

Segal E and Elad D. (2021). Human and Zoonotic Dermatophytoses: Epidemiological Aspects. *Frontiers in microbiology* **12**(

Segal E and Frenkel M. (2015). Dermatophyte infections in environmental contexts. *Res Microbiol* **166**(7):564-9.

Seyedmousavi S, Bosco SdMG, de Hoog S, et al. (2018). Fungal infections in animals: a patchwork of different situations. *Medical Mycology* **56**(suppl_1):165-187.

Shah PC, Krajden S, Kane J, et al. (1988). Tinea corporis caused by Microsporum canis: report of a nosocomial outbreak. *Eur J Epidemiol* **4**(1):33-8.

Sharma R, de Hoog S, Presber W, et al. (2007). A virulent genotype of Microsporum canis is responsible for the majority of human infections. *Journal of Medical Microbiology* **56**(10):1377-1385.

Sittampalam GS, Smith WC, Miyakawa TW, et al. (1996). Application of experimental design techniques to optimize a competitive ELISA. *Journal of immunological methods* **190**(2):151-61.

Snider R, Landers S, and Levy ML. (1993). The ringworm riddle: an outbreak of Microsporum canis in the nursery. *Pediatr Infect Dis J* **12**(2):145-8.

Soderstrom CI, Spriggs FP, Song W, et al. (2011). Comparison of four distinct detection platforms using multiple ligand binding assay formats. *Journal of immunological methods* **371**(1):106-113.

Sparkes A, Werrett G, Stokes C, et al. (1994). Microsporum canis: inapparent carriage by cats and the viability of arthrospores. *Journal of Small Animal Practice* **35**(8):397-401.

Sparkes AH, Gruffydd-Jones TJ, Shaw SE, et al. (1993). Epidemiological and diagnostic features of canine and feline dermatophytosis in the United Kingdom from 1956 to 1991. *Vet Rec* **133**(3):57-61.

Sparkes AH, Robinson A, MacKay AD, et al. (2000). A study of the efficacy of topical and systemic therapy for the treatment of feline Microsporum canis infection. *Journal of feline medicine and surgery* **2**(3):135-42.

Sparkes AH, Stokes CR, and Gruffydd-Jones TJ. (1995). Experimental Microsporum canis infection in cats: correlation between immunological and clinical observations. *Journal of Medical and Veterinary Mycology* **33**(3):177-184.

Stalpers J, Hoog Ad, and Vlug IJ. (1987). Improvement of the straw technique for the preservation of fungi in liquid nitrogen. *Mycologia* **79**(1):82-89.

Stenwig H. (1985). Isolation of dermatophytes from domestic animals in Norway. *Nord Vet Med* **37**(3):161-9.

Stuntebeck R, Moriello KA, and Verbrugge M. (2017). Evaluation of incubation time for Microsporum canis dermatophyte cultures. *Journal of feline medicine and surgery* **20**(10):997-1000.

Subelj M, Marinko JS, and Učakar V. (2014). An outbreak of Microsporum canis in two elementary schools in a rural area around the capital city of Slovenia, 2012. *Epidemiol Infect* **142**(12):2662-6.

Summerbell RC, Kushwaha RKS, and Guarro J. *Form and function in the evolution of dermatophytes*. 2000.

Taghipour S, Pchelin IM, Zarei Mahmoudabadi A, et al. (2019). Trichophyton mentagrophytes and T interdigitale genotypes are associated with particular geographic areas and clinical manifestations. *Mycoses* **62**(11):1084-1091.

Taylor JW. (2011). One Fungus = One Name: DNA and fungal nomenclature twenty years after PCR. *IMA fungus* **2**(2):113-120.
Theel ES, Hall L, Mandrekar J, et al. (2011). Dermatophyte identification using matrix-assisted laser desorption ionization-time of flight mass spectrometry. *Journal of clinical microbiology* **49**(12):4067-4071.
Tran VD, De Coi N, Feuermann M, et al. (2016). RNA Sequencing-Based Genome Reannotation of the Dermatophyte Arthroderma benhamiae and Characterization of Its Secretome and Whole Gene Expression Profile during Infection. *mSystems* **1**(4).
Turin L, Riva F, Galbiati G, et al. (2000). Fast, simple and highly sensitive double-rounded polymerase chain reaction assay to detect medically relevant fungi in dermatological specimens. *Eur J Clin Invest* **30**(6):511-8.
Uhrlaß S, Verma SB, Gräser Y, et al. (2022). Trichophyton indotineae-An Emerging Pathogen Causing Recalcitrant Dermatophytoses in India and Worldwide-A Multidimensional Perspective. *Journal of fungi (Basel, Switzerland)* **8**(7).
Vanbreuseghem R and De Vroey C. (1970). Geographic distribution of dermatophytes. *Int J Dermatol* **9**(2):102-9.
Veraldi S, Genovese G, and Peano A. (2018). Tinea corporis caused by Trichophyton equinum in a rider and review of the literature. *Infection* **46**(1):135-137.
Veraldi S, Schianchi R, Benzecry V, et al. (2019). Tinea manuum: A report of 18 cases observed in the metropolitan area of Milan and review of the literature. *Mycoses* **62**(7):604-608.
Verma SB. (2018). Emergence of recalcitrant dermatophytosis in India. *Lancet Infect Dis* **18**(7):718-719.
Verma SB, Panda S, Nenoff P, et al. (2021). The unprecedented epidemic-like scenario of dermatophytosis in India: III. Antifungal resistance and treatment options. *Indian J Dermatol Venereol Leprol* **87**(4):468-482.
Vermout S, Tabart J, Baldo A, et al. (2008). Pathogenesis of Dermatophytosis. *Mycopathologia* **166**(5):267.
Viani FC, Dos Santos JI, Paula CR, et al. (2001). Production of extracellular enzymes by Microsporum canis and their role in its virulence. *Med Mycol* **39**(5):463-8.
Voisard JJ, Weill FX, Beylot-Barry M, et al. (1999). Dermatophytic granuloma caused by Microsporum canis in a heart-lung recipient. *Dermatology* **198**(3):317-9.
Wang MZ, Guo R, and Lehman JS. (2017). Correlation between histopathologic features and likelihood of identifying superficial dermatophytosis with periodic acid Schiff-diastase staining: a cohort study. *Journal of Cutaneous Pathology* **44**(2):152-157.
Watanabe J, Anzawa K, and Mochizuki T. (2017). Molecular Epidemiology of Japanese Isolates of Microsporum canis Based on Multilocus Microsatellite Typing Fragment Analysis. *Japanese Journal of Infectious Diseases* **70**(5):544-548.
Weitzman I and Padhye AA. (1978). Mating behaviour of Nannizzia otae (=Microsporum canis). *Mycopathologia* **64**(1):17-22.
Weitzman I and Summerbell RC. (1995). The dermatophytes. *Clinical microbiology reviews* **8**(2):240-259.
White TC, Findley K, Dawson TL, Jr., et al. (2014). Fungi on the skin: dermatophytes and Malassezia. *Cold Spring Harbor perspectives in medicine* **4**(8):a019802.
White TC, Oliver BG, Gräser Y, et al. (2008). Generating and testing molecular hypotheses in the dermatophytes. *Eukaryotic Cell* **7**(8):1238-1245.

Wickes BL and Wiederhold NP. (2018). Molecular diagnostics in medical mycology. *Nature Communications* **9**(1):5135.
Wiegand C, Burmester A, Tittelbach J, et al. (2019). [Dermatophytosis caused by rare anthropophilic and zoophilic agents]. *Hautarzt* **70**(8):561-574.
Wolf FT. (1957). Chemical nature of the fluorescent pigment produced in Microsporum-infected hair. *Nature* **180**(4591):860-1.
Wolf FT, Jones EA, and Nathan HA. (1958). Fluorescent Pigment of Microsporum. *Nature* **182**(4633):475-476.
Wu Y, Yang J, Yang F, et al. (2009). Recent dermatophyte divergence revealed by comparative and phylogenetic analysis of mitochondrial genomes. *BMC Genomics* **10**(1):238.
Yamada S, Anzawa K, and Mochizuki T. (2019). An Epidemiological Study of Feline and Canine Dermatophytoses in Japan. *Med Mycol J* **60**(2):39-44.
Yamada S, Anzawa K, and Mochizuki T. (2022). Molecular Epidemiology of Microsporum canis Isolated from Japanese Cats and Dogs, and from Pet Owners by Multilocus Microsatellite Typing Fragment Analysis. *Japanese Journal of Infectious Diseases* **75**(2):105-113.
Zanna G, Auriemma E, Arrighi S, et al. (2015). Dermoscopic evaluation of skin in healthy cats. *Vet Dermatol* **26**(1):14-7, e3-4.
Zaror L. (1974). [Dermatomycosis in the south of Chile]. *Rev Med Chil* **102**(4):299-302.
Ziółkowska G, Nowakiewicz A, Gnat S, et al. (2015). Molecular identification and classification of Trichophyton mentagrophytes complex strains isolated from humans and selected animal species. *Mycoses* **58**(3):119-126.
Zurita J and Hay RJ. (1987). Adherence of Dermatophyte Microconidia and Arthroconidia to Human Keratinocytes In Vitro. *Journal of Investigative Dermatology* **89**(5):529-534.

CHAPTER 2: GENETIC CHARACTERIZATION OF *MICROSPORUM CANIS* CLINICAL ISOLATES IN THE UNITED STATES

2.1 Introduction

Microsporum canis is a filamentous fungus that can cause superficial fungal infections in animals and humans [Cafarchia *et al.* 2004, Moriello 2014][2]. It is the primary agent for dermatophytosis cases in domestic cats [Moriello 2014], and for tinea capitis in humans in certain parts of Europe [Ginter-Hanselmayer *et al.* 2007, Fuller 2009, Hay 2017]. Since *M. canis* is a zoonotic disease that is a common infection in domestic cats [Weitzman *et al.* 1995, Moriello 2014], it places veterinarians, animal care staff, and owners at risk of infection. Although dermatophytosis is generally self-limiting in immunocompetent individuals, the zoonotic and contagious nature of the infection and its propensity to infect children and medically underserved populations categorize it as an agent of concern [Mushtaq *et al.* 2020]. Similar to human infections, feline dermatophytosis presents in a variety of forms [Moriello 2014]. Healthy cats can be presented with areas of circular alopecia and potentially an erythematous margin and scaling [Frymus *et al.* 2013]. Cats with concurrent infections (e.g., upper respiratory infections), geriatric or feral cats can experience more severe disease with widespread lesions and generalized disease [Moriello 2014]. Cats can be carriers without presenting with lesions, representing a risk for infection to other animals and people [Moriello 2014]. Since *M. canis* is highly contagious and can be difficult to diagnose, outbreaks can frequently occur in high-density populations such as animal shelters [Moriello 2014, Newbury *et al.* 2014].

[2] Work presented in this chapter has been published with the following citation Moskaluk, Alex, et al. "Genetic Characterization of *Microsporum Canis* Clinical Isolates in the United States." Journal of Fungi, vol. 8, no. 7, June 2022, p. 676. Crossref, https://doi.org/10.3390/jof8070676.

Molecular characterization of disease outbreaks can be used to trace pathogen spread and identify contributing factors [Engelthaler *et al.* 2011, Etienne *et al.* 2012, Pasquetti *et al.* 2013, Di Pilato *et al.* 2021]. Using one microsatellite allele identified by Sharma et al. [Sharma *et al.* 2007], and seven other loci, Pasquetti et al. [Pasquetti *et al.* 2013] identified 22 genotypes from 26 unrelated *M. canis* isolates from 13 non-US countries, including outbreak settings. Transmission between animals and humans was confirmed via identical multilocus genotypes observed in these cases. Understanding the source of *M. canis* infections and pathogen transmission dynamics during outbreaks can inform transmission pathways and mitigate outbreak risk and severity.

In addition to being beneficial in understanding transmission dynamics, genotyping via microsatellite alleles can assess the relationship between clinical presentation and genotype, leading towards better understanding of pathogenesis and providing an opportunity for more informative diagnostic testing [Sharma *et al.* 2007, da Costa *et al.* 2013]. Previous studies have demonstrated differences in virulence associated with different *M. canis* genotypes; however, no correlations between genotypes and clinical presentation (or other clinical parameters) have been identified [Sharma *et al.* 2007, da Costa *et al.* 2013]. Defining the relationship between clinical presentation and genotype would lead towards elucidation of strain virulence characteristics, and geographic isolate associations could assist in understanding regional risk factors, potentially influencing treatment strategies and prognosis including length of infectivity and disease course.

To our knowledge, genotypic characterization of *M. canis* isolates in the United States has not been conducted. Therefore, we utilized eight microsatellite loci [Sharma *et al.* 2007, Pasquetti *et al.* 2013] to evaluate genetic variants among *M. canis* isolates from cats from seven clinics across the US, characterized the mating gene type and searched for polymorphisms in two

candidate *M. canis* virulence genes. We also analyzed demographic, clinic location and clinical presentation data to assess genotypic correlates with these factors and assessed two potential virulence genes for polymorphisms that might relate to pathogenicity.

2.2. Materials and Methods

2.2.1. Sample Acquisition

From May 2019 to June 2021, 258 hair samples were collected from domestic cats with suspected dermatophytosis from animal shelters (California; New Mexico; Boulder Country, Colorado; Larimer County, Colorado; Weld County, Colorado) and veterinary dermatology practices (Massachusetts, New Jersey). Each location consisted of one clinic that was either a shelter or private practice. The criteria for being included in this study were suspicion of dermatophytosis determined by a licensed veterinarian, and no known history of treatment for dermatophytosis. All protocols were approved by Colorado State University (CSU) clinical review board (VCS #2019-223) and biosafety committee (#145399) and were granted an Institutional Animal Care and Use Committee (IACUC) waiver prior to initiation of this study. Samples were collected in shelters upon initial intake examination and were not collected from patients who developed dermatophytosis while housed at the shelter. Veterinarians collected the hair samples using a sterile toothbrush, following the "Mackenzie" brush technique [Mackenzie 1963, Moriello *et al.* 2017]. This method was used to ensure sufficient hair was collected from each cat as it is sensitive at acquiring spores from the hair coat [Moriello *et al.* 2017]. Samples were mailed overnight to CSU, where they were stored at 4 °C until processed.

2.2.2. Clinical Survey

At each participating clinic, veterinarians were provided with an online survey to record clinical and demographic information for each patient sampled. This tool included questions about the individual performing the sampling and analysis, as well as patient ID, date presented for evaluation, age, sex and neuter status, breed, previous and current housing environment, current medications, concurrent medical conditions, diagnostic tests administered, history of anti-fungal treatment, number of lesions present, average size of the lesions, lesion distribution, lesion types, and lesion severity (Suppl. Table 2.1). Age was based on dentition for animals with an unknown date of birth. Cats less than one year old were categorized as kittens and over one year old as adults.

2.2.3. Reference Fungal Isolate

M. canis isolate CBS 113480 was purchased from Westerdijk Fungal Biodiversity Centre (Utrecht, The Netherlands) and was used as a reference isolate. This isolate was previously used to assemble the published *M. canis* reference genome [Martinez *et al.* 2012].

2.2.4. Fungal Culture and DNA Extraction

Toothbrush samples were cultured on Dermatophyte Test Medium (DTM) plates (Hardy Diagnostics, Santa Maria, CA, USA) or Sabouraud's Dextrose Agar (SDA) plates with chloramphenicol and gentamicin (Hardy Diagnostics, Santa Maria, CA, USA) by gently pressing the toothbrush bristles multiple times on each side of the plate. Plates were inverted and incubated at room temperature (20–25 °C) in the dark and were monitored every 24–48 h for colony growth for up to 4 weeks or until fungal growth was detected. Positive dermatophyte culture was determined by colony morphology; if multiple saprophytes were present, samples

were re-plated by culturing the toothbrush on a new SDA plate. Plates that were overgrown with saprophytes were re-plated at least two times and observed for dermatophyte growth. All culture negative samples were also replated at least two times.

DNA from fungal cultures were extracted using a protocol developed by Brillowska-Dąbrowska [Brillowska-Dąbrowska 2006]. Fungal cells were transferred via a sterile swab to a tube containing 100 µL of extraction buffer (100 µL of 60 mM sodium bicarbonate, 250 mM potassium chloride, and 50 mM Tris, balanced to pH 9.5). This mixture was incubated at 95 °C for 10 min, followed by addition of 100 µL of 2% bovine serum albumin buffer and then stored at −80 °C until needed.

2.2.5. Dermatophyte Detection and Identification

Qualitative PCR was performed using primers designed specifically for dermatophyte detection that target the ITS-1 gene: DERMF3 (5′-GGTTGCCTCGGCGGGCC) and B-DERMR2 (5′-CGGAATTCTGCAATTCACATTACT) [Bergmans *et al.* 2010]. The following protocol was used for each sample with a reaction volume of 20 µL: 10 µL of 2× KAPA Taq ReadyMix with dye (Roche, Indianapolis, IN, USA), 6 µL UltraPure DNase/Rnase-free distilled water (Invitrogen, Carlsbad, CA, USA), 1 µL of 10 µM forward primer, 1 µL of 10 µM reverse primer and 2 µL of DNA template solution (DNA concentration ranged between 0.1–8.5 ng/µL). The reaction was run in a C1000 Touch thermocycler (Bio-Rad, Hercules, CA, USA) for one cycle at 95 °C for 3 min, 34 cycles at 95 °C for 30 s, 60 °C for 30 s, 72 °C for 1 min, and one cycle at 72 °C for 5 min. Five microliters of PCR product was run on 1.5% agarose gel for 30 min at 80 volts and images were recorded using an ImageQuant LAS 4000 (GE healthcare, Chicago, IL, USA). A 280 bp amplicon was considered positive for dermatophytes. To confirm

the identity of the dermatophyte, the PCR products were purified using ExoSAP-IT PCR product cleanup reagent (Applied Biosystems, Carlsbad, CA, USA) and sent for Sanger sequencing (Psomagen, Rockville, MD, USA). The resulting sequences were entered into NIH NCBI's Basic Local Alignment Search Tool (BLAST) (https://blast.ncbi.nlm.nih.gov/Blast.cgi (accessed on September 25, 2019 to June 19, 2021)).

For determining the mating type gene for the *M. canis* isolates, qualitative PCR using primers that target the alpha-box region (for the MAT1-1 locus) were utilized: Mc_alpha_F (5′-TCTCCTGCTGCCATGGCAACT) and Mc_alpha_R (5′-CAATGGGATTGATGTGGGCA) [Kosanke *et al.* 2018]. PCR and agarose gel conditions were identical to those used for ITS-1 PCR listed above. A 420 bp amplicon was considered positive for the alpha-box gene. Reference strain CBS 113480 was utilized as a positive control as it has been previously identified as belong to the MAT1-1 mating gene type [Li *et al.* 2010].

Qualitative PCR and agarose gel analysis was used to amplify and characterize SSU1 and SUB3 genetic content using the same as detailed above for the ITS-1 PCR, except the annealing temperature was 57 °C for SSU1 and 55 °C for SUB3. Primers for targeting the SSU1 gene were designed in Geneious (v10.0.9, Auckland, New Zealand) and primers for SUB3 were previously designed [Descamps *et al.* 2002] (Suppl. Table 2.2). Amplicons between 200 bp to 700 bp were considered positive for SSU1, and a 1149 bp amplicon was considered positive for SUB3. Sequences were compared to reference strain CBS 113480 using Geneious (v10.0.9).

2.2.6. Microsatellite PCR

Eight microsatellite loci (MS) were previously identified and verified in *M. canis* with corresponding primers for these regions [Sharma *et al.* 2007, Pasquetti *et al.* 2013]. To determine

the allele sizes for each of the eight microsatellites, Qiagen Multiplex PCR kit (Qiagen, Valencia, CA, USA) was used with 25 µL of Master Mix, 5 µL of 10× primer mix (each primer is at 2 µM concentration), 15 µL of DNase-free water, and 5 µL of DNA (DNA concentration ranged between 0.1–8.5 ng/µL) with a final reaction volume of 50 µL. Multiplex reactions were performed in two separate panels: Panel 1 contained MS 1, 4, 5, and 8, and Panel 2 contained MS 2, 3, 6, and 7 (Table 2.1). Forward primers were fluorescently labeled on the 5′ end using either 6-FAM, VIC, NED, or PET (Applied Biosystems, Carlsbad, CA, USA) (Table 2.1). The reaction was run on a C1000 Touch thermal cycler (Bio-Rad, Hercules, CA, USA) for 1 cycle at 95 °C for 15 min, 34 cycles at 94 °C for 30 s, 57 °C for 90 s, 72 °C for 1 min, and 1 cycle at 60 °C for 30 min.

When microsatellites had low quality or unusable results following multiplex PCR, singlet PCR was performed using Phusion High-Fidelity PCR master mix (ThermoFisher Scientific, Waltham, MA, USA) with a 50 µL reaction volume containing 25 µL of 2× Phusion master mix, 15 µL of DNase-free water, 2.5 µL of 10 µM primer F, 2.5 µL of 10 µM primer R, and 5 µL of DNA (DNA concentration ranged between 0.1–8.5 ng/µL). The thermocycler conditions were 98 °C for 30 s, 34 cycles of 98 °C for 10 s, annealing temperature for 30 s, 72 °C for 30 s, and 1 cycle of 72 °C for 10 min. The annealing temperatures used were 60 °C (primers of region 1, 2, 3, 4, 5, and 7), 62 °C (primers of region 8), and 58 °C (primers of region 6). CBS 113480 isolate was run as a positive control [Pasquetti *et al.* 2013] and DNase-free water was run as a negative control.

2.2.7. Microsatellite Analysis

PCR product length was assessed using a fragment analyzer (Psomagen, Rockville, MD, USA) and microsatellite allele sizes were classified using Geneious microsatellite plugin (Geneious v10.0.9, plugin v1.4.7) with size standards (GeneScan 500 LIZ, Rockville, MD, USA). To confirm allele calls, each allele was sent for fragment analysis multiple times until at least two high-quality reads produced the same allele size [Selkoe *et al.* 2006]. Loci were considered unusable if low-quality reads were obtained after three replicates.

2.2.8. Statistical Analysis of Genetic Clustering

To evaluate genetic variants among the samples, allele data for each sample were analyzed using the adegenet package (v2.1.3) of R (R version 4.0.4, Vienna, Austria) [Jombart 2008, Jombart *et al.* 2011]. Principal component analysis (PCA) plots were used to visualize dermatophyte microsatellite variation with respect to clinical and demographic characteristics (i.e., clinic location, sex and neuter status, previous housing, number of lesions, size of lesions, and disease severity). Analysis of variance (ANOVA) was performed on the clinical parameters of location, disease severity, lesion size and number of lesions to determine whether these parameters differed among clinics.

To test associations between clinical parameters and genetic distances among individual isolates, distance-based redundancy analysis (db-RDA) [Legendre *et al.* 1999] was performed using the function capscale in the vegan package (v2.5.7) [Oksanen *et al.* 2012] of R. Genetic distances were provided as a pairwise matrix of the inverse of the proportion of shared alleles, which were calculated from microsatellite genotypes using adegenet. ANOVA was performed in R on the db-RDA model to determine which of the explanatory variables were significant predictors of genetic distance. To ensure that results were not biased by low sample sizes and

thus potentially unrepresentative sampling from some clinics, the ANOVA was repeated using data from California and New Mexico clinics, which had 106 and 26 samples, respectively.

To characterize patterns of dermatophyte genetic structure, allele data were analyzed using two distinct approaches: STRUCTURE (v2.3.4, Stanford University, Stanford, CA, USA) [Pritchard *et al.* 2000] and the snapclust.choose.k function in adegenet (v2.1.3) [Jombart 2008, Jombart *et al.* 2011]. STRUCTURE implements Bayesian clustering algorithms to estimate the number of distinct clusters (K) that best describes genetic variation among samples and, for each sample, estimates the probability of belonging to each cluster. Ten independent runs were performed for K values one to eight using the admixture model with a burn-in period of 10,000 replications and then 100,000 Markov chain Monte Carlo (MCMC) replications. To determine the optimal K for our dataset, CLUMPAK's Best K function was utilized [Evanno *et al.* 2005, Kopelman *et al.* 2015]. This program determines the optimal K value using two methods: one where the uppermost level of structure is found and one where Pr(K = k) is the highest [Evanno *et al.* 2005, Kopelman *et al.* 2015]. Additionally, the optimal number of clusters was also estimated using snapclust.choose.k, which utilizes goodness-of-fit statistics to identify genetic clusters [Jombart 2008, Jombart *et al.* 2011]. As before, we tested models for one up to eight genetic clusters.

2.3. Results

2.3.1. Majority of Dermatophytosis Cases Are from Stray Intact Kittens with Multiple Alopecic Lesions

Two hundred and fifty-eight samples were received from seven clinics in five states (165 from California; 53 from New Mexico; eight from Boulder County, CO; 14 from Larimer

County, CO; eight from Weld County, CO; eight from Massachusetts; and two from New Jersey); 206 of these were paired with sample survey data (Table 2.2). Of the received samples, 191 (74%) were culture positive for *M. canis* confirmed by ITS-1 sequencing. 154 of 191 *M. canis* positive samples had accompanying clinical survey data and were included in the study (Table 2.2). Ninety-seven point four percent of 154 samples (n = 150) were collected from shelters and 2.6% (n = 4) from individual cases referred by private practitioners. Ninety-six point eight percent of 154 samples (n = 149) were from kittens (aged to be younger than one year based on dentition), 89% (n = 137) were domestic shorthair (DSH) breed, 89% were intact (n = 137) and 89% (n = 137) were strays upon presentation. Nearly three quarters (73.6%, n = 113) had more than two lesions present and 89% (n = 137) had alopecic lesions (Table 2.3 and Suppl. Table 2.3). Most of the lesions were distributed on the head (81%, n = 125) and legs including the paws (50%, n = 77). The majority of patients (74%, n = 114) did not have concurrent medical conditions reported. The most common concurrent medical condition was upper respiratory infection (18.2%, n = 28), followed by ectoparasites (3.2%, n = 5). In addition, 151 of 154 patients (98.1%) had Wood's lamp performed before sample collection and 87.4% (132 of 151) were Wood's lamp positive (Table 2.3). Based on the clinical presentation, most of the patients were classified with mild (31.8%, n = 49) or moderate (25.3%, n = 39) disease severity. Clinical survey data were not collected for Weld County, CO samples (n = 8), and were not included for New Jersey patients treated with anti-fungal medication before collection of samples (n = 2).

2.3.2. Microsatellite Variation among Samples

Of the 191 culture positive samples, 180 were successfully sequenced at six or more microsatellite loci (Fig. 2.1). The number of alleles per MS ranged from 3 (MS3) to 13 (MS4)

(Fig. 2.2 and Suppl. Table 2.4). Of the 180 genotyped samples, 122 unique multilocus genotypes were observed. There were two genotype combinations observed in nine cats from either California or New Mexico, representing the most frequently observed single genotypes (n = 9) (Suppl. Table 2.4). The genotype combination of reference strain CBS 113480 was not observed amongst the clinical samples (Suppl. Table 2.4). MS4 had the greatest variability with most frequently observed allele occurring in 43% of the samples, while MS3 showed the lowest variation, with the majority of samples (79%) having a 114 bp allele at this locus (Fig. 2.2 and Table 2.4). The other MS ranged in size from 105 bp to 117 bp (MS1), 95 bp to 101 bp (MS2), 96 bp to 106 bp (MS5), 105 bp to 115 bp (MS6), 121 bp to 127 bp (MS7), and 112 bp to 118 bp (MS8) (Table 2.4). Across all MS, the percent of missing alleles per locus ranged from 0% (MS2, 5) to 21% (MS6) (Table 2.4).

2.3.3. All M. canis Isolates Expressed the MAT1-1 Mating Type Locus

For the 180 *M. canis* isolates that were utilized for microsatellite genotyping, qualitative PCR for the mating locus alpha-box gene was performed. An amplification product was observed at 420 bp for each isolate, indicating that all isolates were of the negative mating gene type (MAT1-1) (Suppl. Table 2.4).

2.3.4. Homologous Sequences for SSU1 and SUB3 between Isolates

Of the 180 *M. canis* isolates utilized for the microsatellite PCRs, the SSU1 genes were characterized for 46 isolates from varied sites including Boulder (n = 3); New Mexico (n = 7); California (n = 24); Larimer County, CO (n = 3); Weld County, CO (n = 6); Massachusetts (n = 2); and New Jersey (n = 1) (NCBI GenBank accession numbers ON799017-62). Six isolates

from California were evaluated for SUB3 gene sequence (NCBI GenBank accession numbers ON755064–68). The sequences for SSU1 and SUB3 for all isolates were 100% identical to reference strain CBS 113480 [Descamps *et al.* 2002, Martinez *et al.* 2012].

2.3.5. Clinic Location and Disease Severity Were Associated with Microsatellite Genotype

db-RDA modeling using ANOVA indicated significance among clinical parameters (*p*-value = 0.001, Fig. 2.3). Both clinic location (*p*-value = 0.001) and disease severity (*p*-value = 0.004) were found to be significant predictors of genetic distance (Fig. 2.3 and Suppl. Table 2.5). To test the correlation between disease severity and location, we performed an ANOVA and found that disease severity differed among locations (*p*-value = 0.0049) with number of lesions and size of lesions not varying significantly among locations (*p*-value = 0.34 and *p*-value = 0.57, respectively). However, when db-RDA analysis included only clinics with large sample sizes (California and New Mexico), we found that the association between disease severity and genetic distance was still significant (*p*-value = 0.012 and *p*-value 0.011, respectively, Suppl. Table 2.6).

PCA plots were used to summarize *M. canis* genetic variants with respect to six parameters, including: (1) geographic location of clinic, (2) sex/neuter status, (3) clinical disease severity, (4) number of lesions present, (5) lesion(s) size, and (6) previous housing environment. Three distinct genetic groups were identified in relation to clinic of origin. Samples from the Boulder County, CO and Massachusetts appeared genetically distinct from other sites (Fig. 2.4). One sample from Massachusetts was distinct from all other samples. This sample was coincidentally the only Persian cat analyzed in this study (Fig. 2.4, Suppl. Table 2.3). The third genetic group contained samples from California, where the majority of the samples clustering had been collected during the same month.

2.3.6. Genetic Clustering of M. canis Isolates

STRUCTURE analysis indicated the greatest support for three distinct genetic clusters (K = 3) according to both the ΔK and prob(K) metrics (Suppl. Fig. 2.1). However, snapclust.choose.k indicated five genetic clusters (K = 5; Suppl. Fig. 2.1). To resolve this discrepancy, we scrutinized plots showing genetic cluster membership probabilities of individual *M. canis* isolates for K = 3–5 (Fig. 2.5). We found that neither the K = 4 nor K = 5 models revealed any additional genetic structure among samples that was not evident with K = 3, suggesting that K = 3 was the most biologically informative model (Fig. 2.5).

Because of this, and because K = 3 was most consistent with the PCA results, we concluded that there were most likely three genetic clusters among our *M. canis* isolates. The three *M. canis* genetic clusters appeared to be partly associated with different clinics (Fig. 2.5). Samples from the Boulder County, CO; Larimer County, CO; Massachusetts; and New Jersey clinics clustered in one group (dark blue/purple, Fig. 2.5). California samples comprised two genetic clusters (orange, light blue, Fig. 2.5). The New Mexico and Weld County, CO clinics comprised samples that assigned to both the California and Boulder genetic clusters (Fig. 2.5). Genetic clusters were not related to sex/neuter status, previous housing environment, number of lesions, size of lesions, and disease severity (Suppl. Figs. 2.2–2.6).

2.4. Discussion

Few studies have assessed genotypic or regional factors that influence dermatophyte clinical presentation [Gräser *et al.* 2007, Sharma *et al.* 2007, Viani *et al.* 2007]. These studies have utilized microsatellite DNA polymorphisms as this is an established method for genotypic

comparisons among large sample sets and have been identified in dermatophytes [Sharma *et al.* 2007, Pasquetti *et al.* 2013]. With two microsatellite loci, 101 *M. canis* isolates were classified as three distinct populations [Sharma *et al.* 2007]. One of these populations was found to be over-represented in human samples, implying that this group has a greater ability to infect humans due to higher virulence in humans[Sharma *et al.* 2007]. Clinical presentations were classified based on anatomical location for human samples (e.g., tinea capitis, tinea corporis, etc.) whereas cases in animals were characterized as ringworm [Sharma *et al.* 2007]; however, no associations between genotype and clinical presentation were identified [Sharma *et al.* 2007].

Da Costa et al. [da Costa *et al.* 2013] utilized two microsatellite loci identified by Sharma et al. [Sharma *et al.* 2007] to analyze 102 *M. canis* isolates from Brazil isolated from humans, cats, and dogs. Fourteen distinct multilocus genotypes and six distinct populations were identified [da Costa *et al.* 2013]. Genotypes were compared to age, sex, breed, symptomatology, geographical location, and living conditions, and broadly characterized symptoms (asymptomatic, focal ringworm, multifocal ringworm, ringworm, and pseudomycetoma) [da Costa *et al.* 2013]. No correlations were noted between genotypes at two microsatellite loci and these parameters [da Costa *et al.* 2013]. Notably, these previous attempts to associate genotypes with clinical parameters had limited statistical power owing to the use of a very small number of loci. Further investigation using a greater number of loci is necessary to quantify genetic variants with sufficient precision to identify associations with clinical parameters.

Expanding upon previous microsatellite studies, our results demonstrated that disease severity is associated with genetic distance of *M. canis* isolates, suggesting that *M. canis* genetics play a significant role in clinical presentation. Understanding this difference in virulence between genotypes could be beneficial in implementing treatment plans as strains that cause

more severe disease might require more intensive therapy, particularly if the patient has co-morbidities. Previous studies of dermatophytosis have demonstrated more severe inflammatory infections generally resolve faster, suggesting that the host immune system is effective at clearing the infection [Hube *et al.* 2015]. Knowing that certain *M. canis* genotypes can cause more severe disease can help clinicians better predict when infections will resolve. Although we identified genetic differentiation with respect to disease severity, it is unlikely that the MS analyzed are associated with fungal virulence genes as these loci are not associated with specific gene products. However, our results suggest that variation in *M. canis* virulence may be at least partly genetically determined. Further studies implementing more extensive genome-wide sequencing approaches are warranted to identify the genetic basis of *M. canis* virulence.

Genetic clustering was observed with respect to clinic location, suggesting that location or clinic-specific genotypes of *M. canis* may occur. This finding may represent *M. canis* spread within a specific site or setting. As the sample size for five of seven locations was less than 10 individuals per clinic, it is unlikely that samples from these clinics are truly representative of the genetic variants present in the surrounding regions. These regions that had clinic locations align with the clusters (Boulder County, Massachusetts, and California) have different climates, and represent private practices (Massachusetts) and shelters (Boulder, California), further suggesting that the observed clustering has clinic-specific factors involved. Samples from the Massachusetts clinic were collected over months from different private owners, suggesting that the genotype was more region-specific, since these cats with ringworm were unlikely to have been exposed to one another.

We noted one highly divergent *M. canis* genotype isolated from the only sample from a Persian cat included in this study. Persian cats have been reported to have a higher prevalence of

dermatophytosis [Scott *et al.* 1990, Lewis *et al.* 1991], although it has been suggested that it is due to sampling bias [Moriello *et al.* 2017]. Long-haired cats (including Persians) have also been shown to have higher rates of subclinical dermatophytosis due to their longer coats [Sattasathuchana *et al.* 2020]. Further sample collection from Persian and other long-haired cats could elucidate if certain *M. canis* genotypes preferentially infect these breeds and if clinical disease differs in these infections.

The reference strain CBS 113480 demonstrated a different genotype that was not observed in our data set, with two loci containing novel alleles. While our samples were from domestic cats in the Unites States, this reference strain was originally isolated from a human in Germany, suggesting that different *M. canis* strains could be present in the United States compared to in Europe, and that strains circulating on cats could be different from ones infecting humans. The allele values for the eight microsatellite loci for the reference strain have been previously published and are slightly different from our genotype results, likely due to differences in equipment and software used for genotyping inherent in microsatellite analysis [Ewen *et al.* 2000, Johansson *et al.* 2003].

Given that dermatophytes can utilize both sexual and asexual modes of reproduction [Rippon *et al.* 1969, Weitzman *et al.* 1978, Gräser *et al.* 2007, Kosanke *et al.* 2018], identifying the mating types for different isolates can help understand genetic mixing in the population. Dermatophytes have two mating types, positive and negative, which correspond to the mating type genes high mobility group and alpha-box, respectively [Kosanke *et al.* 2018]. Understanding dermatophyte mating types can reveal if populations have shifted toward one form of reproduction and the possible effect this can have on the genotypes present, which is particularly important for tracking virulence genes.

For our study, all samples that were utilized for microsatellite analysis were determined to possess the MAT1-1 mating locus, suggesting that this mating locus is dominant in the United States, making *M. canis* more reliant on asexual reproduction. It has been previously suggested that the MAT1-2 mating locus for *M. canis* has become extinct [Kosanke *et al.* 2018] with the only known MAT1-2 *M. canis* isolates originating from Japan [Hironaga *et al.* 1980]. The extinction of one mating type and loss of sexual reproduction has been documented for various other dermatophyte species, including *Trichophyton rubrum* morphotype "megninii", *Trichophyton tonsurans*, *Trichophyton interdigitale*, *Trichophyton schonleinii*, *Trichophyton concentricum*, *Microsporum audouinii*, and *Microsporum ferrugineum*, all of which are anthropophilic [Kosanke *et al.* 2018]. It has been suggested that this shift in mating type distribution reflects the fungi becoming more adapted to a particular host species, leading to a loss of interaction between the two mating types [Kosanke *et al.* 2018]. This shift could suggest that *M. canis* is becoming more adapted to cats as they are the primary host, indicating that infections could become more chronic and less inflammatory, similarly to infections caused by anthropophiles that rely on asexual reproduction [Moriello 2014, de Hoog *et al.* 2017, Kosanke *et al.* 2018].

Two potential virulence genes for *M. canis* include sulfite efflux pump (SSU1) and subtilisin 3 (SUB3) as these genes are critical for the beginning stages of infection [Mignon *et al.* 1998, Léchenne *et al.* 2007, Baldo *et al.* 2008, Grumbt *et al.* 2013]. Both genes were 100% identical to the reference isolate CBS 113840 for the samples analyzed, suggesting that these genes are conserved between isolates. Due to the importance of these genes for establishing infections, mutations in these genes would likely be deleterious, reducing the fungus' chances of

survival. Exploring the level of expression of these genes could elucidate the potential differences of clinical presentation for various isolates.

In addition to genetics, another interesting component of our work investigated the demographics of the study populations. Kittens are known to have higher rates of *M. canis* clinical infection [Moriello 2014, Moriello *et al.* 2017], a finding represented in our study. Because our sample set was strongly biased to clinical samples from shelter animals, this undoubtedly affected our findings, though higher rates of infection in kittens compared to adult cats generally is thought to be related to maturation of the immune system [Day 2007]. While the immune system is considered competent by 6–12 weeks of age in cats, the cellular processes critical for eliminating dermatophytes (the maturation of phagocytic and antigen-presenting cells) have not been studied [Day 2007]. Mature versions of these phagocytic and antigen-presenting cells are responsible for removing dermatophytes from the host through extra/intracellular lysis of the fungi and cytokine production [Jartarkar *et al.* 2021]. However, immature versions of these cells could have a delayed or less potent response during the beginning stages of infection, preventing kittens from quickly eliminating infection before clinical signs develop. Further investigation into immature immune systems of cats could help elucidate key differences that occur in neonatal and adolescent cats, particularly during fungal infections.

The majority of patients with clinical data reported positive fluorescence under a Wood's lamp, suggesting that Wood's lamp is an effective screening tool for *M. canis* infections in cats. The reported percentage of *M. canis* strains that fluoresce following Wood's lamp examination ranges from 45.5% [Cafarchia *et al.* 2004] to 100% [DeBoer *et al.* 1994]. Reports from the 1950s associated fluorescence of *M. canis* with production of the compound pteridine [Wolf 1957,

Wolf *et al.* 1958]. It is unclear if different isolates have varying ability to produce pteridine or other fluorescent metabolites, or if this metabolite is only produced during certain stages of infection. The metabolic pathway that produces pteridine and the precursor metabolites have not been investigated. Future studies of pteridine and associated metabolic pathways could help explain the function of this product and whether it represents a potential target for a metabolic-based diagnostic assay.

Table 2.1. Primer sequences with corresponding fluorescent dyes (6-FAM, VIC, NED, and PET) used for the microsatellite loci.

Panel	Microsatellite Locus	Orientation	Primer Sequence 5′ to 3′	Reference
1	1	Forward	[VIC]GAAGGAGGTATATATGGGTGTG	[Pasquetti *et al.* 2013]
		Reverse	GATAAGGTGTTTGGCACTGA	
	4	Forward	[6-FAM]CAGCATCTAAATAACTGGCCTA	[Pasquetti *et al.* 2013]
		Reverse	TTTTCTTTCTACTTCCCGTTG	
	5	Forward	[NED]GGTTTACACGCAGCATGA	[Pasquetti *et al.* 2013]
		Reverse	CGTGGCTGAAGAAGTCTACC	
	8	Forward	[PET]GATCGGAGCATGCCATACAG	[Sharma *et al.* 2007]
		Reverse	TCTTCCCACCCTTCTCAATG	
2	2	Forward	[NED]GGGAACAATCTGCCTTAAAC	[Pasquetti *et al.* 2013]
		Reverse	CACAGAGATATGCCGTATGC	
	3	Forward	[PET]AGGTGTTTGGCACTGAGC	[Pasquetti *et al.* 2013]
		Reverse	CGAAGAGAAGGAGGTATATATGG	
	6	Forward	[6-FAM]CGTCTGGGACTTGGTAGTAA	[Pasquetti *et al.* 2013]
		Reverse	TCGGAGGATCTTTAAACTGT	
	7	Forward	[VIC]GCCAAAGAGCTTGCTGAG	[Pasquetti *et al.* 2013]
		Reverse	CGTTAGCATGCATCTCTCTATAC	

Table 2.2. One hundred forty-seven samples were included in microsatellite analysis associated with reported clinical attributes.

Sample Categories	CA	NM	BC	LC	WC	MA	NJ	Total
Samples received	165	53	8	14	8	8	2	**258**
Culture positive samples	132	42	6	4	6	5	1	**191**
Samples with clinical data	139	36	8	14	0	7	2 *	**206**
Culture + clinical data	109	31	6	4	0	4	1 *	**155**
Microsatellite samples	122	36	6	4	6	5	1	**180**
Microsatellite + clinical data	106	26	6	4	0	4	1 *	**147**

* clinical data from New Jersey samples were excluded from downstream analysis due to the patients being treated from dermatophytosis prior to sample collection. Culture + clinical data samples are samples that were culture positive for *Microsporum canis* and had corresponding clinical data for the patient. Microsatellite + clinical data samples are samples that were successfully sequenced for the microsatellite regions and had corresponding clinical data for the patient. CA = California; NM = New Mexico; BC = Boulder County, CO; LC = Larimer County, CO; WC = Weld County, CO; MA = Massachusetts; NJ = New Jersey.

Table 2.3. Summary of clinical presentation data for *Microsporum canis* positive cats.

Clinical Parameters	**Total (*n* = 154)**
Sample from shelter or private practice	Shelter (150, 97.4%) Private practice (4, 2.6%)
Age	Kitten (149, 96.8%)
Sex	Female (74, 48.1%)
Neuter status	Intact (138, 89.6%)
Breed	DSH (137, 89%) DMH (11, 7.1%) DLH (4, 2.6%) Persian (1, 0.6%) Exotic Shorthair (1, 0.6%)
Previous housing environment	
Stray	1 (138, 89.6%)
Single cat—owned household	2 (0, 0%)
Multi cat—owned household	3 (3, 1.9%)
Previously owned—other animals unknown	4 (2, 1.3%)
Transferred from shelter	5 (11, 7.1%)
Current housing environment	
Shelter/rescue—single cat kennel	1 (40, 26%)
Shelter/rescue—multiple cat kennel	2 (109, 70.8%)
Client owned—single cat household	3 (1, 0.6%)
Client owned—multiple cay household	4 (4, 2.6%)
Current medications *	
Yes—topical parasite preventatives or dewormer	1 (32, 20.8%)
Yes—oral parasite preventatives or dewormer	2 (57, 37%)
Yes—other	3 (2, 1.3%)
No	4 (83, 53.9%)
Concurrent medical conditions *	URI (28, 18.2%) Ectoparasites (5, 3.2%) Superficial pyoderma (1, 0.6%) IBD (1, 0.6%) Diarrhea (1, 0.6%) Otitis media (1, 0.6%) Degloved chin (1, 0.6%) Underweight (1, 0.6%) None (114, 74%)
Diagnostics performed *	
Wood's lamp	1 (151, 98.1%)
Fungal culture	2 (10, 6.5%)
IDEXX PCR	3 (4, 2.6%)
Hair observed under microscope	4 (2, 1.3%)
Other	5 (3, 1.9%)
None	6 (1, 0.6%)
If diagnostics have been performed, what were the results?	Wood's lamp positive (132, 87.4%)
Number of lesions	

1	1 (29, 18.8%)
2–5	2 (67, 43.5%)
5+	3 (46, 29.9%)
None—no lesions present	4 (12, 7.8%)
Size of lesions	
Less than 0.5 inch (smaller than a dime)	1 (62, 40.2%)
Between 0.5 inch and 1 inch (size of a penny)	2 (59, 38.3%)
Greater than 1 inch (larger than a penny)	3 (21, 13.6%)
N/A—no lesions present	4 (12, 7.8%)
Lesion distribution *	
Head	1 (124, 80.5%)
Neck	2 (46, 30%)
Abdomen	3 (46, 30%)
Back	4 (31, 20.1%)
Tail including base of tail	5 (28, 18.2%)
Legs including paws	6 (77, 50%)
N/A—no lesions present	7 (12, 7.8%)
Lesion types *	
Alopecia	1 (137, 89%)
Scales/crusts	2 (95, 61.7%)
Reddened/erythematous	3 (9, 5.8%)
Papules/pustules	4 (0, 0%)
Miliary dermatitis	5 (2, 1.3%)
N/A—no lesions present	6 (12, 7.8%)
Disease severity	
Mild—lesions are small and confined to focal area	1 (49, 31.8%)
Mild to moderate	2 (20, 13%)
Moderate—lesions are found in multiple areas, but is not widespread	3 (39, 25.3%)
Moderate to severe	4 (14, 9.1%)
Severe—lesions are large and found all over the body	5 (20, 13%)
N/A—no lesions present	6 (12, 7.8%)

* = Percentages are greater than 100 as patients can have more than one answer. DSH = domestic shorthair, DMH = domestic medium hair, DLH = domestic long hair, N/A = not applicable, URI = upper respiratory infection, IBD = inflammatory bowel disease.

Table 2.4. Eight microsatellite loci demonstrate different degrees of polymorphism across samples tested.

Microsatellite Locus	Allele Size Range	Most Common Allele (% of Alleles)	% of Missing Genotypes
1	105–117 bp	115 bp (72%)	7.2%
2	95–101 bp	97 bp (78%)	0%
3	110–116 bp	114 bp (79%)	13%
4	103–161 bp	155 bp (43%)	1.7%
5	96–106 bp	102 bp (47%)	0%
6	105–115 bp	109 bp (48%)	21%
7	121–127 bp	125 bp (81%)	2.2%
8	112–118 bp	116 bp (79%)	2.2%

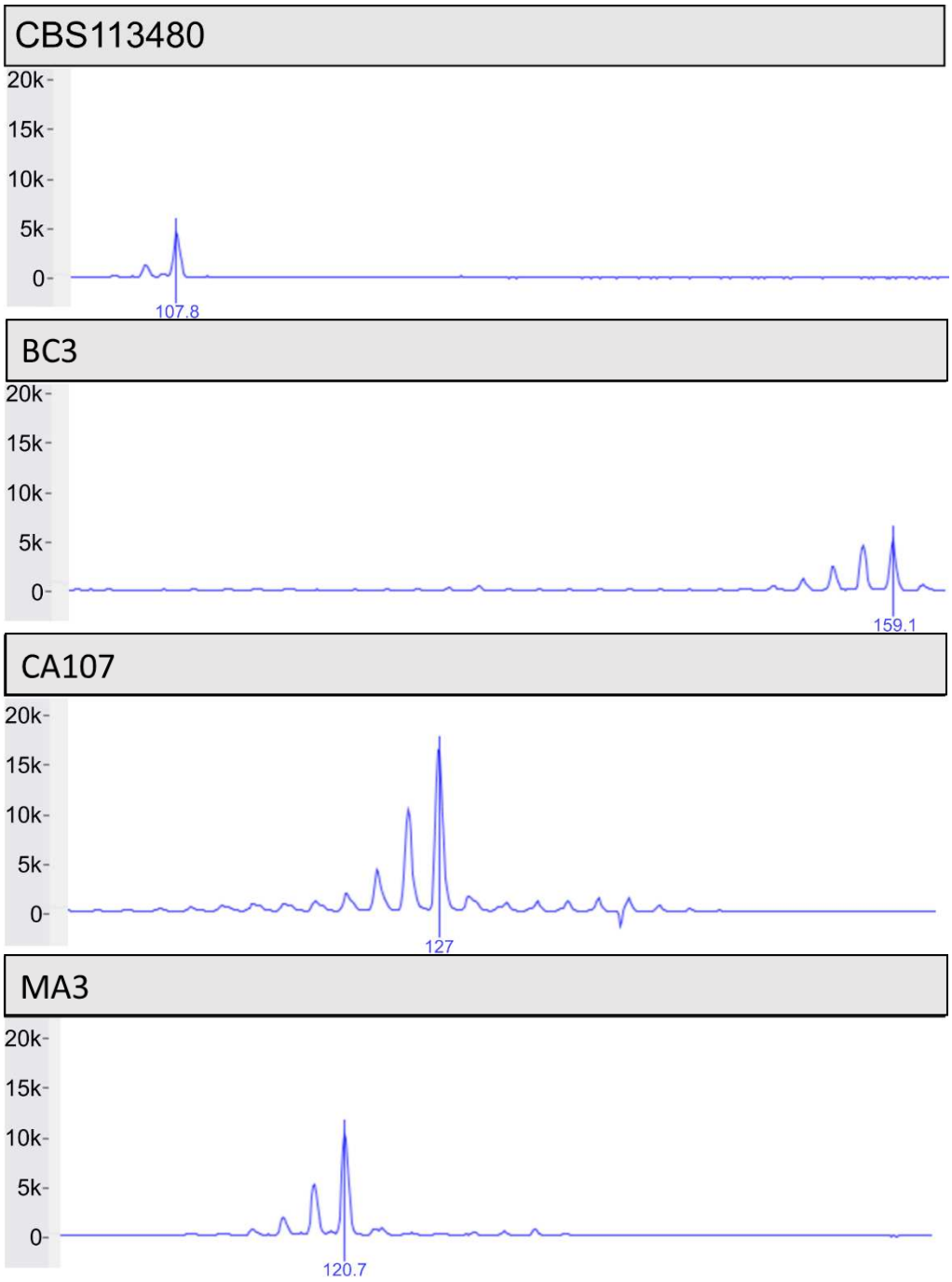

Figure 2.1. Representative images of microsatellite genotypes. MS4 peaks of unrelated isolates (CBS 113480, BC3, CA107, MA3) showing varying allele sizes at 107 bp, 159 bp, 127 bp, and 121 bp, respectively. CBS = Westerdijk Fungal Biodiversity Centre; BC = Boulder County, CO; CA = California; MA = Massachusetts.

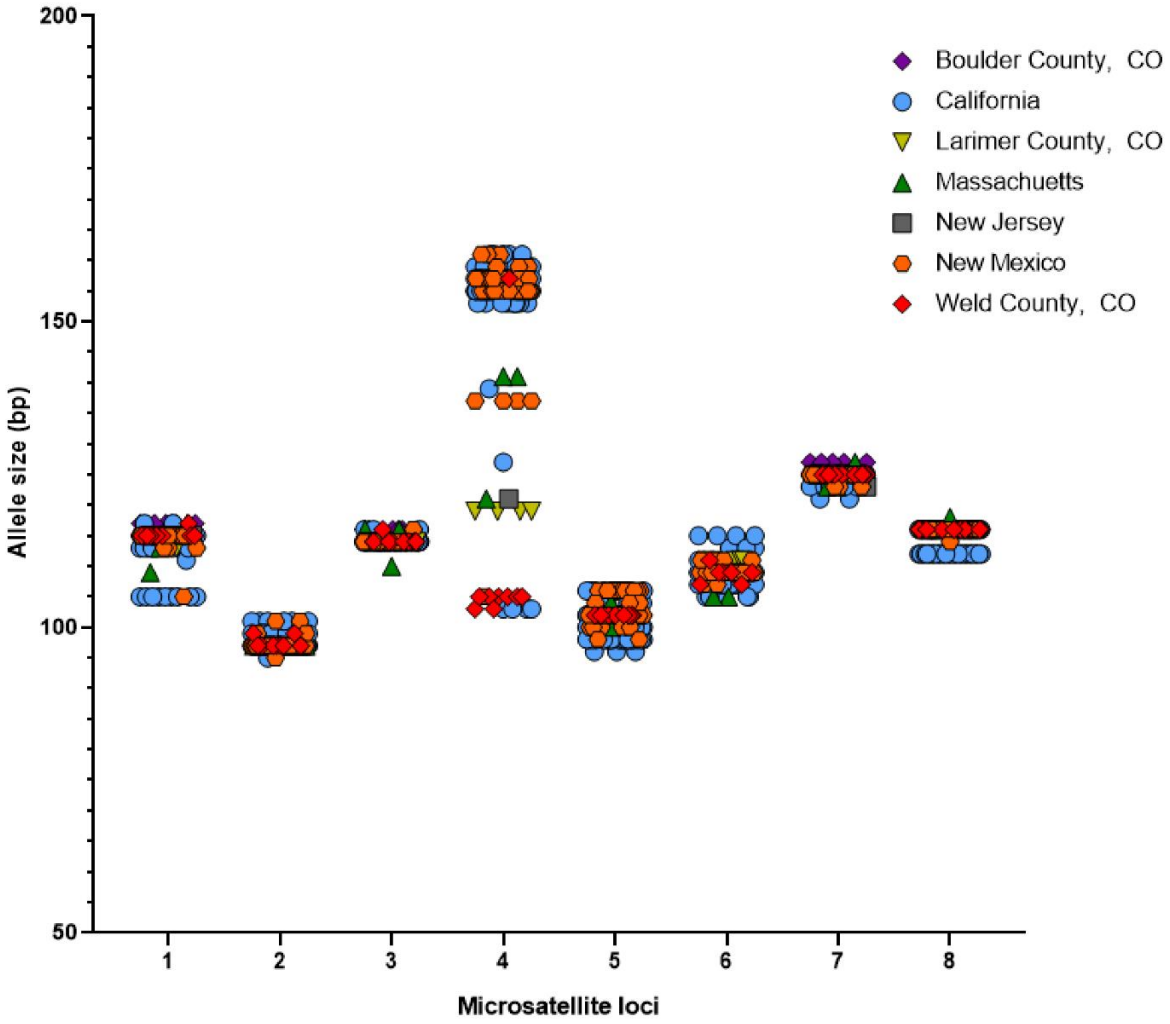

Figure 2.2. Microsatellite locus allelic diversity varies among *Microsporum canis* isolates. Allele sizes for microsatellite loci (MS) 1–8 for each sample are plotted with Boulder County, CO (*n* = 6); California (*n* = 122); Larimer County, CO (*n* = 4); Massachusetts (*n* = 5); New Jersey (*n* = 1); New Mexico (*n* = 36); Weld County, CO (*n* = 9). The microsatellite loci had the following ranges: 105–117 bp (MS1), 95–101 bp (MS2), 110–116 bp (MS3), 103–161 bp (MS4), 96–106 bp (MS5), 105–115 bp (MS6), 121–127 bp (MS7), and 112–118 bp (MS8).

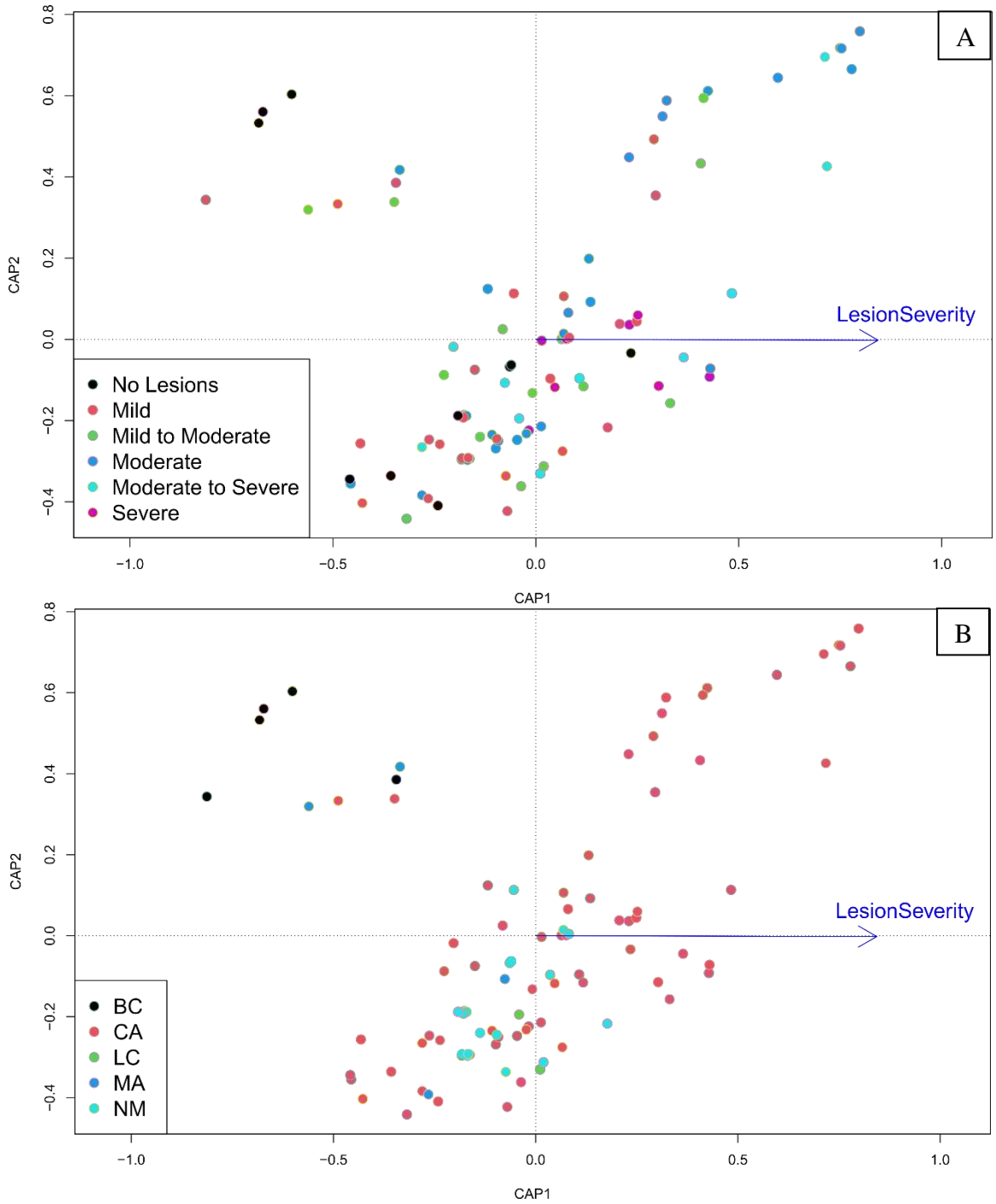

Figure 2.3. Disease severity and location associated with microsatellite genotype. Distance-based redundancy analysis showed significant association between disease severity and microsatellite variation. A—samples colored based on clinic location. B—samples colored by disease severity. Locations included in study are California (CA); New Mexico (NM); Boulder County, CO (BC); Larimer County, CO (LC); and Massachusetts (MA). Position on the plot for each sample depicts genetic differentiation. Arrow = disease severity increases direction of arrow.

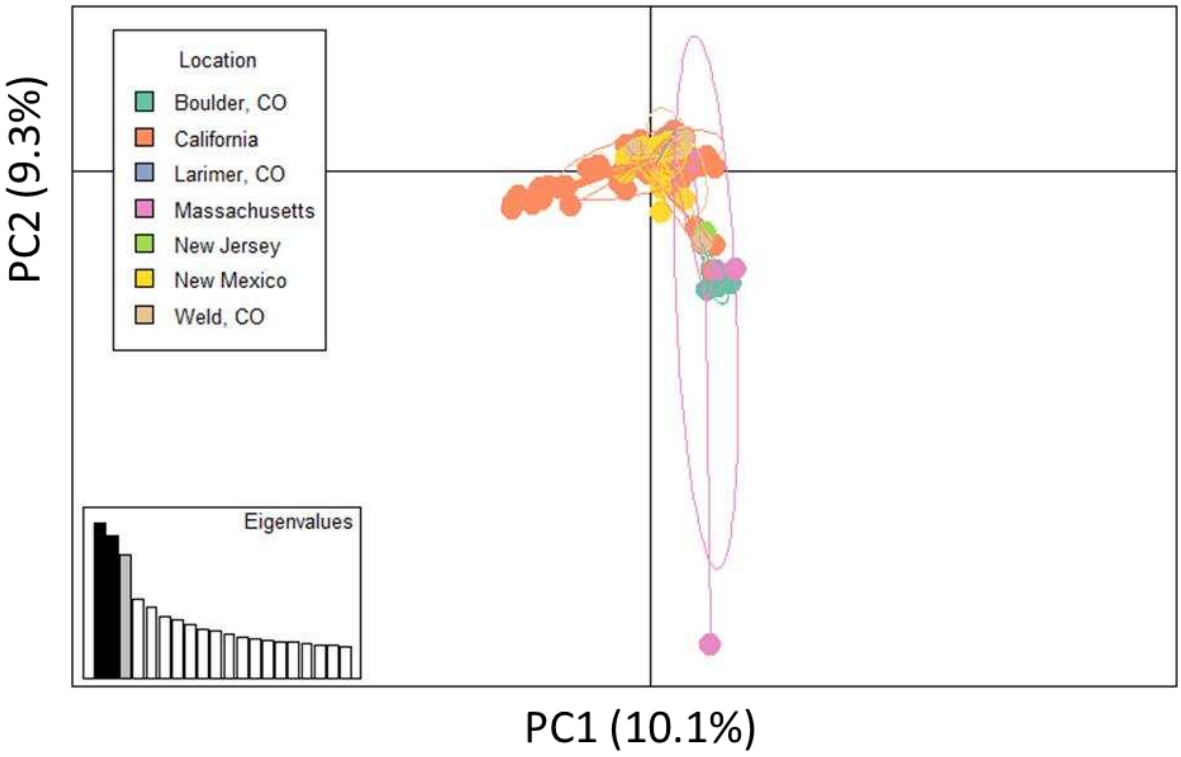

Figure 2.4. Evidence of separation based on clinic location for Boulder, Massachusetts, and part of California. Principal component analysis (PCA) plot for microsatellite regions, with samples colored according to clinic. One sample from Massachusetts was an outlier. The portion of California samples that appear distinct were collected in the same month. Locations included in study are California; New Mexico; Boulder County, CO; Larimer County, CO; Weld County, CO; New Jersey; and Massachusetts.

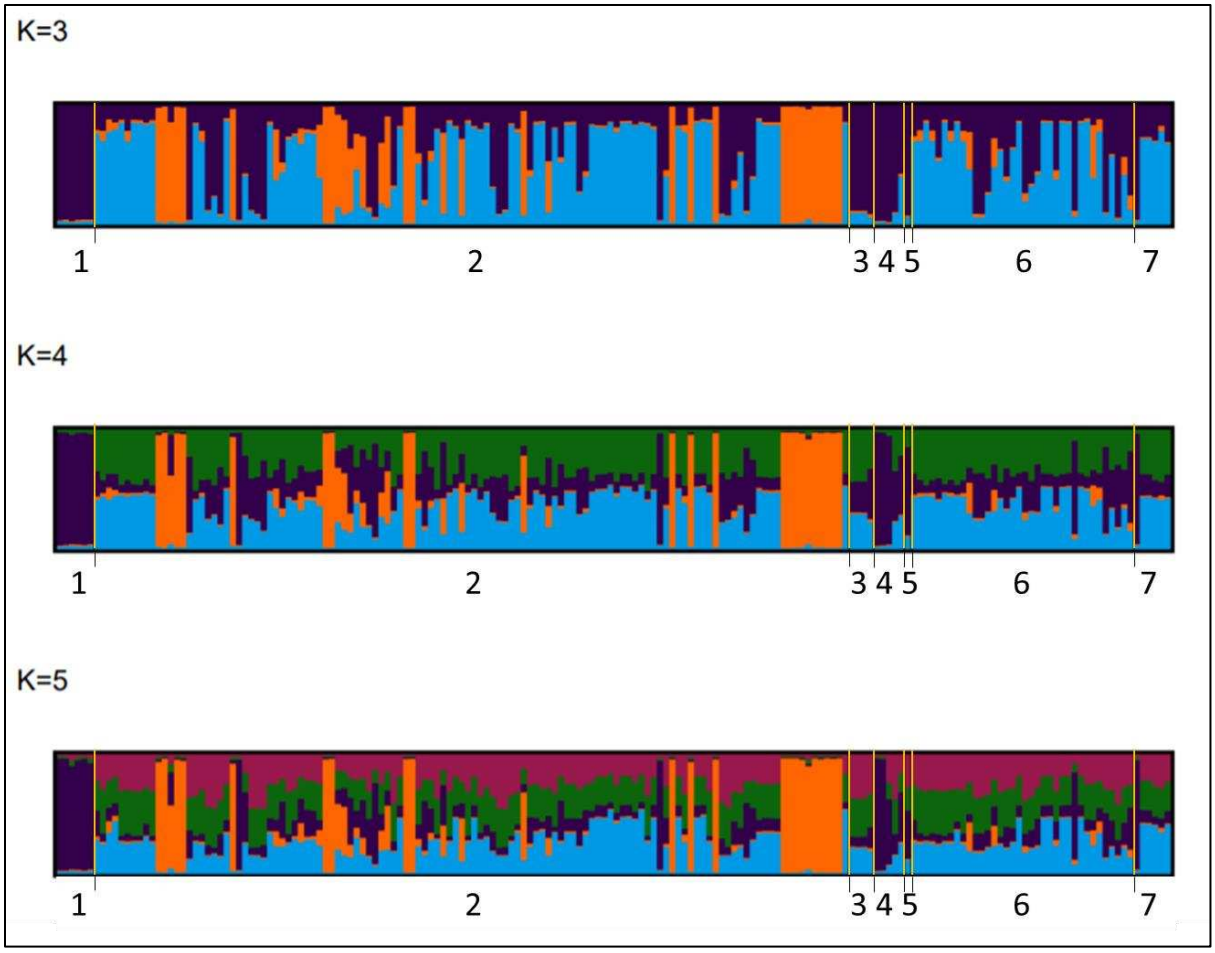

Figure 2.5. Samples from Boulder County, CO and a portion of California clustered apart from other sampled locations. Structure plots with K values 3–5. The amount of vertical color for each sample corresponds with the percentage of belonging to that color cluster. Admixture increased for plots using K = 4 and K = 5. Locations included in study were Boulder County, CO (1); California (2); Larimer County, CO (3); Massachusetts (4); New Jersey (5); New Mexico (6); and Weld County, CO (7).

Literature Cited

Baldo A, Tabart J, Vermout S, et al. (2008). Secreted subtilisins of Microsporum canis are involved in adherence of arthroconidia to feline corneocytes. *Journal of Medical Microbiology* **57**(9):1152-1156.

Bergmans AMC, van der Ent M, Klaassen A, et al. (2010). Evaluation of a single-tube real-time PCR for detection and identification of 11 dermatophyte species in clinical material. *Clinical Microbiology and Infection* **16**(6):704-710.

Brillowska-Dąbrowska A, *DNA preparation from nail samples*, W.I.P. Organization, Editor. 2006: Denmark.

Cafarchia C, Romito D, Sasanelli M, et al. (2004). The epidemiology of canine and feline dermatophytoses in southern Italy. *Mycoses* **47**(11-12):508-513.

da Costa FVA, Farias MR, Bier D, et al. (2013). Genetic variability in Microsporum canis isolated from cats, dogs and humans in Brazil. *Mycoses* **56**(5):582-588.

Day MJ. (2007). Immune System Development in the Dog and Cat. *Journal of Comparative Pathology* **137**(S10-S15.

de Hoog GS, Dukik K, Monod M, et al. (2017). Toward a Novel Multilocus Phylogenetic Taxonomy for the Dermatophytes. *Mycopathologia* **182**(1):5-31.

DeBoer DJ and Moriello KA. (1994). Development of an experimental model of Microsporum canis infection in cats. *Veterinary microbiology* **42**(4):289-295.

Descamps F, Brouta F, Baar D, et al. (2002). Isolation of a Microsporum canis Gene Family Encoding Three Subtilisin-Like Proteases Expressed in vivo. *Journal of Investigative Dermatology* **119**(4):830-835.

Di Pilato V, Codda G, Ball L, et al. (2021). Molecular Epidemiological Investigation of a Nosocomial Cluster of C. auris: Evidence of Recent Emergence in Italy and Ease of Transmission during the COVID-19 Pandemic. *Journal of fungi (Basel, Switzerland)* **7**(2):140.

Engelthaler DM, Chiller T, Schupp JA, et al. (2011). Next-generation sequencing of Coccidioides immitis isolated during cluster investigation. *Emerg Infect Dis* **17**(2):227-32.

Etienne KA, Gillece J, Hilsabeck R, et al. (2012). Whole genome sequence typing to investigate the Apophysomyces outbreak following a tornado in Joplin, Missouri, 2011. *PloS one* **7**(11):e49989.

Evanno G, Regnaut S, and Goudet J. (2005). Detecting the number of clusters of individuals using the software structure: a simulation study. *Molecular Ecology* **14**(8):2611-2620.

Ewen KR, Bahlo M, Treloar SA, et al. (2000). Identification and analysis of error types in high-throughput genotyping. *American journal of human genetics* **67**(3):727-736.

Frymus T, Gruffydd-Jones T, Pennisi MG, et al. (2013). Dermatophytosis in Cats: ABCD guidelines on prevention and management. *Journal of feline medicine and surgery* **15**(7):598-604.

Fuller LC. (2009). Changing face of tinea capitis in Europe. *Curr Opin Infect Dis* **22**(2):115-8.

Ginter-Hanselmayer G, Weger W, Ilkit M, et al. (2007). Epidemiology of tinea capitis in Europe: current state and changing patterns. *Mycoses* **50**(s2):6-13.

Gräser Y, Fröhlich J, Presber W, et al. (2007). Microsatellite markers reveal geographic population differentiation in Trichophyton rubrum. *Journal of Medical Microbiology* **56**(8):1058-1065.

Grumbt M, Monod M, Yamada T, et al. (2013). Keratin Degradation by Dermatophytes Relies on Cysteine Dioxygenase and a Sulfite Efflux Pump. *Journal of Investigative Dermatology* **133**(6):1550-1555.
Hay RJ. (2017). Tinea Capitis: Current Status. *Mycopathologia* **182**(1-2):87-93.
Hironaga M, Nozaki K, and Watanabe S. (1980). Ascocarp production by Nannizzia otae on keratinous and non-keratinous agar media and mating behavior of N. otae and 123 Japanese isolates of Microsporum canis. *Mycopathologia* **72**(3):135-141.
Hube B, Hay R, Brasch J, et al. (2015). Dermatomycoses and inflammation: The adaptive balance between growth, damage, and survival. *Journal de Mycologie Médicale* **25**(1):e44-e58.
Jartarkar SR, Patil A, Goldust Y, et al. (2021). Pathogenesis, Immunology and Management of Dermatophytosis. *Journal of fungi (Basel, Switzerland)* **8**(1):39.
Johansson Å, Karlsson P, and Gyllensten U. (2003). A novel method for automatic genotyping of microsatellite markers based on parametric pattern recognition. *Human Genetics* **113**(4):316-324.
Jombart T. (2008). adegenet: a R package for the multivariate analysis of genetic markers. *Bioinformatics* **24**(11):1403-1405.
Jombart T and Ahmed I. (2011). adegenet 1.3-1: new tools for the analysis of genome-wide SNP data. *Bioinformatics* **27**(21):3070-3071.
Kopelman NM, Mayzel J, Jakobsson M, et al. (2015). Clumpak: a program for identifying clustering modes and packaging population structure inferences across K. *Mol Ecol Resour* **15**(5):1179-91.
Kosanke S, Hamann L, Kupsch C, et al. (2018). Unequal distribution of the mating type (MAT) locus idiomorphs in dermatophyte species. *Fungal Genet Biol* **118**(45-53.
Léchenne B, Reichard U, Zaugg C, et al. (2007). Sulphite efflux pumps in Aspergillus fumigatus and dermatophytes. *Microbiology* **153**(3):905-913.
Legendre P and Anderson MJ. (1999). DISTANCE-BASED REDUNDANCY ANALYSIS: TESTING MULTISPECIES RESPONSES IN MULTIFACTORIAL ECOLOGICAL EXPERIMENTS. *Ecological Monographs* **69**(1):1-24.
Lewis DT, Foil CS, and Hosgood G. (1991). Epidemiology and Clinical Features of Dermatophytosis in Dogs and Cats at Louisiana State University: 1981–1990. *Veterinary Dermatology* **2**(2):53-58.
Li W, Metin B, White Theodore C, et al. (2010). Organization and Evolutionary Trajectory of the Mating Type (MAT) Locus in Dermatophyte and Dimorphic Fungal Pathogens. *Eukaryotic Cell* **9**(1):46-58.
Mackenzie DW. (1963). "Hairbrush Diagnosis" in Detection and Eradication of Non-fluorescent Scalp Ringworm. *Br Med J* **2**(5353):363-5.
Martinez DA, Oliver BG, Gräser Y, et al. (2012). Comparative genome analysis of Trichophyton rubrum and related dermatophytes reveals candidate genes involved in infection. *mBio* **3**(5):e00259-12.
Mignon B, Swinnen M, Bouchara JP, et al. (1998). Purification and characterization of a 315 kDa keratinolytic subtilisin-like serine protease from and evidence of its secretion in naturally infected cats. *Medical Mycology* **36**(6):395-404.
Moriello K. (2014). Feline dermatophytosis: aspects pertinent to disease management in single and multiple cat situations. *Journal of feline medicine and surgery* **16**(5):419-431.

Moriello KA, Coyner K, Paterson S, et al. (2017). Diagnosis and treatment of dermatophytosis in dogs and cats. *Veterinary Dermatology* **28**(3):266-e68.
Mushtaq S, Faizi N, Amin SS, et al. (2020). Impact on quality of life in patients with dermatophytosis. *Australasian Journal of Dermatology* **61**(2):e184-e188.
Newbury S and Moriello KA. (2014). Feline dermatophytosis: steps for investigation of a suspected shelter outbreak. *Journal of feline medicine and surgery* **16**(5):407-418.
Oksanen J, Blanchet FG, Kindt R, et al. (2012). Vegan: Community Ecology Package. R package version 2.0-2.
Pasquetti M, Peano A, Soglia D, et al. (2013). Development and validation of a microsatellite marker-based method for tracing infections by Microsporum canis. *Journal of Dermatological Science* **70**(2):123-129.
Pritchard JK, Stephens M, and Donnelly P. (2000). Inference of Population Structure Using Multilocus Genotype Data. *Genetics* **155**(2):945.
Rippon JW and Garber ED. (1969). Dermatophyte Pathogenicity as a Function of Mating Type and Associated Enzymes**From the Department of Medicine, Section of Dermatology and the Department of Biology, The University of Chicago, Chicago, Illinois 60637. *Journal of Investigative Dermatology* **53**(6):445-448.
Sattasathuchana P, Bumrungpun C, and Thengchaisri N. (2020). Comparison of subclinical dermatophyte infection in short- and long-haired cats. *Vet World* **13**(12):2798-2805.
Scott DW and Paradis M. (1990). A survey of canine and feline skin disorders seen in a university practice: Small Animal Clinic, University of Montréal, Saint-Hyacinthe, Québec (1987-1988). *Can Vet J* **31**(12):830-5.
Selkoe KA and Toonen RJ. (2006). Microsatellites for ecologists: a practical guide to using and evaluating microsatellite markers. *Ecology Letters* **9**(5):615-629.
Sharma R, de Hoog S, Presber W, et al. (2007). A virulent genotype of Microsporum canis is responsible for the majority of human infections. *Journal of Medical Microbiology* **56**(10):1377-1385.
Viani FC, Cazares Viani PR, Gutierrez Rivera IN, et al. (2007). Extracellular proteolytic activity and molecular analysis of Microsporum canis strains isolated from symptomatic and asymptomatic cats. *Rev Iberoam Micol* **24**(1):19-23.
Weitzman I and Padhye AA. (1978). Mating behaviour of Nannizzia otae (=Microsporum canis). *Mycopathologia* **64**(1):17-22.
Weitzman I and Summerbell RC. (1995). The dermatophytes. *Clinical microbiology reviews* **8**(2):240-259.
Wolf FT. (1957). Chemical nature of the fluorescent pigment produced in Microsporum-infected hair. *Nature* **180**(4591):860-1.
Wolf FT, Jones EA, and Nathan HA. (1958). Fluorescent Pigment of Microsporum. *Nature* **182**(4633):475-476.

CHAPTER 3: TWO NOVEL SPECIES OF *ARTHRODERMA* ISOLATED FROM DOMESTIC CATS WITH DERMATOPHYTOSIS IN THE UNITED STATES

3.1 Introduction

Dermatophytes are filamentous fungi that can cause superficial fungal infections in humans and other animals[3]. These fungi are classified as geophilic, zoophilic, and anthropophilic [Kaplan *et al.* 1958, Weitzman *et al.* 1995]. While humans can be infected by numerous dermatophyte species, dermatophytosis in cats and dogs is generally caused by a few specific fungal species [Frymus *et al.* 2013]. Over 90% of infections in cats are caused by *Microsporum canis*, a zoonotic fungus [Moriello 2014]. *Trichophyton* spp., *Arthroderma insingulare* (formerly *Trichophyton terrestre*), *Arthroderma uncinatum* (formerly *Trichophyton ajelloi*), *A. vanbreuseghemii* (formerly *Trichophyton mentagrophytes*), *Nannizzia gypsea* (formerly *Microsporum gypseum*), *Nannizzia persicolor* (formerly *Microsporum persicolor*), and *Nannizzia nana* (formerly *Microsporum nanum*) have been reported as rare causes of feline dermatophytosis [Frymus *et al.* 2013, Moriello 2014, Boehm *et al.* 2019]. These infections frequently occur in high density populations such as animal shelters, and are often transmitted among animals in outbreak situations and may cause zoonotic infection in animal care providers [Newbury *et al.* 2014]. Diagnosis is often symptomatic and presumptive, and thus there is poor understanding of regional differences and variations in etiology and potential causative agents for this common disease.

[3] Work presented in this chapter has been published under the following citation of Moskaluk, Alex, and Sue VandeWoude. "Two novel species of Arthroderma isolated from domestic cats with dermatophytosis in the United States." Medical mycology vol. 60,2 (2022): myac001. doi:10.1093/mmy/myac001

During routine dermatophytosis screening at an animal shelter in California in 2019, three of 164 cats presenting with typical clinical signs of dermatophytosis, and a fourth asymptomatic cat with a positive Wood's lamp screening test, were found to be infected with two dermatophytes belonging to the genera *Arthroderma.* Two of the three animals with clinical signs were also *M. canis* positive. We describe genetic features of these two novel species and assess potential source of infection.

3.2 Materials and Methods

3.2.1 Animal care

Animals involved in this study were a part of a larger investigation involving dermatophytosis cases in domestic cats across the United States. All protocols were approved by Colorado State University clinical review board (VCS #2019-223) and biosafety committee (#145399) and were granted an Institutional Animal Care and Use Committee (IACUC) waiver prior to initiation of this study.

3.2.2 Case Presentations

Case 1: A stray 6-week-old intact female domestic shorthair kitten living outside was presented to San Jose Animal Center on May 25, 2019. Upon physical examination, one lesion (between 1.3-2.5 cm) with scales, crusts and alopecia was identified on the abdomen. A modified UV lamp test (Wood's lamp) was performed to detect fluorescence often associated with *M. canis*, and was found to be positive (Table 3.1). This patient had no prior medical history, and anti-fungal treatment was not performed before hair sample collection. The patient was adopted by a local rescue organization and was lost to medical follow-up.

Case 2: A stray 6-week-old intact domestic shorthair male kitten living outside was presented to San Jose Animal Center on July 10, 2019. Upon physical examination, one lesion described as scales, crusts, and alopecia (between 1.3-2.5 cm) was identified on the head (Table 3.1). The kitten was screened using a Wood's lamp and had a positive fluorescence. This patient had no prior medical history, and anti-fungal treatment was not performed before hair sample collection. The patient was adopted by a local rescue organization and was lost to medical follow-up.

Case 3: A stray 5-month-old intact male domestic shorthair kitten living outside was presented to San Jose Animal Center on July 18, 2019. More than five lesions with alopecia and scales/crusts ranging between 1.3-2.5 cm were distributed on the head, neck, abdomen, back, and legs (Table 3.1). This patient also had a concurrent upper respiratory infection during examination. Wood's lamp testing was performed, and the patient had a positive fluorescence. The patient was adopted by a local rescue organization and was lost to medical follow-up.

Case 4: A stray 2-month-old intact tabby male kitten living outside was presented to San Jose Animal Center on September 24, 2019, with five littermates. Case 4 and its littermates were screened for dermatophytosis upon intake via Wood's lamp and were positive. No lesions were present for Case 4 upon physical examination (Table 3.1). This patient has no prior medical history, and anti-fungal treatment was not performed before hair sample collection. The patient was adopted by a local rescue organization and was lost to medical follow-up.

3.2.3 Sample collection

Following clinical examination, hair samples were collected via MacKenzie toothbrush method [Mackenzie 1963]. Patients were not routinely screened for other infections via skin scraping as ectoparasites were an uncommon diagnosis and lesions were characteristic of

dermatophytosis. All samples were sent to Colorado State University. Upon receipt, hair samples were stored at 4°C, and nail and skin samples were stored at -20°C until utilized for down streaming processing.

3.2.4 Characterization of fungal isolates

Initial colony isolation: Hair samples collected on the toothbrushes were inoculated onto a biplate of Sabouraud dextrose agar (SDA) with chloramphenicol and gentamicin, and Dermatophyte Test Medium (Hardy Diagnostics, Santa Maria, CA, USA) and incubated in the dark at room temperature (range, 20-25°C) for 4 weeks [Robert *et al.* 2008]. Plates were monitored for growth every 24-48 hours. Color (code and terminology) of fungal colonies was recorded using a color identification textbook [Kornerup *et al.* 1967]. To increase sporulation, isolates of the novel taxa were grown on Potato Dextrose Agar (PDA) (Hardy Diagnostics, Santa Maria, CA, USA) at room temperature until colonies reached a sufficient colony size to be utilized for microscope slides.

Microscopic evaluation: 2-3 week old cultures were touched lightly with the sticky side of acetate tape, mounted on a microscope slide, and stained with Lactophenol Cotton Blue Stain (Hardy Diagnostics, Santa Maria, CA, USA) [Kidd *et al.* 2016]. A minimum of 30 conidia was measured on PDA-grown colonies, and the length and width were recorded.

Temperature range testing: Each isolate was tested for ability to grow at 30°C, 33°C, and 37°C on SDA. Two plates were inoculated using one-point inoculation of each of the two isolates that were not co-cultured with *M. canis* and grown at each of the three temperatures for 10-24 days or until colonies were formed. Colony diameter was measured at day 7.

Urease production: Production of urease was tested by growing the isolates that were not co-cultured with *M. canis* on urea agar slants (Becton, Dickinson, and Company BBL, Franklin Lakes, NJ, USA) at room temperature. Swabs of the isolates were streaked across the urea agar slants and monitored for color changed every 24 hours.

Hair perforation test: 5ml of UltraPure DNase/RNase free distilled water (Invitrogen, Carlsbad, CA, USA) was inoculated with autoclaved specific pathogen free cat hair. Fungal isolates that were not co-cultured with *M. canis* were added to the cat hair water via sterile cotton swab of the SDA culture plate. Inoculates were grown at room temperature in the dark for up to four weeks with hair removed approximately twice weekly for microscopic evaluation [Kidd *et al.* 2016]. Hair was examined on a microscope slide with Lactophenol Cotton Blue Stain (Hardy Diagnostics, Santa Maria, CA, USA) and cover slide at 1000x magnification [Kidd *et al.* 2016].

Mating type gene characterization: We tested strains using methods reported for identifying *Microsporum* and *Trichophyton* mating type genes [Kosanke *et al.* 2018]. This methodology has been used as an alternative to traditional mating type cross experiments [Kosanke *et al.* 2018]. DNA was extracted from each unique isolate as described below and subjected to PCR using primers that target the two mating type gene loci: alpha-box and high motility-group (HMG) [Kosanke *et al.* 2018]. Prototypical *T. mentagrophytes* (American Type Culture Collection 44687), and clinical isolates from a domestic cat of *T. mentagrophytes* and *M. canis* were used as positive controls. Amplification was assessed by gel electrophoresis followed by DNA fragment visualization using SYBR Safe DNA gel stain (ThermoFisher Scientific, Waltham, MA, USA).

3.2.5 DNA extraction and conventional PCR

DNA was extracted from SDA plate using a previously published method [Brillowska-Dąbrowska 2006] modified for culture samples. Briefly, a sterile cotton swab collected fungal cells from the plate and added to a 1.5 ml tube with 100 µl of DNA extraction buffer (60 mM sodium bicarbonate, 250 mM potassium chloride, and 50 mM Tris, balanced to pH 9.5). The swab was removed, and the tube was incubated at 95°C for 10 minutes. 100 µl of 2% bovine serum albumin was then added to the tube. The DNA was stored at -80°C until utilized for down streaming processing.

This unpurified DNA was used in conventional PCR for the internal transcribed spacer (ITS), β-tubulin, and translation elongation factor 1-alpha (TEF1) regions. The ITS, β-tubulin, and TEF1 regions were amplified using previously published primers (Table 3.2) [White *et al.* 1990, Glass *et al.* 1995, Rehner *et al.* 2005]. The following protocol was utilized for ITS PCR: 10 µl of 2X KAPA Taq ReadyMix with dye (Roche, Indianapolis, IN, USA), 6 µl UltraPure DNase/RNase free distilled water (Invitrogen, Carlsbad, CA, USA), 1 µl forward primer, 1 µl reverse primer and 2 µl of DNA template solution. The reaction was run in a C1000 Touch thermal cycler (Bio-Rad, Hercules, CA, USA) for one cycle at 95°C for 3 min, 34 cycles at 95°C for 30 sec, 60°C for 30 sec, 72°C for 1 min, and one cycle at 72°C for 5 min. The protocol was modified for amplifying the β-tubulin and TEF1 regions by adjusting the annealing temperatures to 55°C and 56°C, respectively. PCR products were run on a 1.5% agarose gel, and a band at 600bp, 500bp, and 1,000bp was visualized for ITS, β-tubulin, and TEF1 PCRs, respectively. PCR products were purified using ExoSAP-IT kit (Applied Biosystems, Carlsbad, CA, USA) and Sanger sequenced at a commercial laboratory (Psomagen, Rockville, MD, USA). Each region was sequenced a minimum of two times.

3.2.6 Phylogenetic analysis

The ITS and β-tubulin sequences from all four isolates were aligned with 51 isolates of other dermatophytes (Suppl. Table 3.1) using MUSCLE Alignment (Geneious v10.0.9) with a maximum of 8 iterations. Available sequences were downloaded from NCBI's GenBank database (https://www.ncbi.nlm.nih.gov/). These alignments were utilized for constructing a maximum likelihood tree (Geneious v10.0.9, RAxML plugin v8.2.11)[Stamatakis 2014] with 1,000 bootstrap replicates. Additionally, a neighbor-joining tree was constructed (Geneious v10.0.9) with 1,000 bootstrap replicates and CBS269.89 *Guarromyces ceretanicus* was classified as the outgroup. Bootstrap values greater than 50% were displayed in phylogenetic trees.

The sequences for ITS, β-tubulin, and TEF1 for the four cases were separately aligned with available sequences for *A. redellii* and *A. quadrifidum* (Suppl. Tables 3.1 and 3.2) of the same regions using MUSCLE Alignment (Geneious v10.0.9) with a maximum of 8 iterations. Only one sequence was available on NCBI's database for β-tubulin and TEF1 from *A. redellii* and one sequence for the full length of TEF1 from *A. quadrifidum* (Suppl. Tables 3.1 and 3.2). These genes were utilized for analysis based on a previous report for distinguishing species within the *Arthroderma* genus [Hainsworth *et al.* 2021].

3.3 Results

3.3.1 Initial fungal isolation

Culture of the hair sample from Case 1 exclusively grew a single fungus on the biplate. Colonies first appeared after 3 days of incubation at room temperature without bacterial contamination. Biplate cultures from hair samples from Cases 2-4 grew multiple saprophytes and were re-cultured from the hair samples a second time. During regrowth a single fungus was

identified from Case 4 starting 3 days post-incubation at room temperature. For Cases 2 and 3, colonies of *M. canis* first appeared 3-4 days after incubation at room temperature, followed by growth of a second white, fluffy fungus (Fig. 3.1K) that outgrew *M. canis*. The singular fungi from Cases 1 and 4, and overgrowth fungi from Cases 2 and 3 had colony morphology similar to *Trichophyton* spp. and *Arthroderma* spp. (Fig. 3.1, Table 3.3) [Dawson *et al.* 1961, Gräser *et al.* 2000, de Hoog *et al.* 2017]. Additional morphologic and physiologic characterization are described below.

3.3.2 Phylogenetic analysis

3.3.2.1 Two previously uncharacterized Arthroderma spp. were isolated from four cats.

ITS and β-tubulin maximum likelihood and neighbor-joining trees for all four isolates placed them within the genus *Arthroderma* (Figs. 3.2 and 3.3). Dermatophytes speciated from Cases 1 and 2 are most closely related to *Arthroderma redellii* as analyzed by both ITS maximum-likelihood (Fig. 3.2) and the neighbor-joining tree (Fig. 3.3A). While the isolate associated with Case 1 has high nucleotide alignment with *A. redellii* ITS and TEF1 (both over 99%), it had a lower nucleotide alignment for β-tubulin (less than 98.5%) and had different growth characteristics than reported for *A. redellii* (Tables 3.3 & 3.4). Case 2 non-*M. canis* dermatophyte isolate had 98.5% or greater alignment for all three *A. redellii* genes (Table 3.4). Case 1 and 2 ITS and β-tubulin amplicons were > 99% identical, suggesting the same or very similar species (Table 3.5).

Genetic analysis of Case 3 and 4 indicated 100% nucleotide alignment for ITS, β-tubulin, and TEF1 (Table 3.5) and were closely related by phylogenetic analysis (Figs. 3.2 and 3.3). These cases had less than 98% homology; in particular, β-tubulin homology distinguished Cases

3 and 4 from Cases 1 and 2 (less than 95% identity, Table 3.5). When compared to *A. redellii* and *A. quadrifidum*, both Case 3's and 4's dermatophytes have low nucleotide alignment with the TEF1 region; the highest agreement is less than 98.5% (Table 3.4).

M. canis and *T. mentagrophytes* mating type gene strains were amplified by PCR specific for mating type genes for these species. No amplification products were detected for any of the novel *Arthroderma* spp. using the *Trichophyton* specific primers. Two of the novel species that grew as pure isolates (Cases 1 and 4) were negative for bands using *Microsporum* specific primers. A single product of approximately 420 base-pairs was amplified from the two cases (2 and 3) that has been originally co-cultured with *M. canis* (Suppl. Fig. 3.1). We conducted Sanger sequencing on these products (Psomagen, Rockville, MD, USA) and via comparison with the NCBI GenBank database (https://www.ncbi.nlm.nih.gov/), determined that these bands were 100% identical to *M. canis* alpha-box (data not shown). We therefore conclude these products reflected DNA from *M. canis* DNA present in co-cultured materials and were not primary *Arthroderma spp.* fragments.

3.3.3 Species Description

Arthroderma lilyanum: Moskaluk, sp. nov. Figure 3.1. MycoBank: MB841894

Holotype: US, California, San Jose Animal Care Center, hair of a domestic cat, 25 May 2019, collected by Dr. Katherine Tyson, isolated by A. Moskaluk, dried culture on SDA (holotype, Westerdijk Fungal Biodiversity Centre CBS 148461); ex-living culture CSU CA002.1, GenBank ITS: OK623475, β-tubulin: OL342744, TEF1: OL342746.

Etymology: The species name honors Lily Moskaluk for her invaluable support during this study.

Diagnosis: This species can infect domestic cats, causing clinical signs similar to other dermatophytes that infect cats, including producing a positive fluorescence on Wood's lamp testing. This species is morphologically similar to *Arthroderma redellii*, but can grow well at room temperature.

Holotype culture characteristics: Colonies exhibited growth on SDA after 3 days at room temperature. Colony diameter was 17.5 mm after 7 days and 49 mm after 14 days grown on SDA at room temperature. Colonies had flat topography, cottony texture with surface color being lily white (1A1) and reverse color being oxide yellow (5C7) in the center with the color progressing to amber yellow (4B6) at the periphery. Colonies exhibited a similar growth rate on PDA at room temperature with colonies first visible after 2 days. Colony diameter was 22 mm after 7 days on PDA at room temperature. Colonies had flat topography with lacy margins, granular texture with surface color being milk white (1A2) and reverse color being light orange (5A4) at the center progressing to orange white (5A2) at the margins. Cultures grew on SDA at 30°C and were 11 mm at 7 days, which was smaller than that observed at room temperature (17.5 mm, as noted above). No growth was observed at 33°C for 10 days and at 37°C for 24 days. Cultures were urease positive after 2 days of growth on urea agar slants at room temperature.

Description of micromorphology: Vegetative mycelium consisted of hyaline, septate hyphae. Spiral hyphae were rarely observed. No racquet hyphae were observed. No ascomata were observed. Few conidia were observed from cultures grown on SDA. Numerous conidia were present from cultures grown on PDA. Conidia ranged from 2.3-4.9 µm length (mean ± standard deviation: 3.3 ± 0.7 µm) and 1.4-2.1 µm width (mean ± standard deviation: 1.7 ± 0.2 µm) with a length to width ratio ranging from 1.2-3.2 (mean ± standard deviation: 2 ± 0.5). Arthrospores were occasionally present. Hair perforation test was negative at 24 days.

Habitat and distribution: Found on domestic cats in California, US.

Additional cultures examined: US, California, San Jose Animal Care Center, hair of a domestic cat, 10 July 2019, collected by Dr. Katherine Tyson, isolated by A. Moskaluk, living culture CSU CA018, GenBank ITS: OK597194, β-tubulin: OL342745, TEF1: OL342747.

Arthroderma mcgillisianum: Moskaluk, sp. nov. Figure 3.1. MycoBank: MB841895

Holotype: US, California, San Jose Animal Care Center, hair of a domestic cat, 24 September 2019, collected by Dr. Sharon Ostermann, isolated by A. Moskaluk, dried culture on SDA (holotype, CBS 148462); ex-living culture CSU CA033.1, GenBank ITS: OK631727, β-tubulin: OL342748, TEF1: OL342750.

Etymology: The species name honors the late Gladys "Beth" McGillis, honorably discharged Leading Aircraftwoman of the Royal Canadian Air Force for her inspiration of women in STEM and dedication to feline medicine.

Diagnosis: This species can infect domestic cats, causing clinical signs similar to other dermatophytes that infect cats, including producing a positive fluorescence on Wood's lamp testing. This species is morphologically similar to *Arthroderma quadrifidum*.

Holotype culture characteristics: Colonies exhibited growth on SDA after 3 days at room temperature. Colony diameter was 11 mm after 7 days and 33 mm after 14 days grown on SDA at room temperature. Colonies had flat topography, cottony texture with surface color being satin white (2A1) and reverse color being apricot yellow (5B6) in the center progressing to butter yellow (4A5) at the margins. Colonies exhibited a slightly faster growth rate on PDA at room temperature with colonies first visible after 2 days. Colony diameter was 17.5 mm after 7 days on PDA at room temperature. Colonies had flat topography with lacy margins, granular texture

with surface color being snow white (1A1) and reverse color being pale orange (5A3) in the center progressing to orange white (5A2) at the periphery. Growth was similar growth at 30°C to room temperature (colony diameter 12.7 mm at 7 days). No growth was observed at 33°C for 10 days and for 24 days at 37°C. Species was urease positive after 3 days on urea agar slants at room temperature.

Description of micromorphology: Vegetative mycelium consisted of hyaline, septate hyphae. No spiral or racquet hyphae were observed. No ascomata were observed. Numerous conidia were observed from cultures grown on SDA. Conidia ranged from 3.8-9.6 µm length (mean ± standard deviation: 6.7 ± 1.3 µm) and 2.1-3.4 µm width (mean ± standard deviation: 2.7 ± 0.3 µm) with a length to width ratio ranging from 1.3-3.5 (mean ± standard deviation: 2.5 ± 0.4). Arthrospores were occasionally present. Hair perforation test was negative at 24 days.

Habitat and distribution: Found on domestic cats in California, US.

Additional cultures examined: US, California, San Jose Animal Care Center, hair of a domestic cat, 18 July 2019, collected by Dr. Sharon Ostermann, isolated by A. Moskaluk, living culture CSU CA022, GenBank ITS: OK631735, β-tubulin: OL342749, TEF1: OL342751.

3.4 Discussion

Dermatophytosis is a common skin infection that can be caused by a variety of fungal species. In domestic cats, the main agent is *M. canis* with reports of other dermatophytes causing dermatophytosis from the genera *Arthroderma, Nannizzia,* and *Trichophyton*[Moriello 2014, Boehm *et al.* 2019]. Investigators in Turkey found that while *M. canis* was responsible for over 60% of dermatophytosis cases in cats in Western Turkey, almost 20% of the cases were caused by *N. nana*, *N. gypsea* and *A. vanbreuseghemii* [Seker *et al.* 2011]. Cats that spend all or part of

their time outdoors may be exposed to a variety of dermatophytes through the soil or contact with other animals [Frymus *et al.* 2013].

In 2019, four cats were presented to an animal shelter in California, US for suspected dermatophytosis. While three of these animals had clinical signs consistent with dermatophytosis at the time of examination, hair samples from all four cases grew fungi with morphology similar to *Trichophyton* spp. and *Arthroderma* spp. Microscopic features of these isolates were consistent with dermatophyte species. Through maximum likelihood trees and neighbor-joining trees for ITS and β-tubulin, Cases 1 and 2 were determined to be strains of a novel dermatophyte species described herein as *Arthroderma lilyanum* sp. nov. Cases 3 and 4 were found to be 100% identical in the markers that were investigated and determined to be a novel dermatophyte species described herein as *Arthroderma mcgillisianum* sp. nov. Mating type gene analysis using reagents that successfully typed *M. canis* and *T. mentagrophytes* were unable to genotype these novel strains. Strains were found to be urease positive and hair perforation negative, consistent with other species of *Arthroderma* [Takahashi *et al.* 2002, Zhang *et al.* 2009, Brasch *et al.* 2019]. Other *Arthroderma* species that have been reported to be urease positive include *Arthroderma chiloniense* [Brasch *et al.* 2019] and *Arthroderma vanbreuseghemii* [Zhang *et al.* 2009], while negative hair perforation test species include *A. chiloniense* [Brasch *et al.* 2019] and *Arthroderma benhamiae*[Takahashi *et al.* 2002]. Investigators have reported that hair from domestic cats may be resistant to perforation due to thicker diameter of the different hair layers and less favorable nutritional composition for fungal growth compared to human hair, thus further studies could be conducted to assess ability of these isolates to attach to and degrade other types of hair samples [Al-Janabi *et al.* 2016].

While the sequences of the ITS, β-tubulin, and TEF1 regions for the two *A. lilyanum* isolates had high nucleotide agreement with *A. redellii*, the host and growing conditions are different between the species (Table 3.3). *A. redellii* has only been isolated from bats in Indiana, Texas, and Wisconsin, with the distinguishing feature of being unable to grow at ambient room temperature [Lorch *et al.* 2015]. As noted here, the strain isolated here grew within the temperature range of 20-30°C. Given the genetic similarities, it is suggestive of these two species sharing a recent ancestor and possibly diverging to better suit their respective hosts.

We identified these novel fungal species in California, however, given the low frequency of dermatophyte species identification via culture or genetic sequence analysis in clinical settings [Bistis 1959, Weitzman *et al.* 1995, Mohanty *et al.* 1999], these species could be more widespread but undiagnosed. Two cases (one isolate for each of the novel species) were co-cultured with *M. canis.* Given that *M. canis* colonies grew more rapidly, *A. lilyanum* and *A. mcgillisianum* could be missed without fastidious examination of culture plates. While Case 2 (*A. lilyanum* co-cultured with *M. canis*) was presented with similar clinical signs as Case 1 (*A. lilyanum* only), Case 3 (*A. mcgillisianum* co-cultured with *M. canis*) had a more severe presentation than Case 4 (*A. mcgillisianum* only), suggesting that *A. mcgillisianum* might be less pathogenic as a primary pathogen than when infected in concert with *M. canis*.

All four of the cases exhibited positive Wood's lamp fluorescence during examination. While *M. canis* are classically known to exhibit fluoresce under UV light with a blue-green color, other dermatophytes including *M. audouinii*, *M. ferrugineum*, *M. disortum*, *N. gypsea*, and *Trichophyton schoenleinii* have also been reported to have positive fluorescence [Asawanonda *et al.* 1999]. The compound reportedly responsible for *M. canis* and *N. gyp*sea fluorescence has been reported to be pteridine [Wolf 1957, Wolf *et al.* 1958], and pteridine and xanthurenic acid

derivatives have been reported to contribute to fluorescence of *T. schoenleinii* [Chattaway *et al.* 1966]. It is unclear what benefit or purpose these compounds serve, and what the metabolic pathway for the production of these fluorescent compounds is. It is unknown if *A. lilyanum* and *A. mcgillisianum* are geophilic or zoophilic, and whether they are zoonotic or can infect other animals. Determining the natural history, mating scheme, prevalence, fluorescent principle, and geographic distribution of these strains presents interesting questions for future studies.

Table 3.1. Demographic information for four cases presenting with novel fungal species. All four cases occurred in stray (i.e. unowned) cats that were younger than 6 months. Lesion presentation was similar between Case 1 and 2. Case 4 presented asymptomatically but was from a litter found to be positive during Wood's lamp screening. DSH = domestic shorthair. N/A = not applicable.

Clinical Parameters	**Case 1**	**Case 2**	**Case 3**	**Case 4**
Age	6 weeks	6 weeks	5 months	2 months
Sex/Neuter Status	Female Intact	Male Intact	Male Intact	Male Intact
Breed	DSH	DSH	DSH	Tabby
Date of Presentation	05/25/2019	07/10/2019	07/18/2019	09/24/2019
Number of Lesions	1	1	5	0
Lesion Types	Scales, crusts, alopecia	Scales, crusts, alopecia	Scales, crusts, alopecia	N/A
Lesion Location	abdomen	head	head, neck, abdomen, back, legs	N/A
Lesion Size	1.3-2.5 cm	1.3-2.5cm	1.3-2.5 cm	N/A
Wood's Lamp Results	positive	positive	positive	positive
Presumptive diagnosis	*Arthroderma lilyanum*	*Arthroderma lilyanum* and *Microsporum canis*	*Arthroderma mcgillisianum* and *Microsporum canis*	*Arthroderma mcgillisianum*

Table 3.2. Primers used for targeting internal transcribed spacer (ITS), β-tubulin, and translation elongation factor 1-alpha (TEF1) regions.

Target region	**Primer**	**Sequence**	**Reference**
ITS	ITS5F	5'- GGAAGTAAAAGTCGTAACAAGG	[White *et al.* 1990]
	ITS4R	5'- TCCTCCGCTTATTGATATGC	
β-tubulin	Bt2a	5'- GGTAACCAAATCGGTGCTGCTTTC	[Glass *et al.* 1995]
	Bt2b	5'- ACCCTCAGTGTAGTGACCCTTGGC	
TEF1	983F	5′-GCYCCYGGHCAYCGT-GAYTTYAT	[Rehner *et al.* 2005]
	2218R	5′-ATGACACCRA-CRGCRACRGTYTG	

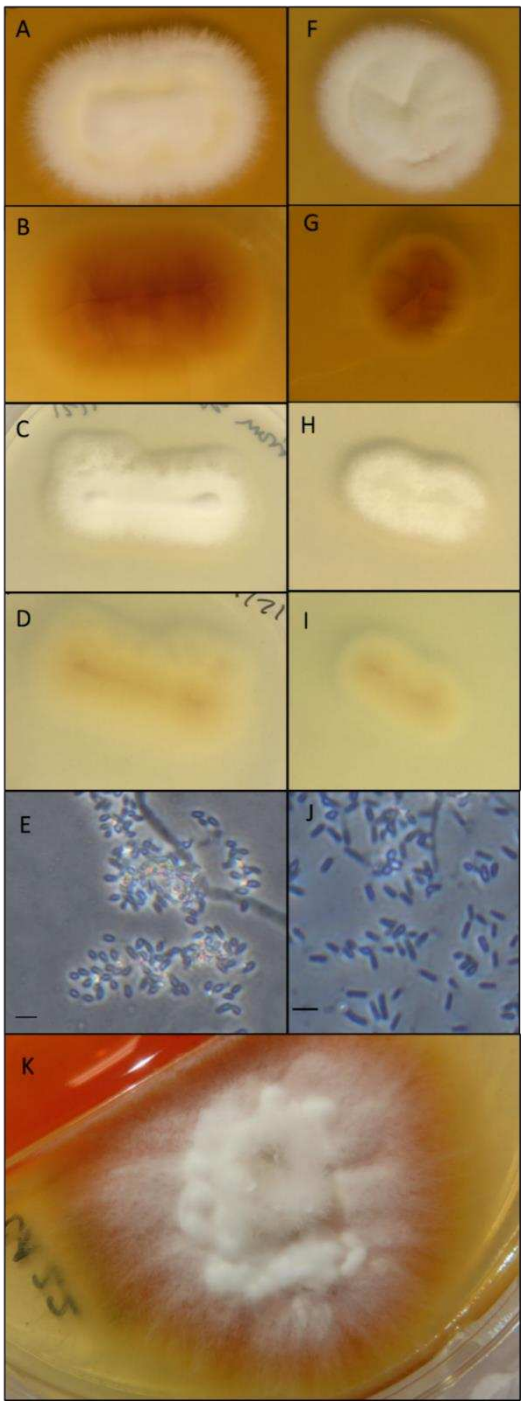

Figure 3.1. *Arthroderma lilyanum* (ex-type living culture) – (A) colony surface grown on SDA, (B) colony reverse grown on SDA, (C) colony surface grown on PDA, (D) colony reverse grown on PDA, (E) conidia and hyphae under dark field at 400X magnification. Bar = 10µm. *Arthroderma mcgillisianum* (ex-type living culture) – (F) colony surface grown on SDA, (G) colony reverse grown on SDA, (H) colony surface grown on PDA, (I) colony reverse grown on PDA, (J) conidia observed under dark field at 400X magnification. Bar = 10µm. Co-culture of *A. mcgillisianum* and *M. canis* – (K) colony surface grown on SDA. SDA plates were incubated for 10 days for single isolates and 9 days for co-culture colonies, and PDA plates for 7 days, at room temperature in the dark.

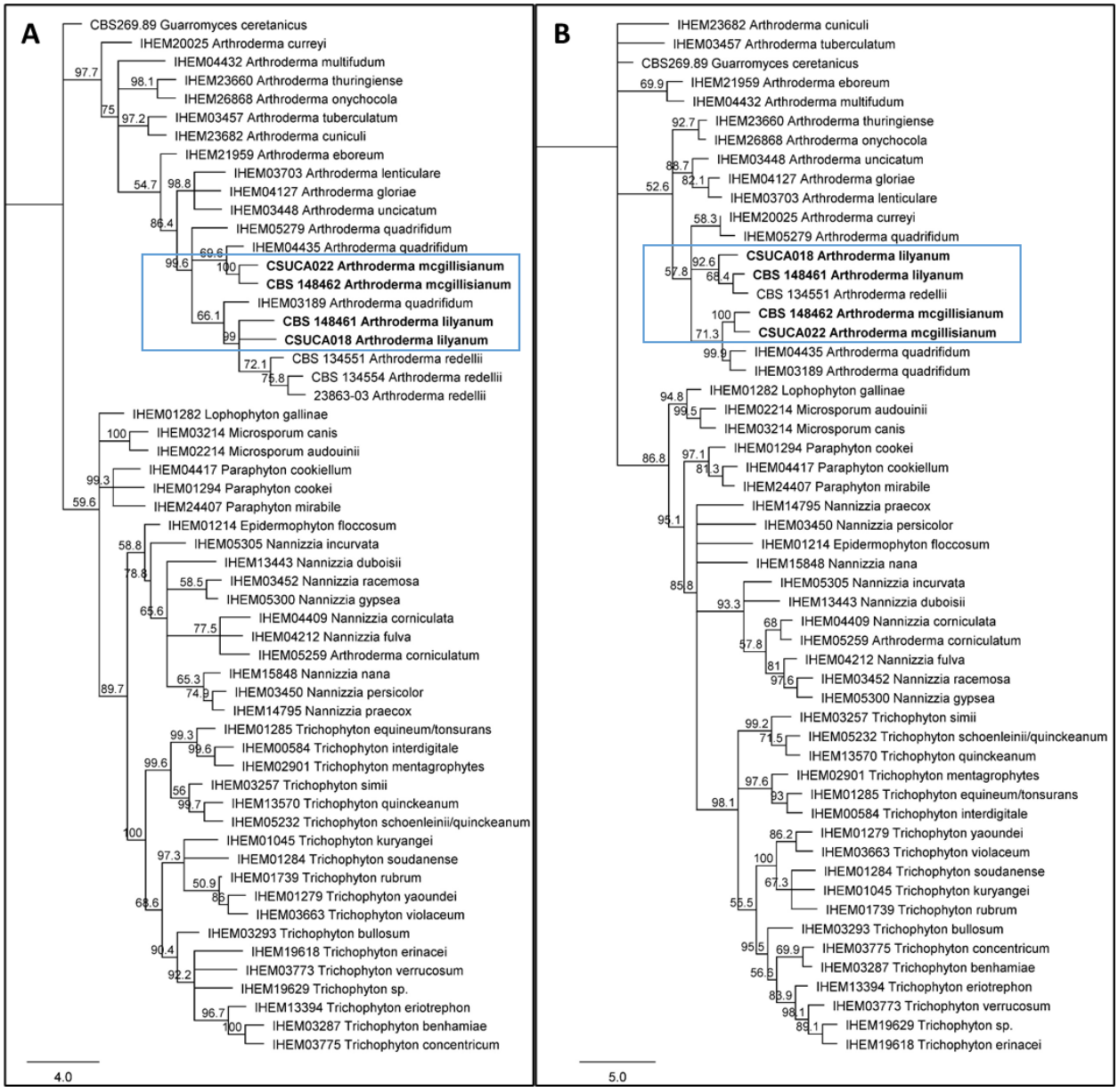

Figure 3.2. Consensus trees for maximum likelihood analysis of novel dermatophytes. A) ITS analysis. B) β-tubulin. All four dermatophyte isolates are placed with the genus *Arthroderma* (blue box indicates location of new isolates). Using 1,000 iterations for RAxML analysis, bootstrap support values ≥50% are placed above the branches. Westerdijk Fungal Biodiversity Centre (CBS), Belgian Co-ordinated Collections of Micro-organisms/Institute of Hygiene and Epidemiology Mycology (BCCM/IHEM), Center for Forest Mycology Research, or Colorado State University strain number is placed before isolate name. Scale bar represents mean number of nucleotide substitutions per site.

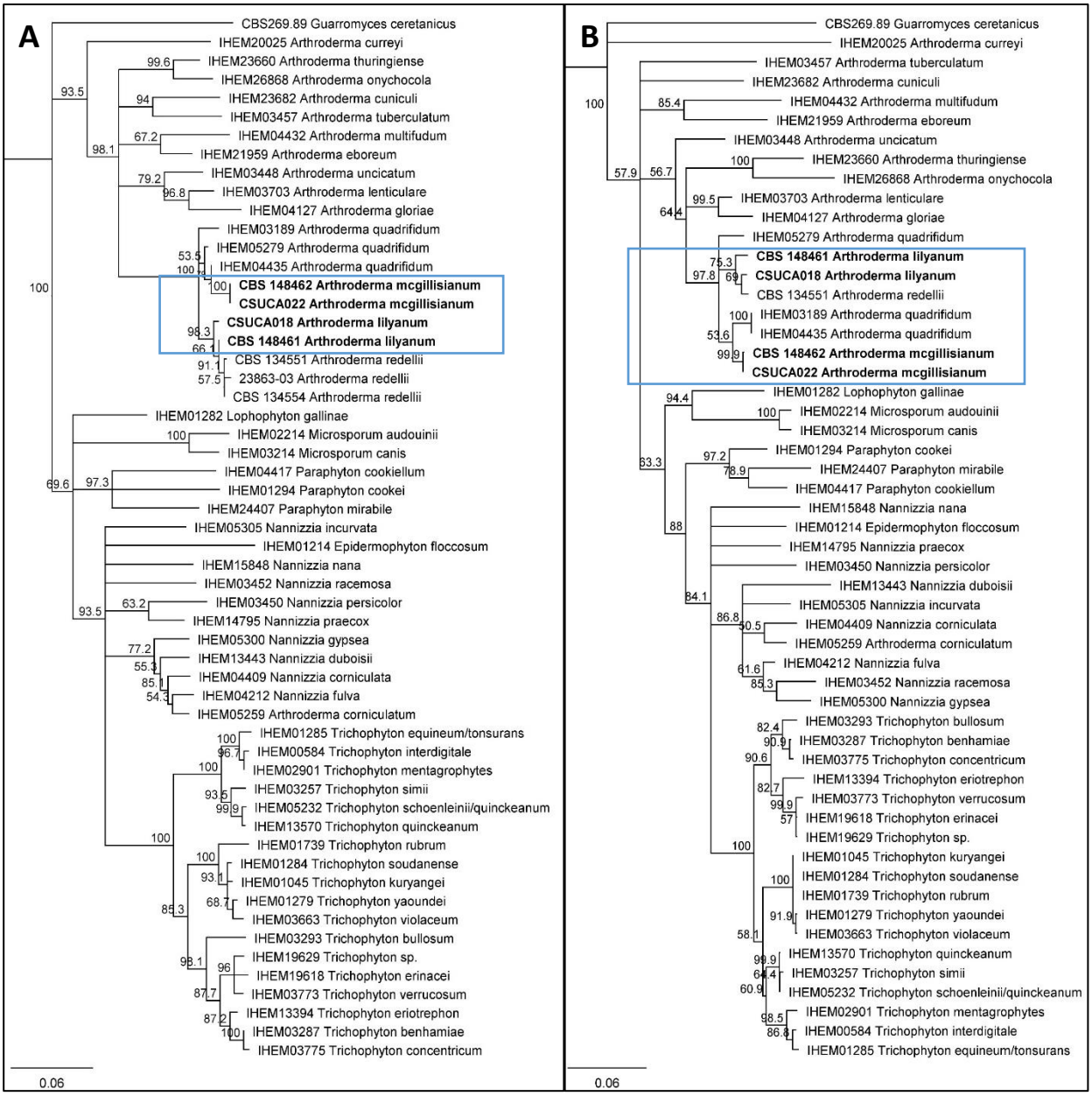

Figure 3.3. Neighbor-joining analysis of novel dermatophytes. A) ITS region. B) β-tubulin. All novel dermatophytes were placed with the genus *Arthroderma* (blue box indicates new isolates). Using 1,000 iterations, bootstrap support values ≥50% are placed above the branches. Westerdijk Fungal Biodiversity Centre (CBS), Belgian Co-ordinated Collections of Micro-organisms/Institute of Hygiene and Epidemiology Mycology (BCCM/IHEM), Center for Forest Mycology Research, or Colorado State University strain number is placed before isolate name. Scale bar represents substitutions per nucleotide site.

Table 3.3. Description of *Arthroderma lilyanum* and *Arthroderma mcgillisianum*, and similar genetic or clinical presentation fungi. CA = California. TN = Tennessee. TX = Texas. WI = Wisconsin. * = culture characteristics of fungi grown on Sabouraud dextrose agar (SDA). ** = major reservoir species listed, there are reports of other animals harboring this fungus.

Fungal Species	**Culture characteristics***	**Micromorphology**	**Habitat**	**Distribution**
Arthroderma lilyanum	• growth at 20-25°C, 30°C • no growth at 33°C, 37°C • surface color: lily white • reverse color: oxide yellow • texture: cottony	• hyaline, septate hyphae • spiral hyphae rare • ellipsoidal microconidia • hair perforation test: negative • urease positive	domestic cats	USA: CA
Arthroderma mcgillisianum	• growth at 20-25°C, 30°C • no growth at 33°C, 37°C • surface color: satin white • reverse color: apricot to butter yellow • texture: cottony	• hyaline, septate hyphae • ellipsoidal microconidia • hair perforation test: negative • urease positive	domestic cats	USA: CA
Microsporum canis[18]	• growth at 20-25°C • surface color: greyish- to tannish-white • reverse color: deep ochraceous-yellow • texture: woolly	• tear-shaped microconidia • spindle-shaped macroconidia • hair perforation test: positive • urease positive	domestic cats, dogs, rabbits**	Worldwide
Arthroderma quadrifidum[19]	• growth at 25°C • surface color: white to pale yellowish • reverse color: yellowish brown • texture: fluffy to powdery	• cylindrical macroconidia • elongate pyriform microconidia • pale yellow, septate hyphae	soil, feathers, hair	Worldwide
Arthroderma redellii[26]	• no growth at 25°C	• hyaline, septate hyphae	bats (*Myotis lucifugus* and	USA: TN, TX, WI

	• surface color: white • reverse color: yellow • texture: velutinous	• thallic conidia	*Myotis velifer*)	

Table 3.4. Nucleotide homology illustrates two novel dermatophyte strains. Case 1 and 2 have high homology with *A. redellii* (over 98% for internal transcribed spacer (ITS), partial β-tubulin, and translation elongation factor 1-alpha (TEF1) regions). They are distinguished from *A. redellii* phenotypically since they grew readily at room temperature. Cases 3 and 4 are less than 98.5% homologous to *A. quadrifidum* and *A. redellii* across ITS, partial β-tubulin, and TEF1 regions. N/A = sequence data not available.

		Arthroderma quadrifidum IHEM05279	*Arthroderma quadrifidum* IHEM03189	*Arthroderma quadrifidum* IHEM04435	*Arthroderma quadrifidum* UAMH2941	*Arthroderma redellii* CBS 134551	*Arthroderma redellii* CBS 134554	*Arthroderma redellii* 23863-03
Case 1	ITS	96.3%	96%	96%	N/A	99.1%	99.5%	99.4%
	β-tubulin	93.4%	93.1%	93.1%	N/A	98.1%	N/A	N/A
	TEF1	N/A	N/A	N/A	97.8%	99.7%	N/A	N/A
Case 2	ITS	96.1%	95.8%	95.8%	N/A	98.9%	99.4%	99.2%
	β-tubulin	94.1%	93.8%	93.8%	N/A	98.5%	N/A	N/A
	TEF1	N/A	N/A	N/A	98.2%	99.3%	N/A	N/A
Case 3	ITS	96.1%	95.1%	96.8%	N/A	96.9%	97.2%	97.1%
	β-tubulin	96.3%	96.1%	96.1%	N/A	94.6%	N/A	N/A
	TEF1	N/A	N/A	N/A	98.4%	98.4%	N/A	N/A
Case 4	ITS	96.2%	95.1%	96.8%	N/A	96.9%	97.2%	97.1%
	β-tubulin	96.3%	96%	96%	N/A	94.6%	N/A	N/A
	TEF1	N/A	N/A	N/A	98.5%	98.5%	N/A	N/A

Table 3.5. Pairwise homology across three dermatophytes identified in this study. Case 2 and 3 have 100% nucleotide agreement for the internal transcribed spacer (ITS), partial β-tubulin, and translation elongation factor 1-alpha (TEF1) regions. Case 1 had less than 98% identity within ITS, β-tubulin, and TEF1 to Cases 3 and 4, while having over 99% nucleotide agreement with Case 2 for ITS and TEF1 regions.

		Case 1	**Case 2**	**Case 3**	**Case 4**
Case 1	ITS	-	99.2%	97.1%	97.1%
	β-tubulin	-	97.6%	94.3%	94.2%
	TEF1	-	99%	97.8%	97.8%
Case 2	ITS	99.2%	-	96.9%	96.9%
	β-tubulin	97.6%	-	94.8%	94.8%
	TEF1	99%	-	98.1%	98.6%
Case 3	ITS	97.1%	96.9%	-	100%
	β-tubulin	94.3%	94.8%	-	100%
	TEF1	97.8%	98.1%	-	100%
Case 4	ITS	97.1%	96.9%	100%	-
	β-tubulin	94.2%	94.8%	100%	-
	TEF1	97.8%	98.6%	100%	-

Literature Cited

Al-Janabi AAHS, Ai-Tememi NN, Ai-Shammari RA, et al. (2016). Suitability of hair type for dermatophytes perforation and differential diagnosis of T. mentagrophytes from T. verrucosum. *Mycoses* **59**(4):247-252.

Asawanonda P and Taylor CR. (1999). Wood's light in dermatology. *International Journal of Dermatology* **38**(11):801-807.

Bistis GN. (1959). Pleomorphism in the Dermatophytes. *Mycologia* **51**(3):440-452.

Boehm T and Mueller RS. (2019). Dermatophytosis in dogs and cats - an update. *Tierarztl Prax Ausg K Kleintiere Heimtiere* **47**(4):257-268.

Brasch J, Beck-Jendroschek V, Voss K, et al. (2019). Arthroderma chiloniense sp. nov. isolated from human stratum corneum: Description of a new Arthroderma species. *Mycoses* **62**(1):73-80.

Brillowska-Dąbrowska A, *DNA preparation from nail samples*, W.I.P. Organization, Editor. 2006: Denmark.

Chattaway FW and Barlow AJE. (1966). Further studies of the fluorescent compounds produced in vivo by Trichophyton schoenleinii. *Sabouraudia* **4**(4):265-272.

Dawson CO and Gentles JC. (1961). The perfect states of Keratinomyces ajelloi Vanbreuseghem, Trichophyton terrestre Durie & Frey and Microsporum nanum Fuentes. *Sabouraudia* **1**(49-57.

de Hoog GS, Dukik K, Monod M, et al. (2017). Toward a Novel Multilocus Phylogenetic Taxonomy for the Dermatophytes. *Mycopathologia* **182**(1):5-31.

Frymus T, Gruffydd-Jones T, Pennisi MG, et al. (2013). Dermatophytosis in Cats: ABCD guidelines on prevention and management. *Journal of feline medicine and surgery* **15**(7):598-604.

Glass NL and Donaldson GC. (1995). Development of primer sets designed for use with the PCR to amplify conserved genes from filamentous ascomycetes. *Applied and environmental microbiology* **61**(4):1323-1330.

Gräser Y, Kuijpers AF, El Fari M, et al. (2000). Molecular and conventional taxonomy of the Microsporum canis complex. *Med Mycol* **38**(2):143-53.

Hainsworth S, Kučerová I, Sharma R, et al. (2021). Three-gene phylogeny of the genus Arthroderma: Basis for future taxonomic studies. *Medical Mycology* **59**(4):355-365.

Kaplan W, Georg LK, and Ajello L. (1958). RECENT DEVELOPMENTS IN ANIMAL RINGWORM AND THEIR PUBLIC HEALTH IMPLICATIONS. *Annals of the New York Academy of Sciences* **70**(3):636-649.

Kidd S, Halliday CL, Alexiou H, et al., *Descriptions of Medical Fungi*. 2016: CutCut Digital.

Kornerup A and Wanscher JH, *Methuen handbook of colour*. 2nd ed., revised. ed. 1967, London: Methuen.

Kosanke S, Hamann L, Kupsch C, et al. (2018). Unequal distribution of the mating type (MAT) locus idiomorphs in dermatophyte species. *Fungal Genet Biol* **118**(45-53.

Lorch JM, Minnis AM, Meteyer CU, et al. (2015). The fungus Trichophyton redellii sp. Nov. Causes skin infections that resemble white-nose syndrome of hibernating bats. *J Wildl Dis* **51**(1):36-47.

Mackenzie DW. (1963). "Hairbrush Diagnosis" in Detection and Eradication of Non-fluorescent Scalp Ringworm. *Br Med J* **2**(5353):363-5.

Mohanty JC, Mohanty SK, Sahoo RC, et al. (1999). Diagnosis of superficial mycoses by direct microscopy - A statistical evaluation. *Indian J Dermatol Venereol Leprol* **65**(2):72-4.
Moriello K. (2014). Feline dermatophytosis: aspects pertinent to disease management in single and multiple cat situations. *Journal of feline medicine and surgery* **16**(5):419-431.
Newbury S and Moriello KA. (2014). Feline dermatophytosis: steps for investigation of a suspected shelter outbreak. *Journal of feline medicine and surgery* **16**(5):407-418.
Rehner SA and Buckley E. (2005). A Beauveria phylogeny inferred from nuclear ITS and EF1-alpha sequences: evidence for cryptic diversification and links to Cordyceps teleomorphs. *Mycologia* **97**(1):84-98.
Robert R and Pihet M. (2008). Conventional Methods for the Diagnosis of Dermatophytosis. *Mycopathologia* **166**(5):295-306.
Seker E and Dogan N. (2011). Isolation of dermatophytes from dogs and cats with suspected dermatophytosis in Western Turkey. *Prev Vet Med* **98**(1):46-51.
Stamatakis A. (2014). RAxML version 8: a tool for phylogenetic analysis and post-analysis of large phylogenies. *Bioinformatics* **30**(9):1312-3.
Takahashi Y, Haritani K, Sano A, et al. (2002). An isolate of Arthroderma benhamiae with Trichophyton mentagrophytes var. erinacei anamorph isolated from a four-toed hedgehog (Atelerix albiventris) in Japan. *Nihon Ishinkin Gakkai Zasshi* **43**(4):249-55.
Weitzman I and Summerbell RC. (1995). The dermatophytes. *Clinical microbiology reviews* **8**(2):240-259.
White TJ, Bruns T, Lee S, et al., *38 - AMPLIFICATION AND DIRECT SEQUENCING OF FUNGAL RIBOSOMAL RNA GENES FOR PHYLOGENETICS*, in *PCR Protocols*, M.A. Innis, et al., Editors. 1990, Academic Press: San Diego. p. 315-322.
Wolf FT. (1957). Chemical nature of the fluorescent pigment produced in Microsporum-infected hair. *Nature* **180**(4591):860-1.
Wolf FT, Jones EA, and Nathan HA. (1958). Fluorescent Pigment of Microsporum. *Nature* **182**(4633):475-476.
Zhang H, Ran Y, Liu Y, et al. (2009). Arthroderma vanbreuseghemii infection in three family members with kerion and tinea corporis. *Medical Mycology* **47**(5):539-544.

CHAPTER 4: CHRACTERIZATION OF *MICROSPORUM CANIS* SUB3 EXPRESSION AND DETECTION UNDER VARIOUS GROWTH CONDITIONS

4.1 Introduction

Dermatophytes are a category of fungi that can infect and degrade keratinized tissues [Weitzman *et al.* 1995]. There are seven currently recognized genera of dermatophytes: *Microsporum*, *Trichophyton*, *Arthroderma*, *Lophophyton*, *Paraphyton*, *Nannizzia*, and *Epidermophyton* [de Hoog *et al.* 2017]. Of these groups, the main genera that cause infections in humans and animals are *Trichophyton*, *Microsporum*, and *Epidermophyton* [Weitzman *et al.* 1995]. *Microsporum canis* is the main agent that causes dermatophytosis in cats [Moriello *et al.* 2017] and one of the primary species responsible for tinea capitis in humans [Achterman *et al.* 2011, Leung *et al.* 2020]. While clinical disease can be similar between humans and animals, managing dermatophytosis cases depends on numerous factors [Kaul *et al.* 2017]. Humans generally can treat and monitor the infection at home and can continue most regular activities [Kaul *et al.* 2017]. However, infections in animals, particularly in high density populations, often necessitate extended quarantine or euthanasia as management options, with potentially devastating consequences in these settings [Newbury *et al.* 2014]. Given the potential outcomes of a diagnosis, accurately and rapidly detecting dermatophytes would be significantly benefit these populations.

Standard diagnostic tests for detecting viable dermatophytes are often confounded by prior treatments that limit culture efficacy and fomite carriage [Garg *et al.* 2009, de Hoog *et al.* 2017, Gnat *et al.* 2020]. Current diagnostic approaches for this infection in clinical settings include fungal cultures, microscopy, Wood's lamp fluorescence, and commercial polymerase

chain reaction (PCR). Wood's lamp testing can be used to identify *M. canis* infection, but not all isolates fluoresce, and accurate diagnosis requires experience [Moriello *et al.* 2017]. Direct examination via microscopy is not always practical and achievable, especially in a shelter setting [Rezusta *et al.* 2016, Pihet *et al.* 2017, Stuntebeck *et al.* 2018]. Fungal culture is perhaps the most commonly used diagnostic approach, but false negatives and positives can occur, and up to 21 days may be required to complete the analysis [Moriello *et al.* 2017]. PCR diagnosis is more costly, takes several days to complete, and non-infected fomite carriers or dead fungal organisms cannot be distinguished from active infections [Panasiti *et al.* 2006]. Thus, there is a significant need for an accurate, rapid point-of-care diagnostic test for active *M. canis* infection.

Dermatophytes express unique proteases compared to other groups of fungi, particularly during keratin metabolism during invasion, presenting novel targets for diagnostic assay development [Martinez *et al.* 2012, Tran *et al.* 2016]. Proteases are a classification of enzymes that can degrade proteins into amino acids or peptides [Monod 2008]. The proteases involved in keratin hydrolysis include endoproteases that break internal bonds of polypeptides and exoproteases that target the polypeptide bonds at the N- or C-terminus [Monod 2008, Mercer *et al.* 2019]. While the major categories of endoproteases are fungalysins, subtilisins, and neutral proteases [Rawlings *et al.* 2016, Mercer *et al.* 2019], the most important class of proteases for dermatophytes is the secreted subtilisin proteases as this family of enzymes is responsible for degrading keratin [Mercer *et al.* 2019]. One of these proteases (subtilisin 3, Sub3) has been found to be produced extracellularly by *M. canis* and is essential for adherence to keratinized tissues during early infection [Mignon *et al.* 1998, Monod 2008, Baldo *et al.* 2010, Băguţ *et al.* 2012]. Given that SUB3 expression is active during infection, detecting this protein is an indicator of metabolically active *M. canis* [Grumbt *et al.* 2013]. Sub3 produced by *M. canis*

fungal cells has been previously detected via immunohistochemistry in domestic cat hair follicles in clinical biopsy specimens [Mignon *et al.* 1998], suggesting that antibodies can be created to specifically target this protein.

Modulating metabolic pathways associated with Sub3 can affect the production of this essential protein during infection. Thus, understanding how environmental factors such as external forces from motion, nutrient supplementation, and light conditions influence Sub3 expression and production could help elucidate how future therapies could target these metabolic pathways. These factors are commonly assessed for fungi grown at scale in industrial settings to maximize particular metabolites [Serrano-Carreón *et al.* 2015]. For example, the presence of keratinized tissue (or L-cysteine, the major amino acid of keratin) could upregulate the production of certain metabolites [Kasperova *et al.* 2013, Martins *et al.* 2020]. Furthermore, when fungi are grown in culture flasks, fungal pellets develop from the growth of the mycelium under agitation [Grimm *et al.* 2005] and the size of these pellets has been shown to influence metabolite production [Metz *et al.* 1977, Miyazawa *et al.* 2016, Kelliher *et al.* 2020]. Flask type and motion can also directly affect the size of the fungal pellets produced [Metz *et al.* 1977, Miyazawa *et al.* 2016]. Additionally, light-dependent circadian cycle of fungi has been shown to influence the metabolism of the organism [Montenegro-Montero *et al.* 2015]. Investigating the influence of these factors (motion, flask type, supplementation, and light conditions) on Sub3 metabolism can be helpful for directing future studies on the adherence phase of dermatophytosis infections.

We aimed to demonstrate *M. canis* expression and production of Sub3 under different culture conditions using clinical samples from suspected dermatophytosis cats. We developed and optimized a sandwich enzyme-linked immunosorbent assay (ELISA) that detects Sub3

protein levels. SUB3 expression was measured by RT-qPCR and antigen production was determined by ELISA. Sub3 detection was confirmed via immunohistochemistry on dermatophytosis biopsies. While clinical samples had Sub3 levels below the assay's limit of detection, we were able to detect Sub3 from cultured *M. canis* samples. *M. canis* isolates were grown in different culture conditions that tested the effect of shear forces induced by different flask types (baffled, unbaffled), motion (shaking, stationary), broth supplements (hair, L-cysteine), and light conditions (24 hours of darkness or light) on Sub3 production and SUB3 expression. Use of baffled flasks with broth supplements resulted in higher Sub3 production and expression over the study period. Our findings demonstrated the influence of culture conditions on *M. canis* metabolism of Sub3. Understanding the factors that can influence Sub3 metabolism can help reduce production of this protein as Sub3 is essential for *M. canis* adherence to initiate infection. Modulating the factors to increase production of Sub3 can be utilized for screening suspected dermatophytosis cases.

4.2 Materials and Methods

4.2.1 Clinical samples and fungal isolates

Clinical samples: Clinical samples were collected from domestic cats with suspected dermatophytosis in shelters or private practices; full description can be found in Materials and Methods 2.2 of this dissertation. All protocols were approved by Colorado State University (CSU) clinical review board (VCS #2019-223) and biosafety committee (#145399) and were granted an Institutional Animal Care and Use Committee (IACUC) waiver prior to initiation of this study. Hair samples were collected from cats with suspected dermatophytosis via brushing with a toothbrush (Materials and Methods 2.2). The head of the toothbrush containing the bristles

was removed and placed in a 50ml conical tube. Two ml of MilliQ® water or ELISA diluent was added and the tube was vortexed on high for 30 seconds. The toothbrush bristles were soaked in the water for 1 minute and then vortexed on high for another 30 seconds. The water or ELISA diluent eluted from the toothbrush was used in downstream processing. Nail and skin scrapings from the same cats were processed in the same manner as hair samples, except 1.5 ml of ELISA diluent was used.

Culture samples: *M. canis* and *Aspergillus* spp. isolates utilized for this study originated from clinical samples collected from domestic cats in the United States mentioned in the previous section (see Materials and Methods 2.2 for full description of sample collection). These isolates were isolated on biplates of Dermatophyte Test Medium and Sabouraud dextrose agar (SDA) with chloramphenicol and gentamicin (Hardy Diagnostics, Santa Maria, CA, USA). Colonies were maintained on SDA plates at 20-25°C in the dark. Isolates were identified as *M. canis* and *Aspergillus* spp. via culture morphology and internal transcribed spacer region PCR.

4.2.2 Broth culture experiments

Culture setup: A 2 cm x 2 cm section of *M.* canis culture grown on an SDA plate was swabbed using a sterile cotton swab and then added to 6 ml of Sabouraud dextrose broth (Hardy Diagnostics, Santa Maria, CA, USA) (Fig. 4.1). After swirling the swab in the broth to dislodge the fungal cells, 1 ml of the inoculated broth was added to sterile Erlenmeyer shaker flasks (Greiner Bio-One, Monroe, North Carolina, USA) containing 35-36 ml of Sabouraud dextrose broth (SDB) with gentamicin and chloramphenicol (Fig. 4.1). The flask conditions included additives (100 mg autoclaved specific pathogen free cat hair or 200 mg L-cysteine), shaking (shaking at 200 rpm or stationary), light conditions (24 hours darkness, 24 hours light, 8 hours

light), and flask type (baffled or unbaffled flask) (Table 4.1 and Fig. 4.1). For negative controls, unbaffled flasks with Sabouraud dextrose broth without the addition of fungal cells (+/- cat hair or L-cysteine) were stored in the cabinet in 24 hours darkness without shaking as negative controls (Fig. 4.1).

Broth experiment 1: Broth was collected sequentially from 5 days post inoculation (DPI) to 14 DPI from multiple isolates of *M. canis* grown without shaking and either with (HU) or without hair (NU), and exposed to 8 hours of light (Table 4.2). Samples collected for this experiment were unbaffled flask with hair (HU), unbaffled flask with no broth additives (NU), negative control broth with hair (no fungi added, NTCH), and negative control broth with no broth additives (no fungi added, NTCN) (Tables 4.1 and 4.2).

Broth experiment 2: Isolates were regrown in Sabouraud dextrose broth with shaking, either with or without hair and exposed to 8 hours of light (Table 4.2). Broth was collected sequentially from 1 DPI to 17 DPI. Broth samples collected for this experiment included unbaffled flask with hair (HU), baffled flask with hair (HB), unbaffled flask with no broth additives (NU), baffled flask with no broth additives (NB), negative control broth with hair (no fungi added, NTCH), and negative control broth with no broth additives (no fungi added, NTCN) (Tables 4.1 and 4.2).

Broth experiment 3: Isolates of *M. canis* were regrown in Sabouraud dextrose broth with the following conditions: shaking, baffled or unbaffled flasks, supplemented with hair or L-cysteine, and exposed to 8 hours of light (Table 4.2). Broth samples collected were baffled flask with hair (HB), unbaffled flask with hair (HU), baffled flask with L-cysteine (CB), unbaffled flask with L-cysteine (CU), baffled flask with no broth additives (NB), unbaffled flask with no broth additives (NU), negative control broth with no broth additives (no fungi added, NTCN), negative control broth with hair (no fungi added, NTCH), and negative control broth with L-cysteine (no fungi

added, NTCC) (Tables 4.1 and 4.2). Broth from each sample was concentrated five-fold before use in downstream applications. This experiment was repeated twice with collection days ranging (1) 3-16 DPI, and (2) 1-18 DPI.

Broth experiment 4: Isolates of *M. canis* were regrown in Sabouraud dextrose broth with the following conditions: shaking, baffled flasks, supplemented with hair or L-cysteine, and exposed to 24 hours light or darkness (Table 4.2). Broth samples collected were 24 hours light with hair (HBL), 24 hours darkness with hair (HBD), 24 hours light with L-cysteine (CBL), 24 hours darkness with L-cysteine (CBD), 24 hours light with no broth additives (NBL), 24 hours darkness with no broth additives (NBD), negative control broth with no broth additives (no fungi added, NTCN), negative control broth with hair (no fungi added, NTCH), and negative control broth with L-cysteine (no fungi added, NTCC) (Tables 4.1 and 4.2). Broth from each sample was concentrated five-fold before use in downstream applications.

Broth sample processing: Broth was collected one to two times per week for up to three weeks in a 2 ml tube from each flask and stored at -20°C until utilized for downstream processing. Samples with visible fungal cellular debris were thawed and centrifuged for 2 minutes at 8,000xg and the supernatant was removed. This step removed enough debris to avoid clogging of filters used in subsequent steps. For samples that were concentrated (broth experiments 3 and 4), 1.5 ml of the sample was added to an ultra-centrifugal filter (Amicon Ultra-10K Centrifugal Filter Deice, 10,000 MWCO, Millipore, Ireland) and centrifuged following manufacturer's protocol; first spin at 4,000xg for 10 minutes and second spin at 1,000xg for 2 minutes. The concentrated solute was thoroughly mixed with 200 µl of diluent (2 g bovine serum albumin, 4 ml fetal bovine serum, 95.5ml wash buffer, and 0.5 ml Triton X-100) and tested using ELISA protocols described below.

4.2.3 Sub3 ELISA

Baseline ELISA protocol: High binding 96-well plates (Immulon 2 HB, ThermoFisher Scientific, Houston, Texas, USA), were coated with either 10 ng/µl or 15 ng/µl of commercially produced polyclonal antibodies to Sub3 (Ab93) (GenScript, Piscataway, NJ, USA) diluted in 50 mM carbonate buffer (44 mM sodium biocarbonate, 6 mM sodium carbonate, 1 L of MilliQ® water, pH 9.5), and incubated overnight at 4°C. The contents of the wells were discarded and 300 µl of 2% bovine serum albumin was added to each well. The plate was incubated at room temperature on a plate shaker for at least 2 hours and then the contents were discarded. Positive controls consisted of either a serial dilution of recombinant Sub3 (rSub3) or 100 µl of 3.2 µg/µl rSub3 (GenScript, Piscataway, NJ, USA) in triplicate wells (n=3). One hundred microliters of MilliQ® water or 2% bovine serum albumin (BSA) was added in triplicate wells as negative controls. One hundred microliters of broth was added in triplicate wells (n=3) for sample assessment. The plate was incubated at room temperature for 2 hours on a plate shaker. Contents were discarded and the plate was washed five times with wash buffer containing 0.2% TWEEN 20 (2 mM imidazole, 160 mM sodium chloride, 0.5 mM EDTA, 0.162 mM TWEEN 20). 100 µl of conjugated anti-Sub3 rabbit antibodies (Ab93) diluted in diluent with 5% mouse sera was added to each well, and the plate was incubated in the dark at room temperature on a plate shaker for 1 hour. Anti-Sub3 antibodies were purified and conjugated with horseradish peroxidase (HRP) using antibody concentration and conjugation kits (Abcam, Waltham, MA, USA). Contents were discarded and washed five times with wash buffer containing 0.2% TWEEN 20. 100 µl of TMB was added to each well for 7 minutes, then was stopped with 50 µl of 2.5 N

sulfuric acid. Optical density (OD) was read on a Multiskan® Spectrum spectrophotometer (ThermoFisher Scientific, Waltham, MA, USA) at 450 nm.

Assay optimization: The baseline ELISA protocol was further optimized to enhance sensitivity and specificity for assessment of clinical samples. Optimization protocols included (1) comparisons of ELISA plate types, (2) variation in coating antibody concentration, and type of antibody, (3) variation in blocking incubation time, (4) type of antibody conjugate used, (5) variation in detection antibody concentration and type, and (6) direct coating of plates versus use of a sandwich assay. (1) Plate types evaluated were Immulon 2 HB, Immulon 4 HBX, and Nunc-Immuno MaxiSorp (ThermoFisher Scientific, Houston, Texas, USA). (2) Coating antibody concentrations tested ranged from 10 ng/µl to 20 ng/µl for both anti-Sub3 rabbit antibodies produced commercially (Ab92 and Ab93) (GenScript, Piscataway, NJ, USA). (3) Blocking incubation time was increased from two hours to overnight at 4 °C. (4) Two conjugation systems were evaluated: horseradish peroxidase (HRP) and biotin-streptavidin. For the biotin-streptavidin system, non-specific binding of streptavidin was evaluated regarding ELISA reagents (2% BSA, ELISA diluent) and the ELISA protocol in the absence of biotinylated antibodies. For testing the ELISA reagents, each reagent was utilized for the coating, blocking and sample steps of the protocol, followed by the addition of biotinylated antibodies and streptavidin. (5) Detection antibodies were conjugated with either HRP or biotin (Abcam, Waltham, MA, USA) and optimal concentrations of the antibody were determined. For the biotin-streptavidin system, optimal ratio of biotinylated antibody to streptavidin (Abcam, Waltham, MA, USA) was also determined. Additionally, using the biotin-streptavidin system, indirect sandwich ELISAs were evaluated using the unconjugated version of the rabbit antigen-detection antibody (Ab93) followed by polyclonal biotinylated goat anti-rabbit antibody that was preadsorbed (Abcam, Waltham, MA,

USA). (6) Direct ELISAs were also evaluated using both the HRP and biotin-streptavidin systems where the plates were coated overnight at 4 °C with the sample.

Optical density threshold for positive result: The cutoff value for sample positivity was calculated using the following equation $Cutoff = \left(OD_{avg}\right) + (3 * OD_{std})$, where OD_{avg} is the average optical density of the negative control and OD_{std} is the standard deviation of the optical density results for the negative control [Lardeux *et al.* 2016]. The indeterminate range was determined as 1-2 times the cutoff value. The limit of detection (LoD) was considered to be the lowest concentration of rSub3 that produced an OD value above the indeterminate range.

Statistical analysis: Samples were run in technical triplicates (n=3) and the standard deviation was calculated for each sample. OD values from different groups were compared using Student's t-test in R (v4.0.4) and p-values less than 0.05 were considered significant.

4.2.4 Immunohistochemistry of skin biopsy samples

To confirm anti-Sub3 antibody detection of Sub3 from clinical samples, immunohistochemistry was performed on skin biopsy samples. Biopsy samples included (1) two presumptive dermatophytosis cases from domestic cats (unconfirmed fungal species) and (2) two negative control cases (no known history of dermatophytosis). Slides of the biopsy tissues were stained using an automated stainer (Leica Bond III automated IHC stainer, Newcastle, UK) using Bond Polymer Refine Red Detection kit (Leica Biosystems, Newcastle, UK). Unconjugated anti-Sub3 antibodies (Ab93 and Ab92) were used for antigen detection at 1:600 dilution (533 ng/ml and 680 ng/ml, respectively).

4.2.5 RNA collection and conversion to cDNA

RNA extraction: RNA was collected from broth containing fungal pellets on the same collection days as broth samples (Section 4.2.2). Fungal cells were degraded by using a published protocol as a prior step for RNA collection [Brillowska-Dąbrowska 2006]. Briefly, 500 µl of fungal pellets was added to 100 µl of extraction buffer (60 mM sodium bicarbonate, 250 mM potassium chloride, and 50mM Tris, balanced to pH 9.5) in a 1.5 ml tube and incubated at 95°C for 10 minutes. Then, 100 µl of 2% bovine serum albumin was added to the tube and vortexed. This solution was used in the RNeasy Plant Mini Kit (Qiagen, Valencia, CA, USA) as the lysate following the manufacturer's protocol.

RNA quality check: RNA concentration was measured for each sample as well as purity using a spectrophotometer (Nanodrop ND-1000, Thermofisher Scientific, Waltham, MA, USA). The wavelength 260/280 ratio measures nucleic acid purity of samples [Desjardins *et al.* 2010]. RNA samples with a value of 2.0 were considered to have high purity [Desjardins *et al.* 2010].

cDNA conversion: After the RNA collection, DNase was added to remove any remaining DNA using the following protocol: 50 µl of RNA, 12 µl of Reaction Buffer (New England BioLabs, Ipswich, MA, USA), and 12 µl DNase 1 (New England BioLabs, Ipswich, MA, USA). The reaction was run on a C1000 Touch thermal cycler (Bio-Rad, Hercules, CA, USA) for 30 minutes at 37°C. To stop the enzyme, 6 µl of EDTA was added to each tube and run again for 10 minutes at 65°C. To convert the RNA into cDNA, equal parts of DNA-free RNA and master mix were mixed together and run on the thermal cycler for 50 minutes at 42°C then 5 minutes at 95°C. The master mix consisted of 10 µl 5X first-strand buffer (Invitrogen, Carlsbad, CA, USA), 2.5 µl of 10 mM dNTP mix (ThermoFisher Scientific, Waltham, MA, USA), 2.5 µl of 100 mM DTT (Invitrogen, Carlsbad, CA, USA), 0.625 µl RNase OUT (Invitrogen, Carlsbad, CA, USA), 0.625 µl SuperScript II Reverse Transcriptase (Invitrogen, Carlsbad, CA, USA), 5 µl Random

Primers (Invitrogen, Carlsbad, CA, USA), and 3.75 µl UltraPure DNase/RNase free distilled water (Invitrogen, Carlsbad, CA, USA). The cDNA was stored at -20°C for no longer than 1 month before use in RT-qPCR.

4.2.6 RT-qPCR

RT-qPCR: In a 96-well plate (96-well Hard-Shell PCR plates, BioRad, Hercules, CA, USA), 10 µl of SYBR Green Supermix (BioRad, Hercules, CA, USA), 3 µl UltraPure DNase/RNase free distilled water (Invitrogen, Carlsbad, CA, USA), 1 µl of forward primer and 1 µl of reverse primer were added per well. Primers were utilized for targeting the reference genes [Ciesielska *et al.* 2018] and SUB3 gene (created using Geneious v10.0.9) (Table 4.3). The three reference genes included were multiubiquitin chain binding protein 1 (mbp1), β-actin, and succinate dehydrogenase complex flavoprotein subunit A (sdha). For negative control wells, either 5 µl of UltraPure DNase/RNase free distilled water or 5 µl of DNased RNA were added. Five microliters of cDNA was added into wells for each sample and each sample was run in technical triplicates (n=3). After sealing the plate, the plate was centrifuged at 1,000xg for 2 minutes. The plate was run on a CFX Connect Real-Time system machine (BioRad, Hercules, CA, USA) for the following protocol: 1 minute at 95°C; 40 cycles of 20 seconds at 95°C, 30 seconds at 72°C; melt curve from 72°C to 95°C with increments of 0.5°C for 10 seconds.

Relative gene expression calculations: RNA was collected at the specific timepoints for each broth experiment, and RT-qPCRs were performed to measure the gene expression of SUB3 relative to the reference gene mbp1. Samples collected from broth experiment 3 were baffled flask with hair (HB), unbaffled flask with hair (HU), baffled flask with L-cysteine (CB), unbaffled flask with L-cysteine (CU), baffled flask with no broth additives (NB), unbaffled flask

with no broth additives (NU), and negative control broth with no broth additives (no fungi added, NTCN). Samples collected for broth experiment 4 were all from baffled flasks that had the following condition combinations: hair with 24 hrs darkness (HBD), hair with 24 hrs light (HBL), L-cysteine with 24 hrs darkness (CBD), L-cysteine with 24 hrs light (CBL), no broth additives in 24 hrs darkness (NBD), no broth additives in 24 hrs light (NBL), and negative control broth with no broth additives (no fungi added, NTCN). Relative gene expression was reported as $\Delta C_T = \left(C_{T,Sub3} - C_{T,mbp1}\right)_{sample}$ and C_T = threshold cycle. where positive ΔCT means that SUB3 gene had lower expression than the reference gene, while negative ΔCT means SUB3 had higher expression than the reference gene. C_T values above 40 were not reported.

Statistical analysis: Samples were run in technical triplicates (n=3) and the standard deviation was calculated for each sample. C_T values from different groups were compared using Student's t-test in R (v4.0.4) and p-values less than 0.05 were considered significant.

4.3 Results

4.3.1 Optimization of Sub3 ELISA

Using the baseline ELISA protocol, the LoD of rSub3 was 2.6 pg/µl for plates coated with either 10 ng/µl or 15 ng/µl of antibody Ab93 (Fig. 4.2). The indeterminate range was calculated to be 0.11-0.22 for 10 ng/µl of coating antibody and 0.14-0.29 for 15 ng/µl of coating antibody.

Each step of the ELISA protocol was optimized to lower the LoD of Sub3. Between the three types of 96-well plates, Immunlon 4 HBX had lower sensitivity than Immunlon 2 HB or Nunc-Immun MaxiSorp, while the latter two plate types had similar OD values for the same rSub3 concentration (Fig. 4.3). As the Immunlon 2 HB plate had slightly lower LoD (Fig. 4.3),

this plate type was used for all remaining optimization steps. Coating antibody Ab92 at 20 ng/µl was found to have the lowest LoD of rSub3 at 0.65 pg/µl compared to other concentrations of Ab92 and Ab93 (Fig. 4.4). Adjustments that did not increase sensitivity or specificity included overnight incubation of the blocking solution and increasing the concentration of the antigen detection antibody for the HRP system (Suppl. Figs. 4.1 and 4.2). Using the biotin-streptavidin system, the optimal ratio of biotinylated antibody to streptavidin was achieved at 1:10,000 dilution of 100 µl of biotinylated antibody and 1:10,000 dilution of 100 µl of streptavidin (Fig. 4.5, Suppl. Fig. 4.3). This system resulted in a LoD higher than 2.6 pg/µl of rSub3 which is higher than the HRP system (Figs. 4.4 and 4.5). Non-specific binding of streptavidin was not observed regarding ELISA reagents (OD values were less than 0.05 for 2% BSA and ELISA diluent) or in the absence of biotinylated antibodies (Suppl. Fig. 4.4). Sandwich ELISAs conducted using goat anti-rabbit antibody resulted in high background signal (Suppl. Fig. 4.5). Direct ELISAs where the antigen was coated directly onto the plate resulted in very low OD values (Suppl. Fig. 4.6). Final optimized parameters are indicated in Table 4.4 to achieve the LoD of 0.65 pg/µl, a four-fold improvement from the baseline protocol.

4.3.2 Sub3 was undetectable in clinical samples and culture plates via ELISA

Using the baseline ELISA protocol, OD values for direct plate samples of *M. canis* and *Aspergillus* spp. were below the indeterminate range (Fig. 4.6). These OD values were similar to the negative controls of 2% bovine serum albumin (BSA) and MilliQ® water. Hair suspended in MilliQ® water from confirmed dermatophytosis via positive culture for *M. canis* cats also had OD values below the indeterminate range, even when samples were concentrated 5x via ultracentrifugation (Fig. 4.6). OD values were measured on ELISA plates with 10 ng/µl of coating antibody which has a LoD of 2.6 pg/µl of rSub3.

Using the optimized ELISA protocol where the LoD was 0.65 pg/µl of rSub3, OD values for 5x concentrated clinical hair, nail, and skin scrape samples suspended in ELISA diluent from the same four cats were below the indeterminate range (Fig. 4.7).

4.3.3 Anti-Sub3 antibodies detected Sub3 from dermatophytosis biopsies

Sub3 was detected in dermatophytosis skin biopsies (two presumptive cases in domestic cats) using our anti-Sub3 antibodies Ab93 and Ab92 in immunohistochemistry (Fig. 4.8). Staining was observed on approximately 50% of arthroconidia present in dermatophytosis biopsies (Fig. 4.8). No staining was observed in cases with no known history of dermatophytosis (Fig. 4.8).

4.3.4 Variable shaking and supplementation protocols did not influence Sub3 detection

All but three samples grown with hair from broth experiment 1 had OD values below the indeterminate range; samples with OD values within the indeterminate range included *M. canis* grown with hair collected on 10 DPI and negative control broths grown with hair collected on 7 and 10 DPI (Fig. 4.8). Fungal mats developed for all samples inoculated with *M. canis* by 14 DPI (data not shown). In order to disperse the fungi more evenly throughout the broth and to attempt to increase Sub3 production, broth experiment 1 was repeated with shaking. Fungal pellets developed for all samples inoculated with *M. canis* by 7 DPI with smaller pellets forming for samples without hair (NU, NB) compared to samples with hair (HB, HU) (data not shown). Similar to stationary isolates, all of the OD values for samples that were shaken (broth experiment 2) were below the indeterminate range (Fig. 4.9). OD values were measured using the baseline ELISA protocol coated with 10 ng/µl of antibody for broth experiments 1 and 2

samples. There was no significant difference between OD values of samples grown in baffled or unbaffled flasks (Table 4.5). Between samples grown with hair and without hair, the difference between OD values was only significant on 14 DPI (Table 4.5).

4.3.5 Sub3 could be detected in concentrated M. canis broth solute

Broth experiment 2 was repeated, but samples were concentrated five-fold before undergoing ELISA (broth experiment 3). When broth experiment 3 samples were measured using the baseline ELISA protocol coated with 10 ng/µl of antibody, OD values for all three baffled flask samples (HB, CB, NB) were above the indeterminate range by 16 DPI (Fig. 4.10). While the OD value for CU sample was above the indeterminate range by 16 DPI, the OD values for other unbaffled flask samples were within the indeterminate range at the same timepoint (Fig. 4.10). Fungal pellets developed for all samples inoculated with *M. canis* by 6 DPI with smaller pellets forming for samples without hair (CB, CU, NB, NU) compared to samples with hair (HB, HU) (data not shown).

When broth experiment 3 samples were run using the baseline ELISA protocol coated with 15ng/µl of antibody, the OD value for HB sample was above the indeterminate range by 8 DPI, continuing to increase at later timepoints (Fig. 4.11). The OD value of HU sample took longer than the OD value of HB sample to surpass the indeterminate range (11 DPI versus 8 DPI) (Fig. 4.11). By 18 DPI, the OD value of HB sample was higher than the OD value of HU sample (Fig. 4.11). Both OD values of NB and NU samples peaked at 15 DPI and decreased at 18 DPI (Fig. 4.11). The OD value of CB sample was slightly higher than the indeterminate range at 11 DPI, but decreased for later timepoints, falling below the indeterminate range by 18 DPI (Fig 4.11). CU sample became contaminated by 8 DPI (data not shown), leading to a low growth

of *M. canis* and Sub3 production. Fungal pellets developed for all samples inoculated with *M. canis* except CU by 4 DPI (data not shown). Fungal pellets were smaller for baffled flask samples (HB, CB, NB) compared to unbaffled flask samples (HU, NU).

4.3.6 Similar Sub3 production when fungi exposed to 24 hours of light or darkness

Using baffled flasks, broth experiment 4 was performed comparing light and dark cycles. Similar OD values were observed between flasks grown in light and darkness for un-supplemented samples and those supplemented with hair or L-cysteine when run using the baseline ELISA protocol with a coating antibody concentration of 15 ng/µl (Fig. 4.12). Fungal pellets developed for all samples inoculated with *M. canis* by 4 PDI with smaller pellets forming for samples without hair (CBD, CBL, NBD, NBL) compared to samples with hair (HBD, HBL) (Suppl. Fig. 4.7).

4.3.7 Quantifying M. canis gene expression

Reference genes for *M. canis* were analyzed via qPCR to ensure consistent expression in our laboratory setting. Three reference genes (β-actin, sdha, and mbp1) for *M. canis* were tested on RNA (converted into cDNA) from isolates of *M. canis* grown on SDA plates and similar expression was seen between the three reference genes (Fig. 4.13, Suppl. Table 4.1). Five primer sets targeting SUB3 were tested on *M. canis* isolates grown on SDA plates and similar expression was observed for all SUB3 primer sets (Fig. 4.14, Suppl. Table 4.2).

4.3.8 Highest SUB3 expression is detected in M. canis samples grown in baffled flasks with L-cysteine

For broth experiment 3 samples, HB sample had increasing ΔCT from 1 to 8 DPI, then decreased for later time points (Fig. 4.15). HU, CB, and NU samples had decreasing ΔCT from 8 to 15 DPI (Fig. 4.15). From 11 to 15 DPI, NU sample had an increasing ΔCT (Fig. 4.15). CT values were missing for CU sample due to contamination by 8DPI (Suppl. Table 4.3). At 4 and 18 DPI, all samples had CT values above 40 (Fig. 4.15). All samples except HB had CT values above 40 for 1 DPI due to low fungal growth (Suppl. Fig. 4.7 and Suppl. Table 4.3).

4.3.9 Higher expression of SUB3 in samples grown in 24-hour light cycle conditions

For broth experiment 4 samples, CBL sample had a negative change in ΔCT from 8 DPI to 11 DPI, going from 0 to -7.27 (Fig. 4.16). The ΔCT values for CBL sample continued to increase at 15 and 18 DPI, ending at -1.13 by 18 DPI (Fig. 4.16). The ΔCT values for NBL sample followed a similar trend with the ΔCT value at 15 DPI being the most negative (Fig. 4.16). HBD sample had a decreasing ΔCT value trend from -1.19 to -2 at 8 and 15 DPI, respectively (Fig. 4.16). Both HBL and CBD samples had CT values above 40 for all collection days except one: 15 DPI for HBL sample and 18 DPI for CBD sample (Fig. 4.16 and Suppl. Table 4.4). All samples had CT values above 40 for 1 and 4 DPI due to low fungal growth (Suppl. Fig. 4.7 and Suppl. Table 4.4).

4.4 Discussion

We have developed and optimized an antibody-based assay that can detect Sub3 protein produced by *M. canis*. Although this assay could not detect Sub3 directly from clinical samples (hair, nails, and superficial skin scrapes), the antibodies developed were able to identify Sub3 from skin biopsy samples of dermatophytosis cases. Isolates of *M. canis* were grown in various

culture conditions and were collected for measuring Sub3 production (via anti-Sub3 ELISA) and SUB3 expression (via RT-qPCR). When compared between culture conditions of flask type, broth supplementation and lighting, a greater amount of Sub3 was produced when samples were grown in baffled flasks and supplemented with either L-cysteine or cat hair with either a 24-hour darkness or light cycle, allowing for a deeper understanding of Sub3 metabolism in *M. canis.* Our results also demonstrated that *M. canis* can produce Sub3 in the absence of a keratin source, suggesting that other environmental factors contribute to activating SUB3 expression and production.

We optimized our Sub3 ELISA to have a limit of detection of 0.65 pg/µl of Sub3 after determining the optimal assay conditions, comparable to other sandwich ELISA assays [Dutaud *et al.* 2002, Vashist *et al.* 2014, Wang *et al.* 2014]. However, clinical hair sample solutions had ELISA OD values below the indeterminate range, suggesting low Sub3 levels. These levels could be due to the low quantity of fungi present or low fungal metabolic activity on the hair samples. To increase the amount of Sub3 present, clinical hair samples were concentrated five-fold, slightly increasing the OD values, but still below the indeterminate range. Nail and skin scrape samples were also tested and concentrated five-fold, resulting in similarly low value OD results as the hair samples. Further concentration could increase the Sub3 levels high enough to result in OD values above the indeterminate range. Additionally, hair samples may be suboptimal for Sub3 detection, as *M. canis* can perforate hair, which could result in Sub3 being trapped within the hair shaft [Gräser *et al.* 2000, Kidd *et al.* 2016]. Testing with deeper skin scrape samples might yield more favorable results for detecting this protein as Sub3 was detected from skin biopsy samples using immunohistochemistry. If accurate detection of Sub3 from clinical samples is achieved, this ELISA could be utilized for rapidly screening clinical samples

for *M. canis* infections, which would be highly useful in animal shelters with high population densities [Moriello 2001, Moriello 2014]. Additionally, this assay could be further modified to include antibodies to other subtilisins that are expressed during other timepoints of infection to cover a broader range of infections at different stages.

To optimize the ELISA, we tested different assay conditions and compared the limit of detection to our baseline protocol. Although the biotin-streptavidin conjugation system has been reported as a more sensitive system compared to HRP [Mishra *et al.* 2019], we experienced higher levels of background noise and lower sensitivity with biotin-streptavidin even after testing for non-specific binding between streptavidin and assay reagents, suggesting that there is cross-reactivity between the coating and antigen detecting antibodies. There were also high OD values for negative controls when anti-rabbit goat antibodies were used, showing that these antibodies interacted with the coating antibodies. Developing new coating antibodies from another animal species (such as mouse) could help reduce or eliminate high background signals, leading to greater assay sensitivity.

To increase the quantity of metabolically active fungi and amount of Sub3 present, we grew *M. canis* samples in media. Sub3 was undetectable in fungal samples grown on solid media as OD values for these samples were below the indeterminate range. As vegetative hyphae of filamentous fungi burrow into solid media [Samanta 2015], Sub3 could be produced within the agar, but would be difficult to measure without digesting the agar. *M. canis* was switched to growing in liquid media to allow for the suspension of Sub3. *M. canis* isolates that were grown with shaking and broth supplementation had OD values below the indeterminate range, resulting in undetectable levels of Sub3. To increase the concentration of Sub3, these samples were concentrated five-fold, resulting in OD values above the indeterminate range as early as 8 DPI.

Baffled flasks led to greater ELISA OD values compared to unbaffled flasks for all three culture conditions (HB, CB, and NB), likely due to the baffled flask samples developing smaller fungal pellets during the experiments. Clumping of filamentous fungi into pellets has been documented in industrial fermentation as reducing metabolite production [Miyazawa *et al.* 2016]. While the outer layer of the pellets has direct contact with nutrients, the inner layers lack access, leading to nutrient deficiencies and decreased metabolism [Kelliher *et al.* 2020]. For future metabolic studies of *M. canis*, growing the cultures in baffled flasks could lead to a greater efficiency of metabolite production. Increased agitation may further reduce pellet size and increase metabolite production [Metz *et al.* 1977]. Modifying the current experimental setup to explore different agitation rates could help increase Sub3 metabolism, leading to earlier detection of Sub3.

Samples from broth experiments 3 and 4 had low Sub3 production and expression at 1 and 4 DPI, most likely due to low growth observed at those timepoints. While *M. canis* has been shown to have a faster growth rate than other dermatophyte species [Achterman *et al.* 2011], previous studies have shown that dermatophytes are still in the lag phase after 72 hours after media inoculation [Alió S *et al.* 2005, Achterman *et al.* 2011]. During this phase, fungi focus on absorbing nutrients and germinating spores then elongating hyphae before entering the first transition phase characterized by further elongation of hyphae [Meletiadis *et al.* 2001]. The maximum growth slope occurs afterward in the log phase followed by the second transition phase, where the growth curve decreases, and finally enters the stationary phase defined by a flat growth curve [Meletiadis *et al.* 2001]. As filamentous fungi have long transition phases compared to yeast [Meletiadis *et al.* 2001], it would be beneficial to select a medium that reduces time in this phase and quickly shifts the fungi to the log phase. Media composition has been shown to affect growth rates of fungi and hyphae to conidia growth ratios [Achterman *et al.*

2011, Faway *et al.* 2021]. Switching *M. canis* growth toward hyphal and arthroconidia development would increase Sub3 production, as hyphae and arthroconidia can produce Sub3 [Mignon *et al.* 1998, Baldo *et al.* 2008]. For *M. canis* growth, Sabouraud dextrose broth has been shown to have the lowest yield of conidia compared to other media such as malt extract agar, oatmeal agar, and yeast extract peptone dextrose agar [Achterman *et al.* 2011]. Another medium that has been shown to produce lower quantities of conidia for *M. canis* is yeast extract nitrogen agar [Faway *et al.* 2021]. Compared to Sabouraud dextrose broth, this media lacks glucose and has added yeast extract [Faway *et al.* 2021]. Repeating our broth experiments using these other mediums could result in higher production of Sub3 at earlier timepoints, leading to earlier detection of Sub3.

Samples grown in baffled flasks with L-cysteine supplementation had the highest SUB3 gene expression via RT-qPCR. Although SUB3 gene expression was higher during L-cysteine supplementation compared to hair, the overall quantity of Sub3 protein produced was lower. Given these results and that hair is structurally more complex and is only made of 18% cysteine [Kasperova *et al.* 2013], it suggests that fungi interact with other components of hair such as other amino acids to initiate and maintain production of Sub3 protein. The levels of L-cysteine supplementation could have been toxic to *M. canis* as L-cysteine has been found have negative impacts on other fungal species [Hennicke *et al.* 2013]. Furthermore, samples grown without hair or L-cysteine supplementation were also able to express and produce Sub3, suggesting that while keratin may enhance Sub3 metabolism, it is not critical for Sub3 metabolism. While this has been demonstrated for *Trichophyton rubrum* through *in vitro* growth experiments [Giddey *et al.* 2007, Maranhão *et al.* 2007, Leng *et al.* 2009, Zaugg *et al.* 2009, Chen *et al.* 2010], this is the first reported study for *M. canis*. A factor to explore for increasing Sub3 production and

expression is the base media composition of SDB. While this media supports growth of *M. canis*, other nutrients could be utilized to shift fungal metabolism toward pathways that induce and support Sub3 expression and production. Urea supplementation could be explored as it has been demonstrated in *T. rubrum* to aid in keratin degradation by increasing pH which allows the fungi to initiate infection and grow [Martins *et al.* 2020]. pH could also be monitored in this experimental setup to elucidate how the fungi change their environment during different growth phases and how manipulation of pH can affect their metabolism. However, it has been demonstrated for other fungal species that metabolism enhancement via changes to media composition can vary between strains of the same species [Vandermolen *et al.* 2013], suggesting that further testing of the effects of media on *M. canis* metabolism would be helpful in fully understanding the influence of media on Sub3 production.

When compared to 24 hours of darkness, samples that were exposed to 24 hours of light had similar growth and pellet size at the same time points post inoculation, indicating that constant light and darkness have a similar influence on overall growth of the fungal cells. However, samples without any additives had a higher expression of SUB3 when exposed to 24 hours of darkness compared to 24 hours of light, implying that light can affect metabolic pathways of the adherence phase of infection. Circadian rhythms are directly affected by the absence or presence of light and can influence metabolism [Montenegro-Montero *et al.* 2015]. While circadian rhythms have been discovered in fungi including the class Eurotiomycetes [Brody 2019], these rhythms have not been established in dermatophytes, even though they belong to the same fungal class. Investigating whether *M. canis* possesses the genes responsible for circadian rhythms and the conditions they optimally run under could help improve our understanding of important factors that affect this species' metabolism.

Similar trends were observed between Sub3 production and expression for the different growth conditions, suggesting a relationship between expression and production. Given that *M. canis* grows as hyphae in media, it is difficult to quantify the amount of fungi present when collecting samples, making it challenging to standardize our measurements between assays (i.e. comparing our Sub3 ELISA results to our Sub3 qPCR results). For biological systems that use discrete, single cells, mRNA expression can be standardized to copy number per cell [Kanno *et al.* 2006]. As hyphae can vary in length and can have different stages of metabolism occurring, comparing mRNA expression to cell number is not feasible for filamentous fungi [Serrano-Carreón *et al.* 2015]. Numerous methods have been developed to standardize hyphae samples, however, many of these techniques still have to be standardized for individual fungal species [Petrikkou *et al.* 2001]. Further investigations into methods to standardized hyphae samples would greatly benefit the filamentous myology field.

In summary, we found that while clinical samples and solid media cultures of *M. canis* had low production of Sub3, Sub3 could be detected from concentrated liquid media isolates as early as 8 DPI. In order to have this ELISA become useful in a clinical setting, further optimizations are required to increase the level of detection of Sub3 from clinical samples. Additionally, we were able to increase the production of this protein by culturing the fungus in baffled flasks supplemented with L-cysteine or hair and demonstrated that these supplements are not vital for initiating Sub3 metabolism. Given that the production of this protein can be modulated by environmental factors and is essential for the initial stage of infection, novel therapies could be designed to target the production of Sub3, preventing *M. canis* from establishing an infection. This type of therapy would be beneficial in exposure cases such as littermates where one animal has dermatophytosis and the others lack clinical signs. These

findings could also help direct future studies for metabolic studies investigating *M. canis* and potentially other dermatophyte species, such as *T. tonsurans* and *T. rubrum* during adherence phase of infections.

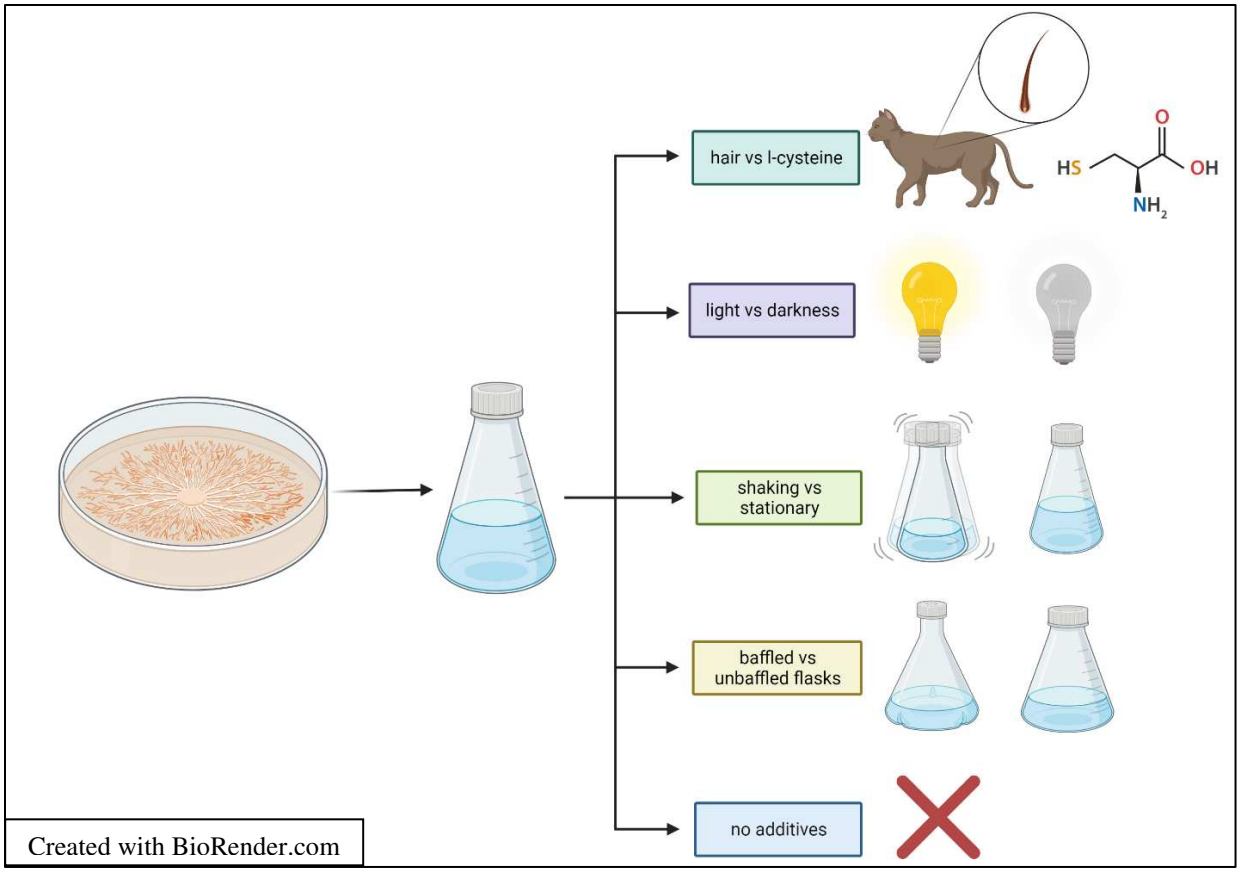

Figure 4.1. Experimental design of broth experiments. *M. canis* was first grown on solid media until sufficient mycelium size was reached. A section of mycelium was added to a flask and grown under certain conditions including (1) hair or l-cysteine supplementation, (2) 24-hour light or darkness cycle, (3) shaking or stationary, (4) baffled or unbaffled flask, or (5) no additives.

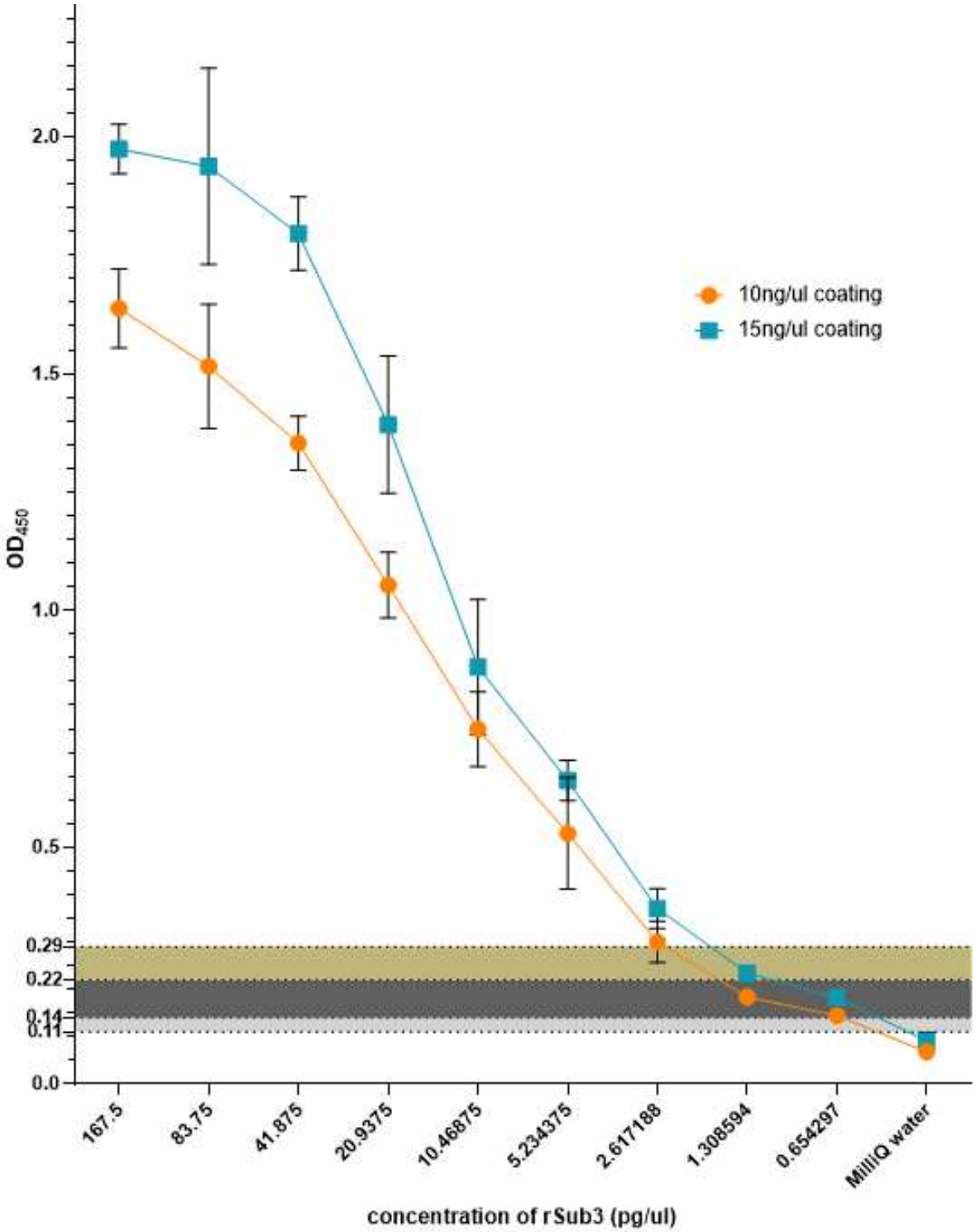

Figure 4.2. Same limit of detection (LoD) of rSub3 for both coating antibody concentrations. Both plates (10 ng/µl and 15 ng/µl of coating antibody) had a LoD of 2.6 pg/µl of rSub3. The indeterminate range was determined as 1-2x cutoff value for each coating antibody concentration. The indeterminate range for 10 ng/µl ELISA plates was 0.11-0.22 (light gray to dark gray region) and 0.14-0.29 (dark gray to gold region) for the 15 ng/µl ELISA plates. Samples were run in triplicate (n=3) and standard deviation was less than 0.21 for all points.

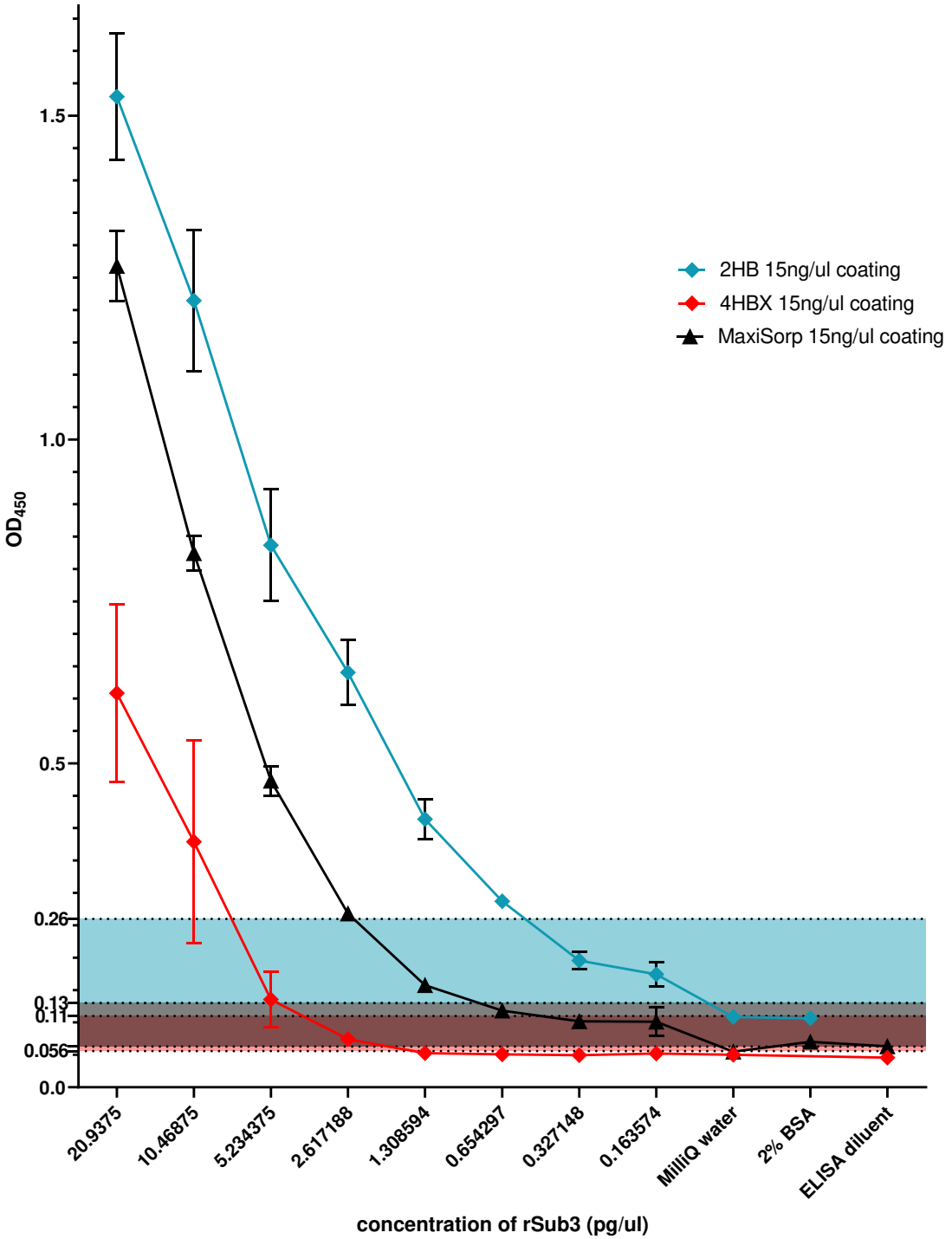

Figure 4.3. 2HB plate had lowest limit of detection (LoD) of rSub3 compared to other plate types. The LoD for 2HB plates was 0.65 pg/µl of rSub3, while it was 1.3 pg/µl for MaxiSorp plates and 5.23 pg/µl for 4HBX plates. The indeterminate range was determined as 1-2x cutoff value for each coating antibody concentration. The indeterminate range for 2HB plates was 0.13-0.26 (blue shaded region), for 4HBX plates was 0.056-0.11 (red shaded region), and for MaxiSorp plates was 0.063-0.13 (gray shaded region). Samples were run in triplicate (n=3) and standard deviation was less than 0.16 for all points.

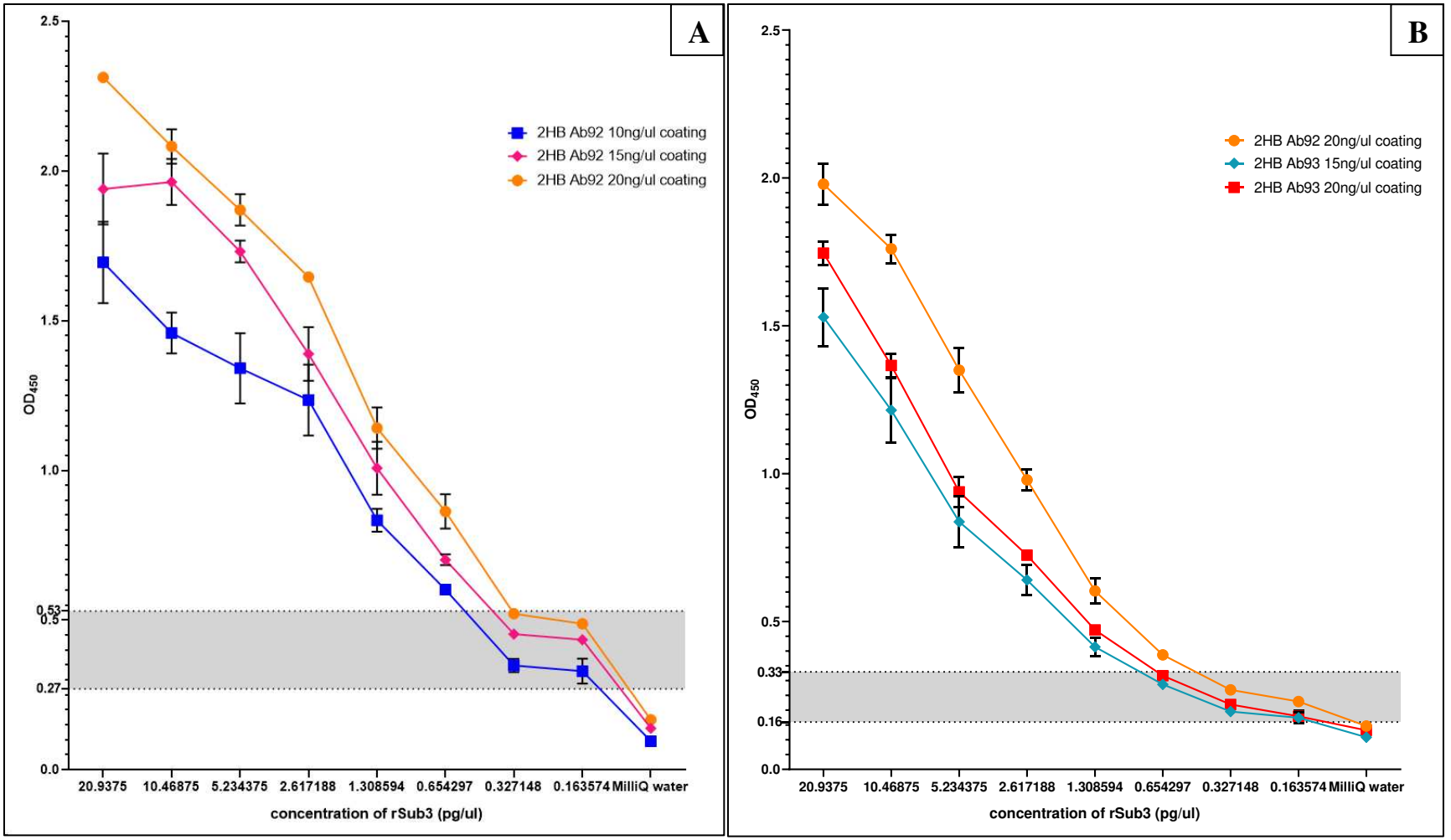

Figure 4.4. Coating antibody Ab92 lead to lower limit of detection (LoD) compared to antibody Ab93. (A): Compared LoD for plates coated with different concentration of coating antibody Ab92. Lowest LoD was seen for 20 ng/µl of coating antibody Ab92. (B): Compared LoD for plates coated with either antibody Ab92 or Ab93. Lowest LoD was seen for 20 ng/µl of coating antibody Ab92. The indeterminate range was determined as 1-2x cutoff value for each plate. The indeterminate range for (A) and (B) was 0.16-0.33 (gray shaded region). Samples were run in triplicate (n=3) and standard deviation was less than 0.136 for all points.

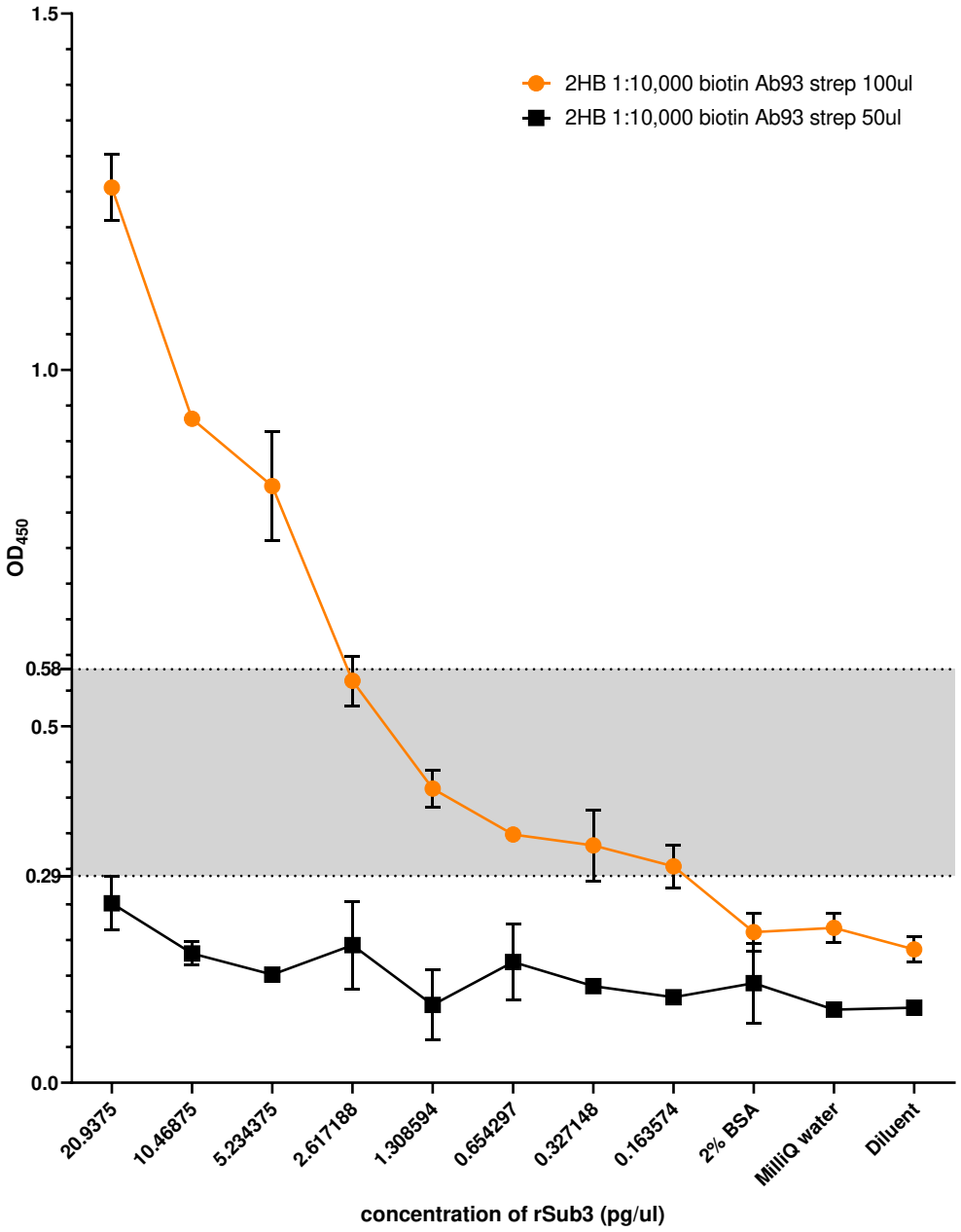

Figure 4.5. Biotin-streptavidin conjugation system led to higher background noise compared to HRP system. Optimal biotin to streptavidin ratio was determined to be 1:10,000 dilution of biotinylated antibodies to 100 µl of 1:10,000 streptavidin (orange color). The limit of detection for the optimized ratio (orange) was 2.6 pg/µl of rSub3. The indeterminate range was determined as 1-2x cutoff value. The indeterminate range was 0.29-0.58 (gray shaded region). Samples were run in triplicate (n=3) and standard deviation was less than 0.077 for all points.

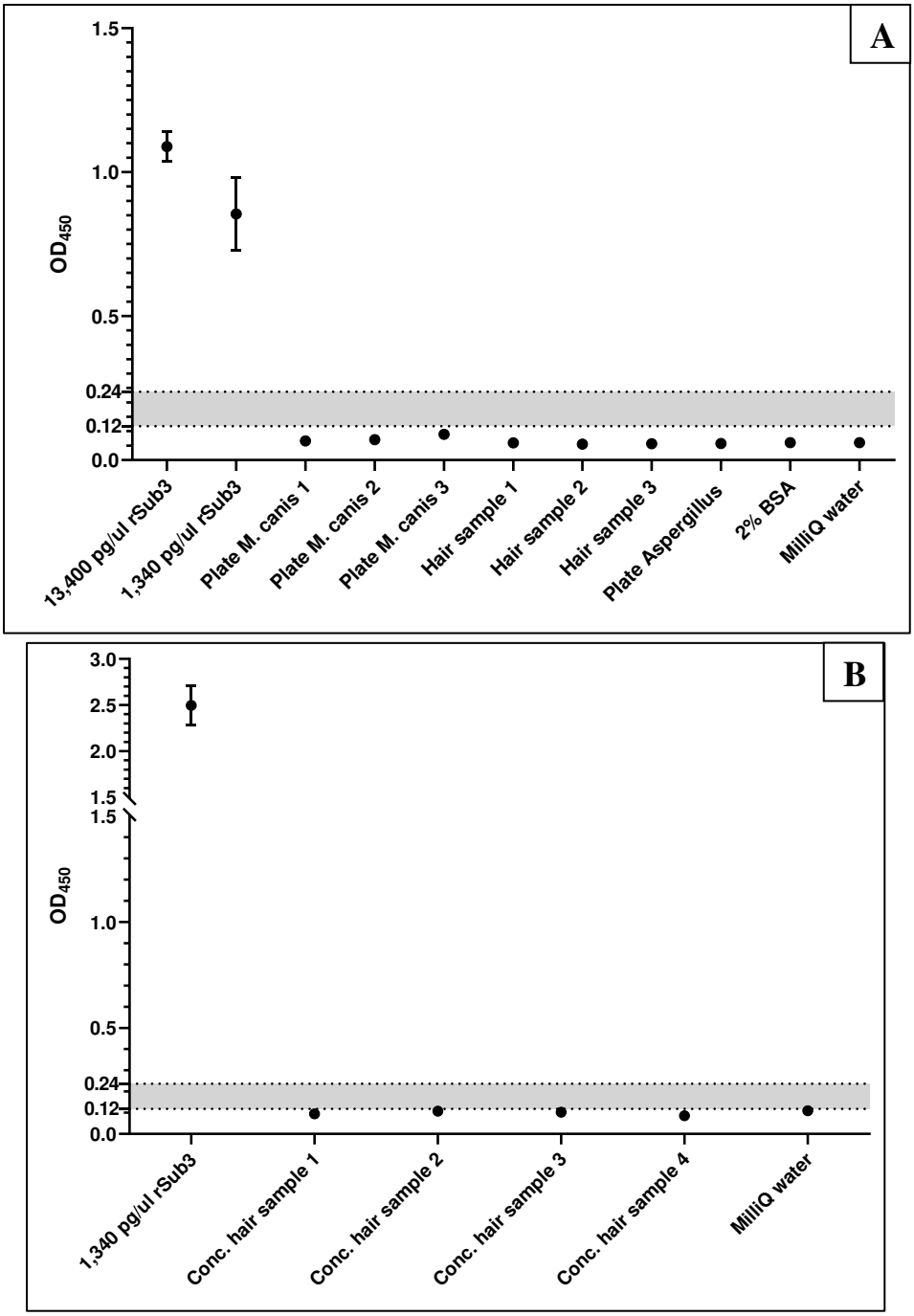

Figure 4.6. Non-detectable levels of Sub3 from culture plates of *Microsporum canis* and *Aspergillus* spp. and clinical hair samples. (A) Swabs of mycelium from *M. canis* (n=3) and *Aspergillus* spp. (n=1) that were grown on solid media agar plates were added to ELISA diluent then added to the ELISA plate. Hair from culture positive (of *M. canis*) samples were added to water then either (A) added to the ELISA plate (n=3) or (B) concentrated 5x then added to the ELISA plate (n=4). ELISA plates were coated with 10ng/µl of antibody Ab93. The indeterminate range (gray shaded region) was calculated as 1-2x the cutoff value. Samples were run in triplicate (n=3) and standard deviation was less than 0.213 for all points.

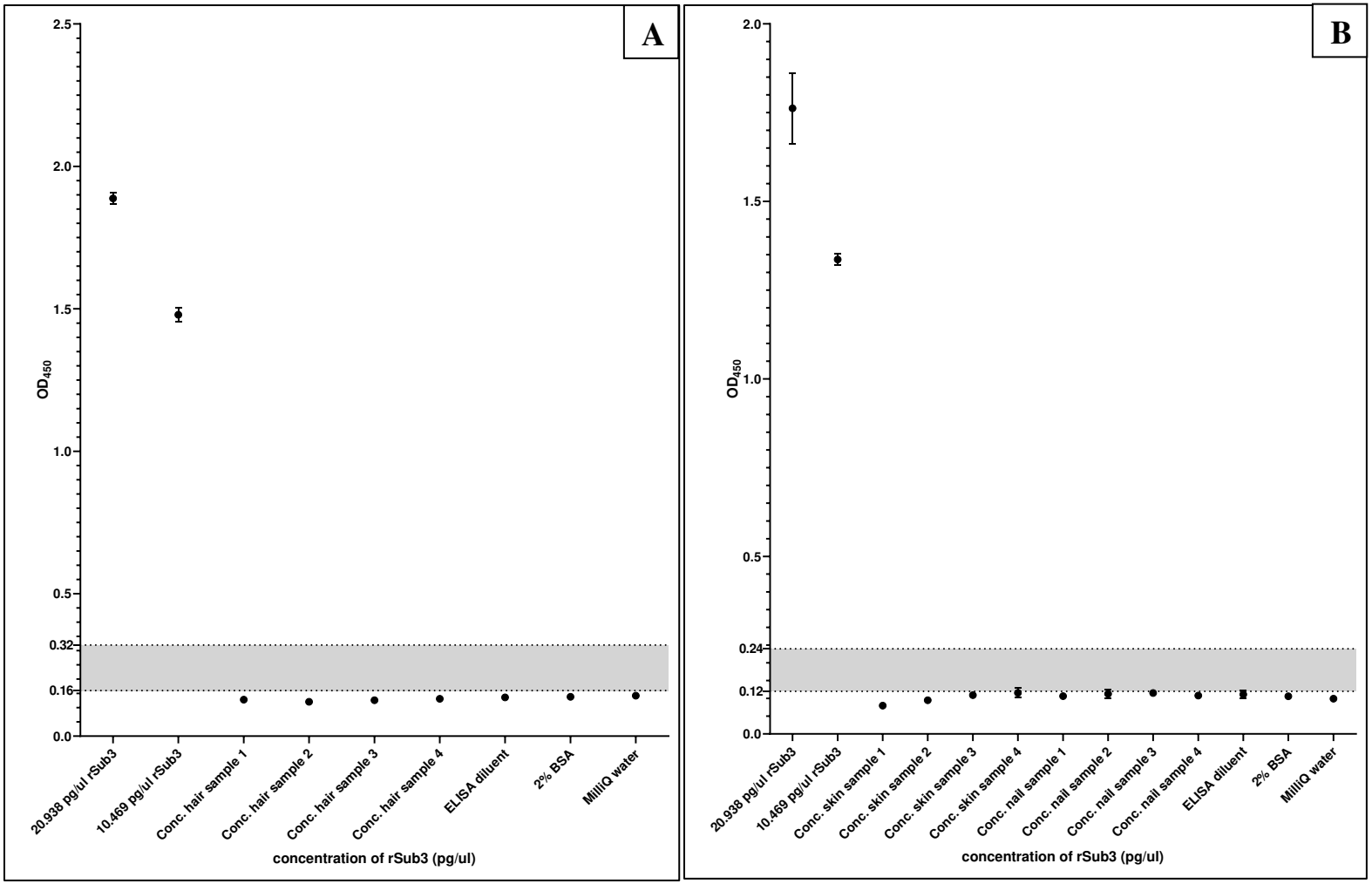

Figure 4.7. Non-detectable levels of Sub3 from clinical hair, nail, and skin scrap samples using optimized ELISA. (A) Hair from culture positive (of *M. canis*) samples were added to ELISA diluent then concentrated 5x then added to the ELISA plate (n=4). (B) Nail and skin scraps from the same cat samples in (A) were added to ELISA diluent then concentrated 5x then added to the ELISA plate (n=4). ELISA plates were coated with 20ng/µl of antibody Ab92. The indeterminate range (gray shaded region) was calculated as 1-2x the cutoff value. Samples were run in triplicate (n=3) and standard deviation was less than 0.099 for all points.

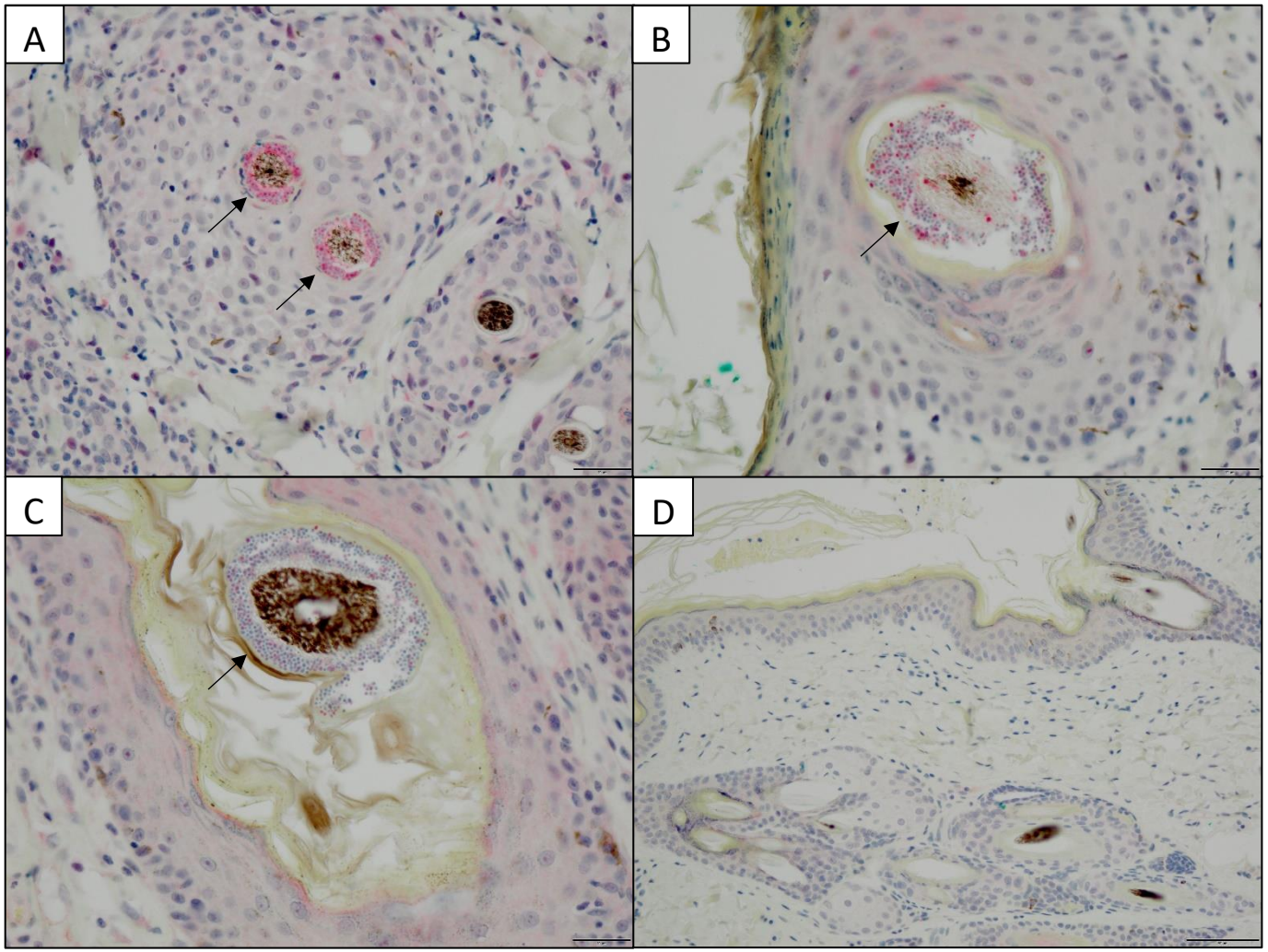

Figure 4.8. Detection of Sub3 observed in dermatophytosis skin biopsies. A, B, C – Staining of Sub3 (red stain, arrow) observed where arthroconidia can be observed, surrounding hair shafts. A, B, C – Skin biopsy samples of presumptive dermatophytosis in a domestic cat, anti-Sub3 antibody was used (A, B = antibody Ab93, C = Ab92), 40x magnification, scale bar = 20 µm. D – Skin biopsy of domestic cat with no known history of dermatophytosis, anti-Sub3 antibody Ab92 was used, 20x magnification, scale bar = 50 µm.

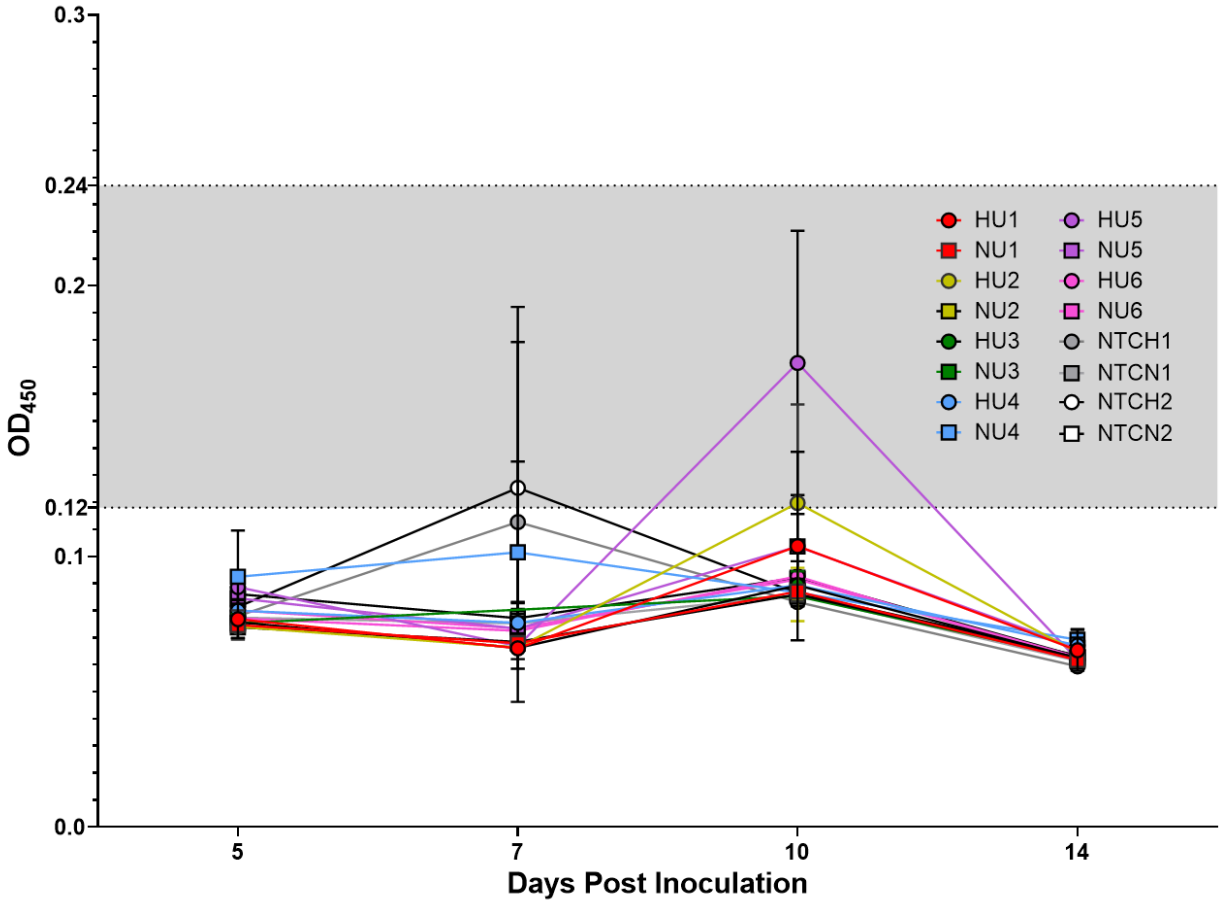

Figure 4.9. Sub3 from *Microsporum canis* isolates grown in broth without shaking was not detectable. Isolates of *M. canis* were grown in Sabouraud dextrose broth either with or without the addition of specific-pathogen free cat hair (broth experiment 1). Broth was collected periodically from each sample and used directly on the ELISA plate. ELISA plate was coated with 10ng/µl of antibody. The indeterminate range (gray shaded region) was calculated as 1-2x the cutoff value. HU = unbaffled flask with hair. NU = unbaffled flask with no broth additives. NTCH = negative control broth with hair (no fungi added). NTCN = negative control broth with no broth additives (no fungi added). Samples were run in triplicate (n=3) and standard deviation was less than 0.066 for all points.

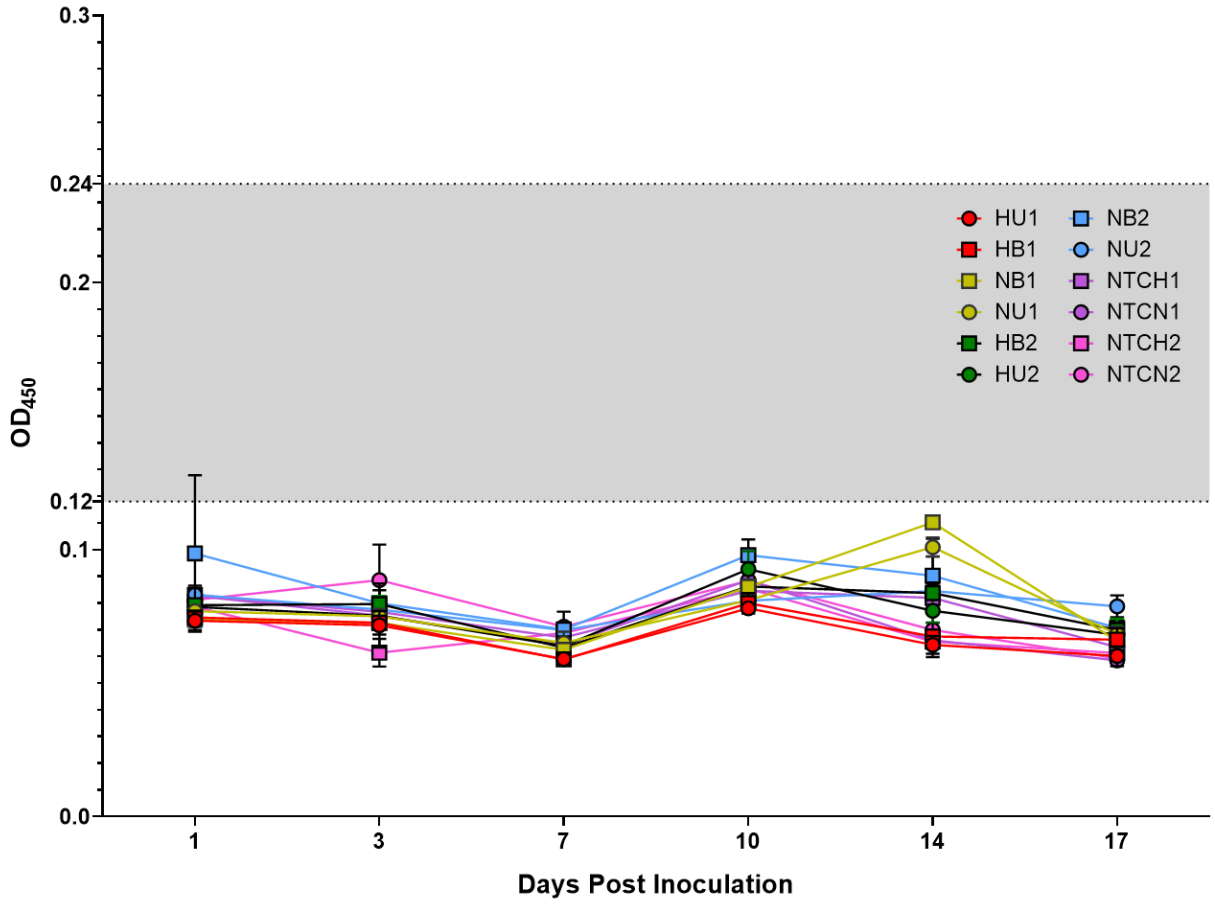

Figure 4.10. Sub3 from *Microsporum canis* isolates grown in broth with shaking was not detectable. Isolates of *M. canis* were grown in Sabouraud dextrose broth either with or without the addition of specific-pathogen free cat hair in either baffled or unbaffled flasks (broth experiment 2). Broth was collected periodically from each sample and used directly on the ELISA plate. ELISA plate was coated with 10ng/µl of antibody. The indeterminate range (gray shaded region) was calculated as 1-2x the cutoff value. HU = unbaffled flask with hair. HB = baffled flask with hair. NU = unbaffled flask with no broth additives. NB = baffled flask with no broth additives. NTCH = negative control broth with hair (no fungi added). NTCN = negative control broth with no broth additives (no fungi added). Samples were run in triplicate (n=3) and standard deviation was less than 0.089 for all points.

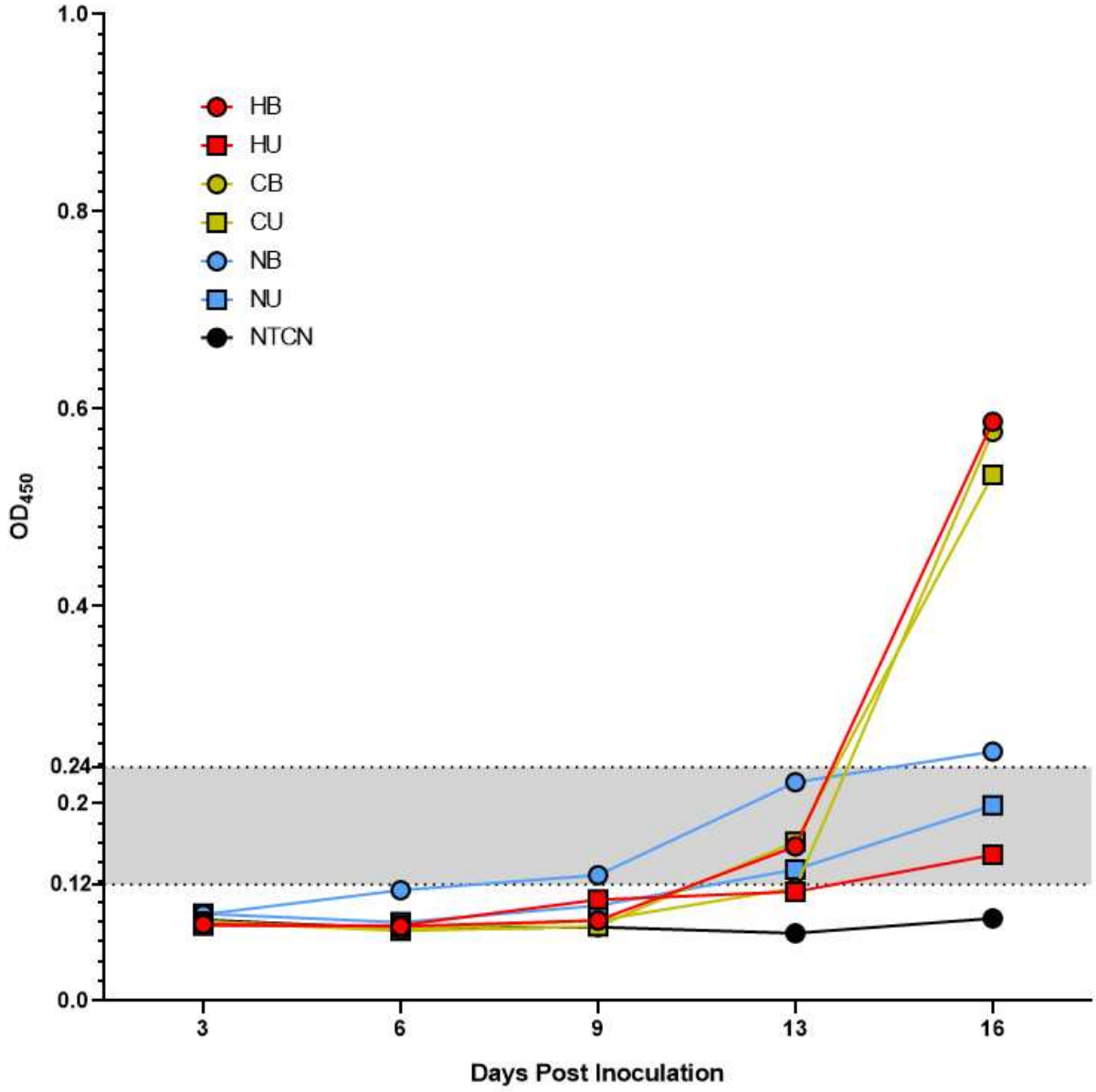

Figure 4.11. Detectable levels of concentrated Sub3 from *Microsporum canis* isolates grown in broth with shaking. Isolates of *M. canis* were grown in Sabouraud dextrose broth either with or without the addition of specific-pathogen free cat hair in either baffled or unbaffled flasks (broth experiment 3). Broth was collected periodically from each sample and ultracentrifuged to concentrate the solute 5x before adding to the ELISA plate. ELISA plate was coated with 10ng/µl of antibody. The indeterminate range (gray shaded region) was calculated as 1-2x the cutoff value. HB = baffled flask with hair. HU = unbaffled flask with hair. CB = baffled flask with L-cysteine. CU = unbaffled flask with L-cysteine. NB = baffled flask with no broth additives. NU = unbaffled flask with no broth additives. NTCN = negative control broth with no broth additives (no fungi added). Samples were run in triplicate (n=3) and standard deviation was less than 0.218 for all points.

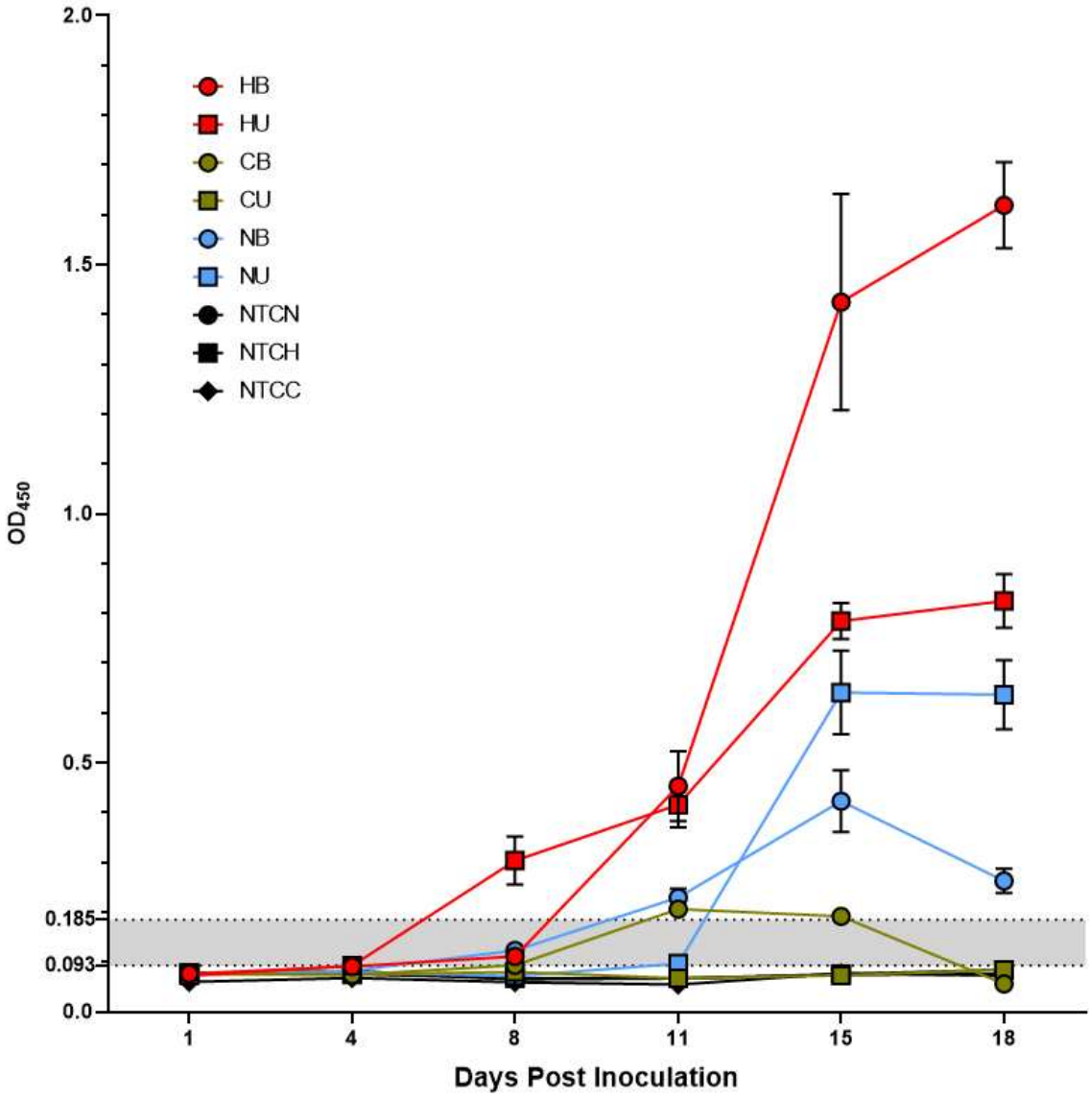

Figure 4.12. Detectable levels of concentrated Sub3 from *Microsporum canis* isolates grown in broth with shaking. Isolates of *M. canis* were grown in Sabouraud dextrose broth either with or without the addition of specific-pathogen free cat hair in either baffled or unbaffled flasks (broth experiment 3). Broth was collected periodically from each sample and ultracentrifuged to concentrate the solute 5x before adding to the ELISA plate. Unbaffled flask of L-cysteine became contaminated by day 8. ELISA plate was coated with 15ng/µl of antibody. The indeterminate range (gray shaded region) was calculated as 1-2x the cutoff value. HB = baffled flask with hair. HU = unbaffled flask with hair. CB = baffled flask with L-cysteine. CU = unbaffled flask with L-cysteine. NB = baffled flask with no broth additives. NU = unbaffled flask with no broth additives. NTCN = negative control broth with no broth additives (no fungi added). NTCH = negative control broth with hair (no fungi added). NTCC = negative control broth with L-cysteine (no fungi added). Samples were run in triplicate (n=3) and standard deviation was less than 0.136 for all points.

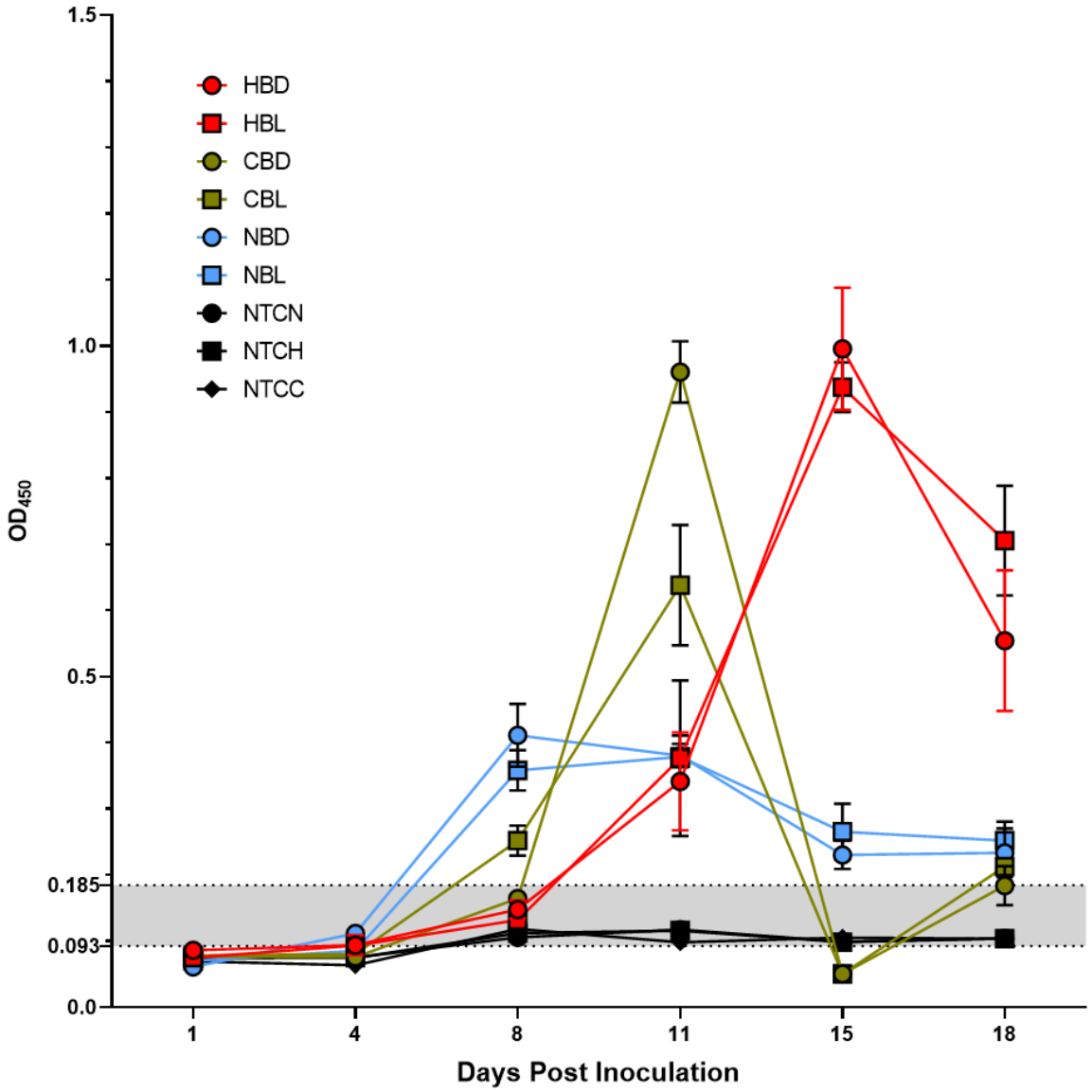

Figure 4.13. Similar levels of Sub3 detected between *Microsporum canis* isolates grown in broth in 24 hours of light and darkness. Isolates of *M. canis* were grown in Sabouraud dextrose broth in baffled flasks either with or without the addition of specific-pathogen free cat hair in either 24hrs light or 24hrs darkness (broth experiment 4). Broth was collected periodically from each sample and ultracentrifuged to concentrate the solute 5x before adding to the ELISA plate. ELISA plate was coated with 15ng/µl of antibody. The indeterminate range (gray shaded region) was calculated as 1-2x the cutoff value. Samples were run in triplicate (n=3) and standard deviation was less than 0.118 for all points.

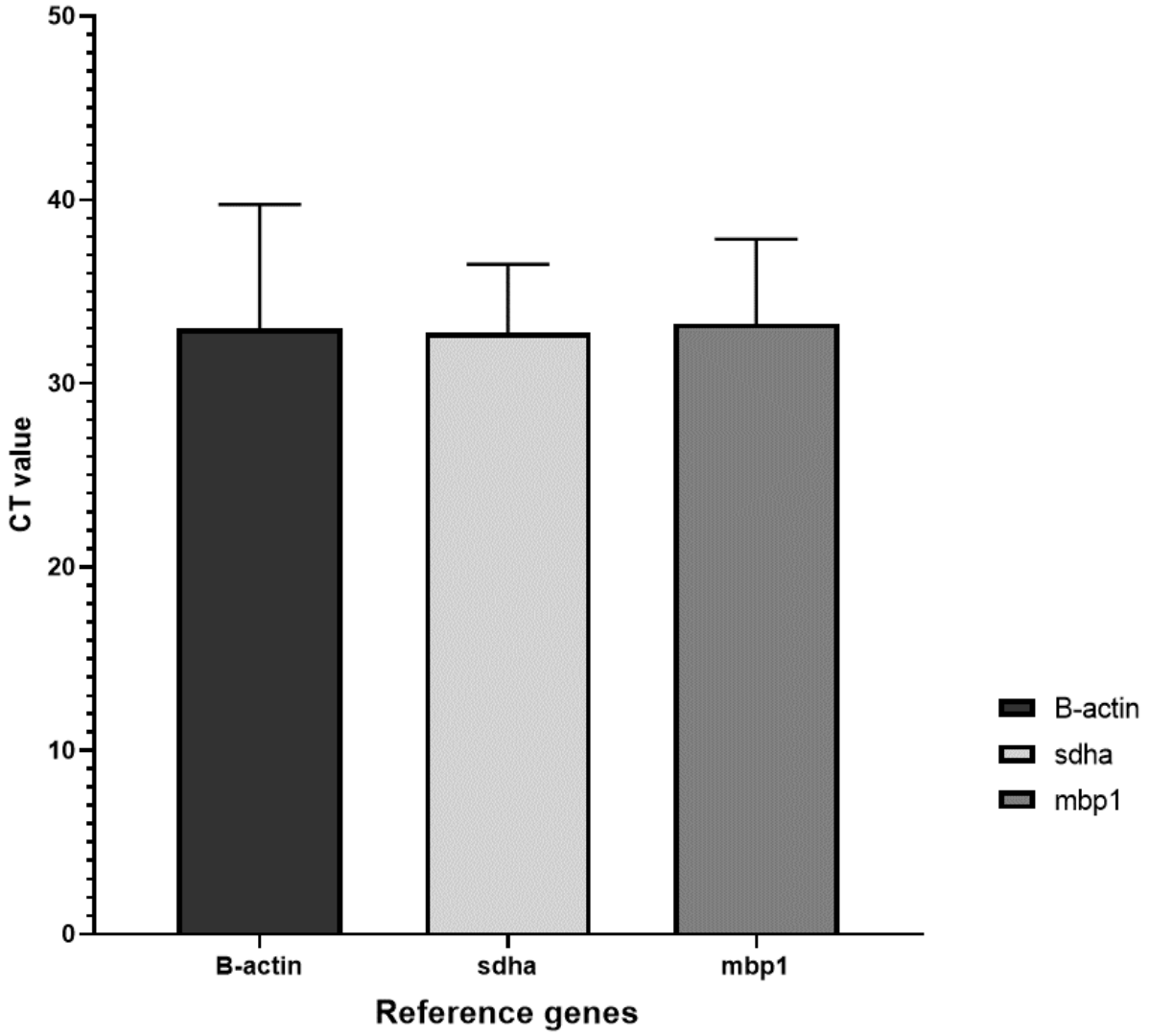

Figure 4.14. Similar expression of *Microsporum canis* between reference genes. Three reference genes were analyzed: β-actin, sdha, and mbp1. *M. canis* culture samples grown on solid media culture plates (n=5). Mbp1 = multiubiquitin chain binding protein. Sdha = succinate dehydrogenase complex flavoprotein subunit A. Each gene was run five times in triplicate and standard deviation was 6.76 for β-actin, 3.72 for sdha, and 4.6 for mbp1.

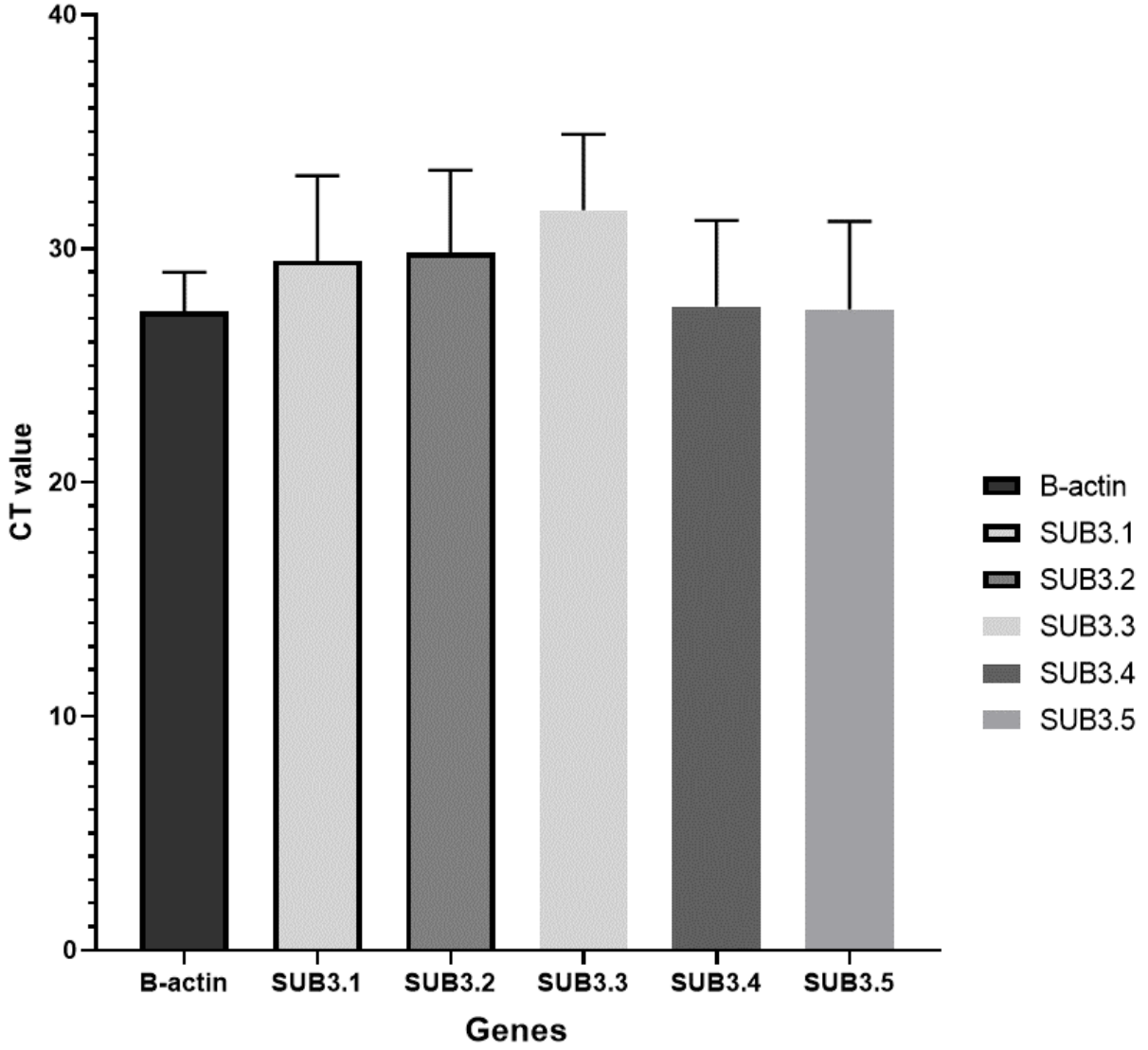

Figure 4.15. Similar expression of different primer sets for SUB3 in *Microsporum canis* isolates. Five primer sets targeting the SUB3 gene in *M. canis* were tested (n=2). *M. canis* isolates were grown on solid media. Samples were run in triplicate (n=3) and standard deviation was less than 0.51 for all points.

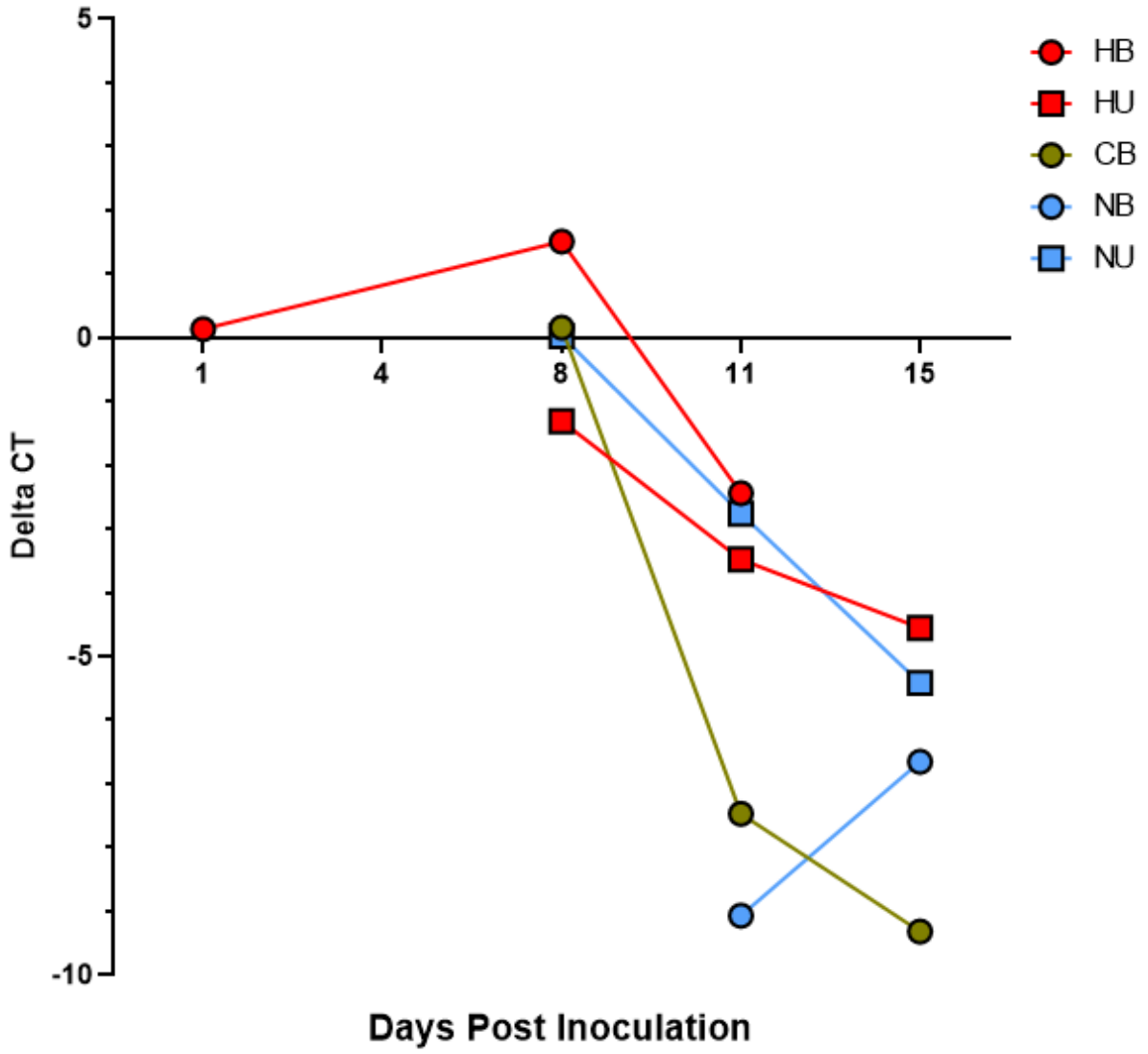

Figure 4.16. Relative expression of Sub3 from different culture conditions for *Microsporum canis*. $\Delta C_T = \left(C_{T,Sub3} - C_{T,mbp1}\right)_{sample}$ and C_T = threshold cycle. Missing data for L-cysteine in the unbaffled flask due to contamination by 8 DPI. Data not shown for 18 DPI due to poor quality C_T values. Missing data for different collection days for samples shown due to poor quality C_T values. HB = baffled flask with hair. HU = unbaffled flask with hair. CB = baffled flask with L-cysteine. NB = baffled flask with no broth additives. NU = unbaffled flask with no broth additives. Samples were run in triplicate (n=3) and standard deviation was less than 3.02 for all points.

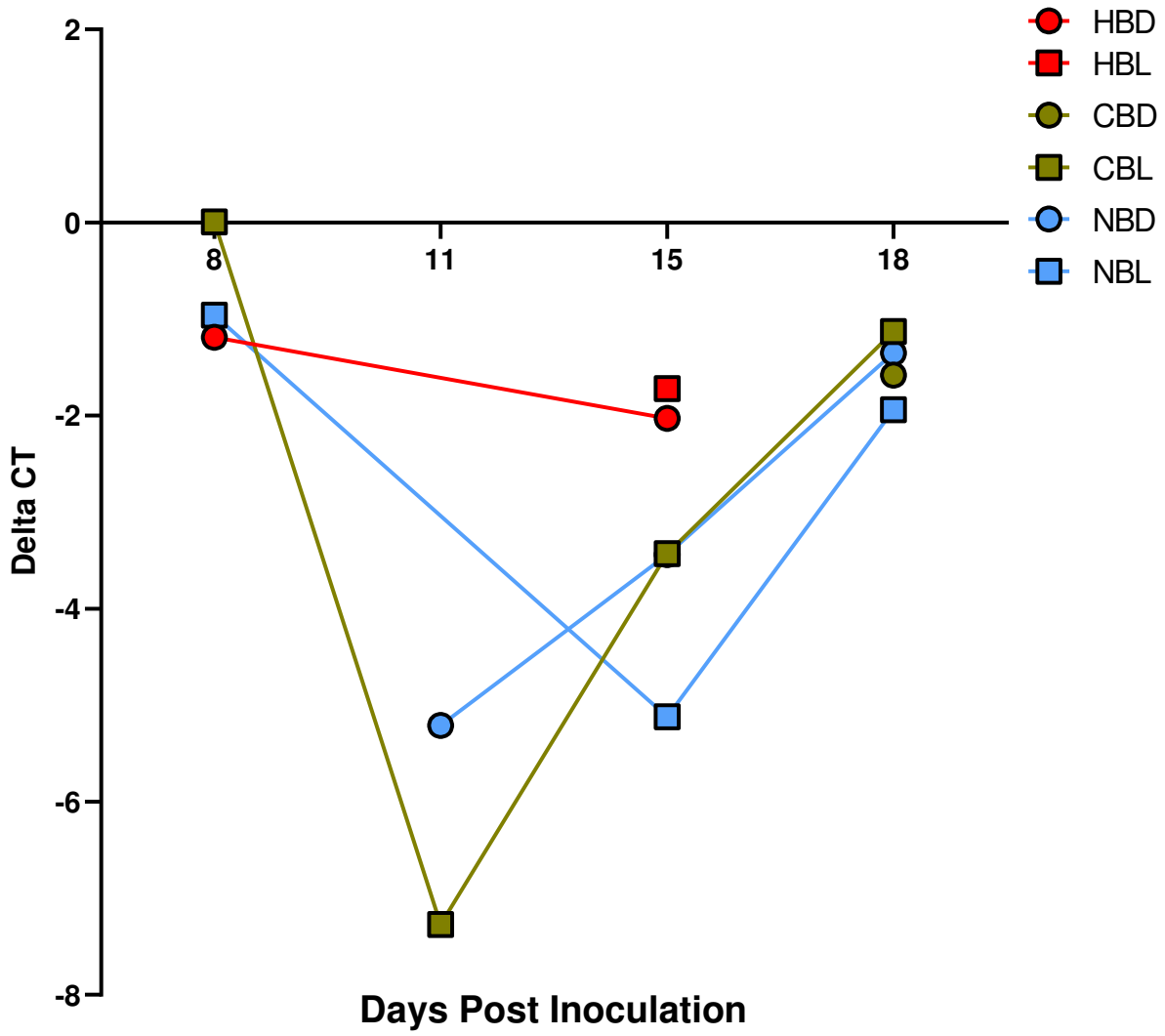

Figure 4.17. Relative expression of Sub3 from different culture conditions for *Microsporum canis*. $\Delta C_T = \left(C_{T,Sub3} - C_{T,mbp1}\right)_{sample}$ and C_T = threshold cycle. Data not shown for 1 and 4 DPI due to poor quality C_T values. Missing data for different collection days for samples shown due to poor quality C_T values. HBD = baffled flask with hair in 24 hr darkness. HBL = baffled flask with hair in 24 hr light. CBD = baffled flask with L-cysteine in 24 hr darkness. CBL = baffled flask with L-cysteine in 24 hr light. NBD = baffled flask with no broth additives in 24 hr darkness. NBL = baffled flask with no broth additives in 24 hr light. Samples were run in triplicate (n=3) and standard deviation was less than 1.5 for all points.

Table 4.1. Culture conditions of each flask inoculated with *Microsporum canis* including flask type, broth additives, and lighting conditions. Flask types = baffled or unbaffled. Broth additives = 200mg L-cysteine or 100mg of specific pathogen free cat hair. Light conditions = 24 hours of darkness, 24 hours of light, or 8 hours light. 8 hours light was based on typical light usage for the laboratory space.

Flask Name	**Flask type**	**Fungus additive**	**Broth additives**	**Light condition**
HB	Baffled	*M. canis*	Hair	8hrs light
HU	Unbaffled	*M. canis*	Hair	8hrs light
CB	Baffled	*M. canis*	L-cysteine	8hrs light
CU	Unbaffled	*M. canis*	L-cysteine	8hrs light
NB	Baffled	*M. canis*	None	8hrs light
NU	Unbaffled	*M. canis*	None	8hrs light
HBL	Baffled	*M. canis*	Hair	24hrs light
HBD	Baffled	*M. canis*	Hair	24hrs darkness
CBL	Baffled	*M. canis*	L-cysteine	24hrs light
CBD	Baffled	*M. canis*	L-cysteine	24hrs darkness
NBL	Baffled	*M. canis*	None	24hrs light
NBD	Baffled	*M. canis*	None	24hrs darkness
NTCN	Unbaffled	None	None	24hrs darkness
NTCH	Unbaffled	None	Hair	24hrs darkness
NTCC	Unbaffled	None	L-cysteine	24hrs darkness

Table 4.2. Culture conditions of each broth experiment inoculated with *Microsporum canis* including motion, flask type, broth additives, and lighting conditions. X = condition was utilized for that experiment. Flask types = baffled or unbaffled. Broth additives = 200mg L-cysteine or 100mg of specific pathogen free cat hair. Light conditions = 24 hours of darkness, 24 hours of light, or 8 hours light. 8 hours light was based on typical light usage for the laboratory space.

	Broth experiment	**1**	**2**	**3**	**4**
Motion	Stationary	X			
	Shaking		X	X	X
Flask type	Baffled		X	X	X
	Unbaffled	X	X	X	
Additives	Hair	X	X	X	X
	L-cysteine			X	X
	No additives	X	X	X	X
Light cycle	24hr light				X
	24hr dark				X
	8hr light	X	X	X	

Table 4.3. Primers used for RT-qPCR targeting the reference genes and gene of interest (SUB3) for *Microsporum canis*. Mbp1 = multiubiquitin chain binding protein. Sdha = succinate dehydrogenase complex flavoprotein subunit A.

Target Region	**Primer**	**Sequence**	**Reference**
mbp1	mbp1F	5'-AGTCCTAGTTACCTTGACCG	[Ciesielska *et al.* 2018]
	mbp1R	5'-CGGTGTTTAAGTGCTAGATAGG	[Ciesielska *et al.* 2018]
sdha	sdhaF	5'-TCTAGGAAACATGCACAAGG	[Ciesielska *et al.* 2018]
	sdhaR	5'-TTCGATAACACTCTGAGGGG	[Ciesielska *et al.* 2018]
β-actin	BactinF	5'-CTCCTGAGGCTCTCTTCC	[Ciesielska *et al.* 2018]
	BactinR	5'-GTAGTACCGCCGGACATG	[Ciesielska *et al.* 2018]
SUB3.1	59F	5'-GCGCTTTCTTTCACAACCGT	This paper
	231R	5'-GGAGTCCTTGTGTCCGACAG	This paper
SUB3.2	59F	5'-GCGCTTTCTTTCACAACCGT	This paper
	277R	5'-CTTCGTCAAAGTGGCCGTTG	This paper
SUB3.3	532F	5'-ACGGCGTTGACACTGGTATT	This paper
	692R	5'-GGCCTTCTTAGCAACTCCGT	This paper
SUB3.4	673F	5'-ACGGAGTTGCTAAGAAGGCC	This paper
	854R	5'-GTTGTTTGCCTGGCTGAAGG	This paper
SUB3.5	674F	5'-CGGAGTTGCTAAGAAGGCCA	This paper
	854R	5'-GTTGTTTGCCTGGCTGAAGG	This paper

Table 4.4. Optimized ELISA parameters led to limit of detection of 0.65 ng/µl of Sub3. Each sequential test utilized the optimized parameter from the previous test. Final optimized parameters included 2HB plate coated with 20 ng/µl of antibody Ab92 with 2hrs blocking incubation. All steps used horseradish peroxidase (HRP) for antibody conjugation except for biotin-streptavidin conjugation test. Streptavidin's concentration was 1:10,000.

Assay parameter tested	**Options tested**	**Limit of detection (ng/µl)**
Baseline protocol	N/A	2.6
Plate type	2HB plate	0.65
	4HBX	1.3
	MaxiSorp	5.23
Coating antibody type	Ab92	0.65
	Ab93	1.3
Coating antibody concentration	20 ng/µl	0.65
	15 ng/µl	0.65
	10 ng/µl	0.65
Blocking incubation time	Overnight	0.65
	2hrs	0.65
Biotin-streptavidin conjugation	Streptavidin: 200µl Biotin-Ab: 1:5,000	>20.9
	Streptavidin: 100µl Biotin-Ab: 1:5,000	>20.9
	Streptavidin: 50µl Biotin-Ab: 1:5,000	>20.9
	Streptavidin: 100µl Biotin-Ab: 1:10,000	5.23
	Streptavidin: 50µl Biotin-Ab: 1:10,000	>20.9

Table 4.5. Significant difference only observed between hair and no hair samples at 14 DPI. Samples analyzed were isolates of *M. canis* grown with shaking in either baffled or unbaffled flasks supplemented either with hair or no hair. P-values were calculated using Student's t-test and were considered significant if less than 0.05.

	P-values					
Sample Groups	1 DPI	3 DPI	7 DPI	10 DPI	14 DPI	17 DPI
Hair vs No Hair	0.2831	0.5534	0.05054	0.6844	0.01805*	0.2831
Baffled vs Unbaffled	0.588	0.6106	0.8084	0.4154	0.616	0.8666

Literature Cited

Achterman RR, Smith AR, Oliver BG, et al. (2011). Sequenced dermatophyte strains: growth rate, conidiation, drug susceptibilities, and virulence in an invertebrate model. *Fungal Genet Biol* **48**(3):335-341.

Alió S AB, Mendoza M, Zambrano EA, et al. (2005). Dermatophytes growth curve and in vitro susceptibility test: a broth micro-titration method. *Medical Mycology* **43**(4):319-325.

Băguţ ET, Baldo A, Mathy A, et al. (2012). Subtilisin Sub3 is involved in adherence of Microsporum canis to human and animal epidermis. *Veterinary microbiology* **160**(3-4):413-9.

Baldo A, Mathy A, Tabart J, et al. (2010). Secreted subtilisin Sub3 from Microsporum canis is required for adherence to but not for invasion of the epidermis. *Br J Dermatol* **162**(5):990-7.

Baldo A, Tabart J, Vermout S, et al. (2008). Secreted subtilisins of Microsporum canis are involved in adherence of arthroconidia to feline corneocytes. *Journal of Medical Microbiology* **57**(9):1152-1156.

Brillowska-Dąbrowska A, *DNA preparation from nail samples*, W.I.P. Organization, Editor. 2006: Denmark.

Brody S. (2019). Circadian Rhythms in Fungi: Structure/Function/Evolution of Some Clock Components. *Journal of Biological Rhythms* **34**(4):364-379.

Chen J, Yi J, Liu L, et al. (2010). Substrate adaptation of Trichophyton rubrum secreted endoproteases. *Microbial Pathogenesis* **48**(2):57-61.

Ciesielska A and Stączek P. (2018). Selection and validation of reference genes for qRT-PCR analysis of gene expression in Microsporum canis growing under different adhesion-inducing conditions. *Scientific Reports* **8**(1):1197-1197.

de Hoog GS, Dukik K, Monod M, et al. (2017). Toward a Novel Multilocus Phylogenetic Taxonomy for the Dermatophytes. *Mycopathologia* **182**(1):5-31.

Desjardins P and Conklin D. (2010). NanoDrop microvolume quantitation of nucleic acids. *Journal of visualized experiments : JoVE* 45):2565.

Dutaud D, Aubry L, Henry L, et al. (2002). Development and evaluation of a sandwich ELISA for quantification of the 20S proteasome in human plasma. *Journal of immunological methods* **260**(1-2):183-93.

Faway E, Staerck C, Danzelle C, et al. (2021). Towards a Standardized Procedure for the Production of Infective Spores to Study the Pathogenesis of Dermatophytosis. *Journal of Fungi* **7**(12):1029.

Garg J, Tilak R, Garg A, et al. (2009). Rapid detection of dermatophytes from skin and hair. *BMC research notes* **2**(60-60.

Giddey K, Monod M, Barblan J, et al. (2007). Comprehensive analysis of proteins secreted by Trichophyton rubrum and Trichophyton violaceum under in vitro conditions. *Journal of proteome research* **6**(8):3081-3092.

Gnat S, Łagowski D, and Nowakiewicz A. (2020). Major challenges and perspectives in the diagnostics and treatment of dermatophyte infections. *J Appl Microbiol* **129**(2):212-232.

Gräser Y, Kuijpers AFA, El Fari M, et al. (2000). Molecular and conventional taxonomy of the Microsporum canis complex. *Medical Mycology* **38**(2):143-153.

Grimm LH, Kelly S, Völkerding, II, et al. (2005). Influence of mechanical stress and surface interaction on the aggregation of Aspergillus niger conidia. *Biotechnol Bioeng* **92**(7):879-88.
Grumbt M, Monod M, Yamada T, et al. (2013). Keratin Degradation by Dermatophytes Relies on Cysteine Dioxygenase and a Sulfite Efflux Pump. *Journal of Investigative Dermatology* **133**(6):1550-1555.
Hennicke F, Grumbt M, Lermann U, et al. (2013). Factors supporting cysteine tolerance and sulfite production in Candida albicans. *Eukaryot Cell* **12**(4):604-13.
Kanno J, Aisaki K, Igarashi K, et al. (2006). "Per cell" normalization method for mRNA measurement by quantitative PCR and microarrays. *BMC Genomics* **7**:64.
Kasperova A, Kunert J, and Raska M. (2013). The possible role of dermatophyte cysteine dioxygenase in keratin degradation. *Medical Mycology* **51**(5):449-454.
Kaul S, Yadav S, and Dogra S. (2017). Treatment of Dermatophytosis in Elderly, Children, and Pregnant Women. *Indian dermatology online journal* **8**(5):310-318.
Kelliher CM, Loros JJ, and Dunlap JC. (2020). Evaluating the circadian rhythm and response to glucose addition in dispersed growth cultures of Neurospora crassa. *Fungal Biol* **124**(5):398-406.
Kidd S, Halliday CL, Alexiou H, et al., *Descriptions of Medical Fungi*. 2016: CutCut Digital.
Lardeux F, Torrico G, and Aliaga C. (2016). Calculation of the ELISA's cut-off based on the change-point analysis method for detection of Trypanosoma cruzi infection in Bolivian dogs in the absence of controls. *Mem Inst Oswaldo Cruz* **111**(8):501-4.
Leng W, Liu T, Wang J, et al. (2009). Expression dynamics of secreted protease genes in Trichophyton rubrum induced by key host's proteinaceous components. *Sabouraudia* **47**(7):759-765.
Leung AKC, Hon KL, Leong KF, et al. (2020). Tinea Capitis: An Updated Review. *Recent Pat Inflamm Allergy Drug Discov* **14**(1):58-68.
Maranhão FCA, Paião FG, and Martinez-Rossi NM. (2007). Isolation of transcripts over-expressed in human pathogen Trichophyton rubrum during growth in keratin. *Microbial Pathogenesis* **43**(4):166-172.
Martinez DA, Oliver BG, Gräser Y, et al. (2012). Comparative genome analysis of Trichophyton rubrum and related dermatophytes reveals candidate genes involved in infection. *mBio* **3**(5):e00259-12.
Martins MP, Rossi A, Sanches PR, et al. (2020). Comprehensive analysis of the dermatophyte Trichophyton rubrum transcriptional profile reveals dynamic metabolic modulation. *Biochemical Journal* **477**(5):873-885.
Meletiadis J, Meis JF, Mouton JW, et al. (2001). Analysis of growth characteristics of filamentous fungi in different nutrient media. *Journal of clinical microbiology* **39**(2):478-484.
Mercer DK and Stewart CS. (2019). Keratin hydrolysis by dermatophytes. *Medical Mycology* **57**(1):13-22.
Metz B and Kossen NWF. (1977). The growth of molds in the form of pellets–a literature review. *Biotechnol Bioeng* **19**(6):781-799.
Mignon B, Swinnen M, Bouchara JP, et al. (1998). Purification and characterization of a 315 kDa keratinolytic subtilisin-like serine protease from and evidence of its secretion in naturally infected cats. *Medical Mycology* **36**(6):395-404.

Mishra M, Tiwari S, Gunaseelan A, et al. (2019). Improving the sensitivity of traditional Western blotting via Streptavidin containing Poly-horseradish peroxidase (PolyHRP). *Electrophoresis* **40**(12-13):1731-1739.
Miyazawa K, Yoshimi A, Zhang S, et al. (2016). Increased enzyme production under liquid culture conditions in the industrial fungus Aspergillus oryzae by disruption of the genes encoding cell wall α-1,3-glucan synthase. *Bioscience, Biotechnology, and Biochemistry* **80**(9):1853-1863.
Monod M. (2008). Secreted proteases from dermatophytes. *Mycopathologia* **166**(5-6):285-94.
Montenegro-Montero A, Canessa P, and Larrondo LF, *Chapter Four - Around the Fungal Clock: Recent Advances in the Molecular Study of Circadian Clocks in Neurospora and Other Fungi*, in *Advances in Genetics*, T. Friedmann, J.C. Dunlap, and S.F. Goodwin, Editors. 2015, Academic Press. p. 107-184.
Moriello K. (2014). Feline dermatophytosis: aspects pertinent to disease management in single and multiple cat situations. *Journal of feline medicine and surgery* **16**(5):419-431.
Moriello KA. (2001). Diagnostic techniques for dermatophytosis. *Clinical Techniques in Small Animal Practice* **16**(4):219-224.
Moriello KA, Coyner K, Paterson S, et al. (2017). Diagnosis and treatment of dermatophytosis in dogs and cats. *Veterinary Dermatology* **28**(3):266-e68.
Newbury S and Moriello KA. (2014). Feline dermatophytosis: steps for investigation of a suspected shelter outbreak. *Journal of feline medicine and surgery* **16**(5):407-418.
Panasiti V, Borroni RG, Devirgiliis V, et al. (2006). Comparison of diagnostic methods in the diagnosis of dermatomycoses and onychomycoses. *Mycoses* **49**(1):26-29.
Petrikkou E, Rodríguez-Tudela JL, Cuenca-Estrella M, et al. (2001). Inoculum standardization for antifungal susceptibility testing of filamentous fungi pathogenic for humans. *Journal of clinical microbiology* **39**(4):1345-7.
Pihet M and Le Govic Y. (2017). Reappraisal of Conventional Diagnosis for Dermatophytes. *Mycopathologia* **182**(1):169-180.
Rawlings ND, Barrett AJ, and Finn R. (2016). Twenty years of the MEROPS database of proteolytic enzymes, their substrates and inhibitors. *Nucleic Acids Res* **44**(D1):D343-50.
Rezusta A, de la Fuente S, Gilaberte Y, et al. (2016). Evaluation of incubation time for dermatophytes cultures. *Mycoses* **59**(7):416-418.
Samanta I, *Veterinary Mycology*. 2015: Springer India.
Serrano-Carreón L, Galindo E, Rocha-Valadéz JA, et al. (2015). Hydrodynamics, Fungal Physiology, and Morphology. *Adv Biochem Eng Biotechnol* **149**:55-90.
Stuntebeck R, Moriello KA, and Verbrugge M. (2018). Evaluation of incubation time for Microsporum canis dermatophyte cultures. *Journal of feline medicine and surgery* **20**(10):997-1000.
Tran VD, De Coi N, Feuermann M, et al. (2016). RNA Sequencing-Based Genome Reannotation of the Dermatophyte Arthroderma benhamiae and Characterization of Its Secretome and Whole Gene Expression Profile during Infection. *mSystems* **1**(4).
Vandermolen KM, Raja HA, El-Elimat T, et al. (2013). Evaluation of culture media for the production of secondary metabolites in a natural products screening program. *AMB Express* **3**(1):71-71.
Vashist SK, Marion Schneider E, Lam E, et al. (2014). One-step antibody immobilization-based rapid and highly-sensitive sandwich ELISA procedure for potential in vitro diagnostics. *Sci Rep* **4**(4407.

Wang SY, Li Z, Wang XJ, et al. (2014). Development of monoclonal antibody-based sandwich ELISA for detection of dextran. *Monoclon Antib Immunodiagn Immunother* **33**(5):334-9.
Weitzman I and Summerbell RC. (1995). The dermatophytes. *Clinical microbiology reviews* **8**(2):240-259.
Zaugg C, Monod M, Weber J, et al. (2009). Gene expression profiling in the human pathogenic dermatophyte Trichophyton rubrum during growth on proteins. *Eukaryotic Cell* **8**(2):241-250.

CHAPTER 5: DETECTION OF SULFITE-DERIVED METABOLITES PRODUCED BY *MICROSPORUM CANIS*

5.1 Introduction

Dermatophytes are the most ubiquitous fungal pathogens worldwide, responsible for the majority of skin and nail infections and estimated to be the fourth most prevalent human disease [Havlickova *et al.* 2008, Seebacher *et al.* 2008, Hay 2017]. Globally, the estimated lifetime risk of developing dermatophytosis is 10-20%, with tinea pedis being the most common [Drake *et al.* 1996, Nussipov *et al.* 2017]. Given the high infection rates, treating dermatophytes globally costs $500 million annually [Gräser *et al.* 2008]. Dermatophytosis reinfections are common, particularly when nail beds have been infiltrated; these infections (onychomycoses) persist for years [Gupta *et al.* 2008, Dogra *et al.* 2016]. Infections involving the scalp are not only difficult to diagnose but require systemic therapy as the fungi invade the hair follicle root [Elewski 2000, Bennassar *et al.* 2010]. Immunocompromised patients, such as those with HIV, malignancies, or patients on immunosuppressive therapies, are at risk for severe invasive dermatophytosis, which often goes undiagnosed [Rouzaud *et al.* 2015]. While the "gold standard" for diagnosis is fungal culture, reinfection cases have a high rate of false negative cultures [Achterman *et al.* 2012]. Molecular techniques such as PCR have greater sensitivity than culture, and these tests can also be used for fungal species identification [Brillowska-Dabrowska *et al.* 2013, Jacobson *et al.* 2017, Wagner *et al.* 2018]. However, a significant disadvantage of a DNA-based assay such as PCR is that fomite carriage is not differentiated from active infection [Panasiti *et al.* 2006], making it challenging to distinguish resolved from active cases.

Accurate diagnosis is key for patient management and implementation of appropriate therapies. Many forms of dermatophytosis can be difficult to clinically distinguish from other skin aliments as clinical presentation overlaps between the diseases [Garg *et al.* 2009]. Additionally, a significant portion of dermatophyte cases occur in developing countries, where the populations are unable to access health care [Richard *et al.* 1994, Nweze *et al.* 2017]. Misdiagnosis can result in dangerous consequences, particularly in immunocompromised patients, as disease can progress to deeper invasion, disseminated dermatophytosis and invasive dermatitis [Marconi *et al.* 2010, Peres *et al.* 2010, Rouzaud *et al.* 2015, Benedict *et al.* 2018]. A common method of diagnosis that is fast and relatively cheap is microscopic examination where a potassium hydroxide mount facilitates visualization of fungal hyphae [Panasiti *et al.* 2006]. However, this method cannot distinguish between live and dead organisms, and species cannot be identified [Rezusta *et al.* 2016, Pihet *et al.* 2017, Stuntebeck *et al.* 2018]. Another approach is utilizing fungal culture, which is inexpensive and requires minimal equipment, but requires a long incubation time [Rezusta *et al.* 2016, Pihet *et al.* 2017]. Both of these methods have lower sensitivity compared with newer molecular techniques (such as PCR) as clinical samples can be easily contaminated with quick growing saprophytes (soil fungi) [Kupsch *et al.* 2016, Pihet *et al.* 2017, Wagner *et al.* 2018]. PCR can provide a relatively rapid and specific diagnosis, but because of fungal resistance to chemical degradation and contamination of the DNA preparation with keratinized tissue, extraction of sufficient nucleic acids that do not contain inhibitors can be problematic [Kupsch *et al.* 2016, Wickes *et al.* 2018]. A sensitive, specific, and rapid diagnostic test for active dermatophytosis would significantly enhance recognition and appropriate treatment of this condition.

In this study, we aimed to develop rapid, inexpensive, metabolically based diagnostic assays for accurate identification of dermatophytosis. Dermatophytes are unique in their ability to metabolize keratin, since these proteins are by necessity very resistant to microbial degradation [Grumbt *et al.* 2013]. Dermatophytes produce sulfite as well as keratinases in order to accomplish keratinolysis [Grumbt *et al.* 2013]. The *sulfite efflux pump* (SSU1) secretes sulfite to break the disulfide bonds in keratinized tissues, releasing cysteine and S-sulfocysteine (SSC), and furthering the digestion of keratin to supply fungal nutrients [Léchenne *et al.* 2007, Grumbt *et al.* 2013, Mercer *et al.* 2018] (Fig. 5.1). Cysteine, a nonessential amino acid that constitutes approximately 20% of the amino acid residues in hair, is taken up by fungus and internally converted to sulfite through multiple reactions [Kasperova *et al.* 2013] (Fig. 5.1). Once inside the fungal cell, cysteine is oxidized to cysteine sulfinic acid by cysteine dioxygenase (Cdo1) [Grumbt *et al.* 2013] (Fig. 5.1). The conversion of cysteine sulfinic acid to sulfite is theorized to occur by transamination and spontaneous decomposition, allowing for the degradation cycle to continue [Griffith 1983, Mercer *et al.* 2018].

The SSU1 gene of a dermatophyte (*T. mentagrophytes*) has been shown to be essential for keratin degradation and clinical infection, demonstrating the potential role of this gene as a virulence factor [Grumbt *et al.* 2013]. SSU1 thus makes an attractive target for assessment of active infection and virulence and as a factor underlying dermatophyte strain variation. Detecting metabolic products reliant on SSU1 (such as sulfite or SSC) would indicate the presence of metabolically active dermatophytes as other bacteria and yeast on the skin do not actively breakdown keratin as a nutrient source [Irwin *et al.* 2017]. Furthermore, dermatophyte production of sulfite and SSC may serve as an indicator of dermatophyte infections (Fig. 5.1).

When iodine is in the presence of starch/amylose, the solution is a dark blue color, indicating the bond between the molecules [Dhar 1924] (Fig. 5.2). Both sulfite and SSC interfere with the charge transfer complex between iodine-amylose solution, resulting in a change in the color of the indicator solution from blue to clear, a chemical reaction that has been used to detect sulfites in the food industry [Moya *et al.* 2019] (Fig. 5.2). We aimed to develop a point-of-care diagnostic assay with high sensitivity and specificity that takes advantage of the fact that active *M. canis* infection requires digestion of keratin for invasion, and necessarily results in sulfite secretion. While the colorimetric assay we developed was able to detect down to 0.25 µM of sodium sulfite, other compounds were able to interfere with the reaction, causing inaccurate results. While cysteine was utilized to increase sulfite production in fungal samples, the three compounds tested to remove residual free thiols also interfered with the colorimetric assay, leading to inconsistent results when added to the samples.

In addition to developing a colorimetric assay, we developed a protocol to detect SSC using quantitative liquid chromatography mass spectrometry (LC-MS) as a potential alternative assay for diagnosing dermatophytosis. SSC is a secondary metabolite that has also been described in two rare inherited metabolic disorders in people known as molybdenum cofactor deficiency and isolated sulfite oxidase deficiency [Johnson 2003]; consequently, LC-MS is already implemented as a diagnosis method for SSC in clinical settings [Rashed *et al.* 2005]. As clinical assays for other metabolic targets evolve to use MS owing to its superior specificity and wide applications, hospitals have increasing access to the technology needed to analyze SSC [Léchenne *et al.* 2007, Stone 2019]. Similar to other biochemical targets using this technology, the turnaround time to results would be rapid as LC-MS runs can be performed in several minutes and most clinical laboratories have this equipment on site [Grebe *et al.* 2011]. We were

able to detect low levels of SSC from cultured samples of *M. canis* that were grown with hair for 15 and 18 days, suggesting the potential use of LC-MS for detecting the presence of dermatophytes.

5.2 Materials and Methods

5.2.1 Determination of starch-iodine indicator level of sulfite detection

For developing the indicator solution for the colorimetric assay, different amounts of 2.1% Modified Lugol's iodine (HealthLink, Jacksonville, FL, USA) (5 µl, 10 µl, 20 µl, and 40 µl) were added into the indicator solution. The indicator solution consists of 390 µl MilliQ® water, 43 µl 2% starch in salicylic acid, and 2.1% Modified Lugol's iodine (IKI). Different levels of IKI were tested to determine an optimal visual cutoff value. Twenty microliters of the indicator solution with varying IKI amounts were added to serial diluted sodium sulfite solution (diluted from 16 µM to 0.12 µM). Tubes were monitored for reactivity via a visible color change over a 12-hour period. The indicators' level of detection (LoD) of sulfite was determined by the lowest quantity of sodium sulfite that induced a color change from blue to clear.

5.2.2 Utilizing commercial kits for sulfite detection

To compare the accuracy and user-friendliness of our colorimetric assay, we tested two commercial kits that detect sulfite. These kits are marketed for testing sulfite in solutions including beverages, food, groundwater, and wastewater.

Millipore's sulfite kit: This kit (Millipore, Darmstadt, Germany) detects sulfite by oxidizing sulfite to sulfate after oxidizing iodide to iodine. Excess iodine binds with the indicator, changing color. Following the manufacturer's protocol, the kit's reagents were added to 5 ml of samples

tested. To test the accuracy of this kit, a known concentration of sodium sulfite (0.0195 mg/ml) was utilized.

Megazyme's sulfite kit: This kit (Megazyme, Wicklow, Ireland) detects sulfite through enzymatic reactions by first converting sulfite to sulfate and producing hydrogen peroxide. This hydrogen peroxide is then reduced when NADH peroxidase and NADH are added, resulting in NAD^+ formation. The consumption of NADH is measured. Following the manufacturer's protocol, samples were compared to the kit's standard (1 g citric acid, 590 mg sodium sulfite in 1 L water). Readings of optical density (OD) were taken at 4 minutes, 30 minutes, and 50 minutes at 340 nm. To calculate the sulfite concentration in a sample, the following equation was utilized $\left[sulphite\ (^{mg}/_{ml})\right] = \left(\frac{\Delta sample}{\Delta standard}\right) * 0.3$, where $\Delta sample = (A0 - A1)_{sample} - (A0 - A1)_{blank}$ and $\Delta standard = (A0 - A1)_{standard} - (A0 - A1)_{blank}$. Timepoints of 4 minutes (A0) and 30 minutes (A1) were used for calculations for samples, while timepoints of 4 minutes (A0) and 50 minutes (A2) were utilized in calculations for the kit's standard.

5.2.3 Colorimetric assay with fungal samples

Culture samples: For testing sulfite production for fungal samples, swabs of *M. canis*, *Trichophyton mentagrophytes*, and *Nannizzia gypsea* cultures grown on Sabouraud dextrose agar (SDA), potato dextrose agar (PDA) or Dermatophyte Test Media (DTM) (Hardy Diagnostics, Santa Maria, CA, USA) were added to 200 µl MilliQ® water in a 1.5 ml tube. Each tube had 20 µl of the indicator solution (5 µl of IKI) added and then the tube was mixed to thoroughly distribute the solution in the tube. Visual color changes were observed periodically from 0 minutes to 12 hours after the indicator was added.

Clinical hair samples: For hair samples from suspected dermatophytosis cats (Materials and Methods section 2.2.1), the head of the toothbrush containing the bristles was removed and placed in a 50 ml conical tube. Two mililiters of MilliQ® water was added and the tube was vortexed on high for 10 minutes. For each toothbrush, 200 µl of water was removed and added to a 1.5 ml tube. Each tube had 20 µl of the indicator solution (5 µl of IKI) added and then the tube was mixed to thoroughly distribute the solution in the tube. Visual color changes were observed at 0 minutes, 10 minutes, 30 minutes, 40 minutes, 60 minutes, 120 minutes, 150 minutes, and 12 hours after the indicator was added.

5.2.4 Spectrophotometer reading of colorimetric assay samples

Optical density measurements: To quantify the visible color change that occurs in the colorimetric assay, optical densities were measured for the sulfite dilution curve and hair samples from specific-pathogen free (SPF) and suspected dermatophytosis cats. Samples were run in technical duplicates (n=2) or triplicates (n=3), and the average and standard deviation were calculated for each sample. The optical density (OD) was read on a Multiskan® Spectrum spectrophotometer (ThermoFisher Scientific, Waltham, MA, USA) from 265 nm to 700 nm to determine the optimal absorbance for the assay. Once the optimal absorbance was established, measurements of optical density were taken at multiple timepoints including before and after the indicator was added.

Optical density threshold for positive result: The cutoff value for sample positivity was calculated using the following equation $Cutoff = \left(OD_{avg}\right) + (3 * OD_{std})$, where OD_{avg} is the average optical density of the reactive sodium sulfite dilution samples and OD_{std} is the standard

deviation of the optical density results for the reactive sodium sulfite dilution samples [Lardeux *et al.* 2016].

5.2.5 Blocking interference with indicator solution

To block interference from cysteine (present in hair and samples supplemented with cysteine), zinc sulfate ($ZnSO_4$), hydrogen peroxide (30% H_2O_2), and copper sulfate pentahydrate ($CuSO_4 \cdot 5H_2O$) were added into the colorimetric assay as these chemicals have been shown to bind to free thiols in solution [Manonmani *et al.* 1999]. These chemicals were tested first with dilutions of sodium sulfite to ensure they did not interfere with the interaction between sulfite and the indicator solution. In 1.5 ml tubes, either 200 µl of MilliQ® water or 200 µl sodium sulfite (0.49 mM) was added. For testing the thiol binding chemicals, either 200 µl of 125 mM $ZnSO_4$, 10 µl of 30% H_2O_2, or 50 µl of 100 mM $CuSO_4 \cdot 5H_2O$ was added to the tube. Hydrogen peroxide was also tested with D-cysteine (3 µl of 5 mM) as hydrogen peroxide strongly interfered with the indicator solution. Then, 40 µl of the indicator solution was added and any color changes were noted immediately after.

The chemicals that did not interfere with the colorimetric assay were then tested with L-cysteine to see what concentration can block the free thiol interact with the indicator solution. L-cysteine was first tested with just the indicator solution to measure what level of interference can be observed. Varying amounts of 5 mM L-cysteine (0 to 10 µl) were added to 200 µl of MilliQ® water. The solution was mixed and then 40 µl of indicator solution was added. Reactivity was measured immediately after the indicator solution was added. The reaction was repeated with the addition of $CuSO_4$ (50 µl of 100 mM per tube). Next, in a 96-well plate (Corning 96-well nonbinding surface microplates, ThermoFisher Scientific, Houston, TX, USA), sodium sulfite

serial dilutions (16 µM to 0.12 µM) were added in triplicate (200 µl per well). The indicator solution was added to each well to measure the level of reactivity. Then, another 96-well plate with the same sodium sulfite dilutions was prepared and 4 µl of 5 mM L-cysteine was added to each well. The indicator solution was added to each well to measure the level of reactivity. Lastly, another 96-well plate with the same sodium sulfite dilutions and L-cysteine concentrations was prepared and 50 µl of 100 mM $CuSO_4$, followed by 40 µl of indicator solution were added. Samples were run in technical triplicates (n=3). To better visualize the resulting precipitant, 200 µl of 158.7 mM sodium sulfite with 200 µl 100 mM $CuSO_4$ were mixed together either with or without 40 µl of the indicator solution.

5.2.6 Mass spectrometry of measuring SSC

Development and optimization of a liquid chromatography-mass spectrometry protocol for SSC was performed by Madeline C. Roach. Additionally, a calibration curve was generated for this protocol and the limit of detection and limit of quantification were determined by Madeline C. Roach.

Quantification of SSC from *M. canis* samples: Aliquots of Sabouraud dextrose broth (Hardy Diagnostics, Santa Maria, CA, USA) from *M. canis* samples grown in flasks either with or without hair supplementation were collected for mass spectrometry analysis; these samples were the same from Materials and Methods 4.2.2. Samples were collected on 1, 4, 8, 11, 15, and 18 days post inoculation (DPI) of the broth with *M. canis*. The broth was filtered through a 10K molecular weight cut-off filter (Amicon Ultra-10K Centrifugal Filter Deice, Millipore, Ireland) to remove fungal hyphae and other large particulates and the flow-through was collected. The flow-through was then passed through a 0.2 µm filter (Agilent Captiva Econofilters, Palo Alto,

CA, USA) and 0.5 ml aliquots were loaded into the mass spectrometer (Agilent 6470 triple quadrupole, Palo Alto, CA) coupled to a liquid chromatograph (Agilent 1290 high speed, Palo Alto, CA). The running parameters were the same as utilized for the calibration curve (2,500 volts for capillary voltage, 12 L/min for desolvation gas flow rate, 100°C for desolvation line temperature, 50 L/min for nebulizer gas flow rate, 0 volts for nozzle voltage, 11 L/min for shielding gas flow rate, and 350°C for shielding gas temperature). Separations were performed using an Agilent InfinityLab Poroshell 120 EC-C18 column (Palo Alto, CA, USA) with dimensions of 3.0 x 50 mm and 2.7-micron particle size. Mobile phase A was composed of Optima LC-MS grade water (Fisher Chemicals, Waltham, MA, USA) with 0.1% formic acid (CAS number: 61-18-6, Fisher Chemicals, Waltham, MA, USA) by volume. Mobile phase B was Optima LC-MS grade acetonitrile (ACN) (CAS number: 70-05-8, Fisher Chemicals, Waltham, MA, USA) with 0.1% formic acid by volume. The flow rate was 0.35 mL/min, and a 6-minute runtime was used. The elution was isocratic at 80:20 A:B for the duration of the separation. Electrospray ionization was utilized, and the source was used in negative ionization mode. The concentration of SSC for each sample was quantified using the calibration curve.

5.2.7 Statistical analysis

All samples that were quantified via OD readings or mass spectrometry were measured in duplicate (n=2) or triplicate (n=3). The average and standard deviation were reported.

5.3 Results

5.3.1 Sulfite detection of different indicator solutions

Using the same serial dilution of sodium sulfite, the level of detection (LoD) was determined for each indicator solution. Reactive dilutions turned clear, whereas non-reactive dilutions remained blue. For the indicator solution using 40 µl of IKI, a level of 1 µM sodium sulfite was detected (Fig. 5.3). The other indicator solutions' (20 µl of IKI, 10 µl of IKI, and 5 µl of IKI) LoDs were 0.5 µM, 0.25 µM and lower than 0.12 µM sodium sulfite, respectively (Fig. 5.3). The color of the tubes that were below the level of sulfite detection were shades of blue with the shade becoming darker the more IKI was used in the indicator solution (Fig. 5.3). The color of the tubes persisted overnight (time = 12 hours).

To quantify the color change, the optical density of the serial dilution of sodium sulfite was measured before and after the addition of the indicator solution (5 µl of IKI). Samples were run in technical duplicates (n=2) and all samples had a standard deviation below 0.331. Between 265 nm and 700 nm, the peak absorbance occurred at 600 nm for samples that were non-reactive after adding the indicator (Fig. 5.4). These samples had sulfite concentrations (0.063 µM, 0.031 µM and 0.016 µM) that were below the LoD of the indicator. Samples that had sulfite concentrations above the LoD (16 µM to 0.25 µM) had similar absorbance before and after adding the indicator solution, as these samples were reactive after the indicator solution was added (Fig. 5.4). At 0.125 µM, this sample had OD values within the indeterminate range after the addition of the indicator solution (Fig. 5.4).

5.3.2 Variable sulfite detection using commercial sulfite detection kits

Using a dilution of 0.0195 mg/ml of sodium sulfite, the Millipore kit was able to accurately detect this level of sulfite. However, when testing the Megazyme kit, the same dilution was detected as 0.42 mg/ml of sulfite (Suppl. Table 5.1). The Millipore kit was utilized

for detecting sulfite of *Trichophyton mentagrophytes* cultures and compared to our colorimetric assay. Using *T. mentagrophytes* cultures ranging from 2 to 41 days old, all samples remained non-reactive using the Millipore kit through 12 hours of observation (Table 5.1). For our colorimetric assay, samples had similarly non-reactive results during the initial 40 minutes after the indicator solution was added (Table 5.1). However, by 12 hours, the samples were reactive as the solution turned clear (Table 5.1).

5.3.3 Variable reactivity of dermatophyte species with colorimetric assay

M. canis, *T. mentagrophytes*, and *Nannizzia gypsea* cultures grown on different culture media (SDA, PDA, DTM) were tested for sulfite production using our colorimetric assay. While the *T. mentagrophytes* samples did not exhibit reactivity until 6 hours, all four of the *M. canis* samples had some reactivity by 90 minutes including a sample that had immediate color change (Table 5.2). All of the culture samples had color change to clear by 12 hours after the indicator solution was added (Table 5.2).

5.3.4 Clinical hair samples had mild color change with the colorimetric assay

Hair samples from specific-pathogen free (SPF) cats (n=5) were added to the colorimetric assay and the optical density was measured before adding the indicator solution and sequentially measured up to 90 minutes. For all five SPF cat hair samples, the wells remained non-reactive and had optical densities similar to the negative control wells and dilutions of sulfite that are below the LoD (Fig. 5.4). After the indicator was added, the OD values for the SPF cat samples remained above the indeterminate range (Fig. 5.5). Each sample was run in triplicate (n=3) and the standard deviation was below 0.058 for all points.

Hair samples from cases of suspected dermatophytosis cats were added to the colorimetric assay and after 12 hours of incubation, the color remained blue or turned to a dark purple color, indicating non-reactivity to slight reactivity with the indicator solution (Table 5.3). For another set of hair samples from cases of suspected dermatophytosis cats, most of the samples had OD values that remained high at 600 nm after adding the indicator solution (Fig. 5.6). One sample turned an opaque white after adding the indicator solution, resulting in an artificially high OD value (Fig. 5.6). Furthermore, two clinical hair samples turned clear and had low OD values after the addition of the indicator solution (Fig. 5.6). Samples were run in duplicate (n=2) and the standard deviation was below 0.066 for all points.

5.3.5 Blocking cysteine interference with colorimetric assay

The colorimetric assay may also be sensitive to compounds besides sulfite, such as ascorbic acid, hydrogen peroxide, hypochlorite, certain metals, and nonspecific fungal organisms as free thiols can interfere with this assay [Manonmani *et al.* 1999]. As free thiols interfered with the indicator solution, different compounds were evaluated for blocking cysteine's interaction with the colorimetric assay without interfering with sulfite's interaction with the assay. While hydrogen peroxide and zinc sulfate interfered with sulfite's interaction with the indicator solution, copper sulfate did not affect this reaction (Fig. 5.7).

The level of interference of L-cysteine with the indicator solution was determined to be at 3 µl of 5 mM L-cysteine and greater (Fig. 5.8). When 50 µl of 100 mM $CuSO_4$ was added, up to 6 µl of 5 mM L-cysteine was able to be added without interference with the indicator solution (Fig. 5.8). To observe how these compounds interact with sulfite, 50 µl of 100 mM $CuSO_4$ and 4 µl of 5 mM L-cysteine were added to serial dilutions of sodium sulfite with 20 µl of indicator

solution using 10 µl of IKI. When added all together, the L-cysteine with the $CuSO_4$ interfered with the level of detection changing it from 1.98 µM to 0.25 µM of sulfite (Fig. 5.9). At high levels of sulfite (above 4 µM), copper sulfate reacted with sulfite, precipitating out of solution (Fig. 5.9). The resulting precipitant was a muted yellow color when the indicator solution was absent and a burnt yellow color when the indicator was present (Fig. 5.9).

5.3.6 SSC detected from M. canis culture samples

Using the optimized LC-MS protocol, SSC was detected from broth samples collected from *M. canis* cultures grown with hair at 15 and 18 DPI with SSC concentrations calculated to be 0.5 ± 0.1 µg/ml and 0.4 ± 0.1 µg/ml, respectively (performed by Madeline C. Roach). No peaks that correspondent to SSC were detected using the optimized parameters from broth samples grown with hair at 1, 4, 8, and 11 DPI and broth samples grown without hair at 1, 4, 8, 11, 15, and 18 DPI. This assay has a limit of detection of 0.04 µg/ml of SSC using the optimized source parameters (performed by Madeline C. Roach).

5.4 Discussion

We developed two methods for detecting dermatophyte metabolites from keratin degradation (sulfite and S-sulfocysteine). For the first approach, we analyzed the interactions between a starch-iodine based indicator and various chemicals (sodium sulfite, zinc sulfate, copper sulfate, hydrogen peroxide, and L-cysteine), different species of dermatophytes and cat hair from SPF cats and suspected dermatophytosis cases. While reactions between the indicator and samples (either dermatophytes or cat hair) were inconsistent, we were able to inhibit the reaction of free thiols in solution with addition of 50 mM of copper sulfate, given that copper

interferes with cysteine by reductive chelation [Pecci *et al.* 1997]. To reduce off-targeting of our assay, we targeted a more stable metabolite (SSC) using LC-MS, and were able to detect and quantify this compound from *M. canis* cultures, suggesting further investigation into using this method for dermatophyte detection would be warranted.

We developed a colorimetric assay using a starch-iodine indicator solution that had a limit of detection (LoD) of 0.25 μM of sodium sulfite, lower than the reported levels produced by dermatophytes [Grumbt *et al.* 2013]. This LoD was similar to many commercial sulfite detection kits, allowing for a broad range of sulfite detection; these kits LoDs typically range from 0.05-10 mg/L of sulfite [Merck 2022]. The reactivity between the dilutions of sodium sulfite and the indicator solution was measured via absorbance and found that non-reactive solutions had the highest OD value at 600 nm. Having the highest absorbance occur at 600 nm was expected as this wavelength falls within the visible light spectrum and corresponds to orange, the complementary color to blue [Algar *et al.* 2016], allowing for visual assessment of the assay. As reactivity can be distinguished at 600 nm, scanning at this wavelength would be optimal for high throughput screening of samples utilizing this colorimetric assay.

Our colorimetric assay was compared to two commercial sulfite kits to ensure validity in our results and compare how user friendly the kits are. We found that both kits had disadvantages regarding potential use for clinical detection of sulfite from dermatophyte samples. These two kits (Millipore's and Megazyme's sulfite kits) were designed to detect sulfite in solutions, using two different methods. While Millipore's kit was less complicated and used similar equipment as our assay, Megazyme's kit required specialized equipment (spectrophotometer) and required multi-step calculations, potentially contributing to the inaccurate results for measuring sulfite. A major drawback of the Millipore kit was the large

minimum volume required to run a sample. As this kit was designed for sulfite detection in food and beverage, it had been calibrated for using 5 ml of sample liquid, a significantly larger quantity than our assay at 200 µl. Millipore's kit had less reactivity with fungal samples than our colorimetric assay, suggesting that this commercial kit is more robust for detecting only sulfite and not similar compounds such as SSC. Given these results from the commercial kits, it would not be a viable approach to utilize these kits for sulfite detection from dermatophytes.

All of the dermatophyte species tested (*M. canis*, *T. mentagrophytes*, and *N. gypsea*) had reactivity with our colorimetric assay by 12 hours, indicating either the fungi itself was consuming part of the indicator, secreting a compound that interfered with the indicator, or potentially both. Although a part of the indicator is starch, the fungi are unable to utilize this as a source of nutrient [Philpot 1977], suggesting that it is more likely that the fungi's extracellular metabolites are interfering with the indicator, causing the color change. Furthermore, hair samples from SPF and suspected dermatophytosis cats were tested with the colorimetric and had the OD values measured. While the SPF cat hair samples remained non-reactive, a few of the suspected dermatophytosis hair samples had reactivity, suggesting a positive detection of a dermatophyte. Possible reasons for why the other dermatophyte hair samples were non-reactive include sulfite levels below the assay's LoD due to low amount of fungi present, lower metabolic activity from the fungi, or rapid consumption/degradation of sulfite. Given that sulfite interacts with keratin and forms downstream metabolites [Léchenne *et al.* 2007, Grumbt *et al.* 2013], it is reasonable for dermatophytes to have low sulfite levels in the presence of keratinized tissues. Furthermore, the type of clinical sample and the quantity of sample collected can affect the amount of fungi present as skin scrapings have been found to yield higher positive results via fungal culture compared to other sample types [Alshehri *et al.* 2021]. Furthermore, one of the

clinical hair samples that had reactivity with the indicator solution had an opaque white color and a high OD value, suggesting a contaminant compound from the cat was present and interfered with the reaction. As the majority of dermatophytosis cases in cats collected from shelters are strays [Moskaluk *et al.* 2022], various substances from the environment could be present on the cat hair and potentially interact with our colorimetric assay, leading to false positives. Utilizing the OD value in conjunction with visual assessment could allow for distinguishment between different types of reactivities, reducing the rate of false positives.

Given that our colorimetric assay interacted with other compounds present in samples, we investigated additives that could reduce this interference. We targeted free thiols, which can be found in cysteine (the main amino acid of keratin) [Kasperova *et al.* 2013] and found that while the additives tested blocked cysteine's interaction with the starch-iodine indicator, they also interfered with the colorimetric assay. Copper sulfate was found to bind to free thiols without interfering with the colorimetric indicator, however, at high concentrations of sulfite, a side reaction occurred, disrupting the results of the colorimetric assay. The precipitate formed when sodium sulfite was mixed with copper sulfate is most likely copper I sulfide, which insoluble in water [PubChem 2022]. Copper is undergoing an oxidative reduction reaction with sulfite with the by-product of the reaction being copper I sulfide. While zinc sulfate can undergo the same reaction as copper sulfate, the by-product (zinc sulfide) is partially soluble in water [PubChem 2022], making it more difficult to visually detect the by-product and determine if this reaction has occurred. Additionally, at high concentrations of sodium sulfite, hydrogen peroxide interfered with the interaction of sulfite and the colorimetric indicator. Given that hydrogen peroxide is a strong oxidant, it could have reacted with the sulfite before the sulfite was able to react with the indicator solution. Further investigation into chemical reactions that can bind to

thiols without interacting with sulfite could greatly benefit this assay, increasing its specificity for sulfite.

As our colorimetric assay experienced off-target reactions, we pivoted to developing a LC-MS protocol for detecting a more stable metabolite of keratin degradation: SSC. Our LC-MS protocol had a LoD of 0.04 µg/ml of SSC, lower than other mass spectrometry and liquid chromatography protocols for SSC [Rashed *et al.* 2005, Belaidi *et al.* 2012]. Having a low LoD for SSC would be beneficial not only for dermatophytosis, but for early detection of two rare inherited metabolic disorders (molybdenum cofactor deficiency and isolated sulfite oxidase deficiency) [Johnson 2003]. Given that these metabolic disorders can be fatal without proper diagnosis and treatment, early detection is critical for survival and for monitoring the effectiveness of therapies [Misko *et al.* 1993, Mechler *et al.* 2015]. For dermatophyte detection, our initial results using LC-MS detected and quantified SSC in *M. canis* culture samples at day 15 and 18 using the optimized conditions. No SSC was detected using LC-MS prior to day 15, suggesting that this metabolite is being consumed by the fungi faster than it is produced at the beginning growth stages. Keratin metabolites (such as SSC and cysteic acid) have been shown to be rapidly utilized during the growth phase of dermatophytes [Kunert 1985]. Given that SSC has been shown to be consumed by dermatophytes and utilized as a sulfur source [Kunert 1985], detection of these metabolite might depend on the nutrient environment of the fungi and what growth phase the fungi are in. Preventing degradation of this metabolite could lead to accumulation, allowing for earlier detection of dermatophytes from culture and potentially from clinical samples. Furthermore, SSC was only detected in samples grown with hair supplementation, suggesting that this metabolite is not produced during other metabolic processes. Based on these results, determining the levels of SSC can indicate the presence of

dermatophyte metabolism of keratin with the potential to adapt this protocol as a method for diagnosing dermatophytosis.

In summary, we developed a colorimetric assay utilizing starch and iodine that can detect low levels of sulfite and potentially the presence of dermatophytes. The metabolites produced by fungal samples were at too low of levels for some samples, leading to false negatives. Although cysteine could be used as a supplement to increase sulfite production in dermatophytes, it interfered with the colorimetric assay, resulting in reactivity between the free thiol in cysteine and the indicator solution. Chemicals that bind free thiol were tested to block cysteine's interference, but also interfered with the colorimetric assay. Further exploration into chemical reactions that can bind free thiols without interacting with the starch-iodine indicator could aid in increasing the accuracy of this colorimetric assay. Additionally, we developed a LC-MS method for detecting and quantifying SSC from dermatophyte cultures that could be further developed as a potential diagnostic assay for detecting dermatophytes. Understanding how keratin metabolic by-products are produced and consumed by dermatophytes lead to more specific dermatophyte diagnostic assays and potential targets for anti-dermatophytosis therapies.

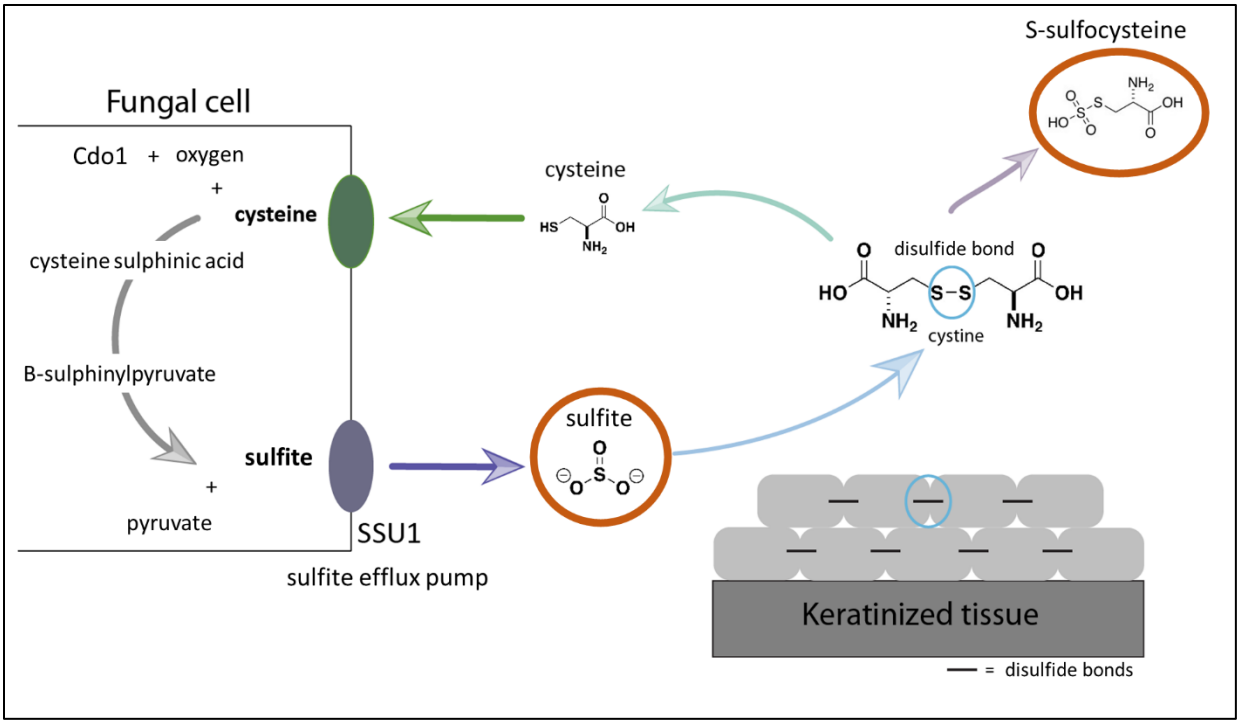

Figure 5.1. Fungal metabolism of keratin results in sulfite production. Fungal cells secrete sulfite via sulfite efflux pump (SSU1) which breaks the disulfide bonds in cystine, resulting in the formation of cysteine and S-sulfocysteine. The fungal cells uptake cysteine and convert it back to sulfite using cysteine dioxygenase (Cdo1).

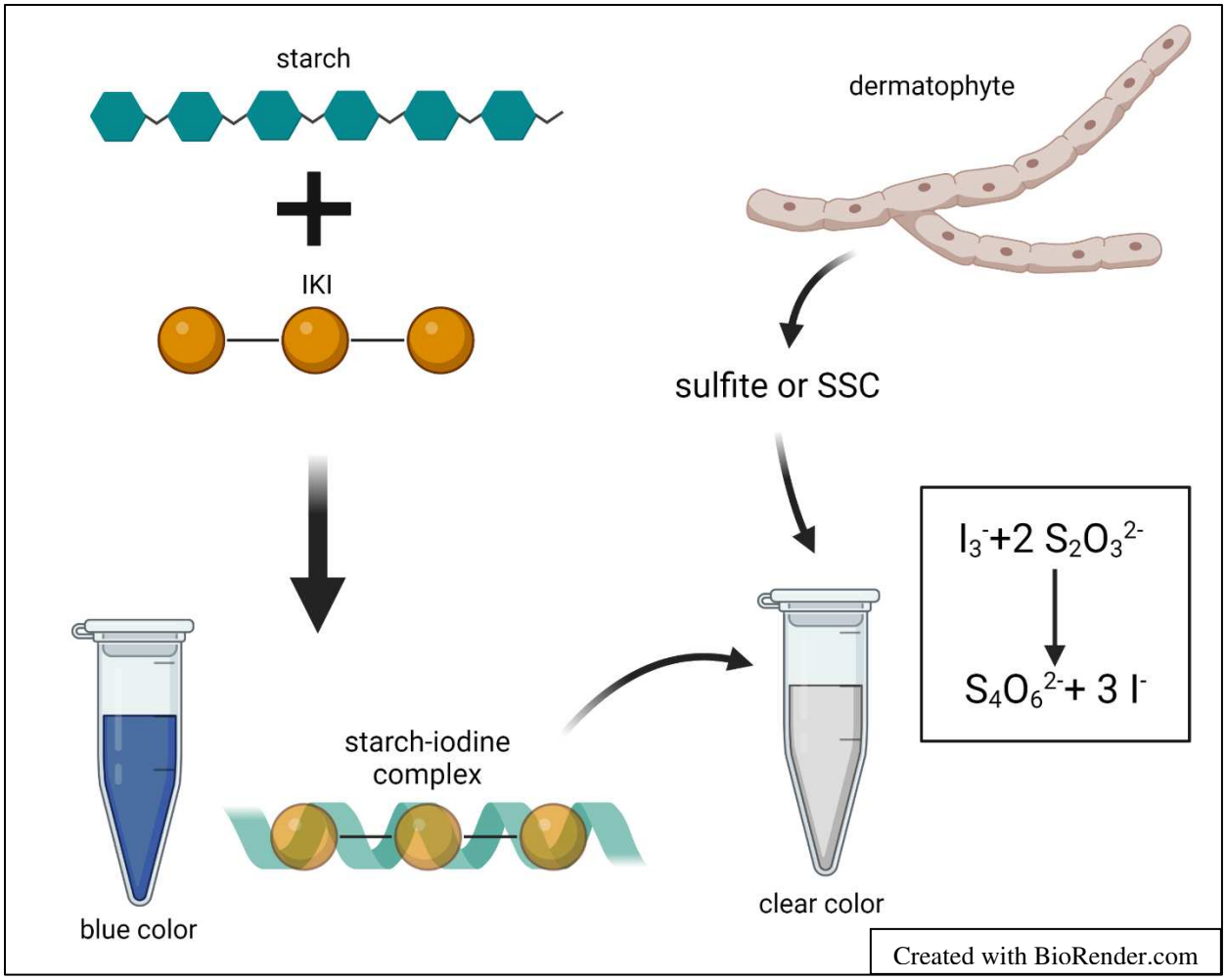

Figure 5.2. Starch-iodine indicator interacts with sulfite turning the solution from blue to clear. When starch is mixed with IKI, it forms a complex and creates a blue solution. When sulfite or S-sulfocysteine (SSC) produced from dermatophytes' metabolism of keratin interact with this complex, it turns the solution clear.

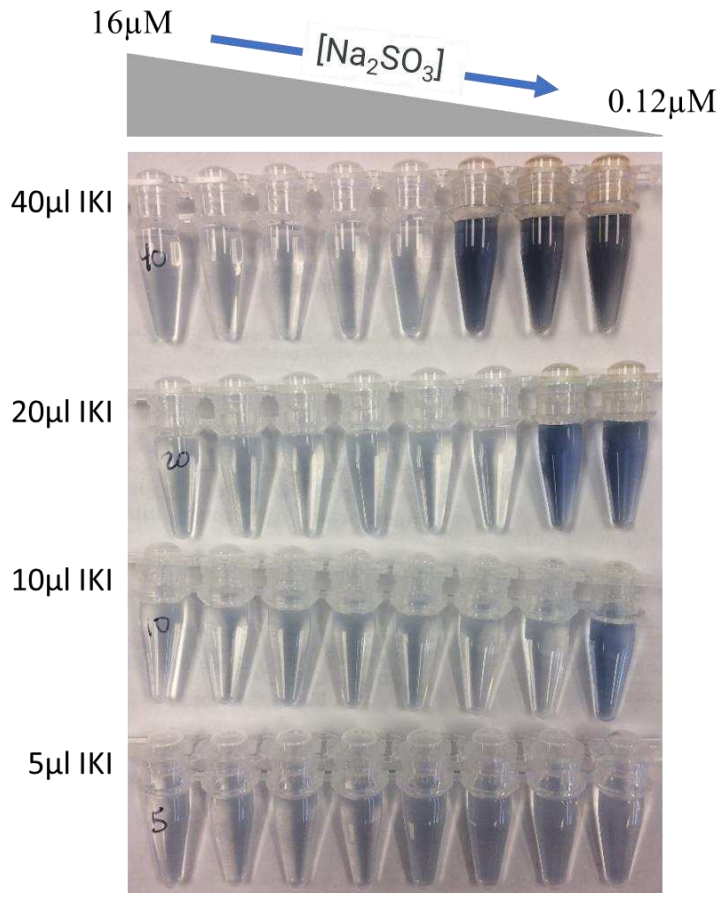

Figure 5.3. Level of sulfite detection for varying concentrations of potassium iodine (IKI). Row (1) – 40 µl of IKI; (2) – 20 µl of IKI; (3) – 10 µl of IKI; (4) – 5 µl of IKI. Tubes 1-8 have serial dilutions of sodium sulfite (diluted from 16 µM to 0.12 µM). Clear = reactive. Blue = non-reactive.

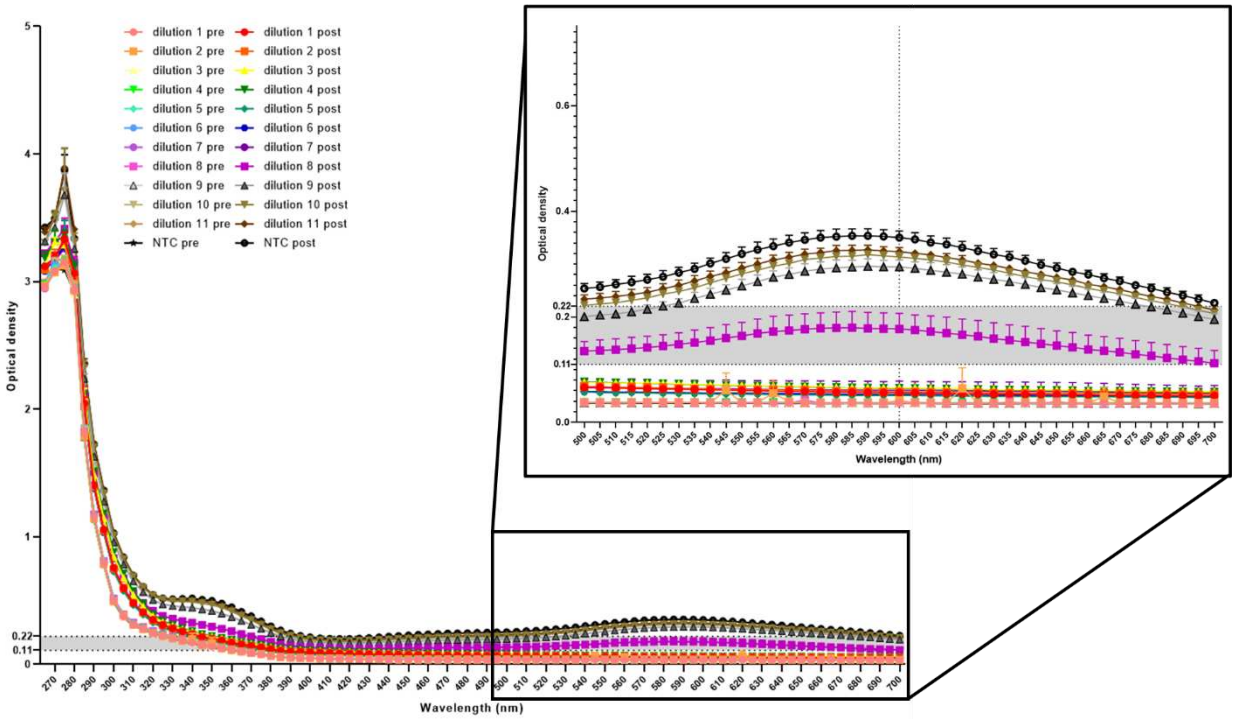

Figure 5.4. Peak optical density for non-reactive samples occurred at 600 nm. Optical densities of serial dilution of sodium sulfite from 16 µM (dilution 1) to 0.016 µM (dilution 11) before and after adding the indicator solution. Concentrations between 16 µM (dilution 1) to 0.25 µM (dilution 7) of sodium sulfite were reactive after the indicator solution was added. Concentrations 0.063 µM (dilution 9), 0.031 µM (dilution 10) and 0.015 µM (dilution 11) of sodium sulfite were non-reactive after the indicator solution was added. Dilution 8 (0.125 µM) was within the indeterminate range. Negative control (NTC) was water with indicator solution. The indeterminate range (gray shaded region) was calculated as 1-2x the cutoff value. Samples were run in duplicate (n=2) and the standard deviation was below 0.331 for all points.

Table 5.1. Samples using Millipore's kit remain non-reactive overnight. Swabs of *Trichophyton mentagrophytes* cultures at different days post inoculated were added to both the colorimetric assay and Millipore's kit. Reactivity was measured via color change from blue to clear up to 12 hours. R = reactive. N = non-reactive. C = colorimetric assay. M = Millipore's kit.

	0min		**5min**		**10min**		**40min**		**12hours**	
Days in culture	**C**	**M**	**C**	**M**	**C**	**M**	**C**	**M**	**C**	**M**
2	N	N	N	N	N/A	N/A	N/A	N/A	R	N
6	N	N	N	N	N	N	N	N	R	N
39	N	N	N/A	N/A	N	N	N/A	N/A	N/A	N/A
41	N	N	N/A	N/A	N	N	N/A	N/A	N/A	N/A

Table 5.2. Fungal cultures turned positive by 12 hours. Swabs of *Trichophyton mentagrophytes*, *Microsporum canis*, and *Nannizzia gypsea* cultures grown on different culture media were added to the colorimetric assay. Reactivity was measured via color change from blue to clear up to 12 hours. R = reactive. S = slightly reactive. N = non-reactive. SDA = Sabouraud dextrose agar. PDA = potato dextrose agar. DTM = dermatophyte test media.

Fungal samples	**0 min**	**5 min**	**10 min**	**30 min**	**60 min**	**90 min**	**2hr**	**6hr**	**12hr**
M. canis 1 SDA	N	N	N	N/A	N/A	S	N/A	N/A	R
M. canis 2 SDA	N	N/A	S	R	R	N/A	R	R	N/A
M. canis 3 SDA	R	N/A	R	R	R	N/A	R	N/A	R
M. canis 1 PDA	N	N	N	N/A	N/A	S	N/A	N/A	R
M. canis 2 PDA	S	N/A	R	R	R	N/A	R	R	N/A
M. canis 1 DTM	N	N/A	N	N	S	N/A	S	N/A	R
T. mentagrophytes 1 SDA	N	N	N	N/A	N/A	N	N/A	N/A	R
T. mentagrophytes 2 SDA	N	N/A	N	N	N	N/A	N	S	N/A
T. mentagrophytes 1 PDA	N	N	N	N/A	N/A	N	N/A	N/A	R
T. mentagrophytes 2 PDA	N	N/A	N	N	N	N/A	N	S	N/A
N. gypsea 1 SDA	N	N/A	N	N	N	N/A	S	N/A	R
Water	N	N	N	N/A	N/A	N	N/A	N/A	N

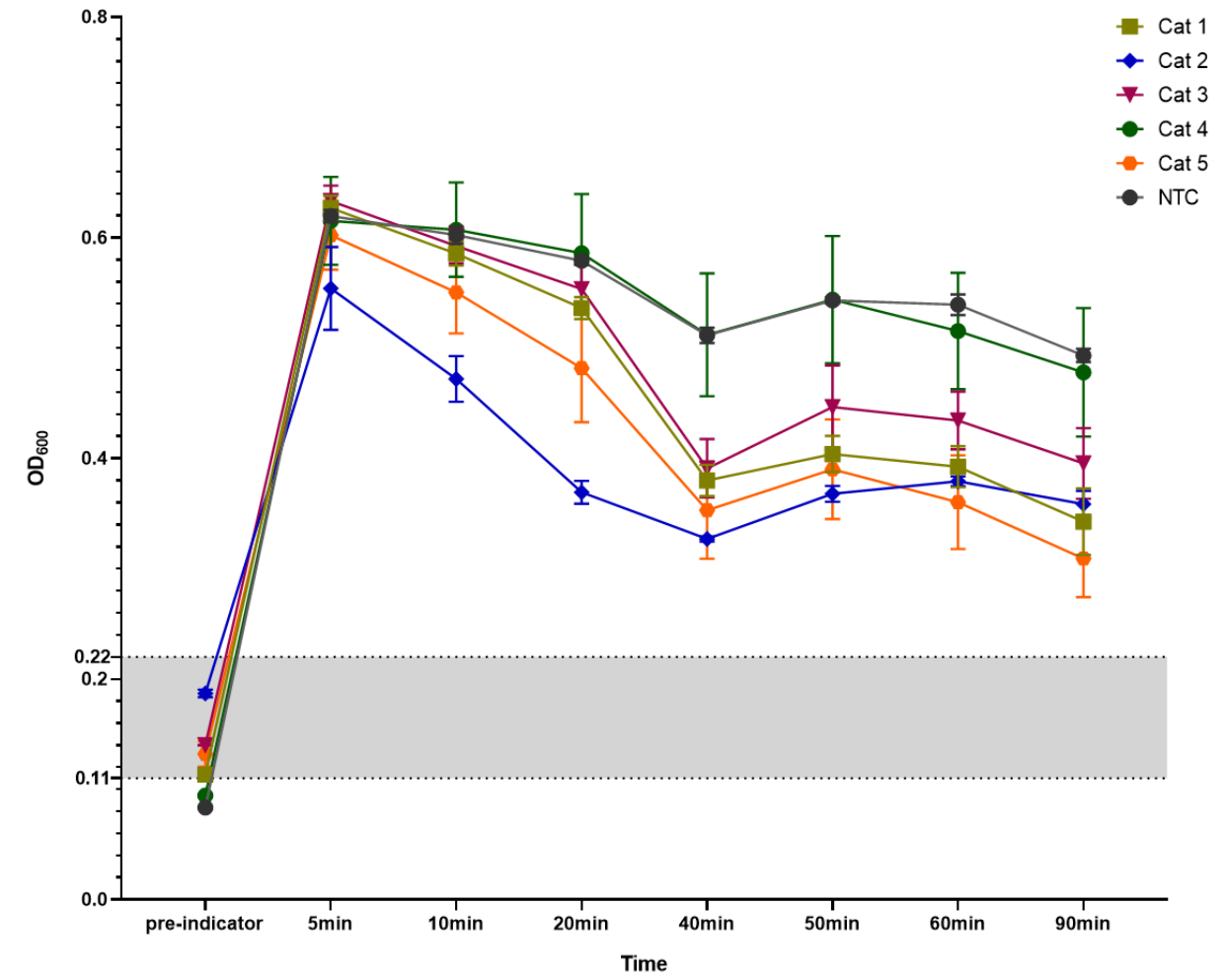

Figure 5.5. High optical density for SPF cat hair samples at 600 nm. Optical densities of specific pathogen free cat hair added to water before and after adding the indicator solution. All SPF cat hair samples remained non-reactive after the indicator was added. Negative control (NTC) was water with indicator solution. The indeterminate range (gray shaded region) was calculated as 1-2x the cutoff value. Samples were run in triplicate (n=3) and the standard deviation was below 0.058 for all points.

Table 5.3. Hair samples had slightly reactivity with colorimetric assay by 12 hours. Hair samples from suspected dermatophytosis cats were added into water then into the colorimetric assay. Reactivity was monitored via color change from blue to clear up to 12 hours. R = reactive. S = slightly reactive. N = non-reactive.

Time	**0 min**	**10 min**	**30 min**	**40 min**	**60 min**	**120 min**	**150 min**	**12hr**
Hair sample 1	N	N	N	N	N	N	N	N
Hair sample 2	N	N	N	N	N	N	N	S
Hair sample 3	N	N	N	N	N	N	N	S
Hair sample 4	N	N	N	N	N	N	N	S
Hair sample 5	N	N	N	N	N	N	N	S
Hair sample 6	N	N	N	N	N	N	N	S
Water	N	N	N	N	N	N	N	N

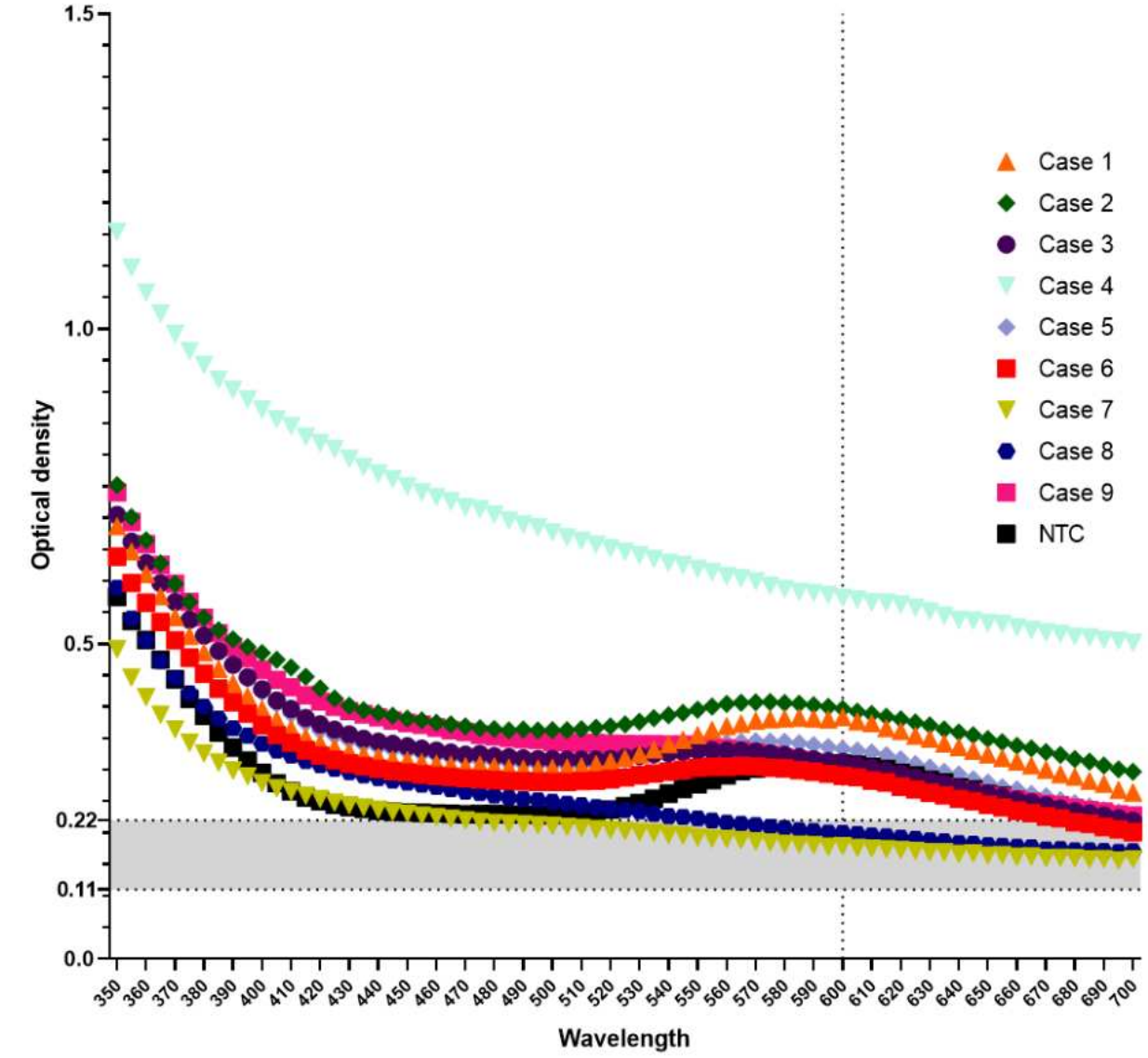

Figure 5.6. High optical density for clinical cat hair samples at 600 nm. Optical densities of cat hair from suspected dermatophytosis cases before and after adding the indicator solution. Most of the clinical cat hair samples (n=6) remained non-reactive after the indicator was added. A sample (Case 4) was an opaque white after the indicator was added, giving a falsely high optical density. Two samples (Cases 7 and 8) were reactive after the indicator was added. Negative control (NTC) was water with indicator solution. The indeterminate range (gray shaded region) was calculated as 1-2x the cutoff value. Samples were run in duplicate (n=2) and the standard deviation was below 0.066 for all points.

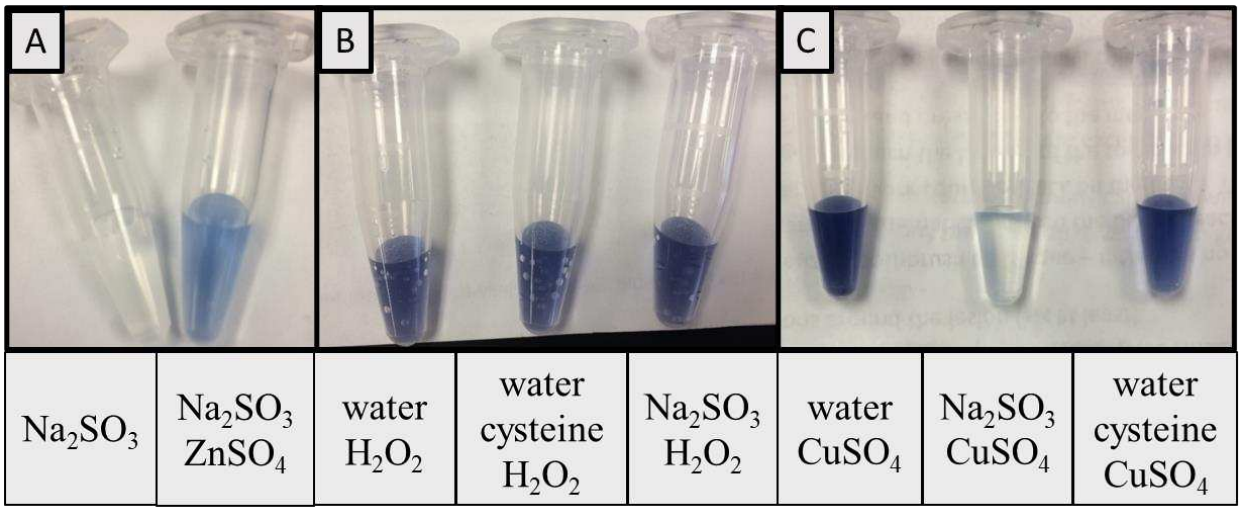

Figure 5.7. $CuSO_4$ did not interfere with indicator solution. All tubes had 40 µl of the indicator solution added. (A) left tube – 200 µl of 0.49 mM sodium sulfite; right tube – 200 µl of 0.49 mM sodium sulfite with 200 µl of 125 mM $ZnSO_4$. (B) left tube – 200 µl water with 10 µl 30% H_2O_2; center tube – 200 µl water with 10 µl 30% H_2O_2 and 3 µl 5 mM D-cysteine; right tube – 200 µl of 0.49 mM sodium sulfite with 10 µl 30% H_2O_2. (C) left tube – 200 µl water with 50 µl of 100 mM $CuSO_4$; center tube – 200 µl of 0.49 mM sodium sulfite with 50 µl of 100 mM $CuSO_4$; right tube – 200 µl water with 50 µl of 100 mM $CuSO_4$ and 3 µl 5 mM D-cysteine.

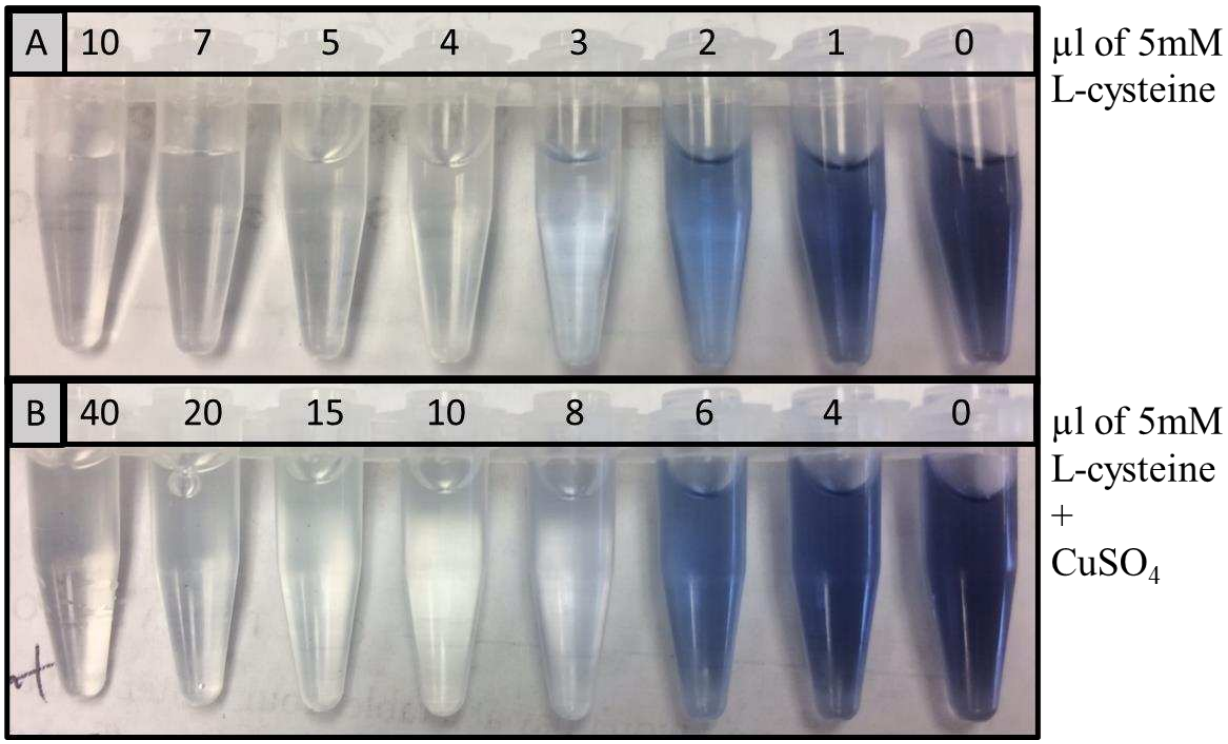

Figure 5.8. $CuSO_4$ blocked L-cysteine interference with indicator solution. All tubes had 40 µl of the indicator solution and 200 µl water added. (A) varying levels of 5 mM L-cysteine added; left to right tubes: 1 – 10 µl; 2 – 7 µl; 3 – 5 µl; 4 – 4 µl; 5 – 3 µl; 6 – 2 µl; 7 – 1 µl; 8 – 0 µl. (B) all tubes had 50 µl 100 mM $CuSO_4$ and varying levels of 5 mM L-cysteine added; left to right tubes: 1 – 40 µl; 2 – 20 µl; 3 – 15 µl; 4 – 10 µl; 5 – 8 µl; 6 – 6 µl; 7 – 4 µl; 8 – 0 µl.

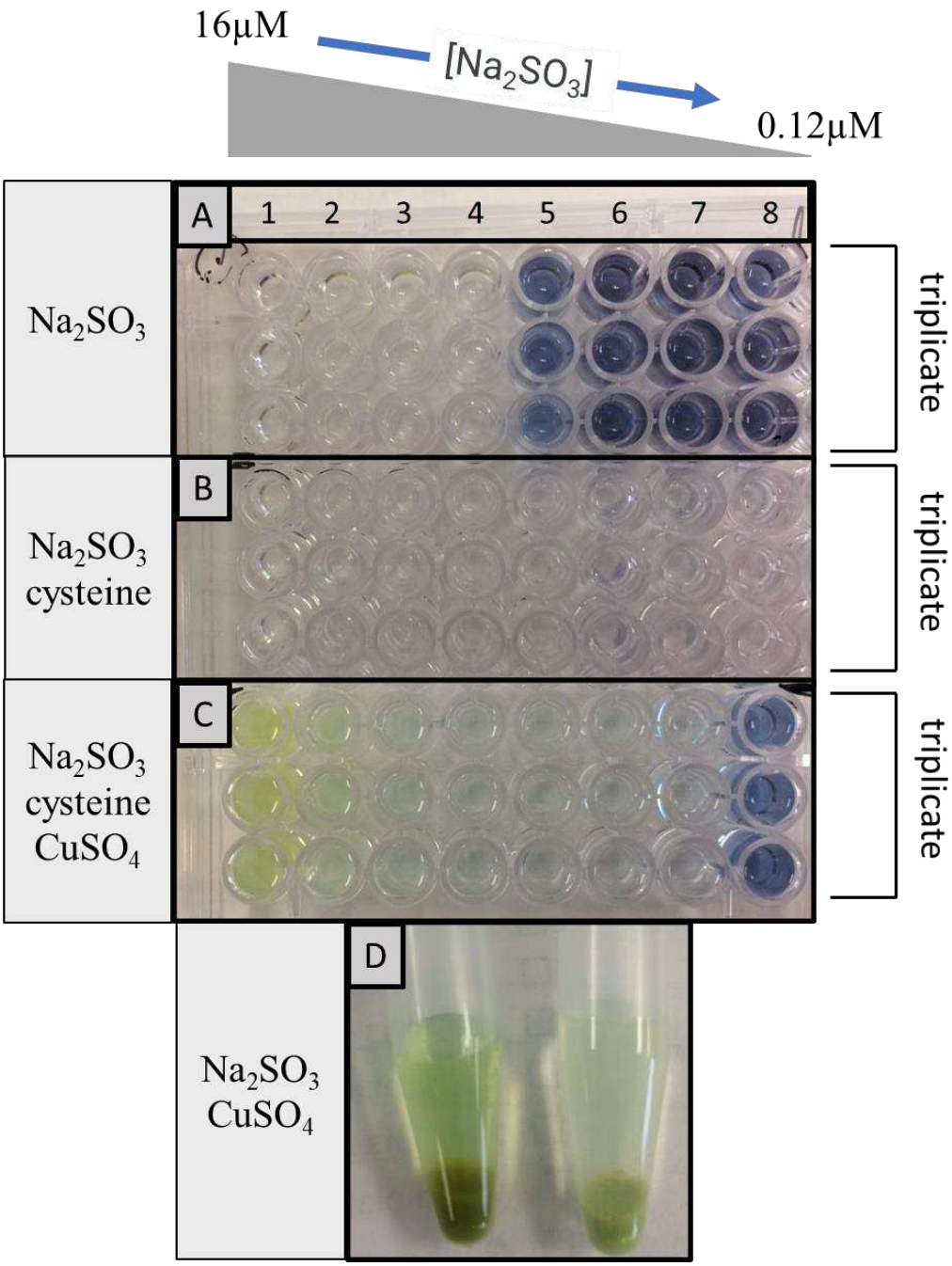

Figure 5.9. $CuSO_4$ interacts with high levels of sodium sulfite. (A-C) each well was run in triplicate (rows 1-3); 20 µl of indicator solution added to each well. (A) serial dilution of sodium sulfite from 16 µM to 0.12 µM with final volume of 200 µl per well. (B) same sulfite dilution as (A) with 4 µl of 5 mM L-cysteine added. (C) same sulfite and L-cysteine as (B) with 50 µl of 100 mM $CuSO_4$ added. (D) left tube – 200 µl 158.7 mM sodium sulfite with 200 µl 100 mM $CuSO_4$ and 40 µl of indicator solution; right tube – 200 µl 158.7 mM sodium sulfite with 200 µl 100 mM $CuSO_4$.

Literature Cited

Achterman RR and White TC. (2012). A foot in the door for dermatophyte research. *PLoS pathogens* **8**(3):e1002564-e1002564.

Algar WR, De Jong CAG, Maxwell EJ, et al. (2016). Demonstration of the Spectrophotometric Complementary Color Wheel Using LEDs and Indicator Dyes. *Journal of Chemical Education* **93**(1):162-165.

Alshehri BA, Alamri AM, Rabaan AA, et al. (2021). Epidemiology of Dermatophytes Isolated from Clinical Samples in a Hospital in Eastern Saudi Arabia: A 20-Year Survey. *J Epidemiol Glob Health* **11**(4):405-412.

Belaidi AA, Arjune S, Santamaria-Araujo JA, et al. (2012). Molybdenum cofactor deficiency: a new HPLC method for fast quantification of s-sulfocysteine in urine and serum. *JIMD Rep* **5**(35-43.

Benedict K, Jackson BR, Chiller T, et al. (2018). Estimation of Direct Healthcare Costs of Fungal Diseases in the United States. *Clinical Infectious Diseases* **68**(11):1791-1797.

Bennassar A and Grimalt R. (2010). Management of tinea capitis in childhood. *Clinical, cosmetic and investigational dermatology* **3**(89-98.

Brillowska-Dabrowska A, Michałek E, Saunte DML, et al. (2013). PCR test for Microsporum canis identification. *Medical Mycology* **51**(6):576-579.

Dhar NR. (1924). The Starch-Iodine Reaction. *The Journal of Physical Chemistry* **28**(2):125-130.

Dogra S and Uprety S. (2016). The menace of chronic and recurrent dermatophytosis in India: Is the problem deeper than we perceive? *Indian dermatology online journal* **7**(2):73-76.

Drake LA, Dinehart SM, Farmer ER, et al. (1996). Guidelines of care for superficial mycotic infectionsof the skin: Tinea corporis, tinea cruris, tinea faciei, tinea manuum, and tinea pedis. *Journal of the American Academy of Dermatology* **34**(2, Part 1):282-286.

Elewski BE. (2000). Tinea capitis: A current perspective. *Journal of the American Academy of Dermatology* **42**(1, Part 1):1-20.

Garg J, Tilak R, Garg A, et al. (2009). Rapid detection of dermatophytes from skin and hair. *BMC research notes* **2**(60.

Gräser Y, Scott J, and Summerbell R. (2008). The New Species Concept in Dermatophytes—a Polyphasic Approach. *Mycopathologia* **166**(5):239.

Grebe SK and Singh RJ. (2011). LC-MS/MS in the Clinical Laboratory - Where to From Here? *The Clinical biochemist. Reviews* **32**(1):5-31.

Griffith OW. (1983). Cysteinesulfinate metabolism. altered partitioning between transamination and decarboxylation following administration of beta-methyleneaspartate. *J Biol Chem* **258**(3):1591-8.

Grumbt M, Monod M, Yamada T, et al. (2013). Keratin Degradation by Dermatophytes Relies on Cysteine Dioxygenase and a Sulfite Efflux Pump. *Journal of Investigative Dermatology* **133**(6):1550-1555.

Gupta AK and Cooper EA. (2008). Update in Antifungal Therapy of Dermatophytosis. *Mycopathologia* **166**(5):353-367.

Havlickova B, Czaika VA, and Friedrich M. (2008). Epidemiological trends in skin mycoses worldwide. *Mycoses* **51**(s4):2-15.

Hay RJ. (2017). Tinea Capitis: Current Status. *Mycopathologia* **182**(1-2):87-93.

Irwin SV, Fisher P, Graham E, et al. (2017). Sulfites inhibit the growth of four species of beneficial gut bacteria at concentrations regarded as safe for food. *PloS one* **12**(10):e0186629-e0186629.
Jacobson LS, McIntyre L, and Mykusz J. (2017). Comparison of real-time PCR with fungal culture for the diagnosis of Microsporum canis dermatophytosis in shelter cats: a field study. *Journal of feline medicine and surgery* **20**(2):103-107.
Johnson JL. (2003). Prenatal diagnosis of molybdenum cofactor deficiency and isolated sulfite oxidase deficiency. *Prenatal Diagnosis* **23**(1):6-8.
Kasperova A, Kunert J, and Raska M. (2013). The possible role of dermatophyte cysteine dioxygenase in keratin degradation. *Medical Mycology* **51**(5):449-454.
Kunert J. (1985). Metabolism of sulfur-containing amino acids in the dermatophyte Microsporum gypseum. II. Acidic amino acid derivatives. *J Basic Microbiol* **25**(2):111-8.
Kupsch C, Ohst T, Pankewitz F, et al. (2016). The agony of choice in dermatophyte diagnostics—performance of different molecular tests and culture in the detection of Trichophyton rubrum and Trichophyton interdigitale. *Clinical Microbiology and Infection* **22**(8):735.e11-735.e17.
Lardeux F, Torrico G, and Aliaga C. (2016). Calculation of the ELISA's cut-off based on the change-point analysis method for detection of Trypanosoma cruzi infection in Bolivian dogs in the absence of controls. *Mem Inst Oswaldo Cruz* **111**(8):501-4.
Léchenne B, Reichard U, Zaugg C, et al. (2007). Sulphite efflux pumps in Aspergillus fumigatus and dermatophytes. *Microbiology* **153**(3):905-913.
Manonmani HK and Kunhi AAM. (1999). Interference of thiol-compounds with dextrinizing activity assay of α-amylase by starch-iodine colour reaction: Modification of the method to eliminate this interference. *World Journal of Microbiology and Biotechnology* **15**(4):485-487.
Marconi VC, Kradin R, Marty FM, et al. (2010). Disseminated dermatophytosis in a patient with hereditary hemochromatosis and hepatic cirrhosis: case report and review of the literature. *Medical Mycology* **48**(3):518-527.
Mechler K, Mountford WK, Hoffmann GF, et al. (2015). Ultra-orphan diseases: a quantitative analysis of the natural history of molybdenum cofactor deficiency. *Genet Med* **17**(12):965-70.
Mercer DK and Stewart CS. (2018). Keratin hydrolysis by dermatophytes. *Medical Mycology* **57**(1):13-22.
Merck. *Water, Environmental and Food and Beverage Analysis: Ready-to-use Test kits, Instruments, and Accessories*. 2022 [cited 2022 August 4]; 1:[Visual and Instrumental Testing Portolio Overview].
Misko A, Mahtani K, Abbott J, et al., *Molybdenum Cofactor Deficiency*, in *GeneReviews(®)*, M.P. Adam, et al., Editors. 1993, University of Washington, Seattle

Mooi E and Sarstedt M, *A concise guide to market research: The process, data, and methods using IBM SPSS Statistics. New York: Springer*. 2011. 307.
Moskaluk A, Darlington L, Kuhn S, et al. (2022). Genetic Characterization of Microsporum canis Clinical Isolates in the United States. *Journal of Fungi* **8**(7).
Moya H and Santana W. (2019). Determination of Free SO2 in Wines Using a Modified Ripper Method with Potentiometric Detection a Comparative Study with an.5.

Nussipov Y, Markabayeva A, Gianfaldoni S, et al. (2017). Clinical and Epidemiological Features of Dermatophyte Infections in Almaty, Kazakhstan. *Open access Macedonian journal of medical sciences* **5**(4):409-413.
Nweze EI and Eke IE. (2017). Dermatophytes and dermatophytosis in the eastern and southern parts of Africa. *Medical Mycology* **56**(1):13-28.
Panasiti V, Borroni RG, Devirgiliis V, et al. (2006). Comparison of diagnostic methods in the diagnosis of dermatomycoses and onychomycoses. *Mycoses* **49**(1):26-29.
Pecci L, Montefoschi G, Musci G, et al. (1997). Novel findings on the copper catalysed oxidation of cysteine. *Amino acids* **13**(3):355-367.
Peres NT, Maranhao FC, Rossi A, et al. (2010). Dermatophytes: host-pathogen interaction and antifungal resistance. *An Bras Dermatol* **85**(5):657-67.
Philpot CM. (1977). The use of nutritional tests for the differentiation of dermatophytes. *Sabouraudia* **15**(2):141-150.
Pihet M and Le Govic Y. (2017). Reappraisal of Conventional Diagnosis for Dermatophytes. *Mycopathologia* **182**(1):169-180.
PubChem. *PubChem Compound Summary for CID 14821, ZINC sulfide*. 2022 [cited 2022 July 30]; Available from: https://pubchem.ncbi.nlm.nih.gov/compound/ZINC-sulfide.
PubChem. *PubChem Compound Summary for CID 14831, Copper(II) sulfide*. 2022 [cited 2022 July 28].
Rashed MS, Saadallah AAA, Rahbeeni Z, et al. (2005). Determination of urinary S-sulphocysteine, xanthine and hypoxanthine by liquid chromatography–electrospray tandem mass spectrometry. *Biomedical Chromatography* **19**(3):223-230.
Rezusta A, de la Fuente S, Gilaberte Y, et al. (2016). Evaluation of incubation time for dermatophytes cultures. *Mycoses* **59**(7):416-418.
Richard JL, Debey MC, Chermette R, et al. (1994). Advances in veterinary mycology. *Journal of Medical and Veterinary Mycology* **32**(Supplement_1):169-187.
Rouzaud C, Hay R, Chosidow O, et al. (2015). Severe Dermatophytosis and Acquired or Innate Immunodeficiency: A Review. *Journal of fungi (Basel, Switzerland)* **2**(1):4.
Seebacher C, Bouchara J-P, and Mignon B. (2008). Updates on the Epidemiology of Dermatophyte Infections. *Mycopathologia* **166**(5):335-352.
Stone J. (2019). The Way Forward for Clinical Mass Spectrometry in Hospital Laboratories. *Clinical Laboratory News*.
Stuntebeck R, Moriello KA, and Verbrugge M. (2018). Evaluation of incubation time for Microsporum canis dermatophyte cultures. *Journal of feline medicine and surgery* **20**(10):997-1000.
Wagner K, Springer B, Pires VP, et al. (2018). Molecular detection of fungal pathogens in clinical specimens by 18S rDNA high-throughput screening in comparison to ITS PCR and culture. *Scientific Reports* **8**(1):6964.
Wickes BL and Wiederhold NP. (2018). Molecular diagnostics in medical mycology. *Nature Communications* **9**(1):5135.

CHAPTER 6: CONCLUSIONS AND FUTURE DIRECTIONS

6.1 Conclusions and Future Directions

Our work in Chapter Two represents the first comprehensive assessment of *M. canis* genetic and clinical associations conducted in the US. Our analysis showed that a small handful of microsatellite loci are capable of distinguishing geographic and virulence characteristics. This provides great optimism that more rigorous genomic comparisons will reveal markers that could be exploited to diagnostic and therapeutic advantage. Disease severity was demonstrated to be a significant predictor of genetic differentiation among *M. canis* isolates. Our finding of MAT1-1 locus homogeneity suggests evolution of domestic cat-associated *M. canis* towards a largely asexual reproduction cycle. These results had significant ecological and biological implications, and again offer potential therapeutic targets for this widespread zoonotic agent. Other genes essential for adhesion and keratin metabolism (SUB3, SSU1) were evaluated in a subset of the cohort and were found to be genetically identical across clinic locations. Follow up studies exploring more comprehensive sequencing methods, such as whole genome sequencing, provide an exciting avenue for in-depth genetic analyses that could reveal differences in clinical presentation, unknown functions inherent in superficial fungal metabolism, and may suggest novel and innovative therapeutic modalities.

Chapter Three revealed two novel dermatophyte species isolated from domestic cats in California: *Arthroderma lilyanum* and *Arthroderma mcgillisianum*. Given the slower growth rate and similar culture morphology to other dermatophytes, these species can easily be missed in clinical settings, making it difficult to know the true geographical range of these fungi and potential other host species they can infect. Molecular characterization of additional

dermatophyte samples from various geographical locations and host species could help elucidate these fungi's distribution and identify new dermatophyte species.

In Chapter Four, we optimized an antibody assay for detecting Sub3 from *M. canis* samples (clinical and culture). While the assay was able to detect Sub3 from concentrated culture samples, Sub3 levels from clinical samples were below the assay's limit of detection, suggesting that *M. canis* utilizes a small quantity of this protein for establishing infections. We were able to increase the production of this protein by culturing the fungus in baffled flasks supplemented with L-cysteine or hair. Gene expression of Sub3 followed a similar pattern as the production levels, however, the RNA for some samples was of low quality. Repeating these broth experiments using liquid nitrogen followed by either (1) RNeasy Plant Mini Kit (Qiagen, Valencia, CA, USA), and (2) Trizol/chloroform extraction methods would hopefully increase the quality of extracted RNA, allowing for a more accurate assessment of Sub3 expression. We also demonstrated that samples not supplemented with L-cysteine or hair also produced Sub3, implying that these compounds are not required for initializing Sub3 metabolism. Given that the production of this protein can be modulated by environmental factors and is essential for the initial stage of infection, novel therapies could be designed to target the production of Sub3, preventing *M. canis* from establishing an infection. This type of therapy would be beneficial in exposure cases such as littermates where one animal has dermatophytosis and the others lack clinical signs.

Chapter Five explored the development of two novel molecular diagnostics targeting dermatophyte metabolism of keratin. While the first approach utilized a starch-iodine indicator and had a limit of detection below reported dermatophyte production of sulfite, this assay had off-target reactions, leading to a low specificity. Our second approach targeted a more stable

metabolite (S-sulfocysteine) using tandem liquid chromatography with mass spectrometry. From this second method, we were able to detect and quantify SSC from *M. canis* culture samples, demonstrating that this metabolite is consumed/degraded at a higher rate in earlier growth phases. Further testing with different types of clinical samples containing different dermatophyte species could be explored as the levels of SSC from clinical samples could potentially be detected, thus diagnosing dermatophytosis rapidly compared to fungal culture. Furthermore, designing therapies that target the production of sulfite and the gene expression of the pump responsible for secreting sulfite would be beneficial in all stages of infection as dermatophytes cannot degrade keratin without sulfite, essentially starving the fungi and decreasing the fungi's ability to invade new tissue.

In summary, we expanded upon the knowledge of the relationship between *M. canis* genetics and disease severity, and the development of assays for detecting key dermatophyte metabolites. Furthermore, we contributed to our understanding of the dermatophyte species that infect domestic cats by identifying and characterizing two novel dermatophyte species. The work presented in these chapters helps elucidate several avenues for future studies involving dermatophyte genetics and diagnostic assay development.

APPENDIX

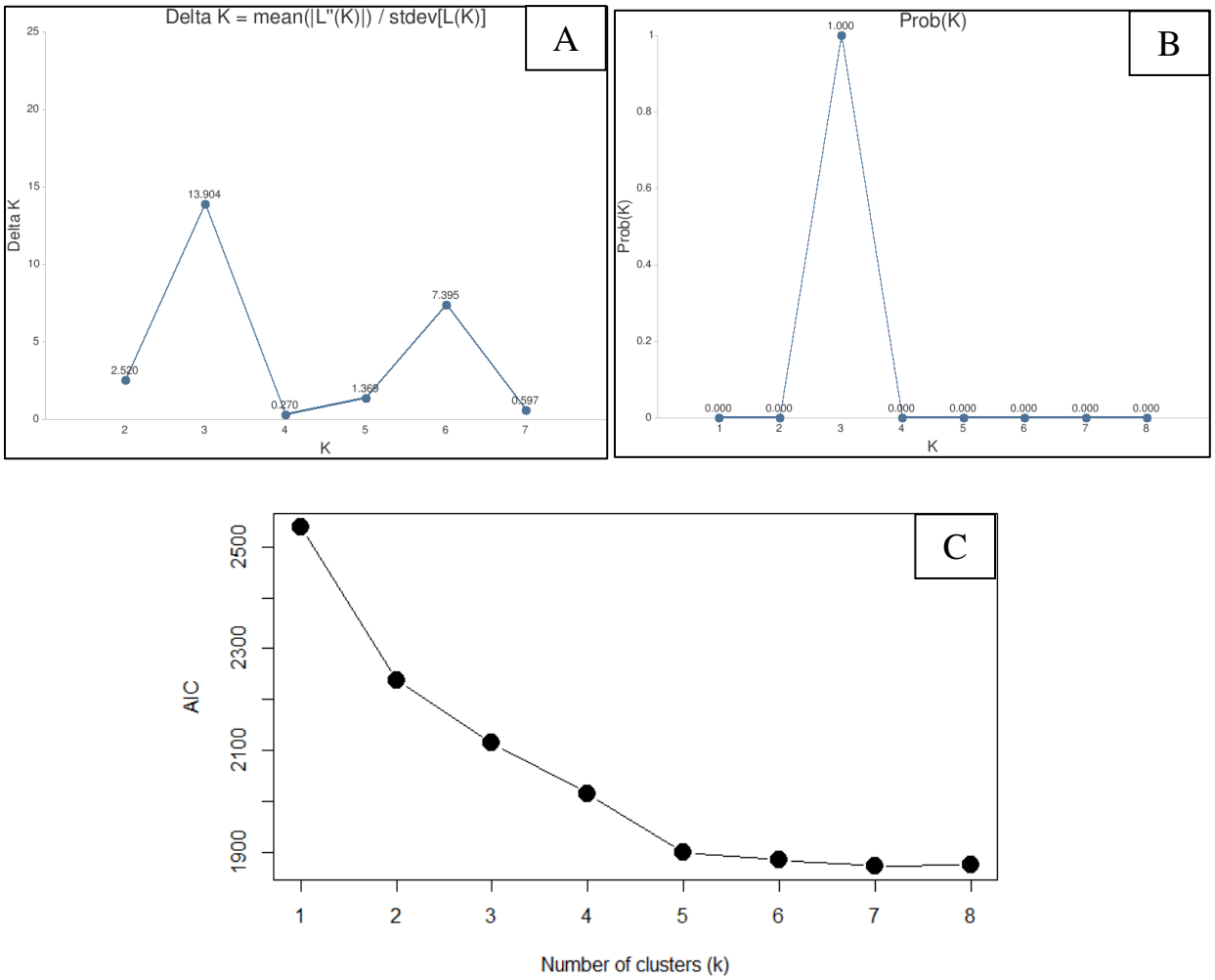

Supplementary Figure 2.1. Optimal clustering of study population ranged between 3 and 5. (A & B) Optimal K output graph generated by CLUMPAK from STRUCTURE results according to delta K and Prob(K) support. Both approaches indicate that K = 3 is the most supported model for explaining genetic structure among *Microsporum canis* isolates. (A) The optimal K was 3 using delta K = mean(lL"(K)l)/stdev[L(K)]. (B) The K for which Pr(K=k) is the highest was 3. (C) Optimal k output graph generated by snapclust.choose.k program. AIC support increased with successive value of k up until 5, after which AIC support did not increase, suggesting that k = 5 is the most supported model.

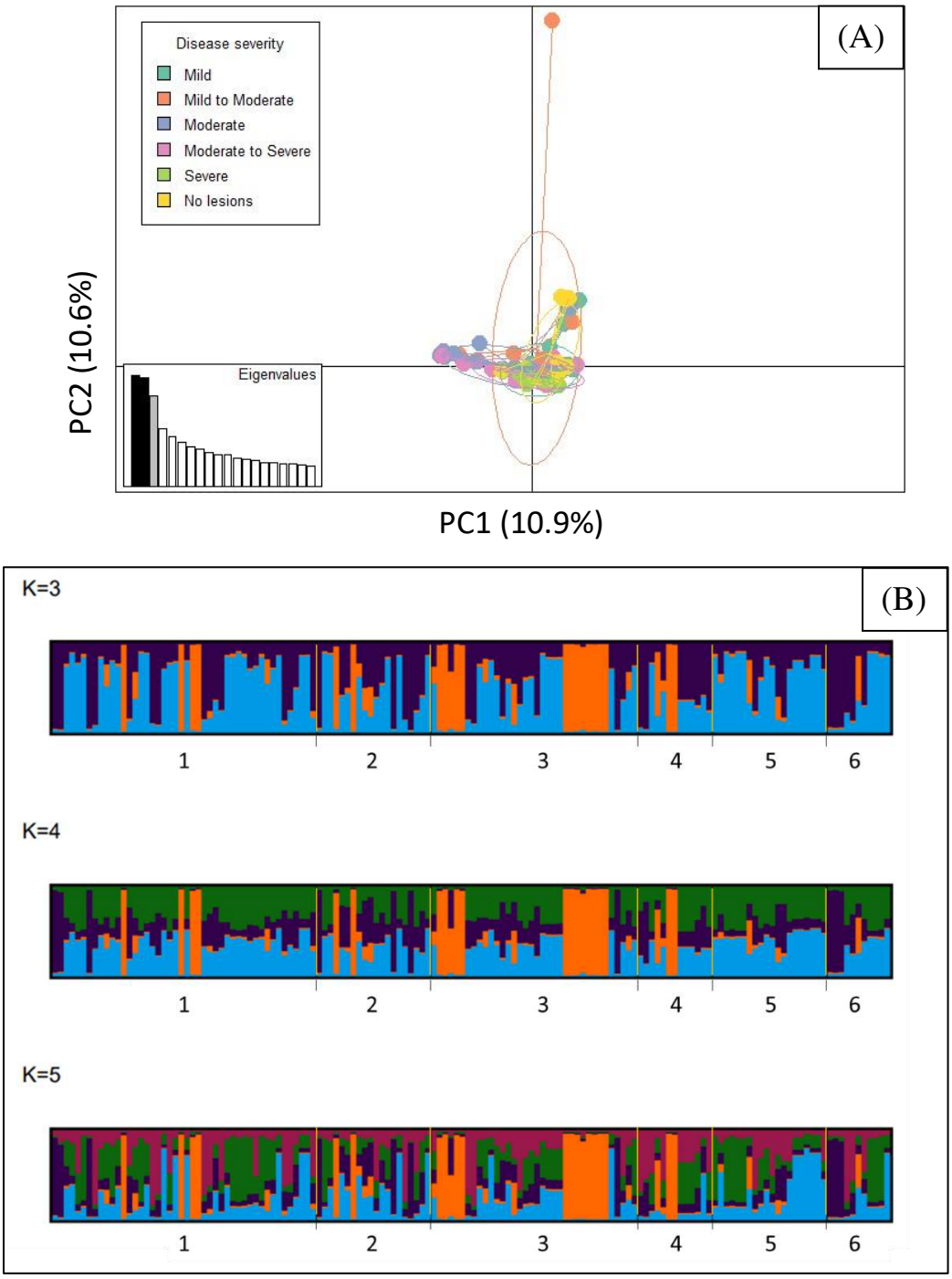

Supplementary Figure 2.2. Genetic clustering is not observed among categories of disease severity. (A) PCA plot for microsatellite regions using disease severity collected from the clinical survey. The outlier point for group mild to moderate was a sample from MA. (B) Structure plots with K values 3-5. The amount of vertical color for each sample corresponds with the percentage of belonging to that color cluster. Admixture increased for plots using K=4 and K=5. Disease severity groups included in study were mild (1), mild to moderate (2), moderate (3), moderate to severe (4), severe (5), and no lesions (6). Locations included in study were California; New Mexico; Boulder County, CO; Larimer County, CO; and Massachusetts.

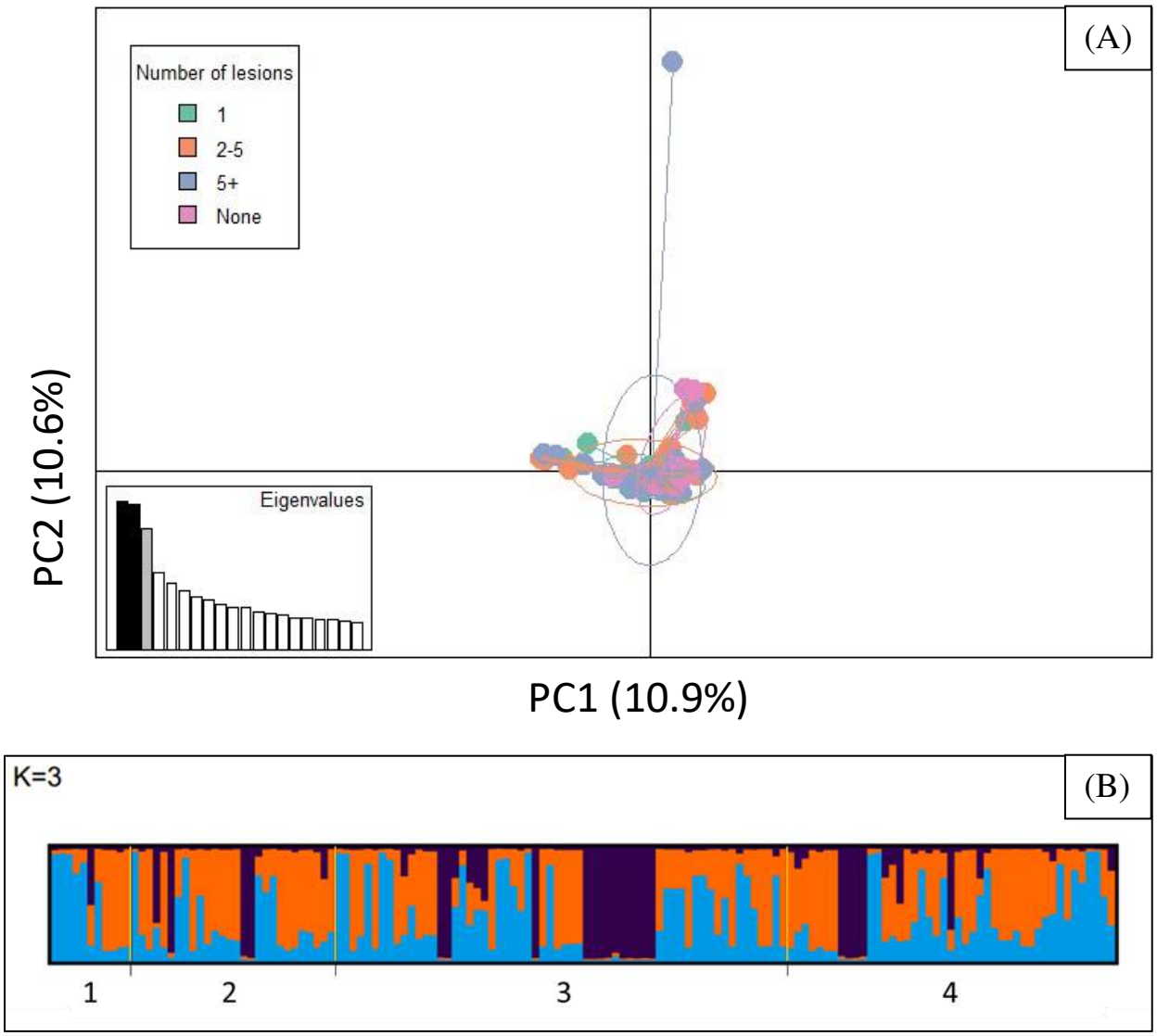

Supplementary Figure 2.3. Genetic clustering is not observed among categories of number of lesions. (A) PCA plot for microsatellite regions using the number of lesions (if present) collected from the clinical survey. The outlier point for 5+ lesions group was a sample from MA. (B) STRUCTURE plot (k=3) grouping samples based on number of lesions where 1 = none, 2 = 1 lesion, 3 = 2-5 lesions, and 4 = 5+ lesions. Locations included in study were California; New Mexico; Boulder County, CO; Larimer County, CO; and Massachusetts.

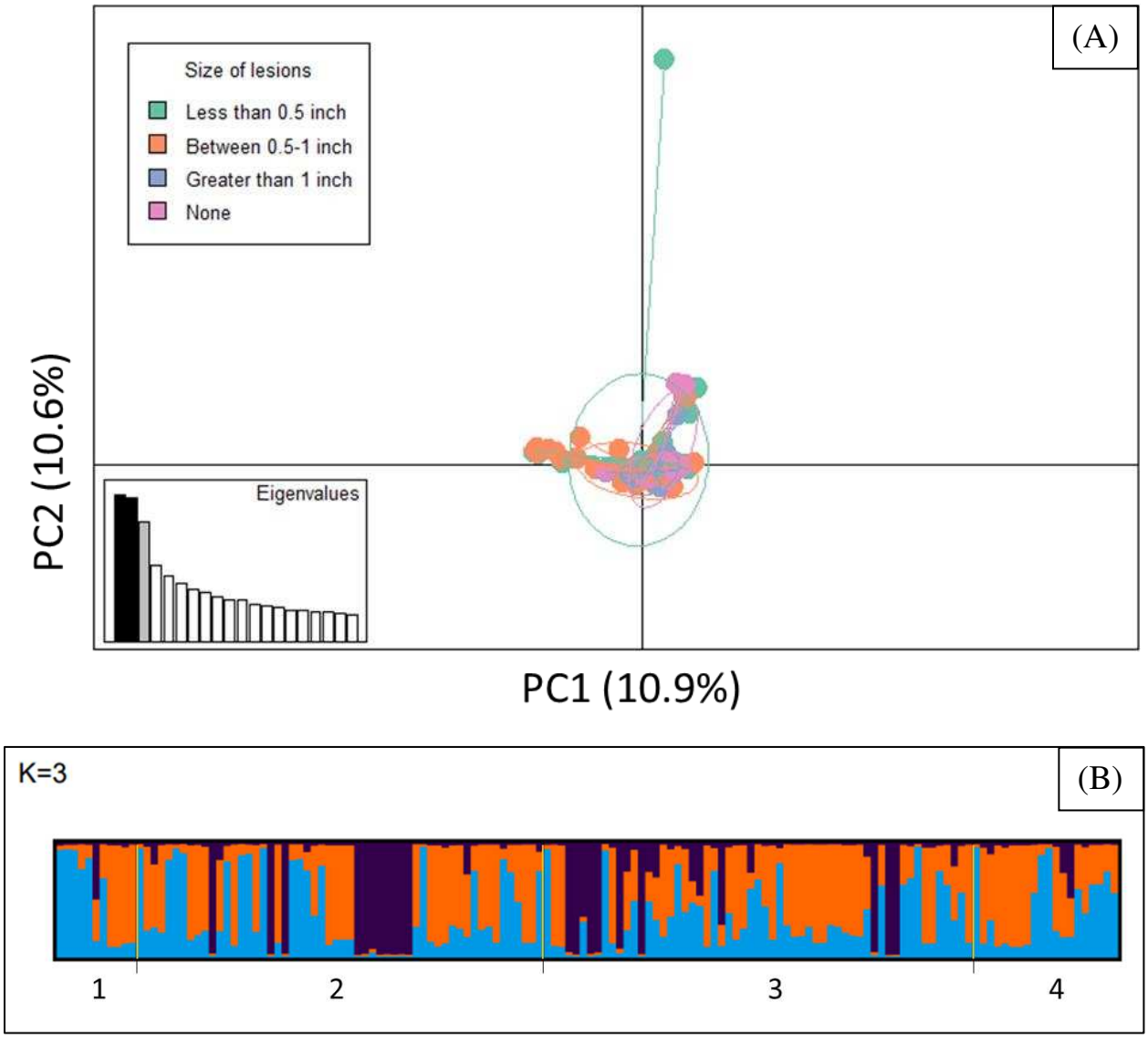

Supplementary Figure 2.4. Genetic clustering is not observed among categories of size of lesions. (A) PCA plot for microsatellite regions using the size of the lesions (if present) collected from the clinical survey. The outlier point for less than 0.5 inch group was a sample from MA. (B) STRUCTURE plot (k=3) grouping samples based on size of lesions where 1 = none, 2 = less than 0.5 inch, 3 = between 0.5 inch and 1 inch, and 4 = greater than 1 inch. Locations included in study were California; New Mexico; Boulder County, CO; Larimer County, CO; and Massachusetts.

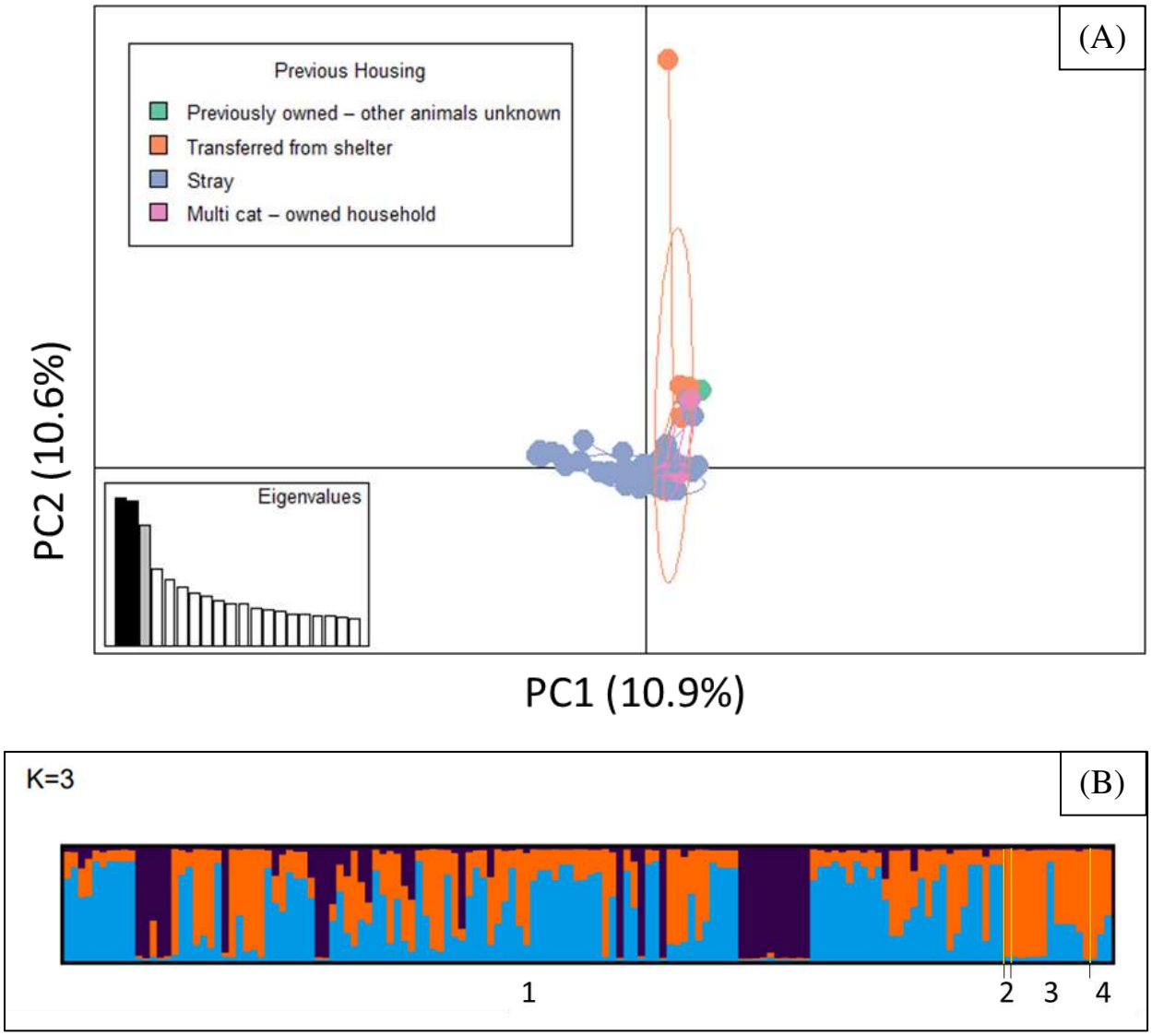

Supplementary Figure 2.5. Genetic clustering is not observed among categories of previous housing environment. (A) PCA plot for microsatellite regions using the previous housing environment collected from the clinical survey. The outlier point for transferred from shelter group was a sample from MA. (B) STRUCTURE plot (k=3) grouping samples based on previous housing environment where 1 = stray, 2 = previously owned – other animals unknown, 3 = transferred from shelter, and 4 = multi cat – owned household. Locations included in study were California; New Mexico; Boulder County, CO; Larimer County, CO; and Massachusetts.

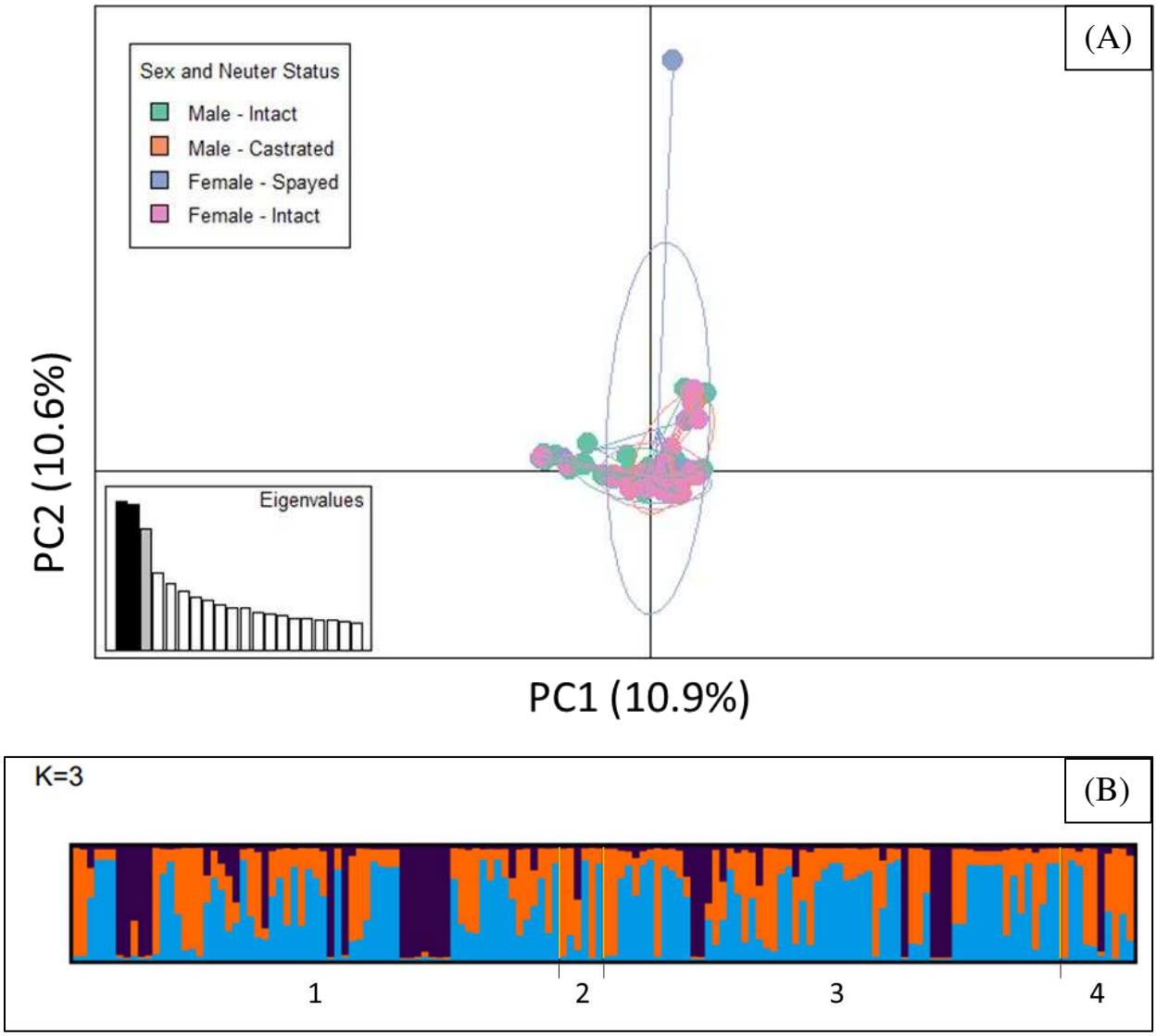

Supplementary Figure 2.6. Genetic clustering is not observed among categories of sex and neuter status. (A) PCA plot for microsatellite regions using sex and neuter status collected from the clinical survey. The outlier point for female spayed group was a sample from MA. (B) STRUCTURE plot (k=3) grouping samples based on neuter status and sex where 1 = male intact, 2 = male castrated, 3 = female intact, 4 = female spayed. Locations included in study were California; New Mexico; Boulder County, CO; Larimer County, CO; and Massachusetts.

Supplementary Table 2.1. Survey provided to shelters and clinics for suspected dermatophytosis patients.

#	Questions	Answer options
1	Please enter the name of the person collecting the sample	Free response
2	Please select your clinic	Free response
3	Patient ID and name	Free response
4	Cat research ID	Free response
5	Date presented for ringworm evaluation	Free response
6	Cat's age	• Kitten – less than 1 year old • Adult – over 1 year old
7	Cat's sex and neuter status	• Female – spayed • Female – intact • Female – unknown • Male – castrated • Male intact
8	Cat's breed	Free response
9	Cat's previous housing environment	• Stray • Single cat – owned household • Multi cat – owned household • Previously owned – other animals unknown • Transferred from shelter
10	Cat's current housing environment	• Shelter/rescue – single cat kennel • Shelter/rescue – multiple cat kennel • Client owned – single cat household • Client owned – multiple cat household
11	Is this cat currently receiving any medications (excluding vaccines)?	• Yes – topical parasite preventatives or dewormer • Yes – oral parasite preventatives or dewormer • Yes – other • No
12	Any other concurrent medical conditions?	Free response
13a	Have diagnostics for ringworm been performed? (select all that apply)	• Wood's lamp • Fungal culture • IDEXX PCR • Hair observed under microscope • Other • None
13b	If diagnostics have been performed, what were the results?	Free response
14a	Has anti-fungal treatment been performed prior to sample collection?	• Yes • No
14b	If yes, what treatment and for how long?	Free response

15	How many lesions are present?	• 1 • 2-5 • 5+ • None – no lesions present
16	What is the average size of the lesions?	• Less than 0.5 inch (smaller than a dime) • Between 0.5 inch and 1 inch (size of a penny) • Greater than 1 inch (larger than a penny) • N/A – no lesions present
17	Lesion distribution (select all that apply)	• Head • Neck • Abdomen • Back • Tail including base of tail • Legs including paws • N/A – no lesions present
18	Lesion types (select all that apply)	• Alopecia • Scales/crusts • Reddened/erythematous • Papules/pustules • Miliary dermatitis • N/A – no lesions present
19	Rate the severity of the lesions	• Mild – lesions are small and confined to focal area • Mild to moderate • Moderate – lesions are found in multiple areas, but is not widespread • Moderate to severe • Severe – lesions are large and found all over the body • N/A – no lesions present
20	Please upload pictures of lesions/alopecia, Wood's lamp or trichogram	Free response
21	Any additional comments?	Free response

Questions with multiple choice answers have all possible answers shown while questions that could have answers written in are listed as free response. N/A = not applicable.

Supplementary Table 2.2. Primers utilized for characterizing SUB3 and SSU1 genes.

Target	Pair	Orientation	Primer sequence 5' to 3'	Reference
SSU1	1	Forward	CAACCCAAGGATCCCAGGTC	This paper
		Reverse	CGGGTGATCGAGATGGTGAG	
SSU1	2	Forward	GAGCTTCAGGTCACAGCCAT	This paper
		Reverse	GCATAGAATGGGCGGGATGA	
SSU1	3	Forward	CTCACCATCTCGATCACCCG	This paper
		Reverse	CGGATCCCCACATCACGTAG	
SSU1	4	Forward	TACCTCTTCGCTCGAGACCA	This paper
		Reverse	ACTCCTTGCCCATCTGTGTG	
SSU1	5	Forward	CCCATTGCCGGTGAGATCTT	This paper
		Reverse	GCGTTTATCGTCGAAGGGGA	
SSU1	6	Forward	CACACAGATGGGCAAGGAGT	This paper
		Reverse	CGGGGTTTTCCTCTGAAGCT	
SUB3	1	Forward	GTTCGAAAAGACGCGCTTTCTTTCACAACCGT	[Descamps *et al.* 2002]
		Reverse	GTAGCCCTATCTTCCACTTCCGTTGTA	

Supplementary Table 2.3. Clinical presentation data for *Microsporum canis* positive cats from CA, NM, CO (Boulder, Larimer), and MA.

Clinical Parameters	**CA (n=109)**	**NM (n=31)**	**BC (n=6)**	**LC (n=4)**	**MA (n=4)**
Age	Kitten (99 %)	Kitten (97 %)	Kitten (100 %)	Kitten (100 %)	Kitten (25 %)
Sex	Female (49 %)	Female (45 %)	Female (50 %)	Female (50 %)	Female (50 %)
Neuter status	Intact (91 %)	Intact (94 %)	Intact (66.7 %)	Intact (100 %)	Intact (25 %)
Breed	DSH (92.6 %) DMH (4.6 %) DLH (2.8 %)	DSH (84 %) DMH (16 %)	DSH (83.3 %) DMH (16.6 %)	DSH (100 %)	DSH (25 %) DLH (25 %) Persian (25 %) Exotic shorthair (25 %)
Previous housing environment 1. Stray 2. Single cat – owned household 3. Multi cat – owned household 4. Previously owned – other animals unknown 5. Transferred from shelter	1 (98 %) 4 (1 %) 5 (1 %)	1 (100 %)	4 (16.6 %) 5 (83.3 %)	5 (100 %)	3 (75 %) 5 (25 %)
Current housing environment 1. Shelter/rescue – single cat kennel 2. Shelter/rescue – multiple cat kennel 3. Client owned – single cat household 4. Client owned – multiple cay household	1 (30 %) 2 (69 %) 3 (1 %)	1 (19 %) 2 (81 %)	1 (16.6 %) 2 (83.3 %)	2 (100 %)	4 (100 %)
Current medications* 1. Yes – topical parasite preventatives or dewormer 2. Yes – oral parasite preventatives or dewormer	1 (27.5 %) 2 (18.3 %) 3 (2 %) 4 (71.5 %)	2 (100 %)	2 (100 %)	4 (100 %)	1 (50 %) 3 (25 %) 4 (25 %)

3. Yes – other 4. No					
Concurrent medical conditions*	URI (24 %) ectoparasites (13 %) Diarrhea (1 %) Otitis media (1 %) Degloved chin (1 %) Underweight (1 %) None (67 %)	URI (6.5 %) Ectoparasites (3.2 %) None (90 %)	None (100 %)	None (100 %)	IBD (25 %) superficial pyoderma (25 %) None (75 %)
Diagnostics performed* 1. Wood's lamp 2. Fungal culture 3. IDEXX PCR 4. Hair observed under microscope 5. Other 6. None	1 (99 %) 6 (1 %)	1 (93.5 %) 5 (6.5 %)	1 (100 %) 2 (100 %)	1 (100 %) 2 (100 %)	1 (100 %) 3 (100 %) 4 (50 %) 5 (25 %)
If diagnostics have been performed, what were the results?	Wood's lamp positive (88 %)	Wood's lamp positive (92.9 %)	Wood's lamp positive (50 %)	Wood's lamp positive (100 %)	Wood's lamp positive (75 %)
Number of lesions 1. 1 2. 2-5 3. 5+ 4. None – no lesions present	1 (16.5 %) 2 (42.2 %) 3 (36.7 %) 4 (4.6 %)	1 (29 %) 2 (51.6 %) 3 (6.5 %) 4 (12.9 %)	1 (16.6 %) 2 (33.3 %) 4 (50 %)	2 (75 %) 3 (25 %)	1 (25 %) 3 (75 %)
Size of lesions 1. Less than 0.5 inch (smaller than a dime) 2. Between 0.5 inch and 1 inch (size of a penny) 3. Greater than 1 inch (larger than a penny) 4. N/A – no lesions present	1 (36.7 %) 2 (44 %) 3 (14.7 %) 4 (4.6 %)	1 (64.5 %) 2 (22.6 %) 4 (12.9 %)	1 (16.6 %) 2 (16.6 %) 3 (16.6 %) 4 (50 %)	2 (50 %) 3 (50 %)	1 (25 %) 2 (25 %) 3 (50 %)
Lesion distribution* 1. Head 2. Neck	1 (88 %) 2 (33 %) 3 (29 %)	1 (64.5 %) 2 (12.9 %) 3 (29 %)	1 (16.6 %)	1 (100 %) 2 (50 %)	1 (75 %) 2 (75 %) 3 (75 %)

3. Abdomen 4. Back 5. Tail including base of tail 6. Legs including paws 7. N/A – no lesions present	4 (24 %) 5 (25 %) 6 (58 %) 7 (4.6 %)	4 (6.5 %) 5 (3.2 %) 6 (32.2 %) 7 (12.9 %)	2 (16.6 %) 3 (33.3 %) 7 (50 %)	4 (25 %) 6 (100 %)	4 (50 %)
Lesion types* 1. Alopecia 2. Scales/crusts 3. Reddened/erythematous 4. Papules/pustules 5. Miliary dermatitis 6. N/A – no lesions present	1 (94.5 %) 2 (64 %) 3 (2.8 %) 5 (1.8 %) 6 (4.6 %)	1 (74 %) 2 (55 %) 3 (9.7 %) 6(12.9 %)	1 (50 %) 3 (33.3 %) 6 (50 %)	1 (100 %) 2 (100 %)	1 (100 %) 2 (100 %) 3 (25 %)
Disease severity 1. Mild – lesions are small and confined to focal area 2. Mild to moderate 3. Moderate – lesions are found in multiple areas, but is not widespread 4. Moderate to severe 5. Severe – lesions are large and found all over the body 6. N/A – no lesions present	1 (24.8 %) 2 (13.8 %) 3 (31.2 %) 4 (7.3 %) 5 (18.3 %) 6 (4.6 %)	1 (61.3 %) 2 (9.7 %) 3 (12.9 %) 4 (3.2 %) 6 (12.9 %)	1 (33.3 %) 2 (16.6 %) 6 (50 %)	4 (100 %)	1 (25 %) 2 (25 %) 3 (25 %) 4 (25 %)

No clinical data was collected for Weld County, CO. CA = California, NM = New Mexico, BC = Boulder County CO, LC = Larimer County CO, MA = Massachusetts, DSH = domestic shorthair, DMH = domestic medium hair, DLH = domestic long hair, N/A = not applicable, URI = upper respiratory infection, IBD = inflammatory bowel disease. * = Percentages are greater than 100 as patients can have more than one answer.

Supplementary Table 2.4. Allele sizes for microsatellite regions one to eight (MS1, MS2, MS3, MS4, MS5, MS6, MS7, MS8) for *Microsporum canis* samples.

Sample ID	MS1 (bp)	MS2 (bp)	MS3 (bp)	MS4 (bp)	MS5 (bp)	MS6 (bp)	MS7 (bp)	MS8 (bp)	Genotype	Mating gene type
BC1	117	97	116	157	102	109	127	116	DF	MAT1-1
BC2	117	97	116	155	102	109	127	116	DD	MAT1-1
BC3	117	97	116	159	102	111	125	116	DI	MAT1-1
BC4	117	97	116	155	106	109	127	116	DE	MAT1-1
BC5	117	97	116	155	102	109	127	116	DD	MAT1-1
BC6	117	97	116	155	100	109	127	116	DC	MAT1-1
CA1	113	97	114	155	102	109	125	116	O	MAT1-1
CA2	115	97	114	155	106	109	125	116	BC	MAT1-1
CA3	115	99	114	155	102	109	125	116	CS	MAT1-1
CA4	115	99	114	157	102	109	125	116	CV	MAT1-1
CA5	115	97	114	155	100	109	125	116	AT	MAT1-1
CA6	115	97	114	155	106	109	125	116	BC	MAT1-1
CA7	115	97	114	155	100	109	125	116	AT	MAT1-1
CA8	115	97	114	155	100	109	125	116	AT	MAT1-1
CA9	115	97	114	157	100	109	125	116	BK	MAT1-1
CA10	115	97	114	155	100	109	125	116	AT	MAT1-1
CA11	NA	101	NA	155	106	109	125	112	DS	MAT1-1
CA12	105	101	NA	155	96	109	125	112	F	MAT1-1
CA13	NA	101	NA	155	104	105	125	112	DR	MAT1-1
CA14	105	99	NA	155	106	109	125	112	E	MAT1-1
CA15	NA	101	NA	153	106	109	125	112	DQ	MAT1-1
CA16	115	97	114	161	102	113	123	116	CI	MAT1-1
CA17	115	97	114	155	100	107	125	116	AS	MAT1-1
CA18	115	97	114	155	106	109	125	116	BC	MAT1-1
CA19	115	97	114	159	100	109	123	116	BY	MAT1-1
CA20	115	97	114	NA	100	107	123	116	CK	MAT1-1
CA21	115	97	114	159	106	109	123	116	CC	MAT1-1
CA22	115	97	114	155	102	109	125	116	AW	MAT1-1
CA23	113	99	NA	155	98	109	125	112	U	MAT1-1
CA24	117	97	116	139	102	109	125	116	DA	MAT1-1
CA25	113	97	114	157	102	105	125	116	R	MAT1-1
CA26	115	97	114	159	102	107	123	116	CA	MAT1-1
CA27	115	97	114	161	102	107	123	NA	CF	MAT1-1
CA28	113	95	114	159	102	107	123	116	J	MAT1-1
CA29	115	97	114	155	102	NA	125	116	AZ	MAT1-1
CA30	115	97	114	155	98	NA	125	116	AR	MAT1-1
CA31	113	97	114	153	102	109	125	116	M	MAT1-1

CA32	115	97	114	NA	100	109	NA	116	CL	MAT1-1
CA33	113	97	114	155	102	107	125	116	N	MAT1-1
CA34	113	99	114	155	102	109	125	116	T	MAT1-1
CA35	113	97	114	155	102	109	125	116	O	MAT1-1
CA36	113	97	114	155	102	109	125	116	O	MAT1-1
CA37	115	97	114	155	98	109	125	116	AN	MAT1-1
CA38	NA	99	NA	153	96	109	125	112	DJ	MAT1-1
CA39	NA	99	NA	153	98	109	125	112	DK	MAT1-1
CA40	115	97	114	157	98	109	125	112	BE	MAT1-1
CA41	115	97	114	157	98	111	125	112	BG	MAT1-1
CA42	115	97	NA	157	104	NA	NA	112	CO	MAT1-1
CA43	115	97	114	157	98	109	125	116	BF	MAT1-1
CA44	115	97	114	157	104	109	125	112	BT	MAT1-1
CA45	115	97	114	155	104	NA	123	116	BB	MAT1-1
CA46	115	97	116	155	106	NA	123	116	CN	MAT1-1
CA47	115	97	114	155	98	111	125	116	AO	MAT1-1
CA48	115	97	114	157	98	NA	125	112	BH	MAT1-1
CA49	115	97	114	159	100	NA	125	116	BZ	MAT1-1
CA50	115	97	114	157	102	NA	125	116	BR	MAT1-1
CA51	NA	99	NA	153	98	NA	125	112	DL	MAT1-1
CA52	NA	99	NA	153	98	109	125	112	DK	MAT1-1
CA53	115	97	114	153	100	109	125	116	AK	MAT1-1
CA54	115	97	114	153	102	113	125	116	AM	MAT1-1
CA55	115	97	114	153	102	109	125	116	AL	MAT1-1
CA56	115	97	114	103	100	107	125	116	W	MAT1-1
CA57	115	97	114	157	96	105	125	112	BD	MAT1-1
CA58	115	97	114	155	100	109	125	116	AT	MAT1-1
CA59	115	97	114	157	102	NA	125	116	BR	MAT1-1
CA60	115	97	114	159	98	NA	125	112	BW	MAT1-1
CA61	115	97	114	155	100	109	125	116	AT	MAT1-1
CA62	115	97	114	157	102	NA	125	116	BR	MAT1-1
CA63	115	97	114	103	100	NA	125	116	X	MAT1-1
CA64	115	97	114	157	100	109	125	116	BK	MAT1-1
CA65	115	97	114	157	100	109	123	116	BI	MAT1-1
CA66	115	97	114	161	102	107	123	116	CE	MAT1-1
CA67	115	97	114	159	100	107	121	NA	BX	MAT1-1
CA68	115	97	114	155	100	107	125	116	AS	MAT1-1
CA69	115	99	114	103	102	107	125	116	CP	MAT1-1
CA70	115	97	114	155	98	NA	125	112	AQ	MAT1-1
CA71	115	97	114	155	102	111	125	116	AX	MAT1-1
CA72	115	97	114	155	102	NA	125	116	AZ	MAT1-1

CA73	115	97	114	155	102	107	125	116	AV	MAT1-1
CA74	115	97	114	155	98	NA	121	NA	AP	MAT1-1
CA75	115	97	114	103	102	107	125	116	Y	MAT1-1
CA76	115	97	114	155	102	105	125	116	AU	MAT1-1
CA77	115	97	114	155	102	NA	125	116	AZ	MAT1-1
CA78	115	97	114	155	102	NA	125	116	AZ	MAT1-1
CA79	115	97	114	157	102	NA	123	116	BQ	MAT1-1
CA80	111	99	114	157	102	107	125	116	I	MAT1-1
CA81	115	97	114	157	102	107	125	116	BM	MAT1-1
CA82	115	97	114	157	102	NA	125	116	BR	MAT1-1
CA83	115	97	114	157	102	NA	125	116	BR	MAT1-1
CA84	115	97	114	157	102	115	125	116	BP	MAT1-1
CA85	115	99	114	157	102	107	125	116	CU	MAT1-1
CA86	115	97	114	157	102	109	125	116	BO	MAT1-1
CA87	115	97	114	157	102	109	125	116	BO	MAT1-1
CA88	115	97	114	157	102	107	125	116	BN	MAT1-1
CA89	115	97	114	157	102	115	125	116	BP	MAT1-1
CA90	115	97	114	155	100	107	125	116	AS	MAT1-1
CA91	115	97	114	157	102	NA	125	NA	BS	MAT1-1
CA92	117	97	116	157	102	113	125	116	DH	MAT1-1
CA93	115	97	114	155	102	111	125	116	AX	MAT1-1
CA94	NA	99	NA	155	98	109	125	112	DM	MAT1-1
CA95	115	97	114	157	102	NA	125	116	BR	MAT1-1
CA96	115	99	114	155	100	107	125	116	CR	MAT1-1
CA97	NA	99	NA	155	106	109	125	112	DO	MAT1-1
CA98	115	97	114	157	102	109	125	116	BO	MAT1-1
CA99	115	97	114	155	102	115	125	116	AY	MAT1-1
CA100	115	97	114	155	100	109	125	116	AT	MAT1-1
CA101	NA	99	NA	155	98	109	125	112	DM	MAT1-1
CA102	115	97	114	161	102	109	123	116	CG	MAT1-1
CA103	115	97	114	161	100	NA	123	116	CD	MAT1-1
CA104	115	99	114	155	102	NA	123	116	CT	MAT1-1
CA105	113	97	114	NA	100	NA	125	116	S	MAT1-1
CA106	115	97	114	157	106	105	123	116	BU	MAT1-1
CA107	115	97	114	127	102	109	125	116	AF	MAT1-1
CA108	115	97	114	155	102	109	125	116	AW	MAT1-1
CA109	115	97	114	155	102	NA	125	116	AZ	MAT1-1
CA110	115	97	114	155	102	NA	125	116	AZ	MAT1-1
CA111	115	97	114	155	102	NA	125	116	AZ	MAT1-1
CA112	105	99	NA	155	98	111	125	112	C	MAT1-1
CA113	105	101	NA	155	98	111	125	112	G	MAT1-1

CA114	105	99	NA	155	98	NA	125	112	D	MAT1-1
CA115	NA	99	NA	155	98	NA	125	112	DN	MAT1-1
CA116	105	99	NA	155	98	107	125	112	B	MAT1-1
CA117	105	99	NA	155	98	NA	125	112	D	MAT1-1
CA118	NA	99	NA	155	98	109	125	112	DM	MAT1-1
CA119	105	99	NA	155	98	NA	125	112	D	MAT1-1
CA120	NA	101	NA	153	98	111	125	112	DP	MAT1-1
CA121	105	99	NA	155	98	NA	125	112	D	MAT1-1
CA122	115	97	114	157	102	115	125	116	BP	MAT1-1
LC1	115	97	114	119	100	111	125	116	AD	MAT1-1
LC2	115	97	114	119	100	111	125	116	AD	MAT1-1
LC3	115	97	114	119	100	111	125	116	AD	MAT1-1
LC4	113	97	114	119	106	111	125	116	L	MAT1-1
MA1	117	97	116	141	102	105	125	116	DB	MAT1-1
MA2	115	97	116	141	102	109	127	116	CM	MAT1-1
MA3	109	97	110	121	104	109	123	118	H	MAT1-1
MA4	115	97	114	157	100	111	123	116	BL	MAT1-1
MA5	113	97	114	157	102	105	125	116	R	MAT1-1
NJ1	115	97	114	121	102	109	123	116	AE	MAT1-1
NM1	115	97	114	157	106	109	125	116	BV	MAT1-1
NM2	115	97	114	155	106	109	125	116	BC	MAT1-1
NM3	115	97	114	155	100	109	125	116	AT	MAT1-1
NM4	115	97	114	155	106	109	125	116	BC	MAT1-1
NM5	115	97	114	137	106	109	125	116	AJ	MAT1-1
NM6	115	97	114	155	100	109	125	116	AT	MAT1-1
NM7	115	97	114	155	106	109	125	116	BC	MAT1-1
NM8	115	97	114	155	102	107	125	116	AV	MAT1-1
NM9	115	97	114	155	106	109	125	116	BC	MAT1-1
NM10	105	97	114	155	100	109	125	116	A	MAT1-1
NM11	115	97	114	161	106	111	125	116	CJ	MAT1-1
NM12	115	97	114	161	106	111	125	116	CJ	MAT1-1
NM13	115	97	114	161	102	109	125	116	CH	MAT1-1
NM14	115	101	114	155	102	109	125	116	CY	MAT1-1
NM15	115	97	114	137	100	109	125	116	AG	MAT1-1
NM16	115	97	114	137	104	109	125	116	AI	MAT1-1
NM17	115	97	114	137	102	109	125	116	AH	MAT1-1
NM18	115	97	114	157	102	109	125	116	BO	MAT1-1
NM19	115	101	114	159	102	107	125	116	CZ	MAT1-1
NM20	115	97	114	159	102	NA	125	116	CB	MAT1-1
NM21	115	97	114	157	100	109	125	114	BJ	MAT1-1
NM22	115	97	114	157	102	109	125	116	BO	MAT1-1

NM23	115	97	114	157	102	109	125	116	BO	MAT1-1
NM24	115	99	114	159	102	109	125	116	CW	MAT1-1
NM25	115	97	114	157	102	109	125	116	BO	MAT1-1
NM26	115	97	114	157	102	109	125	116	BO	MAT1-1
NM27	115	99	116	157	102	111	NA	116	CX	MAT1-1
NM28	115	97	114	157	102	109	125	116	BO	MAT1-1
NM29	115	97	114	155	102	109	125	116	AW	MAT1-1
NM30	115	97	114	155	98	109	125	116	AN	MAT1-1
NM31	115	99	114	155	102	109	125	116	CS	MAT1-1
NM32	113	97	114	105	104	NA	123	116	K	MAT1-1
NM33	113	97	114	157	100	NA	NA	116	Q	MAT1-1
NM34	115	95	114	155	100	111	123	116	V	MAT1-1
NM35	115	97	114	155	104	109	125	116	BA	MAT1-1
NM36	113	97	114	157	98	109	123	116	P	MAT1-1
WC1	117	97	116	157	102	111	125	116	DG	MAT1-1
WC2	115	97	114	105	102	109	125	116	AA	MAT1-1
WC3	115	97	114	105	102	109	125	116	AA	MAT1-1
WC4	115	97	114	105	102	107	125	116	Z	MAT1-1
WC5	115	99	114	103	102	109	125	116	CQ	MAT1-1
WC6	115	97	114	105	102	NA	125	116	AB	MAT1-1
CBS113480	115	97	114	107	104	109	117	116	AC	MAT1-1

Of the clinical samples, 122 unique genotypes were observed with genotypes AT and BO being the most common (n=9 for each genotype). Samples were from Boulder County, CO (BC); California (CA); Larimer County, CO (LC); Massachusetts (MA); New Jersey (NJ); New Mexico (NM); and Weld County, CO (WC). CBS113480 isolate was included as a reference strain. NA = missing genotype.

Supplementary Table 2.5. Clinic location and disease severity were significantly associated with genetic distance.

Clinical parameter	Degrees of Freedom	Sum of Squares	F	P-value
Clinic Location	4	3.0954	4.3127	0.001*
Sex/Intact Status	3	0.6237	1.1586	0.253
Size of Lesions	3	0.7176	1.3332	0.141
Number of Lesions	1	0.1633	0.9099	0.463
Disease Severity	1	0.6206	3.4587	0.004*
Previous Housing	3	0.7955	1.4778	0.139

Analysis of variance of the distance-based redundancy analysis. * = P-values were considered significant if less than 0.05). Samples from California; Boulder County, CO; Larimer County, CO; Massachusetts; and New Mexico were included in this analysis.

Supplementary Table 2.6. Clinic location and disease severity were significantly associated with genetic distance.

Clinical parameter	Degrees of Freedom	Sum of Squares	F	P-value
Clinic Location	1	0.5337	2.998	0.012*
Sex/Intact Status	3	0.7643	1.431	0.127
Size of Lesions	3	0.5680	1.0634	0.348
Number of Lesions	1	0.2162	1.2143	0.234
Disease Severity	1	0.6009	3.3753	0.011*
Previous Housing	1	0.0774	0.4348	0.751

Analysis of variance of the distance-based redundancy analysis. * = P-values were considered significant if less than 0.05). Samples from California and New Mexico were included in this analysis as they had more than 10 individuals per clinic.

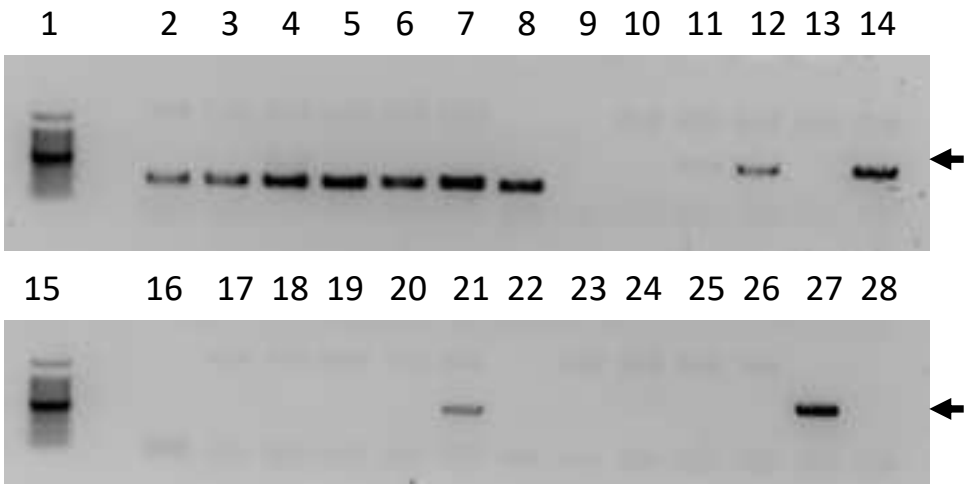

Supplementary Figure 3.1. *Arthroderma lilyanum* and *Arthroderma mcgillisianum* isolate mating loci are not detected using PCR protocols developed for other dermatophytes. Primers and protocol for ITS and mating loci PCR amplification are described in Methods. Lanes: (1, 15) molecular ladder; (2-9) ITS region (est. 280 bp): (2) Case 1, (3) Case 2, (4) Case 3, (5) Case 4, (6) clinical sample of *Trichophyton mentagrophytes*, (7) clinical sample of *Microsporum canis*, (8) American Type Culture Collection 44687 *Trichophyton mentagrophytes*, (9) water; (10-16) alpha-box amplification using primers designed for *Microsporum* spp. (est. 420 bp): (10) Case 1, (11) Case 2, (12) Case 3, (13) Case 4, (14) clinical sample of *Microsporum canis*, (16) water; (17-22) alpha-box amplification using primers designed for *Trichophyton* spp. (est. 432 bp): (17) Case 1, (18) Case 2, (19) Case 3, (20) Case 4, (21) clinical sample of *Trichophyton mentagrophyte*s, (22) water; (23-28) high motility-group amplification using primers designed for *Trichophyton* spp. (est. 860 bp): (23) Case 1, (24) Case 2, (25) Case 3, (26) Case 4, (27) American Type Culture Collection 44687 *Trichophyton mentagrophytes*, (28) water. Arrow = 500 bp. *M. canis* was initially co-cultured with *Arthroderma* spp. isolated from Cases 2 and 3 as described in the text. Amplicons in lanes 11 and 12 were sequenced and found to be identical to *M. canis* alpha-box and hence represent DNA from *M. canis*, not *Arthroderma* spp.

Supplementary Table 3.1. Strains of dermatophytes utilized for constructing phylogenetic trees. Westerdijk Fungal Biodiversity Centre (CBS), Belgian Co-ordinated Collections of Micro-organisms/Institute of Hygiene and Epidemiology Mycology (BCCM/IHEM), or Center for Forest Mycology Research strain number is placed before isolate name. Sequences are available from NCBI database.

Reference #	**Strain name**	**ITS**	**B-tubulin**
IHEM05259	*Arthroderma corniculatum*	MK298673	MK389920
IHEM23682	*Arthroderma cuniculi*	MK298917	MK390164
IHEM20025	*Arthroderma curreyi*	MK298859	MK390106
IHEM21959	*Arthroderma eboreum*	MK298902	MK390149
IHEM04127	*Arthroderma gloriae*	MK298623	MK389869
IHEM03703	*Arthroderma lenticulare*	MK298605	MK389851
IHEM04432	*Arthroderma multifudum*	MK298647	MK389893
IHEM26868	*Arthroderma onychocola*	MK299058	MK390305
IHEM05279	*Arthroderma quadrifidum*	MK298678	MK389925
IHEM03189	*Arthroderma quadrifidum*	MK298572	MK389818
IHEM04435	*Arthroderma quadrifidum*	MK298648	MK389894
CBS 134551	*Arthroderma redellii*	KM091307	LR136818
CBS 134554	*Arthroderma redellii*	KM091311	N/A
23863-03	*Arthroderma redellii*	KM091314	N/A
IHEM23660	*Arthroderma thuringiense*	MK298916	MK390163
IHEM03457	*Arthroderma tuberculatum*	MK298593	MK389839
IHEM03448	*Arthroderma uncicatum*	MK298588	MK389834
IHEM01214	*Epidermophyton floccosum*	MK298428	MK389674
IHEM01282	*Lophophyton gallinae*	MK298460	MK389706
IHEM02214	*Microsporum audouinii*	MK298490	MK389736
IHEM03214	*Microsporum canis*	MK298573	MK389819
IHEM04409	*Nannizzia corniculata*	MK298640	MK389886
IHEM13443	*Nannizzia duboisii*	MK298717	MK389964
IHEM04212	*Nannizzia fulva*	MK298627	MK389873
IHEM05300	*Nannizzia gypsea*	MK298680	MK389927
IHEM05305	*Nannizzia incurvata*	MK298684	MK389931
IHEM15848	*Nannizzia nana*	MK298782	MK390029
IHEM03450	*Nannizzia persicolor*	MK298590	MK389836
IHEM14795	*Nannizzia praecox*	MK298777	MK390024
IHEM03452	*Nannizzia racemosa*	MK298592	MK389838
IHEM01294	*Paraphyton cookei*	MK298464	MK389710
IHEM04417	*Paraphyton cookiellum*	MK298643	MK389889
IHEM24407	*Paraphyton mirabile*	MK298924	MK390171
IHEM03287	*Trichophyton benhamiae*	MK298576	MK389822
IHEM03293	*Trichophyton bullosum*	MK298580	MK389826

IHEM03775	*Trichophyton concentricum*	MK298613	MK389859
IHEM01285	*Trichophyton equineum/tonsurans*	MK298462	MK389708
IHEM19618	*Trichophyton erinacei*	MK298812	MK390059
IHEM13394	*Trichophyton eriotrephon*	MK298715	MK389962
IHEM00584	*Trichophyton interdigitale*	MK298408	MK389654
IHEM01045	*Trichophyton kuryangei*	MK298410	MK389656
IHEM02901	*Trichophyton mentagrophytes*	MK298563	MK389809
IHEM13570	*Trichophyton quinckeanum*	MK298730	MK389977
IHEM01739	*Trichophyton rubrum*	MK298484	MK389730
IHEM05232	*Trichophyton schoenleinii/quinckeanum*	MK298667	MK389914
IHEM03257	*Trichophyton simii*	MK298575	MK389821
IHEM01284	*Trichophyton soudanense*	MK298461	MK389707
IHEM19629	*Trichophyton sp.*	MK298822	MK390069
IHEM03773	*Trichophyton verrucosum*	MK298612	MK389858
IHEM03663	*Trichophyton violaceum*	MK298604	MK389850
IHEM01279	*Trichophyton yaoundei*	MK298459	MK389705
CBS269.89	*Guarromyces ceretanicus*	NR154051	MF898369

Supplementary Table 3.2. Strains of *A. quadrifidum* and *A. redellii* used from translation elongation factor 1-alpha (TEF1) comparisons. Sequences are available from NCBI's database.

Reference #	**Strain name**	**TEF1**
UAMH2941	*Arthroderma quadrifidum*	KM091296
CBS134551	*Arthroderma redellii*	KM091293

Supplementary Table 3.3. Accession numbers for Cases 1-4. Sequences are available from NCBI's database.

Case #	**Case 1**	**Case 2**	**Case 3**	**Case 4**
Reference #	CBS 148461	CSU CA018	CSU CA022	CBS 148462
Strain name	*Arthroderma lilyanum*	*Arthroderma lilyanum*	*Arthroderma mcgillisianum*	*Arthroderma mcgillisianum*
ITS	OK623475	OK597194	OK631735	OK631727
β-tubulin	OL342744	OL342745	OL342749	OL342748
TEF1	OL342746	OL342747	OL342751	OL342750

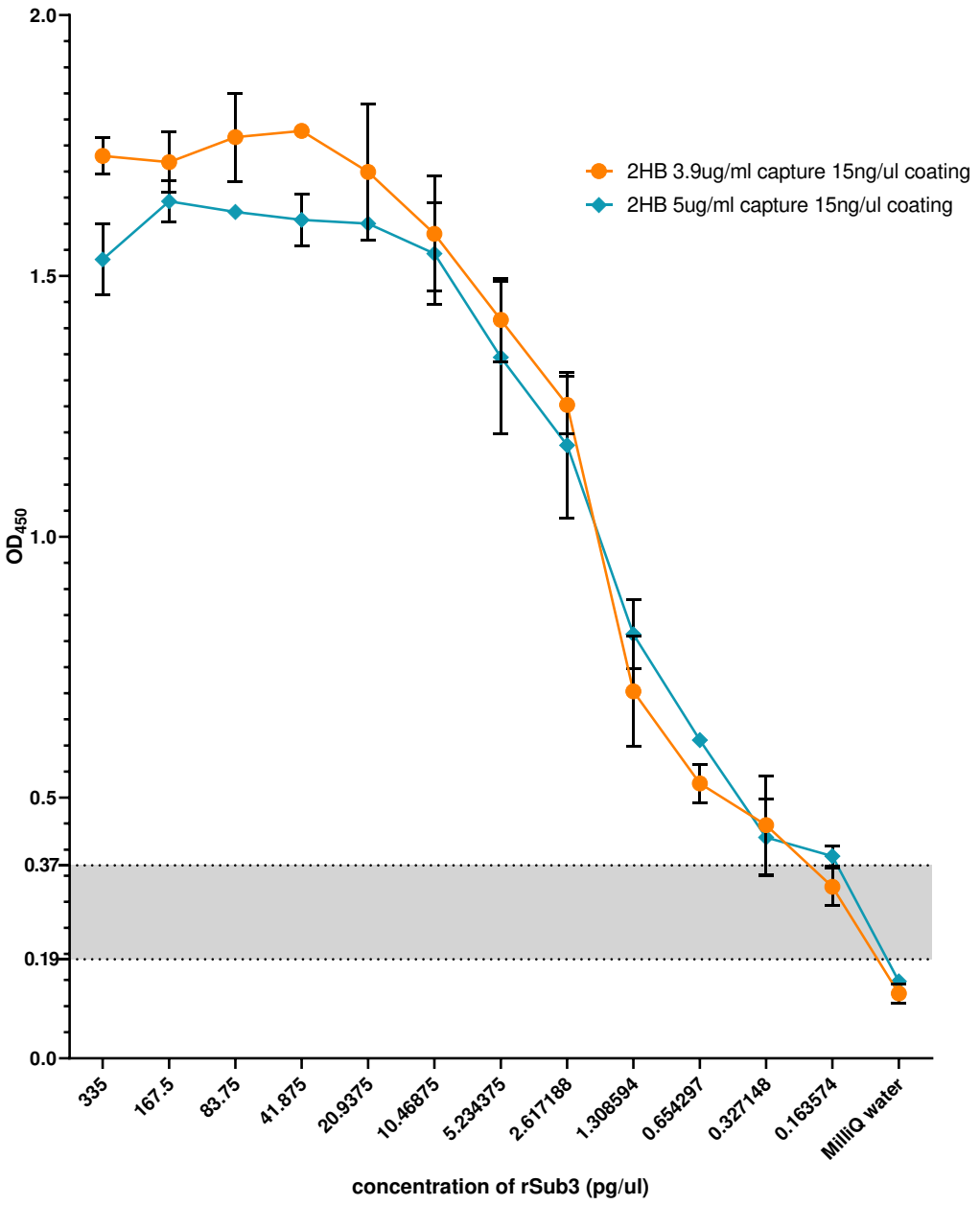

Supplemental Figure 4.1. No increase in assay sensitivity using higher concentration of detection antibody. 2HB plate was coated with 15 ng/µl of coating antibody Ab93 and either 3.9 µg/ml or 5 µg/ml of detection antibody was used. The indeterminate range was determined as 1-2x cutoff value. The indeterminate range was 0.19-0.37 (gray shaded region). Samples were run in triplicate (n=3) and standard deviation was less than 0.146 for all points.

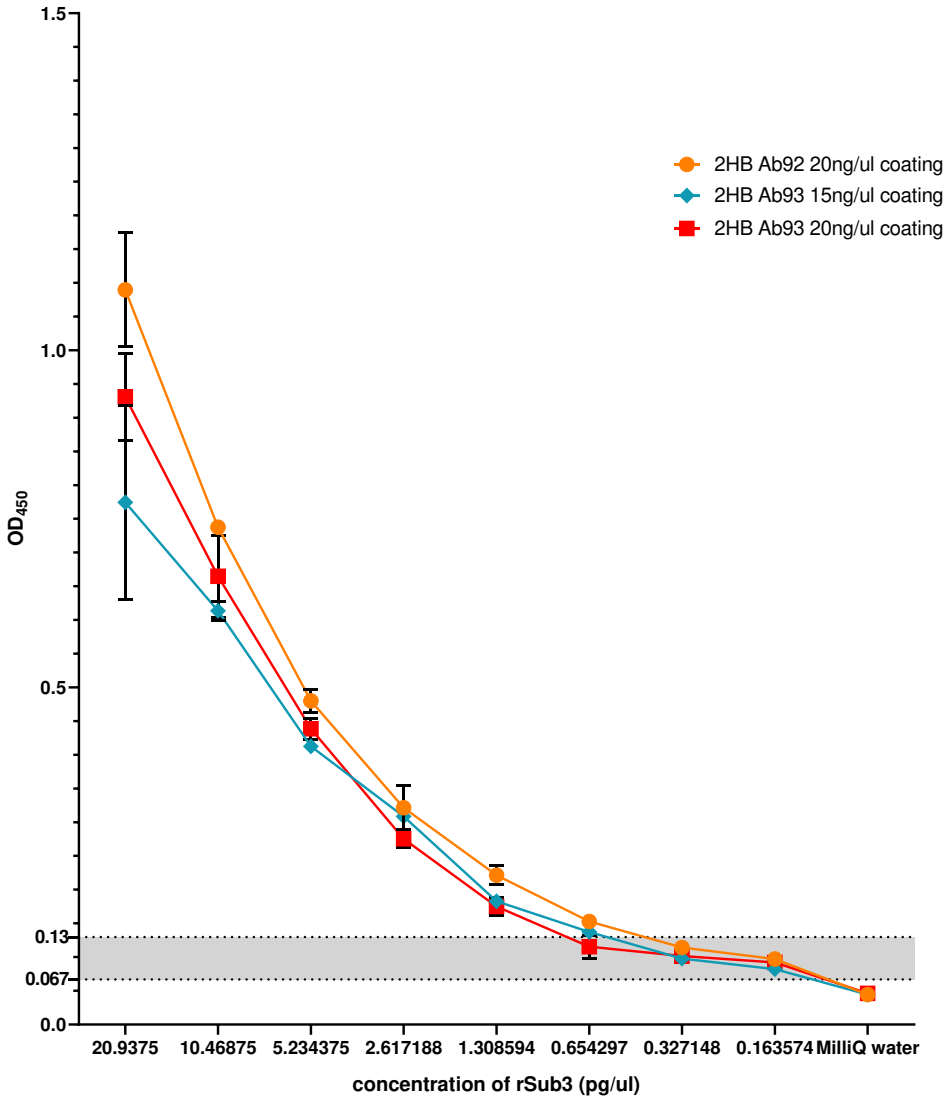

Supplemental Figure 4.2. No increase in assay sensitivity when blocking incubation increased to overnight. Same limit of detection seen when blocking incubation was 2 hrs (Fig. 4.4). 2HB plate was coated with 15 ng/µl or 20 ng/µl of coating antibody Ab93 or 20 ng/µl of coating antibody Ab92. The indeterminate range was determined as 1-2x cutoff value. The indeterminate range was 0.067-0.13 (gray shaded region). Samples were run in triplicate (n=3) and standard deviation was less than 0.144 for all points.

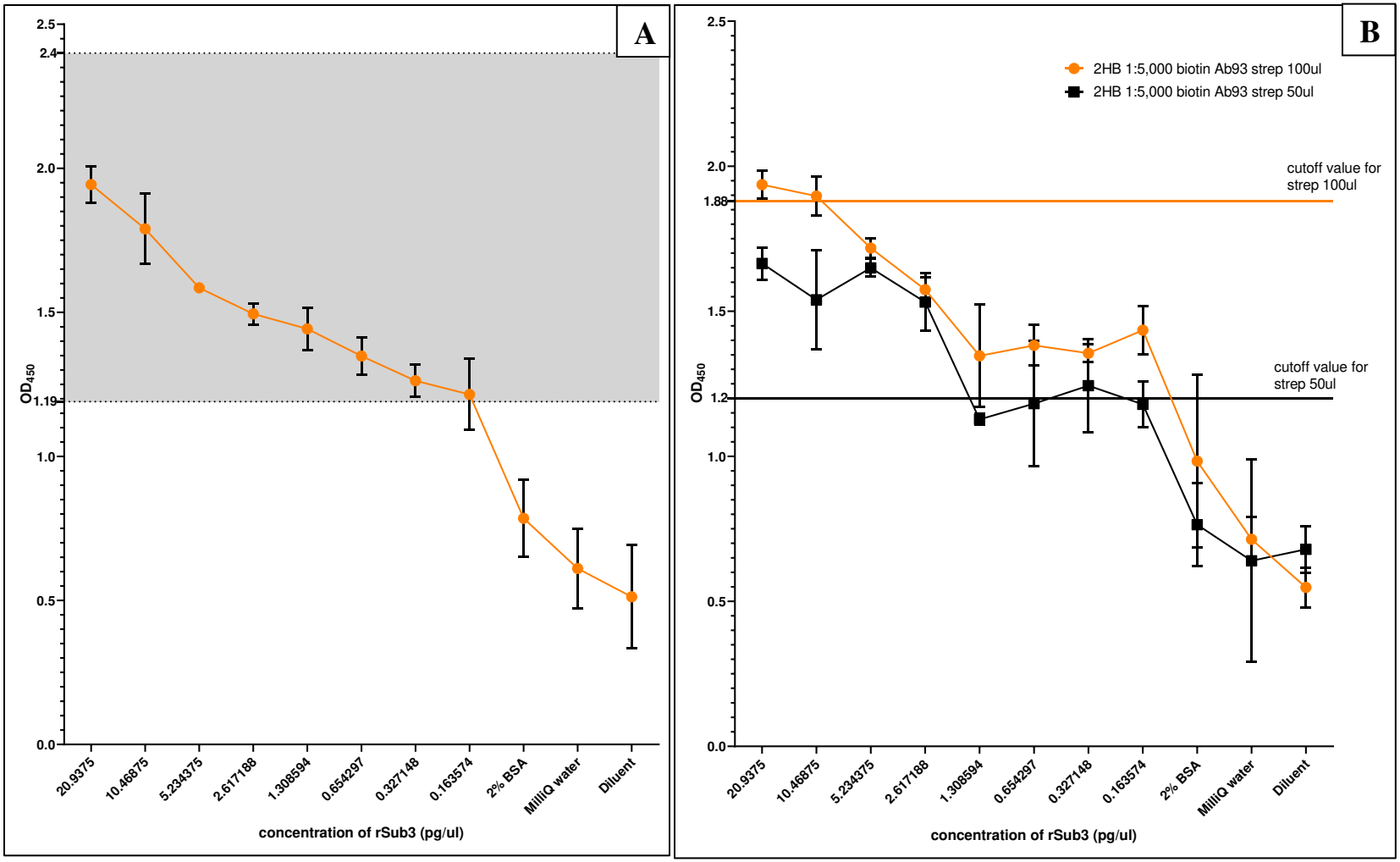

Supplemental Figure 4.3. High assay background noise due to unoptimized ratios of biotin to streptavidin. 2HB plate was coated with 20 ng/µl of coating antibody Ab92 and 1:5,000 dilution of detection biotinylated antibody. (A) Streptavidin was added to wells at 200 µl of 1:10,000 dilution. The indeterminate range was determined as 1-2x cutoff value. The indeterminate range was 1.19-2.4 (gray shaded region). (B) Streptavidin was added to wells at 100 µl (orange) or 50 µl (black) of 1:10,000 dilution. The lower limit of the indeterminate range was 1.2 (black line) and 1.88 (orange line). Samples were run in triplicate (n=3) and standard deviation was less than 0.298 for all points.

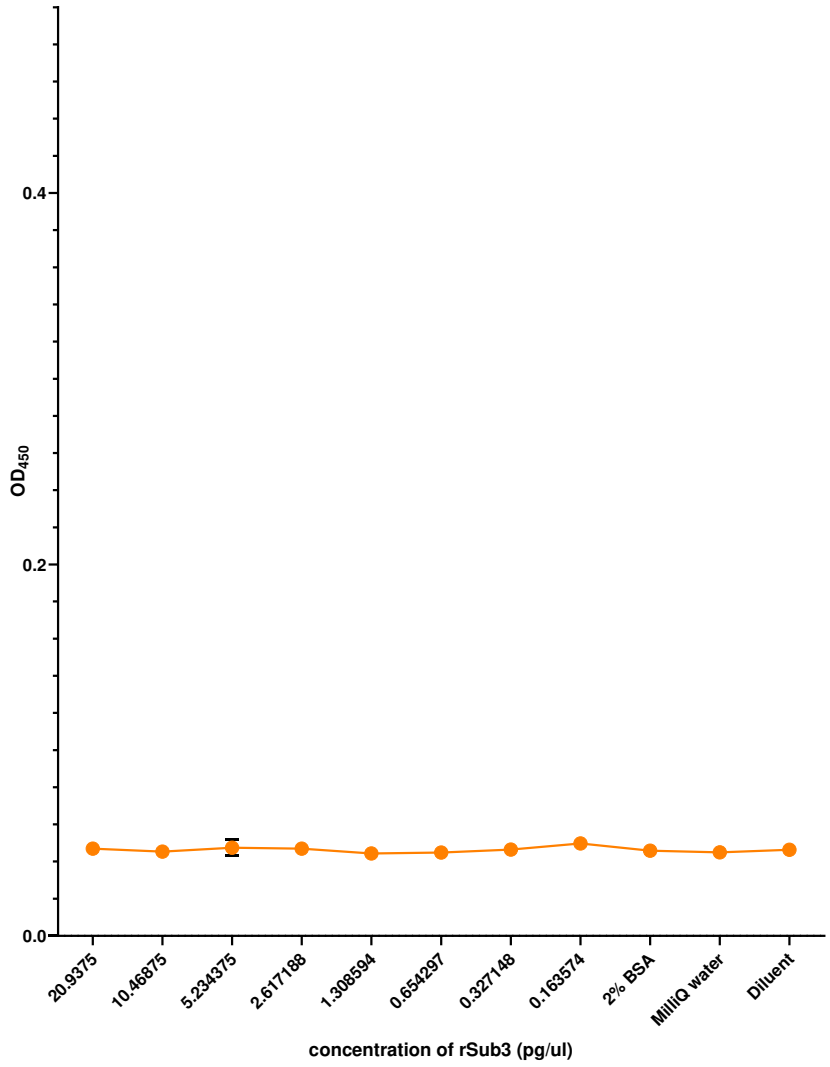

Supplemental Figure 4.4. Absence of non-specific binding of streptavidin to compounds of ELISA. 2HB plate was coated with 20 ng/µl of coating antibody Ab92 and streptavidin was added to wells at 100 µl of 1:10,000 dilution. Samples were run in triplicate (n=3) and standard deviation was less than 0.004 for all points.

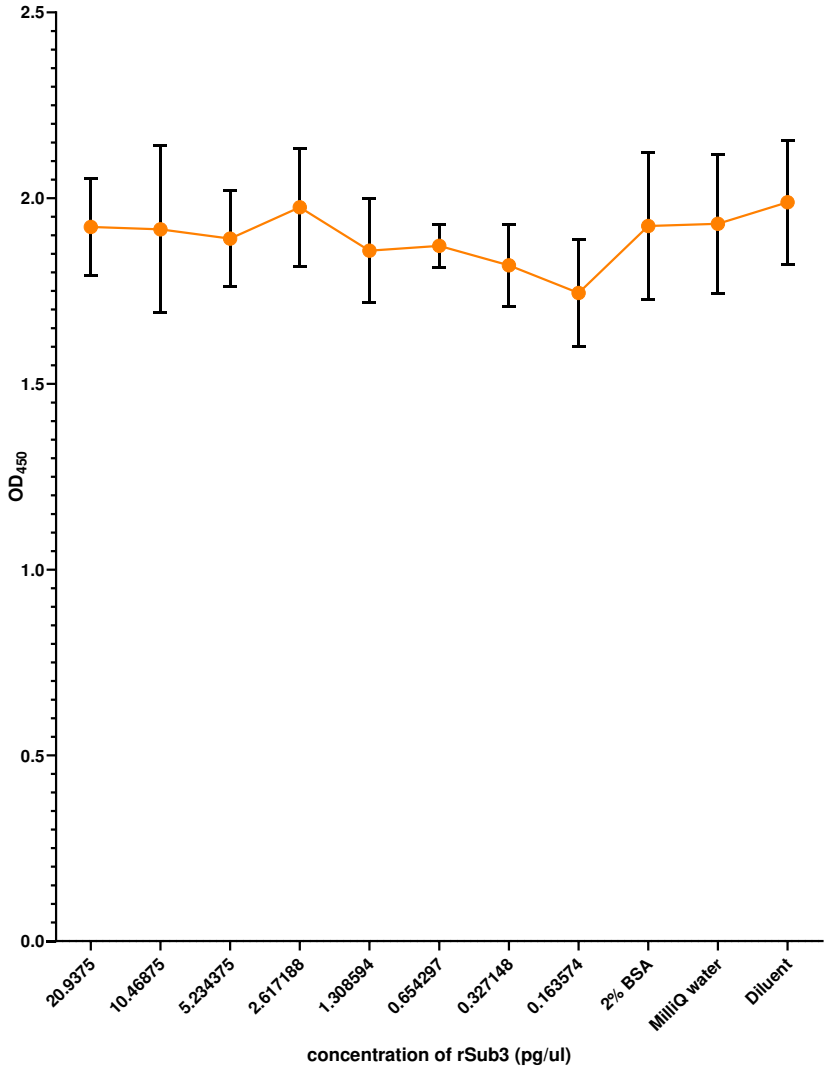

Supplemental Figure 4.5. High assay background noise when using anti-rabbit goat antibodies as detection antibodies. 2HB plate was coated with 20 ng/µl of coating antibody Ab92 and 1:5,000 dilution of antigen detection antibodies, followed by biotinylated goat anti-rabbit antibodies. Samples were run in triplicate (n=3) and standard deviation was less than 0.225 for all points.

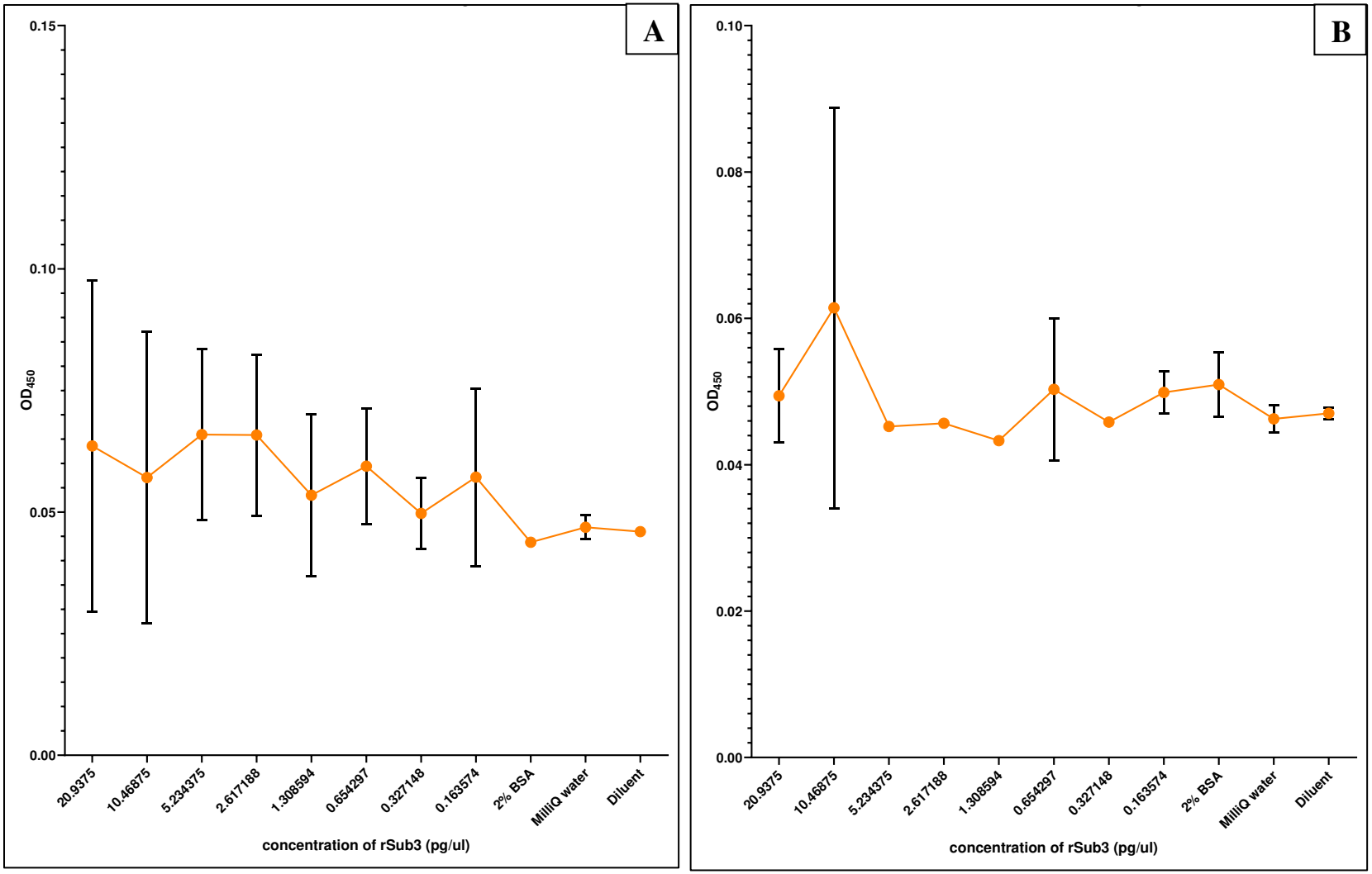

Supplemental Figure 4.6. Low assay signal when directly coating sample on plate. 2HB plate was coated with sample (rSub3, 2% BSA, water, or ELISA diluent). (A) Biotinylated detection antibodies at 1:5,000 dilution were used. (B) Detection antibodies at 1:5,000 dilution of antigen detection antibodies, followed by biotinylated goat anti-rabbit antibodies were used. Samples were run in triplicate (n=3) and standard deviation was less than 0.034 for all points.

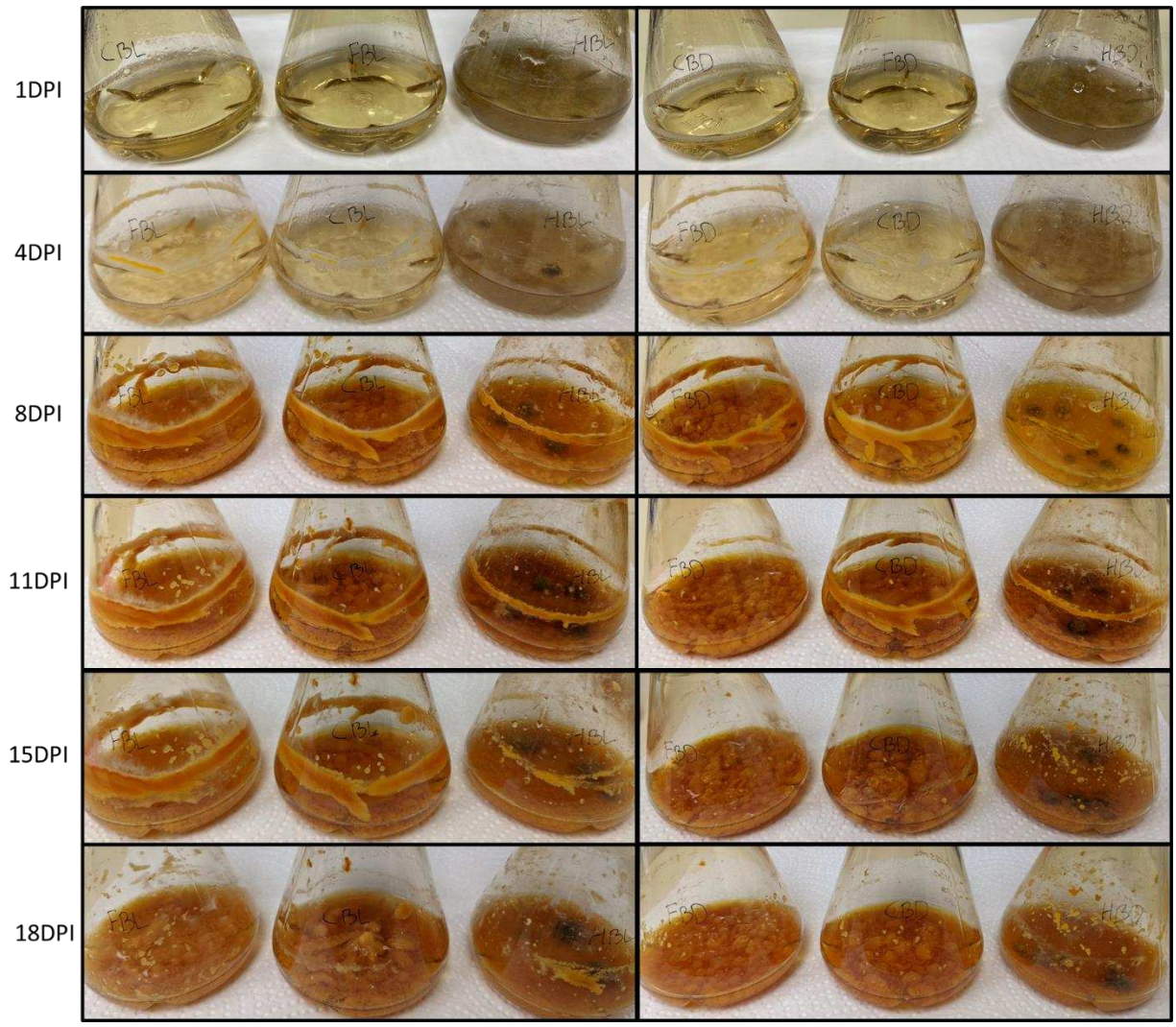

Supplementary Figure 4.7. Grow of *Microsporum canis* in shaken baffled flasks with or without light. Row (1) – 1 day post inoculation (DPI); (2) – 4 DPI; (3) – 8DPI; (4) – 11DPI; (5) – 15DPI; (6) – 18DPI. Visible fungal pellets formed by 4 DPI. Flasks with hair formed small hair balls by 4 DPI.

Supplementary Table 4.1. No significant difference between housekeeping genes. P-values were calculated using Student's t-test and were considered significant if less than 0.05.

Genes	**β-actin**	**sdha**	**mbp1**
	p-values		
β-actin	N/A	0.961	0.948
sdha	0.961	N/A	0.886
mbp1	0.948	0.886	N/A

Supplementary Table 4.2. No significant difference between Sub3 primer sets. P-values were calculated using Student's t-test and were considered significant if less than 0.05.

Primer sets	**SUB3.1**	**SUB3.2**	**SUB3.3**	**SUB3.4**	**SUB3.5**
	p-values				
SUB3.1	N/A	0.934	0.595	0.645	0.63
SUB3.2	0.934	N/A	0.645	0.589	0.576
SUB3.3	0.595	0.645	N/A	0.357	0.351
SUB3.4	0.645	0.589	0.357	N/A	0.977
SUB3.5	0.63	0.576	0.351	0.977	N/A

Supplementary Table 4.3. Nanodrop values for broth experiment 3. Con = concentration of RNA (ng/µl). Ratio = 260/280 ratio measuring nucleic acid purity.

	1 DPI		**4 DPI**		**8 DPI**		**11 DPI**		**15 DPI**		**18 DPI**	
Sample	con	ratio	con	ratio	con	ratio	con	ratio	con	ratio	con	ratio
HB	0.4	0.64	0.8	0.77	0.2	0.21	1.1	0.92	2.1	0.91	-0.8	1.97
HU	1.2	1.68	-0.2	1.47	0.2	-5.57	0.9	0.8	1.5	0.63	0.5	0.9
CB	1.4	1.42	5.4	1.47	0.1	0.01	2.7	1.1	1.5	1.04	1.3	1
CU	2.9	1.53	1.3	0.71	2.2	2.97	0.8	0.74	2.1	0.92	0.6	0.7
NB	0.4	11.85	0.7	1.04	0.5	-1.75	3.2	1.29	2.1	0.71	0.2	0.21
NU	1.1	1.22	1.2	1.43	-0.4	1.18	1.4	1.4	1.7	0.68	0	-0.03
NTCN	1.1	0.97	-0.6	3.04	1.3	-20.55	0.8	0.64	0.7	0.39	-0.2	-0.66
NTCH	-0.1	0.22	-0.1	-0.07	0	10.6	0.5	0.42	0.9	0.71	-0.1	-0.3
NTCC	0.7	2.42	0.2	0.33	-0.6	0.71	1.2	0.79	1.4	0.64	1.3	1.47

Supplementary Table 4.4. Nanodrop values for broth experiment 4. Con = concentration of RNA (ng/µl). Ratio = 260/280 ratio measuring nucleic acid purity.

	1 DPI		**4 DPI**		**8 DPI**		**11 DPI**		**15 DPI**		**18 DPI**	
Sample	con	ratio	con	ratio	con	ratio	con	ratio	con	ratio	con	ratio
HBD	-0.1	-0.21	0	-0.2	1.2	1.24	0.8	16.42	0.2	-0.99	-2.2	0.95
HBL	0.5	0.38	-0.6	3.22	2.2	1.15	2.1	1.67	0.2	-0.87	-1.6	1.05
CBD	3.5	1.29	0.3	0.42	1.7	1.17	0.6	30.19	1.7	2.59	0.9	1.47
CBL	3.2	1.09	0.8	0.85	0.9	2.64	1.1	-31.52	0.3	1.4	-1.1	1.11
NBD	4.2	1.34	0.9	0.72	1.8	1.32	0.3	2.71	0.5	0.48	-2.4	1.26
NBL	0.5	1.45	-0.2	1.01	0.5	0.68	0.4	2.91	1.5	7.43	-1.8	1.09
NTCN	2	0.77	-0.2	-0.56	4.3	1.54	0.8	1.82	1.6	3.24	-2.8	1.07
NTCH	1.1	1.32	1.4	0.97	7.9	1.34	3.8	1.61	0	0.31	-1.5	0.84
NTCC	-0.2	0.71	-0.3	0.39	6.2	1.29	0.6	3.07	0.4	0.86	0.3	-1.3

Supplementary Table 5.1. Optical density values at 340nm for samples using the Megazyme sulfite kit.

	4 mins (A0)	30 mins (A1)	50 mins (A2)
Standard	2.906656561	1.921575698	1.701660522
Sample	2.956891354	1.863415231	1.749595187
Blank	2.784314636	2.072235857	2.169035831